Methods in Molecular Biology 2255

Springer Protocols

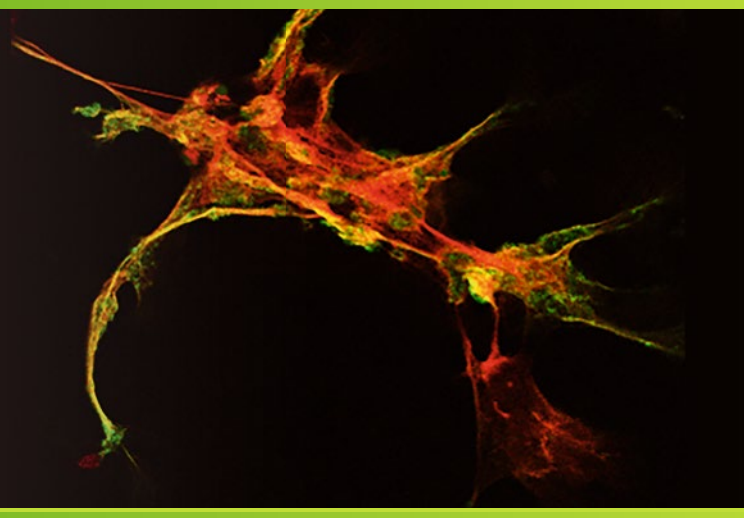

Ayesha B. Alvero
Gil G. Mor *Editors*

Detection of Cell Death Mechanisms

Methods and Protocols

Humana Press

METHODS IN MOLECULAR BIOLOGY

Series Editor
John M. Walker
School of Life and Medical Sciences
University of Hertfordshire
Hatfield, Hertfordshire, UK

For further volumes:
http://www.springer.com/series/7651

For over 35 years, biological scientists have come to rely on the research protocols and methodologies in the critically acclaimed *Methods in Molecular Biology* series. The series was the first to introduce the step-by-step protocols approach that has become the standard in all biomedical protocol publishing. Each protocol is provided in readily-reproducible step-by-step fashion, opening with an introductory overview, a list of the materials and reagents needed to complete the experiment, and followed by a detailed procedure that is supported with a helpful notes section offering tips and tricks of the trade as well as troubleshooting advice. These hallmark features were introduced by series editor Dr. John Walker and constitute the key ingredient in each and every volume of the *Methods in Molecular Biology* series. Tested and trusted, comprehensive and reliable, all protocols from the series are indexed in PubMed.

Detection of Cell Death Mechanisms

Methods and Protocols

Edited by

Ayesha B. Alvero and Gil G. Mor

Department of Obstetrics and Gynecology, Wayne State University, Detroit, MI, USA

Humana Press

Editors
Ayesha B. Alvero
Department of Obstetrics
and Gynecology
Wayne State University
Detroit, MI, USA

Gil G. Mor
Department of Obstetrics
and Gynecology
Wayne State University
Detroit, MI, USA

ISSN 1064-3745 ISSN 1940-6029 (electronic)
Methods in Molecular Biology
ISBN 978-1-0716-1161-6 ISBN 978-1-0716-1162-3 (eBook)
https://doi.org/10.1007/978-1-0716-1162-3

This Humana imprint is published by the registered company Springer Science+Business Media, LLC, part of Springer Nature.
The registered company address is: 1 New York Plaza, New York, NY 10004, U.S.A.

Preface

Cell death mechanisms are diverse yet nonexclusive molecular pathways leading to cell demise. For the past several decades, the field of research in cell death mechanisms had unraveled multiple signaling cascades initiated by a variety of physiological and pathological signals, detected by specific membranal or intracellular sensors, and carried out by different effector proteins leading to a wide range of morphology changes, which precede cell death. Whereas both apoptosis and pyroptosis for instance result in caspase activation and DNA cleavage, the specific caspases involved and the resulting morphology of cell death are different. Similarly, although both apoptosis and necroptosis can be initiated via ligation of membranal death receptors, the downstream signaling in apoptosis is propagated by caspase-8 while necroptosis depends on the kinase activity of RIPK1, RIPK3, and MLKL. Still, these different intracellular mechanisms of cell death lead to diverse host responses. As such pyroptosis and immunogenic cell death are capable of eliciting inflammation and host immune responses, whereas the packaging of apoptotic bodies during apoptotic cell death results in the absence of inflammation.

This book compiles both conventional (Western blot, PCR, etc.) and state-of-the-art (transmission electron microscopy, real-time multiplexed imaging assays, etc.) methodologies for the detection of cell death and more importantly for the determination of the cell death type. Each chapter is written such that students, trainees, and even experienced scientists who are beginning to look into cell death mechanisms will be able to swiftly execute the methodologies described. The chapters are written using readily available systems such as common human and mouse cell lines and commercially available cell death inducers, which can serve as robust positive controls for the assays described. The Notes section in each chapter offers insights into potential problems that can be encountered and troubleshooting tips, which represent the authors' collective experience in the execution of their protocols.

We wish to thank our Senior Editor, Dr. John Walker, and all the authors that contributed to this book. Our authors are both from academia and industry and as such the book offers a variety of techniques that can be executed using either "homemade" buffers or specialized commercially available reagents. Of note is that the latter half of our process occurred during the COVID-19 pandemic. We are especially grateful to the authors who continued their work and contributed to this book during this challenging time.

We hope that each chapter of this book will allow seamless execution of protocols and the demonstration of specific cell death type. Although the protocols are written specifically for the detection of cell death mechanisms, each chapter can be adapted in studying other cellular processes.

Detroit, MI, USA

Ayesha B. Alvero
Gil G. Mor

Contents

Contributors

Vikki M. Abrahams • *Department of Obstetrics, Gynecology and Reproductive Sciences, Yale School of Medicine, New Haven, CT, USA*

Nour N. Al Zouabi • *Department of Obstetrics, Gynecology, and Reproductive Sciences, Yale University School of Medicine, New Haven, CT, USA*

Ayesha B. Alvero • *Department of Obstetrics and Gynecology, C.S. Mott Center for Human Growth and Development, Wayne State University, Detroit, MI, USA*

Daniel M. Appledorn • *Essen Biosciences/Sartorius, Ann Arbor, MI, USA*

Jennifer Carlson Aske • *Translational Oncology Laboratory, Avera Cancer Institute, Sioux Falls, SD, USA*

James J. Cali • *Research and Development, Promega Corporation, Madison, WI, USA*

Guillermina Calo • *CONICET—Universidad de Buenos Aires. Instituto de Química Biológica de la Facultad de Ciencias Exactas y Naturales (IQUIBICEN). Laboratorio de inmunofarmacología, Buenos Aires, Argentina*

Ilana Chefetz • *The Hormel Institute, University of Minnesota, Austin, MN, USA; Masonic Cancer Center, Minneapolis, MN, USA; Stem Cell Institute, Minneapolis, MN, USA; Department of Obstetrics, Gynecology and Women's Health, Minneapolis, MN, USA*

Hussein Chehade • *Department of Obstetrics and Gynecology, C.S. Mott Center for Human Growth and Development, Wayne State University, Detroit, MI, USA*

Mikhail Chesnokov • *The Hormel Institute, University of Minnesota, Austin, MN, USA*

Pradip De • *Translational Oncology Laboratory, Avera Cancer Institute, Sioux Falls, SD, USA; Departmental of Internal Medicine, SSOM, University of South Dakota, Sioux Falls, SD, USA*

Nandini Dey • *Translational Oncology Laboratory, Avera Cancer Institute, Sioux Falls, SD, USA; Departmental of Internal Medicine, SSOM, University of South Dakota, Sioux Falls, SD, USA*

Richard Edelson • *Department of Dermatology, Yale University School of Medicine, New Haven, CT, USA*

Yang Feng • *College of Animal Science & Technology, Sichuan Agricultural University, Chengdu, Sichuan, China*

Alexandra Fox • *Department of Obstetrics and Gynecology, C.S. Mott Center for Human Growth and Development, Wayne State University, Detroit, MI, USA*

Han-Hsuan Fu • *Division of Pediatric Oncology, Sidney Kimmel Cancer Center, Johns Hopkins University, Baltimore, MD, USA*

Naresh Golla • *The Hormel Institute, University of Minnesota, Austin, MN, USA*

Jill E. Granger • *Essen Biosciences/Sartorius, Ann Arbor, MI, USA*

Esteban Grasso • *CONICET—Universidad de Buenos Aires. Instituto de Química Biológica de la Facultad de Ciencias Exactas y Naturales (IQUIBICEN). Laboratorio de inmunofarmacología, Buenos Aires, Argentina*

Katherine Gurdziel • *Office of the Vice President of Research, Wayne State University, Detroit, MI, USA*

Joe L. Guy • *Department of Obstetrics and Gynecology, C.S. Mott Center for Human Growth and Development, Wayne State University, Detroit, MI, USA*

Patrick Han • *Department of Chemical & Environmental Engineering, Yale University School of Engineering and Applied Science, New Haven, CT, USA*
Douglas Hanlon • *Department of Dermatology, Yale University School of Medicine, New Haven, CT, USA*
Peter Hofsteen • *Research and Development, Promega Corporation, Madison, WI, USA*
Linda J. Hong • *Division of Gynecologic Oncology, Department of Gynecology and Obstetrics, Loma Linda University School of Medicine, Loma Linda, CA, USA*
Xiaoli Huang • *College of Animal Science & Technology, Sichuan Agricultural University, Chengdu, Sichuan, China*
Natasha Karassina • *Research and Development, Promega Corporation, Madison, WI, USA*
Irene Angelica Keitelman • *CONICET—Academia Nacional de Medicina. Instituto de Medicina Experimental (IMEX). Laboratorio de Inmunidad Innata, Buenos Aires, Argentina*
Imran Khan • *The Hormel Institute, University of Minnesota, Austin, MN, USA*
Kevin R. Kupcho • *Promega, Madison, WI, USA*
Claudia Pérez Leirós • *CONICET—Universidad de Buenos Aires. Instituto de Química Biológica de la Facultad de Ciencias Exactas y Naturales (IQUIBICEN). Laboratorio de inmunofarmacología, Buenos Aires, Argentina*
Z. Ping Lin • *Department of Obstetrics, Gynecology, and Reproductive Sciences, Yale University School of Medicine, New Haven, CT, USA*
Gil G. Mor • *Department of Obstetrics and Gynecology, C.S. Mott Center for Human Growth and Development, Wayne State University, Detroit, MI, USA*
Andrew L. Niles • *Promega, Madison, WI, USA*
Alexander Paridon • *Department of Obstetrics and Gynecology, C.S. Mott Center for Human Growth and Development, Wayne State University, Detroit, MI, USA*
Harry Qui • *United States Navy, Philadelphia, PA, USA*
Rosanna Ramhorst • *CONICET—Universidad de Buenos Aires. Instituto de Química Biológica de la Facultad de Ciencias Exactas y Naturales (IQUIBICEN). Laboratorio de inmunofarmacología, Buenos Aires, Argentina*
Elena S. Ratner • *Department of Obstetrics, Gynecology, and Reproductive Sciences, Yale University School of Medicine, New Haven, CT, USA*
Cai M. Roberts • *Department of Obstetrics, Gynecology, and Reproductive Sciences, Yale University School of Medicine, New Haven, CT, USA*
Florencia Sabbione • *CONICET—Academia Nacional de Medicina. Instituto de Medicina Experimental (IMEX). Laboratorio de Inmunidad Innata, Buenos Aires, Argentina*
Kazuki Tatsuno • *Department of Dermatology, Yale University School of Medicine, New Haven, CT, USA*
Roslyn Tedja • *Department of Obstetrics and Gynecology, C.S. Mott Center for Human Growth and Development, Wayne State University School of Medicine, Detroit, MI, USA*
Mancy Tong • *Department of Obstetrics, Gynecology and Reproductive Sciences, Yale School of Medicine, New Haven, CT, USA*
Analia Silvina Trevani • *CONICET—Academia Nacional de Medicina. Instituto de Medicina Experimental (IMEX). Laboratorio de Inmunidad Innata, Buenos Aires, Argentina*
Jolanta Vidugiriene • *Research and Development, Promega Corporation, Madison, WI, USA*

Chapter 1

Determination of Caspase Activation by Western Blot

Hussein Chehade, Alexandra Fox, Gil G. Mor, and Ayesha B. Alvero

Abstract

Apoptosis is a type of programmed cell death induced by a cascade of biochemical events, which leads to distinct morphological changes characterized by cell shrinkage, membrane blebbing, chromatin condensation, and DNA fragmentation. Apoptosis is executed by a class of cysteine proteases called caspases. Caspases are synthesized as inactive pro-caspases and activated by a series of cleavage reactions. Active caspases cleave cellular substrates and are thus the main effectors of the apoptotic cell death pathway. Detection of caspase cleavage by western blot analysis is a conventional method to demonstrate the induction of apoptosis. In the context of apoptosis, the proper analysis of western blot results depends on the understanding of the mechanisms and outcomes of caspase processing during the course of its activation. In this chapter, we describe the step-by-step methodology in the western blot analysis of caspase cleavage during apoptosis. We detail protocols for protein extraction, quantitation, casting, and running gel electrophoresis and western blot analysis of caspase -8 and caspase -9 activation. The described methods can be applied to any particular protein of interest.

Key words Apoptosis, Western Blot, Proteins, Caspases, Cleavage, Extrinsic Pathway

1 Introduction

Programmed cell death is an intracellular process activated by cells to induce its death. Apoptosis is a type of programmed cell death and is distinguished morphologically by nuclear condensation, cell shrinkage, and eventually cell fragmentation leading to the formation of apoptotic bodies [1, 2]. A cell undergoes apoptosis due to a myriad of reasons, which include the loss of growth signals, presence of cellular stressors from the environment, or the detection of intracellular events that compromise the survival of the whole organism. These events include overt mistakes in DNA replication and an increase in misfolded proteins. Molecularly, apoptosis is induced by the activation of proteolytic enzymes, termed caspases [3]. Caspases are a family of cysteine proteases, which are synthesized as inactive pro-caspase and are activated by a series of cleavage events, culminating in the production of active enzymes capable of cleaving cellular substrates specifically after aspartate sites.

Ayesha B. Alvero and Gil G. Mor (eds.), *Detection of Cell Death Mechanisms: Methods and Protocols*, Methods in Molecular Biology, vol. 2255, https://doi.org/10.1007/978-1-0716-1162-3_1,

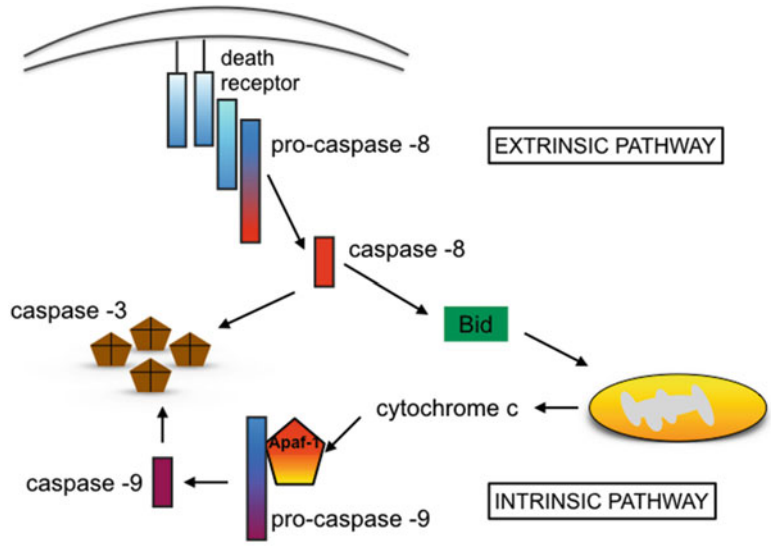

Fig. 1 Schematic diagram of the two arms of the apoptotic pathway. The Extrinsic pathway is activated by ligation of death receptors leading to activation of caspase -8 and subsequently, activation of caspase -3. The Intrinsic pathway is initiated upon the loss of mitochondrial membrane integrity and cytoplasmic translocation of cytochrome c, leading to the activation of caspase -9, which also can subsequently activate caspase -3. Thus, independent of which arm initiates the cascade, caspase -3 is the main effector caspase. Bid connects the Extrinsic pathway to the Intrinsic pathway

In apoptosis, there are two types of caspases: initiator caspases such as caspase -8 and -9, and executor caspases such as caspase -3 and -7. Caspase -8 is the initiator caspase in the extrinsic arm of the apoptotic pathway (Fig. 1). The extrinsic apoptotic pathway is triggered by the ligation of membranal death receptors such as tumor necrosis factor (TNF) or Fas receptors [4]. Upon ligand binding, death receptors are activated leading to the recruitment of adapter proteins and pro-caspase -8. This results in the activation of caspase -8, which occurs via two cleavage events: cleavage of the full-length p55 pro-caspase -8 to p43 and further cleavage to the active p18 caspase -8 [5]. Similarly, upon activation of the intrinsic arm of the apoptotic pathway (Fig. 1), its initiator caspase, caspase -9, is processed and activated in a similar way. Upon the loss of mitochondrial membrane integrity, cytochrome C is released to the cytoplasm leading to the formation of the apoptosome complex [6], which activates caspase -9 via cleavage of the p46 pro-caspase -9 to p35 and p12 subunits [7].

Western blot analysis is a conventional procedure to determine caspase activation. When analyzed by western blot using antibodies that detect full-length caspase, caspase activation is therefore observed as a decrease or loss of the band corresponding to the

full-length pro-caspase and the appearance of smaller cleaved products. This chapter describes the step-by-step procedure required for the detection of caspase activation by western blot or immunoblot technique. The steps are broken down into five parts: (1) induction of apoptosis, (2) protein extraction, (3) protein quantitation, (4) polyacrylamide gel electrophoresis, and (5) western blot analysis. More importantly, we have included tips and recommendations that can enable the swift performance of the methods, rapid analysis of results, and efficient troubleshooting.

2 Materials

2.1 Equipment and Disposables

1. Tissue culture incubator.
2. Refrigerated centrifuge.
3. Microscope.
4. Plate reader for determination of protein quantitation using a colorimetric assay.
5. ECL imager.
6. Heat block.
7. Electrophoresis and transfer tank.
8. Power supply for electrophoresis and transfer tank.
9. Cell counter or hemocytometer.
10. Vortex.
11. Shaker.
12. 100 mm cell culture dish.
13. Scrapers.
14. 50 ml conical tubes.
15. 15 ml conical tubes.
16. Microcentrifuge tubes.
17. Pipet tips.
18. 12 × 75 mm glass tubes.
19. 96-well flat-bottom plate.
20. Parafilm.
21. Glass plates (short and spacer plates) and combs for casting polyacrylamide gels: for this chapter we used the MiniPROTEAN system from BioRad with 1 mm spacers.
22. Casting frame and a holder.
23. Lint-free wipes such as Kimwipes.
24. Transfer cassettes: for this chapter we used the Mini Trans Blot system from BioRad.

25. PVDF membrane.
26. Filter papers.
27. Foam pads for transfer cassettes.

2.2 Reagents and Cell Lines

1. Cell line of choice: for this chapter we used the human ovarian cancer cell line, A2780.
2. Growth media for cell line of choice: for A2780, the growth media is RPMI-1640 + 10% FBS.
3. Inducer of apoptosis: for this chapter we used Paclitaxel (2.5 mM in DMSO).
4. 1× PBS: 137 mM NaCl, 2.7 mM KCl, 10 mM Na_2HPO_4, 1.8 mM KH_2PO_4.
5. 0.05% trypsin.
6. Cell lysis buffer: 1% NP40, 0.1% Sodium dodecyl sulfate (SDS) in 1× PBS (*see* **Note 1**).
7. Commercially available protease inhibitor cocktail (PIC) used according to manufacturer's instructions.
8. Commercially available protein quantitation reagents: for this chapter we used Bicinchoninic assay (BCA).
9. Bovine serum albumin: 1 mg/ml in 1× PBS.
10. 70% ethanol.
11. Ammonium Persulfate.
12. Double distilled water (ddH_2O).
13. 30% acrylamide and bis-acrylamide solution, 29:1.
14. 50% Glycerol in water.
15. Tetramethylethylenediamine (TEMED).
16. Lower-Tris buffer: 36.33 g ultrapure Tris, 0.8 g SDS, 150 ml ddH_2O (adjust pH to 8.8), adjust volume to 200 ml with ddH_2O, mix well and filter using 0.45 μm filter unit.
17. Upper-Tris buffer: 6.05 g ultrapure Tris, 0.4 g SDS, 50 ml ddH_2O (adjust pH to 6.8), adjust volume to 100 ml with ddH_2O, mix well and filter using 0.45 μm filter unit.
18. SDS sample buffer (3×): 3 ml Glycerol, 1.5 ml β-mercaptoethanol, 0.8 g SDS, 3.75 ml upper-Tris buffer, a pinch of Bromophenol Blue, adjust volume to 10 ml with hot ddH_2O and mix well. Incubate in hot water bath for 5 min, then aliquot and store at −20 °C.
19. Commercially available molecular weight marker.
20. PBS-Tween: 1 l 1× PBS, 500 μl Tween 20.
21. Running buffer: 30.3 g Tris, 144.4 g Glycine, 10 g SDS, 1 l ddH_2O.

22. Transfer buffer: 1.44 g Glycine, 3.05 g Tris, 200 ml methanol, 800 ml ddH_2O; keep at 4 °C.
23. Methanol.
24. 10× Ponceau stain: 2% Ponceau S, 30% tricholoracetic acid, 30% sulfosalicylic acid in water; diluted to 1× with water.
25. Nonfat powder dry milk.
26. Primary antibodies for caspase -8 and caspase -9.
27. Primary antibody for a housekeeping gene such as GAPDH or β-actin.
28. Appropriate HRP-tagged secondary antibodies.
29. Commercially available enhanced chemiluminescence (ECL) reagents.

3 Methods

3.1 Induction of Apoptosis

1. Seed cells in 100 mm tissue culture dish. For A2780, we seed 1×10^6 cells per dish in 10 ml growth media.
2. The following day, treat with an apoptosis inducer. In this chapter we treated A2780 cells with 0.02 μM Paclitaxel for 24 h and 48 h.
3. At the end of treatment, collect cells in 15 ml conical tubes by scraping and centrifuge ~500 × *g* for 5 min.
4. Discard supernatant, add 6 ml of 1× PBS and mix to disrupt pellet.
5. Centrifuge ~500 × *g* for 5 min. Discard supernatant and proceed to protein extraction or freeze the dried pellets in −80 °C to store.

3.2 Protein Extraction

1. Keep pellets frozen until ready to use. Keep all reagents on ice at all times.
2. Make a master mix of cell lysis buffer and PIC depending on the number of samples. Pellets from about 1×10^6 cells typically require 100 μl of cell lysis buffer mix (*see* **Note 2**).
3. Add 100 μl of cell lysis buffer mix to each sample and pipet up and down to disrupt the pellet.
4. Vortex samples for 20 s and incubate on ice for 20 min. Keep vortexing the samples every 5 min.
5. Centrifuge at 10,000 × *g* for 15 min at 4 °C.
6. Transfer supernatant to a new microcentrifuge tube and discard the pellet. The supernatant is the protein lysate. Protein lysates should always be kept on ice and stored at −80 °C.

3.3 Protein Quantitation

1. Set up the standards to create a standard curve by labeling 8 microcentrifuge tubes A to H and making serial dilutions according to Table 1 (vortex well after dilution).
2. Label eight 12 × 75 mm glass tubes A to H and transfer 50 µl from each corresponding microcentrifuge tube from above. Discard the microcentrifuge tubes and remaining contents.
3. Label one 12 × 75 mm glass tube as "blank" and add 50 µl of 1× PBS.
4. Set up the protein samples. Label one 12 × 75 mm glass tube per sample and add 45 µl of 1× PBS and 5 µl of protein lysate to create a 1:10 dilution.
5. Prepare BCA reagent mix by mixing Reagent A and Reagent B. For up to 5 protein samples and all protein standards, mix 15 ml of Reagent A and 300 µl of Reagent B (*see* **Note 3**).
6. Add 2 ml of BCA Reagent mix to the "blank" tube and 1 ml to each standard tube and each sample tube.
7. Vortex tubes well and load 200 µl/well of blank, standard mix (A to H) or sample mix (S1 to S20) onto a 96-well flat-bottom plate. An example of loading is shown in Table 2.
8. Cover plate tightly with parafilm and incubate for 30 min at 37 °C, then another 30 min at room temperature.
9. Use plate reader to determine the absorbance of samples and use the absorbance values to determine protein concentration (*see* **Note 4**).

3.4 Polyacrylamide Gel Electrophoresis (See Notes 5–8)

1. Begin the polymerization of the resolving gel by cleaning glass plates with 70% ethanol and wiping with kimwipes.
2. Place the short glass plate in front of the large (spacer) glass plate with raised edges of large glass plate towards the short plate. Align the bottom edges of the two plates and assemble into the casting frame (*see* **Note 9**).
3. Weigh out 0.1 g of ammonium persulfate and dissolve in 1 ml ddH_2O. Vortex well and wrap the tube with an aluminum foil to limit exposure to light.
4. Mix resolving gel solution in a 50 ml conical tube by sequentially adding:
   6 ml lower-Tris buffer.
   9.5 ml of 30% acrylamide (8 ml for a 10% gel).
   200 µl of 50% glycerol in water.
   8.3 ml ddH_2O (9.8 ml for a 10% gel).
5. Add 240 µl of ammonium persulfate and 12 µl of TEMED and pulse vortex or swirl to mix avoiding formation of bubbles.

Table 1
Volumes for serial dilutions for the establishment of a standard curve

Tube	PBS (μl)	BSA Stock (μl)	Concentration (ng/μl)
A	0	400	1000
B	100	300 from A	750
C	100	200 from B	500
D	100	100 from C	250
E	150	100 from D	100
F	50	150 from E	75
G	40	80 from F	50
H	80	20 from G	10

Table 2
Typical layout of 96-well plate for protein quantitation assay

Blank	H	H	H	S1	S1	S1	S9	S9	S9	S17	S19
Blank	G	G	G	S2	S2	S2	S10	S10	S10	S17	S19
Blank	F	F	F	S3	S3	S3	S11	S11	S11	S17	S19
Blank	E	E	E	S4	S4	S4	S12	S12	S12	S18	S20
Blank	D	D	D	S5	S5	S5	S13	S13	S13	S18	S20
Blank	C	C	C	S6	S6	S6	S14	S14	S14	S18	S20
Blank	B	B	B	S7	S7	S7	S15	S15	S15		
Blank	A	A	A	S8	S8	S8	S16	S16	S16		

6. Quickly load 7 ml of resolving gel solution to each cassette slowly, avoiding any bubbles. This can be easily done by placing the tip of a 10 ml pipette into the top corner of the cassette where the two plates come together and slowly load the gel solution.
7. Add 500 μl of ddH_2O evenly across the top of the resolving gel to prevent the gel from drying out while setting. Set aside any remaining resolving buffer solution to check for polymerization as the gel settles (around 20 min).
8. When the resolving gel solution has polymerized, mix stacking gel solution by sequentially adding the following in a 50 ml tube:
   6.5 ml ddH_2O.
   2.5 ml upper-Tris buffer.
   1 ml of 30% acrylamide.

9. Add 45 μl of ammonium persulfate and 22.5 μl of TEMED and pulse vortex or swirl to mix avoiding formation of bubbles.
10. Quickly remove the water from the top of the resolving gel by tipping the cassette holder to one side and collecting water with a Kimwipes or paper towel.
11. Quickly load stacking gel solution into the cassette on top of the resolving gel until the solution starts to spill over the front glass plate (about 3 ml solution) and place the gel comb on the top of the glass cassette. Wipe away the spilled solution on the front of the glass cassette and set aside any remaining stacking gel solution to check for polymerization (around 20 min) (*see* **Note 10**).
12. Prepare protein samples for electrophoresis by calculating the volume of protein sample needed for 20 μg of protein (per well) and adding enough ddH_2O to reach 20 μl volume. Keep protein samples on ice.
13. Add 10 μl of 3× SDS sample buffer to each protein sample and vortex.
14. Boil samples on a heat block set to 100 °C for 5 min and return to ice.
15. Centrifuge all tubes briefly and store on ice until ready to load in the gel.
16. Prepare the molecular weight marker according to manufacturer's instructions.
17. Remove the combs from the gel cassettes and assemble gels in the running tank. The short plates should be facing the center of the tank.
18. Fill the tank with running buffer. Fill the chamber space between the two gels with running buffer and the outer chamber space halfway.
19. Load 25 μl of molecular marker or protein sample in appropriate wells (*see* **Note 11**).
20. Place the lid onto the running tank with the red and black nodes matching properly. Plug into a power source and run at 100 V for about 60–90 min until the blue line of samples has started seeping out at the bottom of the gel.

3.5 Western Blotting

1. Prepare PVDF membranes for transfer by shaking in methanol for about 30 s to activate the membrane. Membranes should be cut to the size of the gel (about 6 cm × 9 cm if using the Mini PROTEAN system).
2. Rinse the membrane with ddH_2O for 5 min to remove the methanol, then shake membranes in transfer buffer until ready to use.

3. Soak 4 pieces of filter paper (7 cm × 10 cm) and foam pads in transfer buffer.
4. Pour transfer buffer about three-quarters into a square plastic container to build the transfer stacks in.
5. Remove the gels from the running tank and carefully separate the glass plates. Run the razor along the edges of the gel and carefully remove it from the glass plate. Soak the gels in transfer buffer until ready to be put on the transfer stack.
6. Build the transfer stack on the black side of the transfer cassette in this exact order: foam pad, filter paper, gel, PVDF membrane, filter paper, and foam pad. Make sure that all components are fully wet with transfer buffer. Ensure that no air bubbles are present by rolling a glass tube or pipet over the transfer stack.
7. Carefully close the transfer cassette and load cassettes into the transfer tank.
8. Place a small stir bar in the tank and completely fill the tank with transfer buffer.
9. Place the lid on the tank, matching up the red and black nodes properly.
10. Plug into a power source and run the transfer at 32 V overnight or at 100 V for 2 h.
11. After transfer is complete, turn off the power supply and remove the cassettes from the transfer tank. Disassemble the transfer stacks and soak the membrane in transfer buffer to keep from drying out. The side of the membrane directly in contact with the gel is the protein side up. Discard the filter paper. Foam pads can be reused.
12. Check that the protein has successfully transferred to the membrane by shaking the membrane for about 30 s in ponceau red stain solution.
13. Wash membranes in PBS-Tween until the washes are clear. At this point, membranes can be air-dried and stored at −20 °C or can be blocked as below.

3.6 Antibody Staining and Enhanced Chemiluminescence

1. Shake membranes in 5% milk in PBS-Tween for 1 h at room temperature to block.
2. After blocking, wash membranes in PBS-Tween for 10 min, three times.
3. Prepare primary antibody according to manufacturer's recommended dilution in 1% milk in PBS-Tween. Incubate membranes in primary antibody solution overnight at 4 °C (*see* **Note 12**).
4. Wash membranes in PBS-Tween for 10 min, three times.

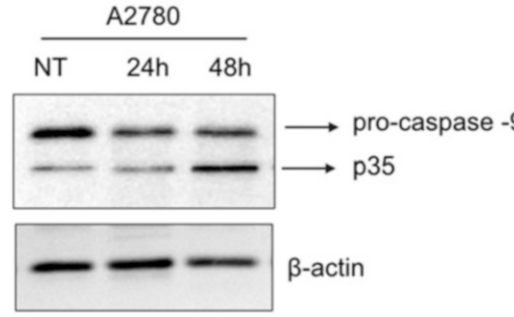

Fig. 2 A2780 human ovarian cancer cells were treated for 24 h and 48 h with 0.02 μM Paclitaxel. Activation of caspase -9 is observed as a decrease in the full-length pro-caspase and an increase in the p35 cleaved and active product

5. Prepare appropriate secondary antibody at a concentration of 1:10,000 in 1% milk in PBS-Tween. A 10 ml total volume is enough to cover a 6 × 9 cm membrane if incubated in a similar-sized tray. Incubate membranes in secondary antibody solution for 1 h at room temperature in the dark (*see* **Note 13**).
6. Wash membranes in PBS-Tween for 10 min, three times. Keep the membranes in the dark.
7. Wash membranes in ddH_2O for 10 min, three times. Keep the membranes in the dark.
8. Prepare ECL solution according to manufacturer's instruction. A 3 ml total volume is sufficient for a 6 × 9 cm membrane. Mix 1.5 ml of oxidizing agent (white bottle) and 1.5 ml enhanced luminol reagent (brown bottle). Be very careful to avoid cross-contamination between bottles!
9. Incubate membrane with ECL while shaking for 1 min.
10. Pick up the membrane carefully from the corner using tweezers and let ECL drip off before imaging.
11. Place the membrane in an imager and capture the image (*see* **Notes 14–16**). Figure 2 shows a representative blot obtained for caspase -9 showing a decrease in pro-caspase -9 and increase in cleaved caspase -9 during treatment.
12. Wash membranes in PBS-Tween for 10 min, three times.
13. Membrane can now be placed in a new primary antibody solution tube (i.e., a housekeeping gene to evaluate loading; *see* **Note 17**) or laid out to air-dry and stored at −20 °C for later use.

4 Notes

1. This cell lysis buffer works well for the western blot analysis of total proteins, but may be too harsh for the detection of phosphorylated proteins.
2. To account for pipetting error, add 20% extra volume to the master mix.
3. 1 ml of BCA reagent mix is added to each tube of standards and samples. The BCA reagent mix is a 50:1 ratio of Reagent A and Reagent B.
4. Most plate readers are equipped with a software that automatically calculates the concentration of protein samples based on the protein standards. This can be manually done in Excel by creating a scatter plot with the known protein standard concentration on the x axis and the obtained absorbance on the y axis. Add trendline to the graph by right clicking on any data point and choosing linear regression and choosing to display the equation. A sample equation is: $y = 0.0149x + 0.1457$. This equation can be used to determine protein sample concentration (x) by substituting each protein sample's absorbance for y and solving for x. Make sure the answer is multiplied by 10 to account for the 1:10 dilution in **step 4** in Subheading 3.2.
5. The described protocol is for the polymerization of a discontinuous gel system with 12% resolving gel under a stacking gel.
6. The described protocol is for the preparation of two gels.
7. To change the percentage of the resolving gel, alter the amount of water and acrylamide solution. Thus, to make 10% resolving gel, add 8 ml (instead of 9.5 ml) of acrylamide solution and 9.8 ml (instead of 8.3 ml) of ddH_2O.
8. We use 12% gel to separate proteins between 15 to 90 kDa and 10% gel to visualize proteins larger than 90 kDa.
9. To check that there are no leaks, use a squeeze bottle to add a small amount of 70% ethanol between the two glass plates and look for any leaking. Before adding the resolving gel solution into the cassette, empty the ethanol by tipping the cassette holder to one side and collect the ethanol with Kimwipe or paper towel.
10. Gels can be used the day they are made or can be stored for a day or two at 4 °C. To store gels, lay a couple pieces of paper towel on top of a plastic wrap and pour running buffer on the paper towel so that it is fully wet. Place glass cassettes onto the paper towels and wrap tightly.
11. If there are empty lanes, load 30 μl of 1× SDS sample buffer to prevent sample lanes from running unevenly.

12. We incubate 6 × 9 cm membranes in 50 ml conical tubes with a total volume of 5 ml. Place membranes inside the tube with the protein side facing inside. Tubes are loaded in a rotator in the refrigerator or cold room overnight.
13. Secondary antibody is incubated in the dark to protect the HRP conjugate from light. From this point on, all washes should be performed in the dark. We typically use opaque trays with lids or cover the membranes with aluminum foil.
14. Most commercially available imagers have an "automatic exposure" feature. We typically use this setting as a start point. In our experience with caspase -8 and caspase -9 antibodies, 5 min of exposure is sufficient to obtain an optimal resolution and minimal background.
15. Housekeeping genes such as GAPDH typically require only 30 s of exposure. In general, the length of exposure greatly depends on the samples, antibody, ECL reagent, and imager used.
16. Highly sensitive ECL reagents are commercially available. Sensitivity varies from the picogram to the attogram range.
17. If you wish to probe with another primary antibody that is close to the same molecular weight as the antibody you have already probed the membrane with, the membrane should be stripped. To strip membranes, soak with enough stripping buffer (Stripping buffer: 62.5 mM Tris–HCl, pH 6.7, 2% SDS, 100 mM β-mercaptoethanol) to completely cover and shake for 15 min at 37 °C. Stripping should be performed in a fume hood. Afterwards, wash the membrane with PBS-Tween for 1 h changing the washes every 10 min. The membrane is now ready for re-probing.

References

1. Elmore S (2007) Apoptosis: a review of programmed cell death. Toxicol Pathol 35 (4):495–516. https://doi.org/10.1080/01926230701320337
2. Taylor RC, Cullen SP, Martin SJ (2008) Apoptosis: controlled demolition at the cellular level. Nat Rev Mol Cell Biol 9(3):231–241. https://doi.org/10.1038/nrm2312
3. Degterev A, Boyce M, Yuan J (2003) A decade of caspases. Oncogene 22(53):8543–8567. https://doi.org/10.1038/sj.onc.1207107
4. Nair P, Lu M, Petersen S, Ashkenazi A (2014) Apoptosis initiation through the cell-extrinsic pathway. Methods Enzymol 544:99–128. https://doi.org/10.1016/B978-0-12-417158-9.00005-4
5. Kallenberger SM, Beaudouin J, Claus J, Fischer C, Sorger PK, Legewie S, Eils R (2014) Intra- and interdimeric caspase-8 self-cleavage controls strength and timing of CD95-induced apoptosis. Sci Signal 7(316):ra23. https://doi.org/10.1126/scisignal.2004738
6. Yuan S, Akey CW (2013) Apoptosome structure, assembly, and procaspase activation. Structure 21(4):501–515. https://doi.org/10.1016/j.str.2013.02.024
7. Twiddy D, Cain K (2007) Caspase-9 cleavage, do you need it? Biochem J 405(1):e1–e2. https://doi.org/10.1042/BJ20070617

Chapter 2

Detection of Unfolded Protein Response by Polymerase Chain Reaction

Alexander Paridon, Alexandra Fox, and Ayesha B. Alvero

Abstract

The unfolded protein response is a cellular adaptive mechanism localized in the endoplasmic reticulum. It involves three phases: the detection of increased presence of unfolded proteins as a result of cellular stressors; the execution of an adaptive cascade of events aimed at the enhancement of proper protein folding and degradation of improperly folded proteins; and finally, when stress is not alleviated, the execution of programmed cell death. The main effectors of the UPR are transcription factors involved in the upregulation of either chaperone proteins or proapoptotic proteins. Two of these transcription factors are CHOP and the spliced variant of XBP-1 (XBP1s). In this chapter, we describe a quantitative PCR method to detect the upregulation of CHOP and XBP1s mRNA during Tunicamycin-induced UPR.

Key words UPR, Real-time PCR, RT-PCR, CHOP, BiP, Spliced XBP1

1 Introduction

Eukaryotic cells rely on proper folding and assembly of both secreted and membrane proteins by the endoplasmic reticulum (ER). The unfolded protein response (UPR) acts as a homeostatic mechanism that allows the ER to adapt to environmental and physiologic stressors [1]. The UPR is composed of three transmembrane proteins housed on the outer membrane of the ER, including, inositol-requiring enzyme-1 (IRE1); PKR-like ER kinase (PERK); and activating transcription factor-6 (ATF6). Each of these proteins has a unique function that helps cells adapt to various stressors.

IRE1 is composed of two subunits, a luminal domain and a cytosolic kinase and RNase domain [2]. IRE1 undergoes oligomerization in response to acute stress and activates its RNase domain through transautophosphorylation [1]. The RNase activity of IRE1 splices out an intron from the mRNA of X-box binding protein-1 (XBP1) to produce spliced XBP1 (XBP1s). The protein product of XBP1s is a transcription factor, whose targets consist of ER protein

Ayesha B. Alvero and Gil G. Mor (eds.), *Detection of Cell Death Mechanisms: Methods and Protocols*, Methods in Molecular Biology, vol. 2255, https://doi.org/10.1007/978-1-0716-1162-3_2,

folding chaperones as well as ER-associated protein degradation factors (ERAD), which allows the ER to fold new proteins with higher fidelity as well as degrade damaged proteins by targeting them for proteasomal degradation in the cytosol [3]. In the setting of chronic stress, IRE1's RNase domain cleaves ER-targeted mRNAs through a process called regulated IRE1-dependent mRNA decay (RIDD) which can result in protective or apoptotic effects depending on the target mRNA's function [4]. IRE1's RNase can also cleave the 3′ untranslated region of BiP mRNA, resulting in stabilization of the mRNA in a process called regulated IRE1-dependent mRNA stabilization (RIDS) [7]. BiP then acts as a molecular chaperone, binding to new proteins and assisting with folding and oligomerization and transporting misfolding proteins across the ER for proteasome degradation.

Like IRE1, PERK undergoes oligomerization in the setting of ER stress and activates a kinase domain within the cytosol [5]. The result is phosphorylation of eukaryotic translation initiation factor 2 subunit alpha (eIF2α), inhibiting conversion of inactive GDP-eIF2 to active GTP-eIF2, which is required for protein translation. This inhibition of protein translation is one mechanism by which PERK can alleviate ER stress in the acute setting. In the face of prolonged stress, PERK switches from a cytoprotective to proapoptotic signaling cascade [6]. In its phosphorylated state, eIF2α-P preferentially translates mRNA encoding CHOP, ATF4, and ATF5 [7]. CHOP has been demonstrated to act as an important proapoptotic transcription factor [8]. Its targets include Bim, Puma, Trb3, and DR5 [6, 9–12]. In addition to transcription of CHOP, ATF4 promotes cell death in a number of ways. ATF4 upregulates GADD34 which acts to dephosphorylate eIF2α-P, thereby inhibiting the translational attenuation and cytoprotective effect of PERK in the setting of acute stress [13]. The resultant increase in protein translation furthers ER stress, leading to cell death [7]. ATF4 also acts on X-linked inhibitor of apoptosis (XIAP) through decreasing de novo synthesis and increasing degradation of existing XIAP [14]. By inhibiting XIAP, the PERK-eIF2α-ATF4 pathway can promote a strong proapoptotic signal by removal of caspase inhibition.

The last of three transmembrane proteins participating in UPR is ATF6, which migrates from the ER to the Golgi apparatus in response to stress [15]. ATF6 consists of a luminal and cytosolic domain, the latter of which is cleaved and released. The cytosolic domain contains a transcriptional activator, bZIP, which migrates to the nucleus and upregulates ERAD factors and ER chaperones, protecting against chronic stress [16]. Working in concert, IRE1, PERK, and ATF6 help cells adapt to ER stress by enhancing protein folding, decreasing de novo protein synthesis, and degrading irreparably damaged proteins.

UPR can be detected by analyzing cellular proteins or mRNA. This chapter discusses the detection of UPR by measuring CHOP and XBP1s mRNA by quantitative PCR (qPCR).

2 Materials and Reagents

2.1 Equipment and Disposables

1. Refrigerated centrifuge.
2. Microcentrifuge.
3. Heat block.
4. Spectrophotometer capable of measuring absorbance at 260 and 280 nm wavelengths.
5. Thermal cycler.
6. Real-time thermal cycler.
7. Tissue culture flasks.
8. 100 mm tissue culture dishes.
9. Scrapers.
10. 15 mL conical tubes.
11. 1.5 mL microcentrifuge tubes.
12. 0.2 mL PCR tubes.
13. 96-well PCR plate.
14. 96-well PCR plate adhesives.
15. Filtered pipet tips.

2.2 Cell Lines and Reagents

1. Cell of interest: in this chapter we used the SKOV3 human ovarian cancer cell line.
2. Appropriate cell growth medium.
3. 0.05% Trypsin.
4. 1× PBS.
5. UPR inducer: in this chapter we used Tunicamycin: 25 mM in DMSO.
6. Phenol and guanidine isothiocyanate solution such as Trizol.
7. Chloroform.
8. Isopropanol.
9. 75% ethanol.
10. Nuclease-free water.
11. Commercially available cDNA synthesis kit.
12. Commercially available SYBR green-based quantitative PCR kit.

13. CHOP primers (20 μM stock solution) [17]: FWD: 5′- CCT AGCTTGGCTGACAGAGG -3′;
    REV: 5′- CTGCTCCTTCTCCTTCATGC -3′.
14. XBP1s primers (20 μM stock solution) [12]: FWD: 5'-CCTG GTTGCTGAAGAGGAGG-3′;
    REV: 5′-CCATGGGGAGATGTTCTGGAG-3'.
15. GAPDH primers (20 μM stock solution): FWD: 5'- GAGT CAACGGATTTGGTCGT-3′;
    REV: 5′-GACAAGCTTCCCGTTCTCAGCC-3′.

3 Methods

3.1 Induction of UPR In Vitro

1. Seed cells in 100 mm tissue culture dish. For SKOV3, we seed 1×10^6 cells per dish in 10 mL growth media.
2. The following day, treat with a UPR inducer. In our system, we use Tunicamycin (2.5 μM × 6 h). The choice of doing a dose-response versus a time-response would depend on the study.
3. At the end of treatment, collect cells in 15 mL conical tubes by scraping and centrifuge ~500 × *g* for 5 min.
4. Discard supernatant and add 6 mL of PBS.
5. Centrifuge ~500 × *g* for 5 min. Discard supernatant and proceed to RNA extraction or freeze in −80 °C to store.

3.2 RNA Extraction Using Trizol

1. Add 1 mL Trizol to each cell pellet (pellets from 5 to 10×10^6 cells) and pipet up and down to resuspend and homogenize.
2. Incubate for 5 min.
3. Add 200 μL of chloroform.
4. Secure the cap and vigorously shake to mix.
5. Incubate for 2 min.
6. Centrifuge for 15 min at 12,000 × *g* at 4 °C.
7. After spinning, three phases become visible: a colorless upper aqueous phase, an interphase, and a red phase of phenol and chloroform. Carefully take out the top aqueous layer and transfer to new microfuge tube.
8. Add 0.5 mL isopropanol to each tube. Invert the tube to mix and incubate for 10 min on ice.
9. Centrifuge for 10 min at 12,000 × *g* at 4 °C.
10. Carefully discard the supernatant. The RNA is pelleted at the bottom.

11. Wash the RNA pellet by resuspending in 75% ethanol (*see* **Note 1**). Use a volume that is at least three times the volume of the resulting pellet.
12. Shake the tubes slightly to dislodge the pellet, then centrifuge for 5 min at 7500 × *g* at 4 °C.
13. Discard as much of the supernatant as possible and air-dry the RNA pellet for 5 min.
14. Resuspend the RNA pellet in 20 to 50 μL nuclease-free water.
15. Incubate at 55 °C for 10 min to make sure pellet is completely dissolved.
16. Quantify RNA using method of choice.

3.3 Reverse Transcription Reaction

1. Convert mRNA isolated in Subheading 3.2 to cDNA using commercially available reverse transcription kit. For this chapter, we used iScript cDNA Synthesis kit from BioRad (*see* **Note 2**).
2. Set up a master mix with the following components (*see* **Note 3**):
   4 μL 5× iScript reaction mix.
   1 μL iScript reverse transcriptase.
3. Load 5 μL master mix to each PCR tube.
4. Add enough volume of each mRNA sample equivalent to up to 1 μg of mRNA.
5. Add enough nuclease-free water to bring final volume to 20 μL.
6. Place PCR tubes in the thermal cycler and run with the following parameters: Priming step—5 min at 25 °C; Reverse transcription step—20 min at 46 °C; and Reverse transcriptase inactivation—1 min at 95 °C.
7. Dilute resulting cDNA product 1:10 by adding 180 μL nuclease-free water. Tubes may be stored at −20 °C for later use.

3.4 qPCR Using SYBR Green

1. Set up qPCR reaction master mix using commercially available qPCR kit. For this chapter, we used the SYBR green dye-based iQ SYBR green supermix from Biorad (*see* **Note 4**). Table 1 shows the volume required for each component per sample and per gene of interest (*see* **Notes 5** and **6**).
2. Load 5 μL of the master mix per well of a 96-well PCR plate.
3. Add 5 μL of cDNA (1:10 dilution from Subheading 3.3). Table 2 shows a typical plate layout for detecting CHOP and XBP1s in Tunicamycin-treated SKOV3.
4. Cover plate with adhesive PCR plate seal and make sure it is well adhered on to the plate.
5. Centrifuge PCR plate to collect contents at the bottom of the well.

Table 1
Components and volumes of qPCR master mix per sample per gene of interest

Component	Volume per sample
SYBR green mix	4.75 μL
Forward primer	0.25 μL (final concentration 500 nM)
Reverse primer	0.25 μL (final concentration 500 nM)
Diluted cDNA	5 μL

Table 2
Typical set up for a 96-well plate for 3 genes of interest, 4 treatment groups, and one cell line with each sample assayed in triplicate

Control CHOP	Control CHOP	Control CHOP	Control XBP1s	Control XBP1s	Control XBP1s	Control GAPDH	Control GAPDH	Control GAPDH
Dose 1 CHOP	Dose 1 CHOP	Dose 1 CHOP	Dose 1 XBP1s	Dose 1 XBP1s	Dose 1 XBP1s	Dose 1 GAPDH	Dose 1 GAPDH	Dose 1 GAPDH
Dose 2 CHOP	Dose 2 CHOP	Dose 2 CHOP	Dose 2 XBP1s	Dose 2 XBP1s	Dose 2 XBP1s	Dose 2 GAPDH	Dose 2 GAPDH	Dose 2 GAPDH
Dose 3 CHOP	Dose 3 CHOP	Dose 3 CHOP	Dose 3 XBP1s	Dose 3 XBP1s	Dose 3 XBP1s	Dose 3 GAPDH	Dose 3 GAPDH	Dose 3 GAPDH

6. Place in qPCR thermal cycler. We use the following parameters for the primers described in Subheading 2:
   Initial denaturation step—2 min at 95 °C.
   Continued denaturation step—15 s at 94 °C.
   Primer annealing step—30 s at 55 °C.
   DNA elongation step—60 s at 74 °C.
   (primer annealing and DNA elongation steps are repeated for 35 cycles)
   Final extension step—5 min at 74 °C.

3.5 Data Analysis

At the end of the qPCR reaction, obtain the cycle thresholds (C_t) for each well and calculate the average for each sample. Calculate the gene of interest's fold expression between samples (i.e., control vs. treated) to determine the effect of treatment (or any variable) to the gene of interest. This is referred to as calculating 2^{-ddCt} using the following equation:

delta C_t = C_t for CHOP—Ct for GAPDH

delta delta C_t = Treated delta C_t—Control delta C_t

2^{-ddCt} = raise the negative delta delta C_t to power of 2 (*see* **Note 7**)

Table 3
Sample calculation to obtain fold gene expression

	C_t for CHOP	C_t for GAPDH	Delta C_t	Delta delta C_t	2^{-ddCt}
Control	30	15	15	0	1
Treated	22	16	6	−9	512

Table 3 shows an example calculation for data obtained for the CHOP gene in Control SKOV3 cells vs. Tunicamycin treatment.

4 Notes

1. RNA can be stored in 75% ethanol for 1 week at 4 °C or 1 year at −20 °C.
2. Commercially available reverse transcription kits typically contain the following components in addition to the reverse transcriptase enzyme: Mg^+ or Mn^+ cofactor; dNTPs; RNase inhibitor; oligodT and/or random hexamer primers.
3. These volumes are for one reaction. To account for pipetting error, add 20% extra volume. Thus, for a total of 10 samples, add 48 μL of iScript reaction mix instead of 40 μL.
4. Commercially available qPCR kits typically contain the following components in addition to the DNA polymerase enzyme: dNTPs; $MgCl_2$; DNA binding dye.
5. The volumes above are for one reaction. To account for pipetting error, add 20% extra volume. Thus, for a total of 10 samples, add 60 μL of SYBR green mix instead of 50 μL.
6. Measuring each gene in triplicates is recommended.
7. C_t values are inversely proportional to the amount of mRNA copies. Thus, if the treatment upregulates the target gene's mRNA expression, the Treated sample's C_t value will be lower than the Control sample's C_t value. Thus, for this relationship, delta delta C_t value in the Treated sample is a negative number. This translates to a 2^{-ddCt} value of greater than 1 as seen in Table 3 for the 2^{-ddCt} for the Treated sample, which shows a 512-fold increase in CHOP mRNA in the Treated sample compared to the Control. Conversely, if the treatment downregulates the target gene's mRNA expression, the Treated sample's C_t value will be higher than the Control sample's C_t value. Thus, for this relationship, delta delta C_t value in the Treated sample is a positive number. This translates to a 2^{-ddCt} value of less than 1.

References

1. Hiramatsu N, Chiang W-C, Kurt TD, Sigurdson CJ, Lin JH (2015) Multiple mechanisms of unfolded protein response–induced cell death. Am J Pathol 185(7):1800–1808. https://doi.org/10.1016/j.ajpath.2015.03.009
2. Hetz C, Glimcher LH (2009) Fine-tuning of the unfolded protein response: assembling the IRE1α interactome. Mol Cell 35(5):551–561. https://doi.org/10.1016/j.molcel.2009.08.021
3. Calfon M, Zeng H, Urano F, Till JH, Hubbard SR, Harding HP, Clark SG, Ron D (2002) IRE1 couples endoplasmic reticulum load to secretory capacity by processing the XBP-1 mRNA. Nature 415(6867):92–96. https://doi.org/10.1038/415092a
4. Hollien J, Lin JH, Li H, Stevens N, Walter P, Weissman JS (2009) Regulated Ire1-dependent decay of messenger RNAs in mammalian cells. J Cell Biol 186(3):323–331. https://doi.org/10.1083/jcb.200903014
5. Harding HP, Zhang Y, Ron D (1999) Protein translation and folding are coupled by an endoplasmic-reticulum-resident kinase. Nature 397(6716):271–274. https://doi.org/10.1038/16729
6. Chang T-K, Lawrence DA, Lu M, Tan J, Harnoss JM, Marsters SA, Liu P, Sandoval W, Martin SE, Ashkenazi A (2018) Coordination between two branches of the unfolded protein response determines apoptotic cell fate. Mol Cell 71(4):629–636.e625. https://doi.org/10.1016/j.molcel.2018.06.038
7. Han J, Back SH, Hur J, Lin Y-H, Gildersleeve R, Shan J, Yuan CL, Krokowski D, Wang S, Hatzoglou M, Kilberg MS, Sartor MA, Kaufman RJ (2013) ER-stress-induced transcriptional regulation increases protein synthesis leading to cell death. Nat Cell Biol 15(5):481–490. https://doi.org/10.1038/ncb2738
8. Zinszner H, Kuroda M, Wang X, Batchvarova N, Lightfoot RT, Remotti H, Stevens JL, Ron D (1998) CHOP is implicated in programmed cell death in response to impaired function of the endoplasmic reticulum. Genes Dev 12(7):982–995. https://doi.org/10.1101/gad.12.7.982
9. Cazanave SC, Elmi NA, Akazawa Y, Bronk SF, Mott JL, Gores GJ (2010) CHOP and AP-1 cooperatively mediate PUMA expression during lipoapoptosis. Am J Physiol Gastrointest Liver Physiol 299(1):G236–G243. https://doi.org/10.1152/ajpgi.00091.2010
10. Puthalakath H, O'Reilly LA, Gunn P, Lee L, Kelly PN, Huntington ND, Hughes PD, Michalak EM, McKimm-Breschkin J, Motoyama N, Gotoh T, Akira S, Bouillet P, Strasser A (2007) ER stress triggers apoptosis by activating BH3-only protein Bim. Cell 129(7):1337–1349. https://doi.org/10.1016/j.cell.2007.04.027
11. Yamaguchi H, Wang H-G (2004) CHOP is involved in endoplasmic reticulum stress-induced apoptosis by enhancing DR5 expression in human carcinoma cells. J Biol Chem 279(44):45495–45502
12. Zhao Y, Li X, Cai M-Y, Ma K, Yang J, Zhou J, Fu W, Wei F-Z, Wang L, Xie D, Zhu W-G (2013) XBP-1u suppresses autophagy by promoting the degradation of FoxO1 in cancer cells. Cell Res 23(4):491–507. https://doi.org/10.1038/cr.2013.2
13. Novoa I, Zeng H, Harding HP, Ron D (2001) Feedback inhibition of the unfolded protein response by GADD34-mediated dephosphorylation of eIF2alpha. J Cell Biol 153(5):1011–1022. https://doi.org/10.1083/jcb.153.5.1011
14. Hiramatsu N, Messah C, Han J, LaVail MM, Kaufman RJ, Lin JH (2014) Translational and posttranslational regulation of XIAP by eIF2α and ATF4 promotes ER stress-induced cell death during the unfolded protein response. Mol Biol Cell 25(9):1411–1420. https://doi.org/10.1091/mbc.E13-11-0664
15. Haze K, Yoshida H, Yanagi H, Yura T, Mori K (1999) Mammalian transcription factor ATF6 is synthesized as a transmembrane protein and activated by proteolysis in response to endoplasmic reticulum stress. Mol Biol Cell 10(11):3787–3799. https://doi.org/10.1091/mbc.10.11.3787
16. Wu J, Rutkowski DT, Dubois M, Swathirajan J, Saunders T, Wang J, Song B, Yau GDY, Kaufman RJ (2007) ATF6α optimizes long-term endoplasmic reticulum function to protect cells from chronic stress. Dev Cell 13(3):351–364. https://doi.org/10.1016/j.devcel.2007.07.005
17. Averous J, Bruhat A, Cl J, Vr C, Thiel G, Fafournoux P (2004) Induction of CHOP expression by amino acid limitation requires both ATF4 expression and ATF2 phosphorylation. J Biol Chem 279(7):5288–5297

Chapter 3

Subcellular Fractionation to Demonstrate Activation of Intrinsic Apoptotic Pathway

Hussein Chehade, Alexandra Fox, Gil G. Mor, and Ayesha B. Alvero

Abstract

Within the cell, proteins are segregated into different organelles depending on their function and activation status. In response to stimulus, posttranslational modifications or loss of organelle membrane integrity lead to the movement of proteins from one compartment to another. This movement of proteins or protein translocation, exerts a significant effect on protein function. This is clearly demonstrated in the context of apoptosis wherein the cytoplasmic translocation of the mitochondrial resident protein, cytochrome C, initiates the activation of the intrinsic arm of the apoptotic pathway. Experimentally, protein translocation can be demonstrated by subcellular fractionation and subsequent western blot analysis of the isolated fractions. This chapter describes the step-by-step procedure in obtaining mitochondrial and cytoplasmic fractions from cell pellets and determining their purity and integrity.

Key words Subcellular fractionation, Protein translocation, Mitochondria, Cytochrome C, Apoptosome

1 Introduction

After translation, proteins are continually modified by processes such as phosphorylation, glycosylation, lipidation, and ubiquitination, to name a few [1]. One possible outcome of these modifications is the determination of the protein's location within the cell [2]. The location of proteins dictates their ability to access binding partners and substrates and therefore contributes to the regulation of protein function.

Apoptosis is a signaling cascade, which is initiated by cellular stress and culminates in the activation of caspases [3]. Caspases are proteases capable of cleaving cellular structures including DNA and are the main effectors of apoptotic programmed cell death [4]. Apoptosis is an example of a biological process that relies on protein translocation for its initiation. The intrinsic arm of the apoptotic pathway is initiated by the loss of mitochondrial membrane integrity, leading to the cytoplasmic translocation of the mitochondrial

Ayesha B. Alvero and Gil G. Mor (eds.), *Detection of Cell Death Mechanisms: Methods and Protocols*, Methods in Molecular Biology, vol. 2255, https://doi.org/10.1007/978-1-0716-1162-3_3,

resident protein, cytochrome C [5]. While in the mitochondria, cytochrome C is an integral component of the electron transport chain and therefore important in the maintenance of cellular bioenergetics. Upon translocation to the cytoplasm, cytochrome C becomes an initiator of cell death since its movement to the cytoplasm allows cytochrome C to bind Apaf-1, which leads to the activation of caspase 9 and the propagation of the intrinsic apoptotic cascade [5]. Similarly, during apoptosis, the nuclear translocation of the antiapoptotic protein X-linked inhibitor of apoptosis protein (XIAP) allows the full induction of the apoptotic cascade. In stress-free conditions, XIAP is mainly localized in the cytoplasm, but the upregulation of XAF-1 during apoptosis leads to its nuclear co-localization with XIAP [6] and ensures the full activation of caspases.

In this chapter, we describe the methods to obtain mitochondrial and cytoplasmic fractions from cell pellets undergoing apoptosis. The occurrence of apoptosis is demonstrated by the translocation of cytochrome C from the mitochondria to the cytoplasm. We also describe how to determine the purity and integrity of the fractions obtained. After cellular fractionation, the analysis and quantification of proteins are determined by Western Blot analysis.

2 Materials

2.1 Equipment and Disposables

1. Refrigerated microcentrifuge.
2. Vortex.
3. Western blot apparatus.
4. Microcentrifuge tubes.
5. Pipet tips.
6. 25-gauge needle.
7. 1 ml syringe.
8. Cover slips.

2.2 Reagents

1. Freshly prepared cell pellets for fractionation (*see* **Notes 1** and **2**).
2. 1× PBS: 137 mM NaCl, 2.7 mM KCl, 10 mM Na_2HPO_4, 1.8 mM KH_2PO_4.
3. Fractionation buffer: 20 mM HEPES, 10 mM KCl, 2 mM $MgCl_2$, 1 mM EDTA, 1 mM EGTA, 1 mM DTT.
4. Organelle lysis buffer: 1% NP40, 0.1% Sodium dodecyl sulfate (SDS) in 1× PBS.
5. Commercially available protease inhibitor cocktail (PIC).

6. Western blot equipment and reagents as described in Chapter 1 of this book.
7. Antibodies to determine integrity of fractions (i.e., Cox-IV assures lack of mitochondrial contamination in the cytoplasmic fraction).

3 Methods

The methods described below provide a step-by-step procedure to obtain mitochondrial and cytoplasmic fractions and validate their purity (*see* **Notes 3** and **4**). It is a modified protocol based on multiple publications, online protocols, and our group's experience [7, 8]. Figure 1 shows the general steps in the protocol. After fractionation, the samples are further analyzed by western blot. The process of western blot is not described in this chapter, but is discussed fully in Chapter 1 of this book.

1. Keep all buffers on ice until ready to use.
2. Add appropriate amount of PIC to fractionation buffer and organelle lysis buffer (according to manufacturer's instructions).
3. Resuspend cell pellets in 200 μl fractionation buffer and vortex. Solution should be cloudy, but there should be no precipitates. If precipitates are observed, add another 100 μl of fractionation buffer and vortex. Keep adding fractionation buffer until there are no precipitates observed.
4. Incubate on ice for 20 min.
5. Pass the cell suspension at least 30 times through a 25-gauge needle fitted onto a 1 ml syringe. This process will shear the cells and break the cell membrane (*see* **Note 5** and Fig. 2).
6. Centrifuge the samples at 750 × *g* for 10 min at 4 °C.
7. Collect the supernatant into a fresh microfuge tube and centrifuge at 10,000 × *g* for 30 min at 4 °C. Discard the pellet (*see* **Note 6**).
8. Collect the supernatant into a fresh microfuge tube: this is the cytoplasmic fraction.
9. Resuspend the pellet in 50 μl organelle lysis buffer with added PIC: this is the mitochondrial fraction.
10. Proceed to protein quantitation and western blot analysis. Figure 3 shows typical western blot results analyzing the cytoplasmic fractions for cytochrome C and Cox-IV.

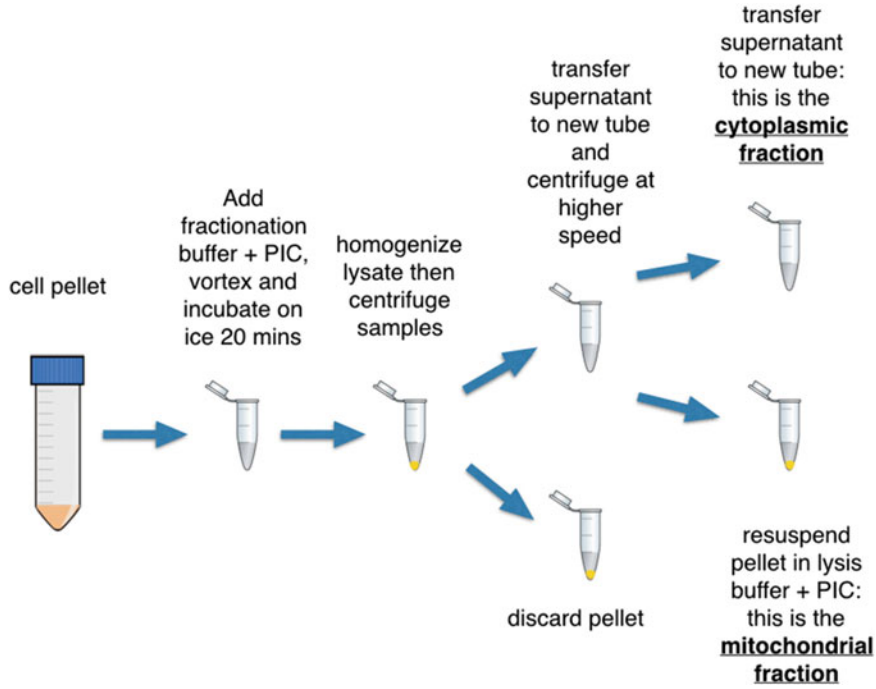

Fig. 1 Schematic diagram of the subcellular fractionation protocol

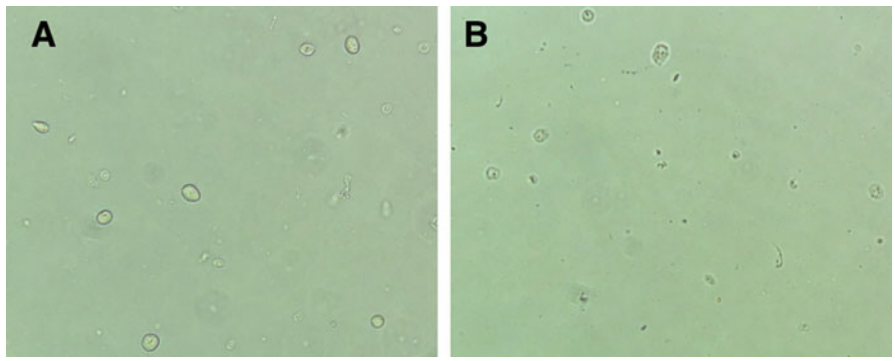

Fig. 2 Microscopic images showing cell morphology before (**a**) and after (**b**) Step 5 wherein cell suspension is passed through a 25-gauge needle. Note the halo around cells in (**a**), which are absent in (**b**)

4 Notes

1. A reliable positive control for observing cytochrome C movement from the mitochondria to the cytoplasm is A2780 human ovarian cancer cells treated with 0.02 μM Paclitaxel for 24 h.
2. We strongly recommend that, if using adherent cells, cultures should be collected by trypsinization since scraping can shear the cells. We also recommend using freshly pelleted cells. Frozen pellets and scraping can limit the reproducibility of results.

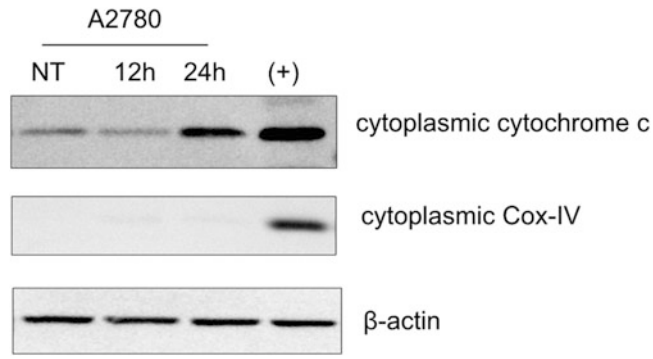

Fig. 3 A2780 human ovarian cancer cells were treated for 12 h and 24 h with 0.02 μM Paclitaxel. After subcellular fractionation, the cytoplasmic fraction is probed for cytochrome C and Cox-IV. Increase in cytoplasmic levels of cytochrome C demonstrates loss of mitochondrial membrane integrity. Absence of Cox-IV in the cytoplasmic fraction demonstrates integrity of cytoplasmic fraction and absence of mitochondrial contamination. (+) positive control, whole cell lysate

3. Volumes are for cell pellets with 1 to 5 × 10^6 pelleted cells.
4. After fractionation, western blot is used to detect protein translocation and integrity of fractions. Cox-IV assures lack of mitochondrial contamination in cytoplasmic fractions.
5. To check for efficiency of cell lysis, pipet 10 μl onto a cover slip and observe under the microscope. Intact cells appear with a shiny halo (Fig. 2). Proceed to the next step only if less than 20% of the cells have intact halo, otherwise perform an additional 20 passes.
6. The supernatant at this step contains both the cytoplasmic and mitochondrial fractions. The pellet contains the nuclear fraction. We have had luck using the nuclear fraction obtained from this step in detecting the movement of AIF from the mitochondria to the nucleus during apoptosis. Nuclear pellets can be resuspended in about 50 μl of organelle lysis buffer with added PIC.

References

1. Bradshaw RA, Medzihradszky KF, Chalkley RJ (2010) Protein PTMs: post-translational modifications or pesky trouble makers? J Mass Spectrom 45(10):1095–1097. https://doi.org/10.1002/jms.1786
2. Sirover MA (2012) Subcellular dynamics of multifunctional protein regulation: mechanisms of GAPDH intracellular translocation. J Cell Biochem 113(7):2193–2200. https://doi.org/10.1002/jcb.24113
3. Elmore S (2007) Apoptosis: a review of programmed cell death. Toxicol Pathol 35 (4):495–516. https://doi.org/10.1080/01926230701320337
4. Salvesen GS (2002) Caspases and apoptosis. Essays Biochem 38:9–19. https://doi.org/10.1042/bse0380009
5. Garrido C, Galluzzi L, Brunet M, Puig PE, Didelot C, Kroemer G (2006) Mechanisms of cytochrome c release from mitochondria. Cell

Death Differ 13(9):1423–1433. https://doi.org/10.1038/sj.cdd.4401950

6. Russell JC, Whiting H, Szuflita N, Hossain MA (2008) Nuclear translocation of X-linked inhibitor of apoptosis (XIAP) determines cell fate after hypoxia ischemia in neonatal brain. J Neurochem 106(3):1357–1370. https://doi.org/10.1111/j.1471-4159.2008.05482.x
7. Baghirova S, Hughes BG, Hendzel MJ, Schulz R (2015) Sequential fractionation and isolation of subcellular proteins from tissue or cultured cells. MethodsX 2:440–445. https://doi.org/10.1016/j.mex.2015.11.001
8. Holden P, Horton WA (2009) Crude subcellular fractionation of cultured mammalian cell lines. BMC Res Notes 2:243. https://doi.org/10.1186/1756-0500-2-243

Chapter 4

A Triple-Parameter-Based Laboratory-Friendly Fluorescence Imaging to Identify Apoptosis in Live Cells

Pradip De, Jennifer Carlson Aske, and Nandini Dey

Abstract

Cellular signals to resist apoptosis have been attributed as one of the mechanisms of tumorigenesis. Hence, apoptosis is a cardinal target for drug development in cancers, and several antitumor drugs have been designed to induce apoptosis in tumor cells. Recently, venetoclax, a Bcl2 inhibitor that induces apoptosis, has been approved by the FDA for the treatment of CLL and SLL patients. Proapoptotic antitumor drugs have been traditionally developed and tested, targeting apoptosis in tumor cells. The mechanism of such drug actions has been functionally connected to the mechanism of apoptosis. The identification of apoptosis in a tumor cell takes into account different characteristics in several steps of apoptosis. Thus, it is understandable that modes of identification of apoptosis observed in tumor cells in a laboratory have also been tuned to different characteristics in several parameters of apoptosis. Here, we present a detailed methodology for a triple-parameter-based co-fluorescence imaging to identify apoptosis in live tumor cells. The procedure involves co-fluorescence staining specific for three cardinal features of apoptosis in live cells. The procedure is simple, time-sensitive, and can be performed successfully in a laboratory-friendly manner.

Key words Apoptosis, Triple-parameter, Laboratory-Friendly, Fluorescence imaging, Live cells

1 Introduction

Oncogenesis is initiated either from within (genomic alteration due to external cues or inherited abnormality/predisposition) or from outside (environmental cues) the cell. Cells respond to an oncogenic signal (oncogenic stress) by altering its signaling circuits. Oncogenesis is an inevitable outcome of cellular response to accommodate oncogenic changes. The signal can be alterations/mutations that are inherited, or induced by environmental factors, or result from DNA replication errors [1]. A cell cannot distinguish between a physiologic signal and a pathologic signal. To a cell, all signals are to be either propagated or blocked. Tumorigenesis occurs when an oncogenic signal is either propagated through the built-in circuitry or when a newly occurred alteration happens in

Ayesha B. Alvero and Gil G. Mor (eds.), *Detection of Cell Death Mechanisms: Methods and Protocols*, Methods in Molecular Biology, vol. 2255, https://doi.org/10.1007/978-1-0716-1162-3_4,

that circuitry in the cell. Tumorigenesis can also occur when an oncogenic signal is not blocked at the cellular level due to the presence of an active oncogene or an absence of a tumor suppressor gene or an alteration of its epigenetic machinery. In a cell that is destined to follow an oncogenic fate, only one or a few alterations take place, while the rest of the signaling circuit remains functional as before.

1.1 Oncogenesis, Cellular Stress, and Apoptosis

During oncogenesis, cells of tissue do not have the intelligence to register or respond to the physiological well-being of the tissue/organ/system/body at large. There exists no mode of identification of the deregulated signal or any feedback system pertaining to the checks and balances of the cell-cycle (for the well-being of the body). So an oncologically transformed cell with its otherwise intact signaling circuitry basically gives in to the oncogenic alteration(s) and increases its cell-cycle either unabated with decreased apoptotic signal or otherwise. To accommodate an oncogenically driven higher rate of cell-cycle, a transforming cell adapts to (1) an altered state of glycolysis-dominated glucose metabolism, (2) higher oxygen consumption-mediated hypoxic stress response, (3) load of DNA damage repair, and (4) ensuing oxidative stress. There occurs new homeostasis within a transformed cell as a result of the cell's relentless effort to adapt/respond to the oncogenic signal. The attempt to adapt/respond to the oncogenic signal causes adaptation-induced stress within transformed cells. The outcome of a cell's struggle to accommodate an oncogenic signal can be messy. A cell in the course of responding to an oncogenic signal often exhibits various stress, including metabolic stress, oxidative stress, genotoxic stress, DNA replication stress [2], and hypoxic stress.

When a cell(s) within a tissue commits to an oncogenic stimulus, it initiates several events towards altered tissue homeostasis, which ultimately becomes clinically recognizable. Tissue homeostasis is managed by (1) proliferation and growth of cells of the tissue and (2) cell death in the tissue [3]. Physiologic cell death in a homeostatic state is mediated through highly regulated apoptotic pathways that involve oxidative stress regulation [4]. The cell's commitment to an oncogenic stimulus tilts the balance towards proliferation and growth of cells either by increasing the proliferation and growth of most cells of the tissue and/or diminishing cell death by reprogramming the regulatory pathways for apoptosis. Reprogramming of the regulatory pathways for apoptosis can occur via several modes, including the inhibition of apoptosis (IAP) protein family [5, 6]. Thus, one of the hallmarks of cancers is the intrinsic or acquired resistance to apoptosis, and evasion of apoptosis contributes to tumor formation and progression, metastasis as well as acquired resistance to various treatment modules. Since an adaptive response to cellular stress accompanies the

process of oncogenic transformation, its relationship with apoptosis has been sought. Studies have proven that cellular stress response in cancer leads to the evasion of apoptosis [7]. A functional relationship between cytotoxic drug-mediated anticancer treatment and apoptotic cell death via key elements of the cellular stress response has been demonstrated [8].

1.2 Apoptosis in Tumor Cells

Apoptosis is a fact of life for tumor cells. Loss or inhibition of apoptotic signals is the ultimate safeguard of a tumor cell against all its proliferation/survival-induced stress. Thus, the mechanisms of apoptosis, intrinsic and extrinsic [9], have been well-understood for the management of the disease using inhibition of apoptosis as a tool to treat various cancers [10]. Several decades of study have helped us to understand the (1) mechanism of apoptosis, (2) role of apoptosis in the development of cancer, its progression, and resistance to treatment, and (3) role of apoptosis to test various target therapies [11–14]. Apoptosis, which can be induced in multiple ways, activates a family of caspases enzymes that disrupt DNA, organelles, and cytoskeleton. Since the suicidal-phenomenon is initiated by cells, the process in its entirety is well-regulated in multiple well-defined steps. Finally, activated caspases recruit scavenging cells to engulf the dying cell's remains. In addition to apoptosis, studies have demonstrated many more types of regulated forms of cell death, including ferroptosis, necroptosis, and entosis. Apoptosis is uniquely integrated into oncogenesis. Studies have shown that, even after committing to the suicidal process of apoptosis, cells may recover via a process called anastasis [15]. However, following anastasis during late apoptosis, the surviving cells can be susceptible to major defects like major chromosomal scars and other genetic deficiencies leading to an oncogenic transformation [16]. The importance of apoptosis compelled the scientific community to device the mode of detection of apoptosis, qualitatively as well as quantitatively, to unveil the different anticancer studies [17].

Inhibition or loss of apoptosis is a trait that all tumor cells share. Tumor cells have survival advantages at the pathological level. Proliferative advantage and loss of programmed cell death jointly empower the tumor to evolve to higher stages and metastatic states. Since the loss of apoptosis is one of the cardinal features of a neoplastic transformation, the induction of apoptosis is one of the items in the "wish list" when designing and developing an anticancer drug. Thus, identification of apoptosis based on its key features is extensively worked out in tumor cells. The literature describes the spectrum of cytomorphological features of apoptosis and the sequence of cellular signaling events of apoptosis, which have been the building blocks of developing methods and protocols to detect apoptosis reported so far. Here, we present laboratory-friendly methods and protocols to identify apoptosis based on the

three critical characteristic features of apoptosis simultaneously in live cells. The features are (1) enzymatic activation of Caspase-3 (cleavage of caspase-3/7, a rate-limiting step), (2) the flipping of phosphatidylserine on the outer surface of the plasma membrane for the recognition of phagocytic cells, and (3) functional state of mitochondria.

2 Materials

2.1 Equipment and Disposables

1. Cell culture hood (biosafety cabinet).
2. CO_2 incubator.
3. Fluorescent microscope with camera.
4. Tissue culture plates and flasks.
5. Coverslips.
6. Conical tubes and Microfuge tubes.
7. Pipets and pipet tips.

2.2 Reagents and Cell Lines

1. Cell line of choice: in this chapter, we used human breast cancer cell line, SUM149, and human ovarian cancer cell line, OVK18.
2. Appropriate cell culture media.
3. 0.25% trypsin.
4. Inducer of apoptosis: in this chapter we used Paclitaxel: 2.5 mM in DMSO; Carboplatin: 1 μM in saline; Olaparib: 2.5 μM in DMSO; AZD5363: 2 μM in DMSO; Trametinib: 500 nM in DMSO.
5. Commercially available Ca^{2+}/Mg^{2+} free 1× Phosphate buffer saline (PBS).
6. Commercially available 5× Binding Buffer: in this chapter we used 5× Binding Buffer from Biotium.
7. Fluorescent stain for mitochondrial membrane potential: in this chapter we used MitoViewBlue.
8. Fluorescent substrate for caspase-3: in this chapter we used NucView® 488 Caspase-3.
9. Fluorescent stain for phosphatidyl serin: in this chapter we used CF®594 Annexin V.
10. Caspase-3 inhibitor Ac-DEVD-CHO: 10 μM.

3 Methods

All experiments are to be performed in a laboratory setting (BSL2). A Good Laboratory Practice (GLP) is to be followed at all stages of the activity. Cell lines should be routinely tested for mycoplasma.

Figure 1a shows the layout of the general plan for discovery and validation experiments. Upon the demonstration of apoptotic events in the discovery set, results can be validated using the other assays listed under the validation set. Table 1 lists the reagents used in this chapter, their final assay concentrations, and their purpose in the triple-co-fluorescence staining in live cells. Table 2 lists the details of the reagents, their concentrations, and their uses

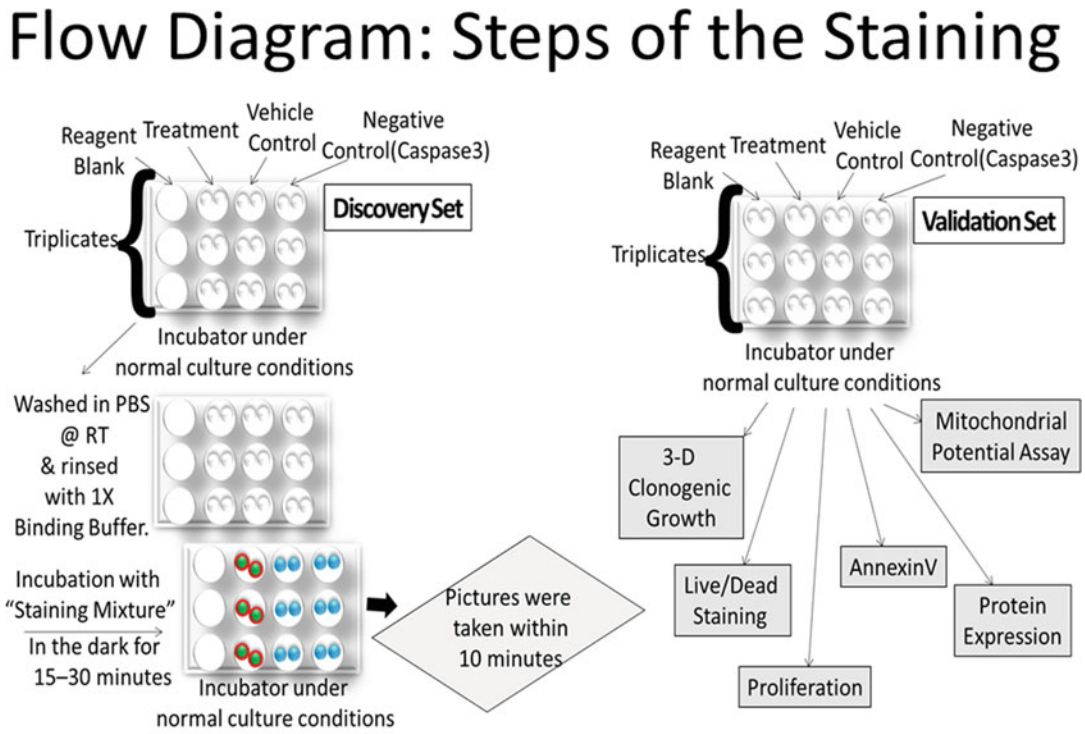

1

Fig. 1 Flow Diagram presenting steps of the triple-fluorescence staining of live cells: For the discovery set, different cell lines were plated on 12 well plates and culture under different conditions; Reagent Blank, Treatment, Vehicle Control, and Negative Control (treatment with a competitive inhibitor for caspase-3/7). Cells are washed in PBS at RT and rinsed with freshly made 1× Binding Buffer. The picture was taken within 10 min following the incubation of the cells in the "Staining Mixture" in the dark for 15–30 min under usual conditions of cell culture. For the validation set, a parallel set of experiments was set up to test the apoptosis by (1) 3-D clonogenic growth, (2) live-dead assay by fluorescence microscopy, (3) real-time confluence assay by Incucyte, (4) annexin V assay by flow cytometry, (5) expression of apoptosis-related signaling proteins by Western blot, and (6) mitochondrial potential assay

Table 1
Reagents Used for the Triple-co-fluorescence staining in Live Cells

Item	Starting concentration	For detection of:	Remarks
MitoView Blue	50 nM	Mitochondrial membrane potential	Visible at the blue filter
NucView® 488 Caspase-3	5 μM	Caspase-3 activity	Visible at FITC filter
CF594 Annexin V	5 μl of 50 μg/ml stock	Flipped phosphatidyl serine	Visible at TRITC filter
Caspase-3 Inhibitor Ac-DEVD-CHO	10 μM	Negative control	Used during standardization

in the respective instruments for the validation of the results obtained from the triple-co-fluorescence staining assay.

1. Plate cells on coverslips in a 12-well plate and induce apoptosis using an agent of choice (*see* **Note 1**).
2. On the day of the assay, prepare fresh 1× Binding Buffer by diluting 5× Binding Buffer with ultrapure water (*see* **Note 2**).
3. Prepare the MitoViewBlue stock solution of 200 μM in DMSO and store in a desiccator at −20 °C in single-use aliquots in light-protected storage conditions.
4. Prepare the NucView488 Caspase-3 substrate stock solution of 0.2 mM in DMSO.
5. Prepare the "staining solution" in a final volume of 1 ml/well in 1× Binding Buffer by adding the following components: MitoViewBlue to a final concentration of 50 nM; NucView488 Caspase-3 to a final concentration of 5 μM; 5 μl of 50 μg/ml stock solution of CF594 AnnexinV. Keep staining solution at room temperature (*see* **Note 3**).
6. Carefully wash control and apoptotic cells with sterile PBS. Repeat PBS washes twice.
7. Carefully wash cells with 1× Binding Buffer once.
8. Incubate cells with the "staining solution" for 30 min. Place the cells back in the tissue culture incubator. Make sure to minimize light exposure during the staining procedure.
9. At the end of the incubation period, obtain images within 10 min using a fluorescence microscope (*see* **Notes 4–10**).

Representative images are shown in Figs. 2, 3, 4, 5 and 6 for both control apoptotic cultures.

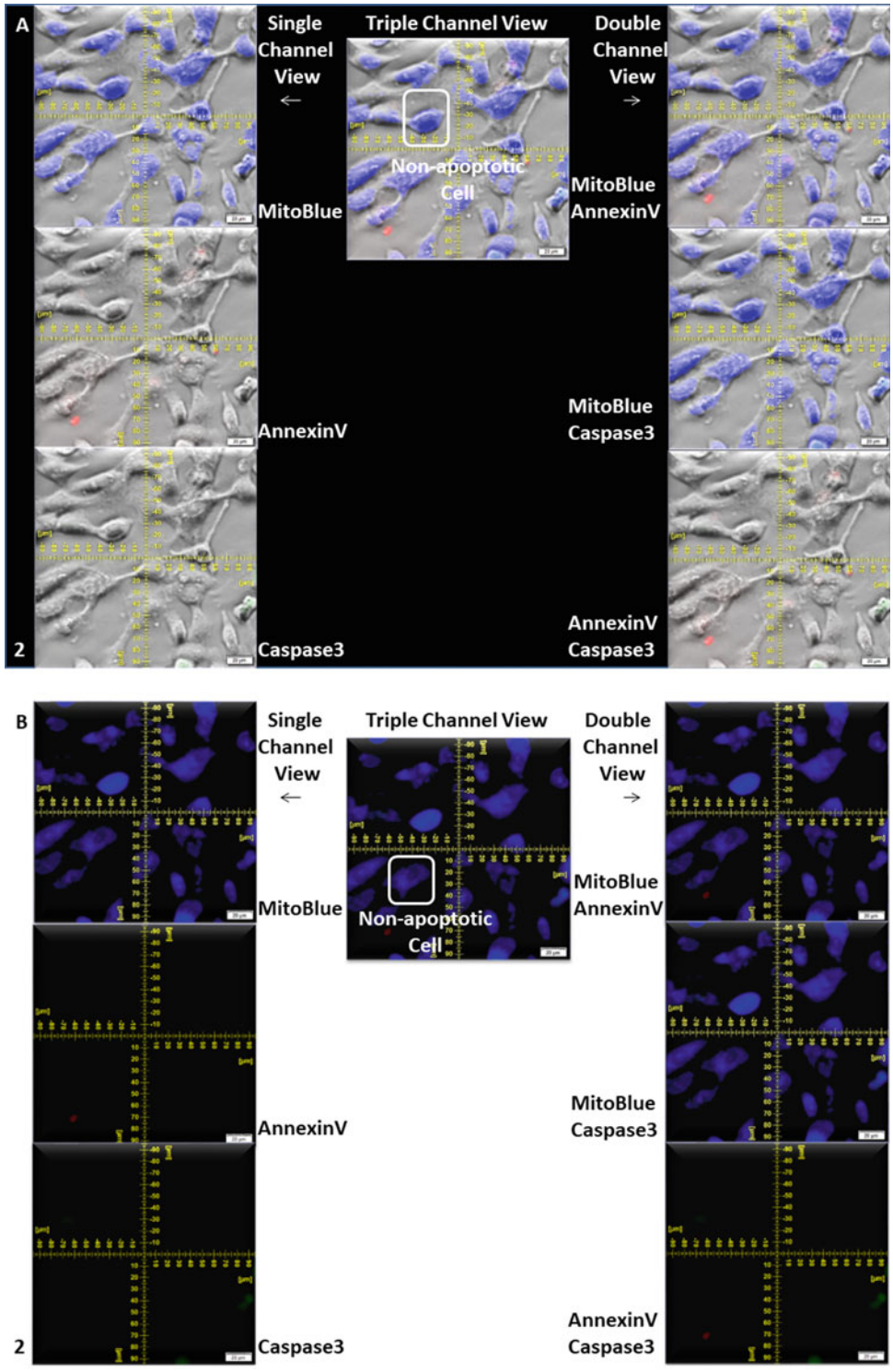

Fig. 2 Triple co-fluorescence of live SUM149 breast cancer cells under the non-treated condition: Single-channel (left panel), double channel merge (right panel), and triple channel merge (middle panel) of pictures with an overlay of the bright-field pictures (of the same field) of live (in culture) SUM149 breast cancer cell line stained by triple co-fluorescence under the non-treated condition for 24 h (**a**). Single-channel (left panel), double channel merge (right panel), and triple channel merge (middle panel) of pictures of live SUM149 breast cancer cell line stained by triple co-fluorescence under the non-treated condition for 24 h (**b**). Picture shows AnnexinV-/Caspase-3-/MitoBlue+ non-apoptotic SUM149 cells

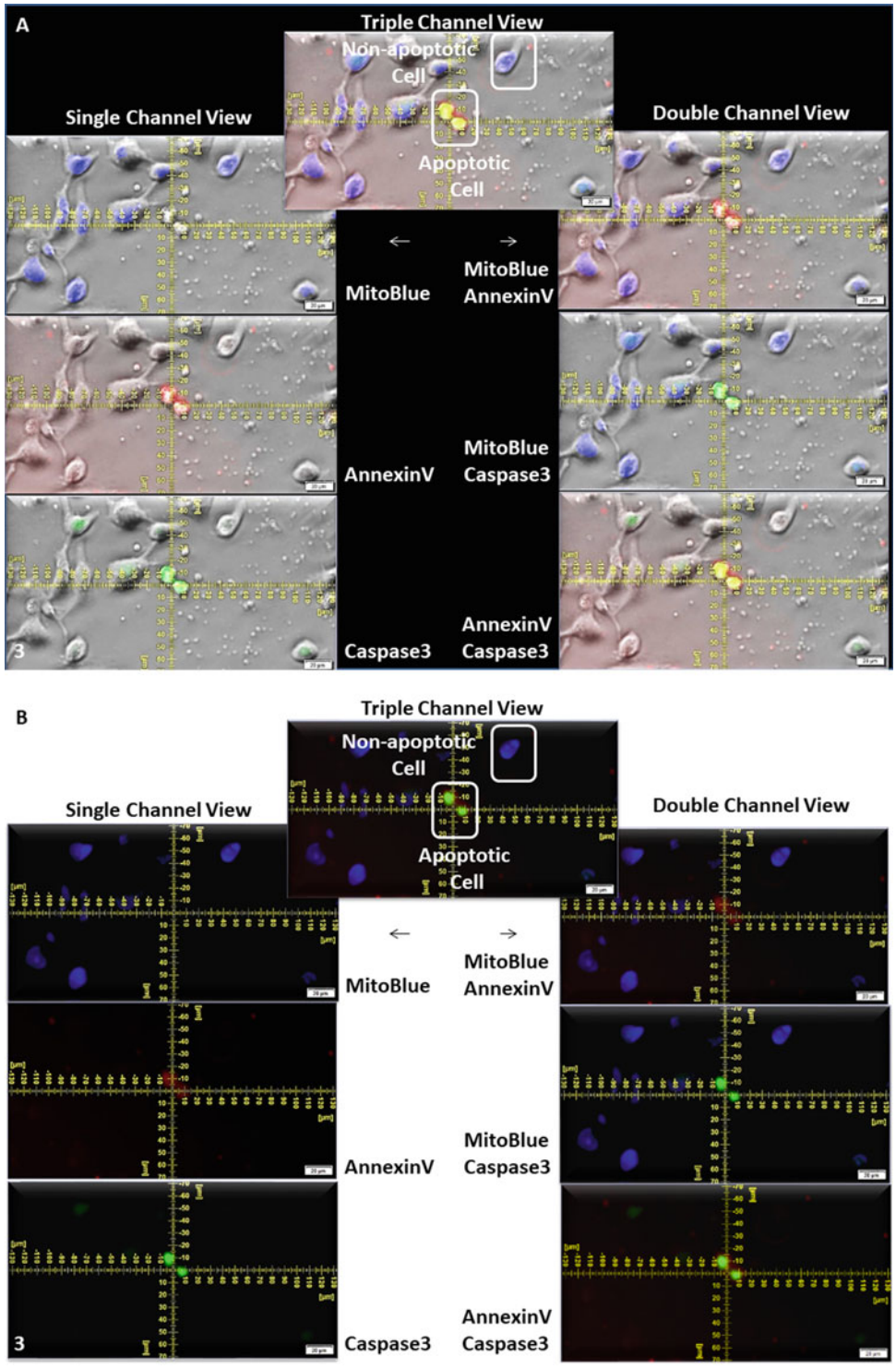

Fig. 3 Triple co-fluorescence of live SUM149 breast cancer cells under the vehicle-treated condition: Single-channel (left panel), double channel merge (right panel), and triple channel merge (middle panel) of pictures with an overlay of the bright-field pictures (of the same field) of live SUM149 breast cancer cell line stained by triple co-fluorescence under the vehicle-treated condition for 24 h (**a**). Single-channel (left panel), double channel merge (right panel), and triple channel merge (middle panel) of pictures of live SUM149 breast cancer cell line stained by triple co-fluorescence under the vehicle-treated condition for 24 h (**b**). Picture shows AnnexinV+/Caspase-3+/MitoBlue- apoptotic SUM149 cells and AnnexinV-/Caspase-3-/MitoBlue+ non-apoptotic SUM149 cells

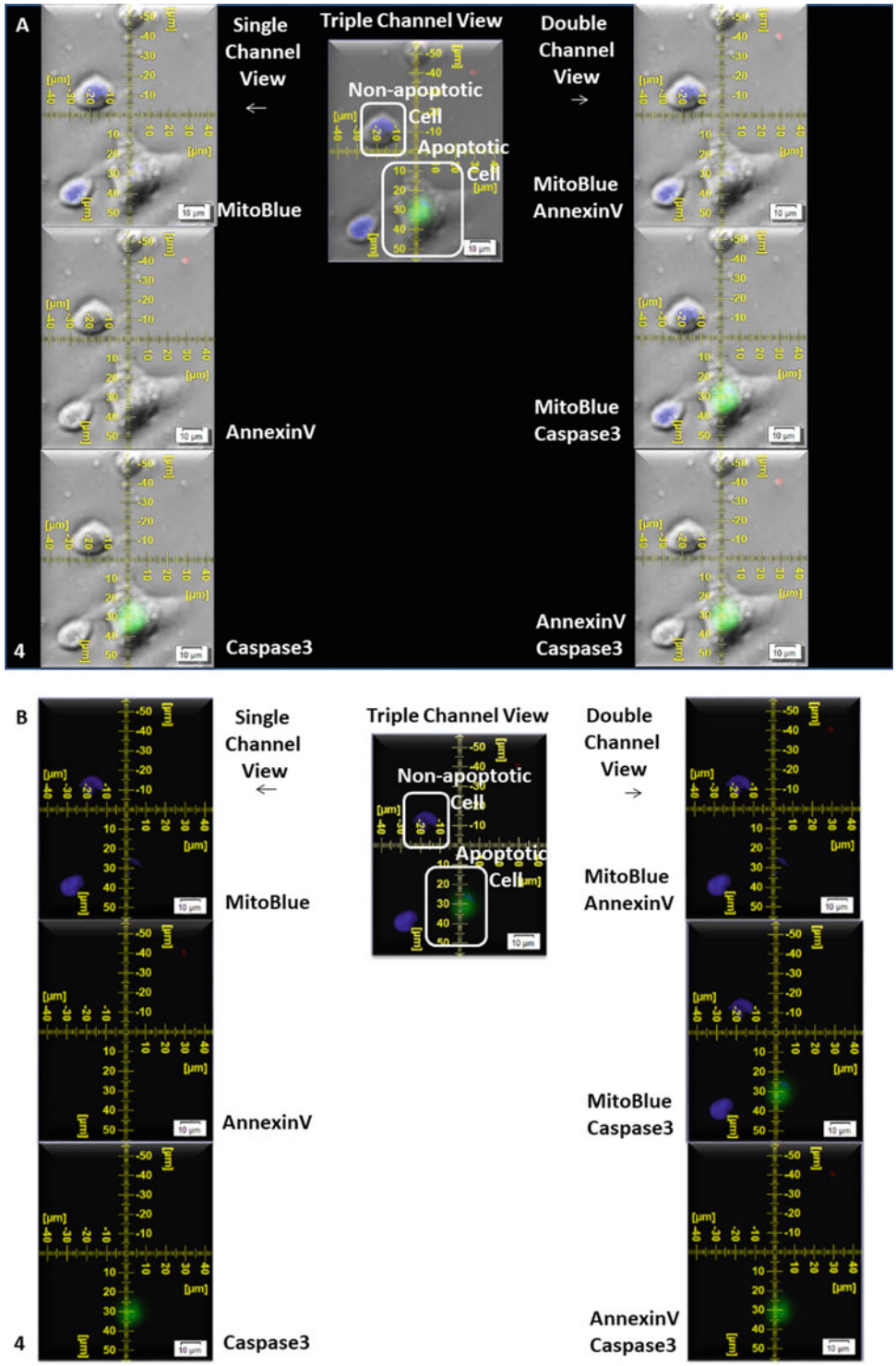

Fig. 4 Triple co-fluorescence of live SUM149 breast cancer cells under condition of treatment with a competitive inhibitor for caspase-3/7 (Ac-DEVD-CHO on the caspase-3/7): Single-channel (left panel), double channel merge (right panel), and triple channel merge (middle panel) of pictures with an overlay of the bright-field pictures (of the same field) of live SUM149 breast cancer cell line stained by triple co-fluorescence under

Validation Assays: After determination of apoptosis using the triple co-fluorescence staining, results can be validated by assays listed in Table 2. These assays include: (1) expression of signaling proteins, markers of apoptosis, and proliferation in cells; (2) microscopic identification of Live-Dead cells; (3) flow cytometric analyses of apoptosis and mitochondrial depolarization assay; (4) real-time confluency assay by time-lapse phase-contrast imaging; and (5) 3-dimensional On-Top clonogenic growth. The detailed description of various assays used for the validation is presented elsewhere [18–20].

4 Notes

1. *Applicability of the Assay*: Although we have developed and standardized the assay for the purpose of testing the effect of combination(s) of various anticancer drugs in cancer cell lines of different organ types, the assay can be applied to cells of various origins in the context of physiological and pathological settings in basic as well as translational research. Similarly, not only is the test suitable for the testing of various drugs, but also for the testing of any physiological and pathological agents/conditions related to the induction or inhibition of apoptosis.
2. *Binding Buffer*: Binding Buffer (1×) should be made fresh every time before the assay.
3. To test the specificity of the caspase-3 enzymatic activity, we recommend the use of Ac-DEVD-CHO at 10 μM, as competitive inhibitor for caspase-3/7. It should be noted that the inhibition of caspase-3 is used only for the purpose of testing the staining and not for testing the effect of drugs.
4. Do not fix cells. Do not use any counterstain.
5. As the staining involves an enzymatic reaction/kinetics (continuous process), carefully monitor the time of exposure to the light source (Microscope) during the acquisition of the picture.
6. *Visualization of the staining*: It is important that the visualization is carried out within 10 min of the ending of the incubation time without any wash. We have observed that a 10 min window has minimum adverse effect on cells, considering the

Fig. 4 (continued) the condition of treatment with a competitive inhibitor for caspase-3/7 (Ac-DEVD-CHO on the caspase-3/7) (**a**). Single-channel (left panel), double channel merge (right panel), and triple channel merge (middle panel) of pictures of live SUM149 breast cancer cell line stained by triple co-fluorescence under the condition of treatment with a competitive inhibitor for caspase-3/7 (Ac-DEVD-CHO on the caspase-3/7) (**b**). Picture shows AnnexinV+/Caspase-3+/MitoBlue- apoptotic SUM149 cells and AnnexinV-/Caspase-3-/MitoBlue+ non-apoptotic SUM149 cells

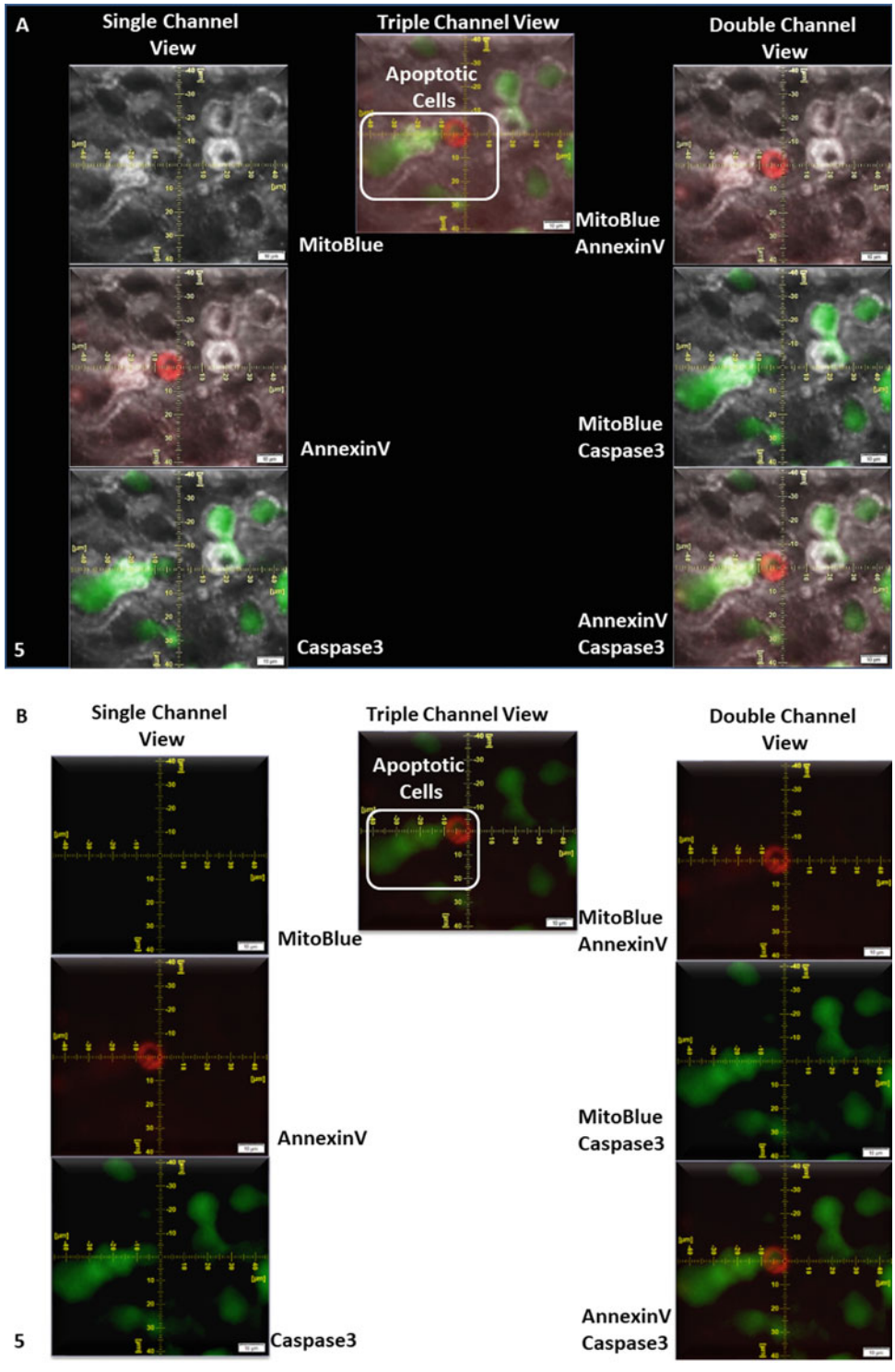

Fig. 5 Triple co-fluorescence of live SUM149 breast cancer cells under condition of treatment with Carboplatin + Olaparib + AZD5363: Single-channel (left panel), double channel merge (right panel), and triple channel merge (middle panel) of pictures with an overlay of the bright-field pictures (of the same field) of live SUM149 breast cancer cell line stained by triple co-fluorescence under the condition of treatment with Carboplatin + Olaparib + AZD5363 for 24 h (**a**). Single-channel (left panel), double channel merge (right panel), and triple channel merge (middle panel) of pictures of live SUM149 breast cancer cell line stained by triple co-fluorescence under the condition of treatment with Carboplatin + Olaparib + AZD5363 for 24 h (**b**). Picture shows AnnexinV+/Caspase-3+/MitoBlue- apoptotic SUM149 cells

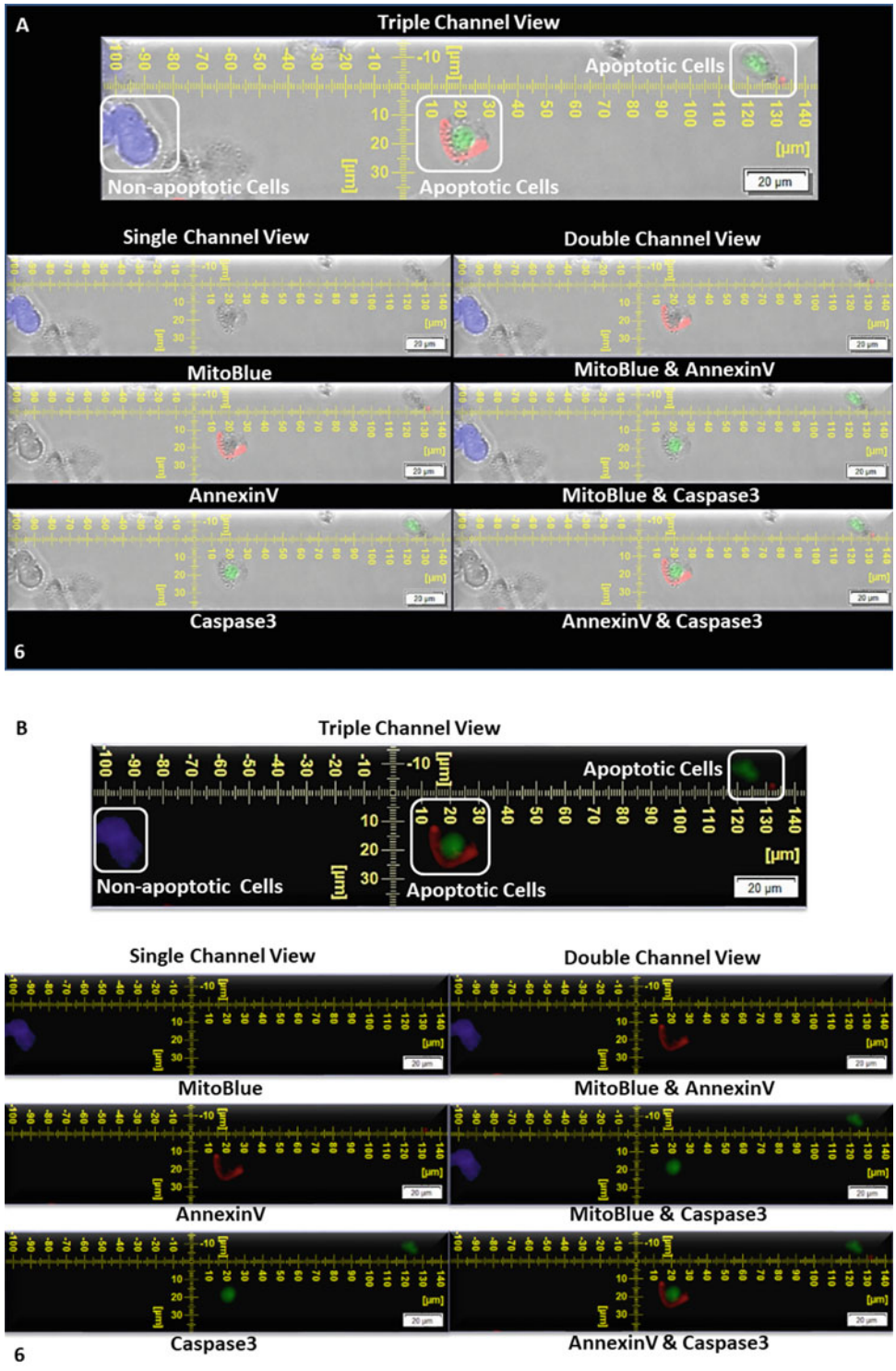

Fig. 6 Triple co-fluorescence of live OVK18 ovarian cancer cells under condition of treatment with Trametinib + Paclitaxel: Single-channel (left panel), double channel merge (right panel), and triple channel merge (middle panel) of pictures with an overlay of the bright-field pictures (of the same field) of live OVK18 ovarian cancer

fact that the cell is live in culture conditions. Activation of Caspase-3 is important for apoptosis, and the staining involves the substrate for the enzyme. It should also be understood that the incubation should be carried out in the dark.

7. *Co-localization between FITC and TRITC and blue channels*: It is strongly suggested that during the initial period of standardization, a co-localization between fluorescence channels should be tested using the programs built in to the microscope software for the imaging of the pictures. This will add confidence to the assay as it provides the "Overlap Coefficient." We have observed that in some cells NucView488 Caspase-3 and CF594 AnnexinV overlap, while in some, it does not. However, in no cases, MitoBlue stain should overlap with NucView488 Caspase-3 and CF594 AnnexinV staining.
8. The treatment of cells with combinations of anticancer drug markedly abrogated MitoBlue staining and parallelly increased AnnexinV+/Caspase-3+ stains. The extent of the staining is a function of the cell line, drug combination, and time as represented in Fig. 5. We have observed three types of apoptotic cells by the triple fluorescent staining: (1) Caspase-3+ cells (nuclear), (2) AnnexinV+ cells (membranous), and (3) AnnexinV+/Caspase-3+ cells (as represented in Fig. 6). All these types were found to be MitoBlue negative cells.
9. We observed a frequent co-localization/overlap between red and green channels. On the contrary, a co-localization/overlap between red and blue or red and green channels was limited, more specifically following the 48 h or 72 h of treatment with drug combinations.
10. *Limitations*: The staining procedure was not designed to quantify the number of apoptotic cells following any treatment. The assays for the accurate methods for the quantification of apoptotic cells and the cell signals associated with it are already well-established by various procedures, including flow-cytometry and western blots, and are beyond the scope of our chapter. Our procedure is designed to visualize apoptosis occurring in live cells in real-time based on a triple-parameters using fluorescence images.

Fig. 6 (continued) cell line stained by triple co-fluorescence under the condition of treatment with Trametinib + Paclitaxel for 24 h (**a**). Single-channel (left panel), double channel merge (right panel), and triple channel merge (middle panel) of pictures of live OVK18 ovarian cancer cell line stained by triple co-fluorescence under the condition of treatment with Trametinib + Paclitaxel for 24 h (**b**). Picture shows AnnexinV+/Caspase-3+/MitoBlue- apoptotic OVK18 ovarian cancer cells and AnnexinV−/Caspase-3−/MitoBlue+ non-apoptotic OVK18 ovarian cancer cells

Table 2
Reagents that can be used for the validation of results from triple-co-fluorescence staining

Items	Source	Concentration (μM)	Instruments used for Assays	Use	Remarks
Expression of signaling proteins, markers of apoptosis and proliferation in cells					
Cleaved-Caspase-3	9661(D175) Cell signaling	1:500	UVP for WB	Validation of Caspase-3 activity	Markers of apoptosis
Cleaved- PARP	9541 (D214) Cell signaling	1:1000		PARP as the physiological substrate of Caspase-3	
BIM	2933 (C34C5) Cell signaling	1:500		A Bcl2 family protein that promotes apoptosis	
PCNA	2586 Cell signaling	1:2000		A nuclear protein which acts as a cofactor of DNA polymerase and helps in the process of DNA replication	Marker of proliferation
Microscopic identification of live-dead cells					
Eth-D-1 (ethidium Homodimer-1)	L3224; Invitrogen, molecular probes	0.5 μM	Fluore-scence microscope Olympus DP72 digital camera	Validation of dead cells	Red (TRITC positive) nuclei of dead cells
Calcein AM	L3224; Invitrogen, molecular probes	0.5 μM		Validation of live cells	Live cells in (FITC positive) green
Flow cytometric analyses of apoptosis and mitochondrial depolarization assay					
TMRE (Tetramethylrhodamine, ethyl ester)	Ab113852; Abcam	200 nM	BD Accuri C6 flow cytometer	Validation of mitochondrial potential in live cells	Mitochon-drial Depolari-zation assay

FCCP (carbonyl cyanide 4-(trifluoromethoxy) Phenylhydrazone)	Ab113852; Abcam	20 μM		Control for the mitochondrial depolarization assay	
Propidium iodide/plus RNaseA	550825; BD biosciences	150 μl per test		Apoptosis	AnnexinV positivity and early apoptosis
AnnexinV-PE	560930; BD biosciences	5 μl per test			
FACS buffer	Phenol red free RPM1 with 1% FBS	Wash			
7aaD	559925; BD biosciences	5 μl per test			
Real-time confluency assay by time-lapse phase-contrast imaging					
96 well format	ESSEN BioScience	As required by the study	IncuCyte ESSEN BioScience	Proliferation	Confluency
3-dimensional on-top Clonogenic growth					
24 well format	Matrigel (BD)	Drug (antitumor) combi-nation	Olympus	Clonogenic growth	Number and size of 3-D colonies

References

1. Tomasetti C, Li L, Vogelstein B (2017) Stem cell divisions, somatic mutations, cancer etiology, and cancer prevention. Science 355 (6331):1330–1334. https://doi.org/10.1126/science.aaf9011
2. Macheret M, Halazonetis TD (2015) DNA replication stress as a hallmark of cancer. Annu Rev Pathol 10:425–448. https://doi.org/10.1146/annurev-pathol-012414-040424
3. Lockshin RA, Zakeri Z (2007) Cell death in health and disease. J Cell Mol Med 11 (6):1214–1224. https://doi.org/10.1111/j.1582-4934.2007.00150.x
4. Mates JM, Segura JA, Alonso FJ, Marquez J (2012) Oxidative stress in apoptosis and cancer: an update. Arch Toxicol 86 (11):1649–1665. https://doi.org/10.1007/s00204-012-0906-3
5. Fulda S, Vucic D (2012) Targeting IAP proteins for therapeutic intervention in cancer. Nat Rev Drug Discov 11(2):109–124. https://doi.org/10.1038/nrd3627
6. Silke J, Vucic D (2014) IAP family of cell death and signaling regulators. Methods Enzymol 545:35–65. https://doi.org/10.1016/B978-0-12-801430-1.00002-0
7. Fulda S (2010) Evasion of apoptosis as a cellular stress response in cancer. Int J Cell Biol 2010:370835. https://doi.org/10.1155/2010/370835
8. Herr I, Debatin KM (2001) Cellular stress response and apoptosis in cancer therapy. Blood 98(9):2603–2614. https://doi.org/10.1182/blood.v98.9.2603
9. Fulda S (2015) Targeting extrinsic apoptosis in cancer: challenges and opportunities. Semin Cell Dev Biol 39:20–25. https://doi.org/10.1016/j.semcdb.2015.01.006
10. Pistritto G, Trisciuoglio D, Ceci C, Garufi A, D'Orazi G (2016) Apoptosis as anticancer mechanism: function and dysfunction of its modulators and targeted therapeutic strategies. Aging 8(4):603–619. https://doi.org/10.18632/aging.100934
11. Hassan M, Watari H, AbuAlmaaty A, Ohba Y, Sakuragi N (2014) Apoptosis and molecular targeting therapy in cancer. Biomed Res Int 2014:150845. https://doi.org/10.1155/2014/150845
12. Wong RS (2011) Apoptosis in cancer: from pathogenesis to treatment. J Exp Clin Cancer Res 30:87. https://doi.org/10.1186/1756-9966-30-87
13. Goldar S, Khaniani MS, Derakhshan SM, Baradaran B (2015) Molecular mechanisms of apoptosis and roles in cancer development and treatment. Asian Pac J Cancer Prev 16 (6):2129–2144. https://doi.org/10.7314/apjcp.2015.16.6.2129
14. Kaczanowski S (2016) Apoptosis: its origin, history, maintenance and the medical implications for cancer and aging. Phys Biol 13 (3):031001. https://doi.org/10.1088/1478-3975/13/3/031001
15. Sun G, Guzman E, Balasanyan V, Conner CM, Wong K, Zhou HR, Kosik KS, Montell DJ (2017) A molecular signature for anastasis, recovery from the brink of apoptotic cell death. J Cell Biol 216(10):3355–3368. https://doi.org/10.1083/jcb.201706134
16. Tang HL, Yuen KL, Tang HM, Fung MC (2009) Reversibility of apoptosis in cancer cells. Br J Cancer 100(1):118–122. https://doi.org/10.1038/sj.bjc.6604802
17. Diaz D, Prieto A, Reyes E, Barcenilla H, Monserrat J, Alvarez-Mon M (2015) Flow cytometry enumeration of apoptotic cancer cells by apoptotic rate. Methods Mol Biol 1219:11–20. https://doi.org/10.1007/978-1-4939-1661-0_2
18. De P, Sun Y, Carlson JH, Friedman LS, Leyland-Jones BR, Dey N (2014) Doubling down on the PI3K-AKT-mTOR pathway enhances the anti-tumor efficacy of PARP inhibitor in triple negative breast cancer model beyond BRCA-ness. Neoplasia 16 (1):43–72. https://doi.org/10.1593/neo.131694
19. Dey N, Sun Y, Carlson JH, Wu H, Lin X, Leyland-Jones B, De P (2016) Anti-tumor efficacy of BEZ235 is complemented by its anti-angiogenic effects via downregulation of PI3K-mTOR-HIF1alpha signaling in HER2-defined breast cancers. Am J Cancer Res 6(4):714–746
20. De P, Carlson JH, Leyland-Jones B, Williams C, Dey N (2018) Triple fluorescence staining to evaluate mechanism-based apoptosis following chemotherapeutic and targeted anti-cancer drugs in live tumor cells. Sci Rep 8 (1):13192. https://doi.org/10.1038/s41598-018-31575-3

Chapter 5

Flow Cytometric Analyses of p53-Mediated Cell Cycle Arrest and Apoptosis in Cancer Cells

Nour N. Al Zouabi, Cai M. Roberts, Z. Ping Lin, and Elena S. Ratner

Abstract

Phenotypic analysis of the effects of a gene of interest may be limited because stable expression of some genes leads to adverse consequences in cell survival, such as disturbance of cell cycle progression, senescence, autophagy, and programmed cell death. One of the best examples is tumor suppressor p53. p53 functions as a tumor suppressor by inducing cell cycle arrest and apoptosis in response to genotoxic and environmental insults. The choice and timing of either pathways induced by p53 depend on cellular context, cell types, and the degree of cellular/genomic damage (For review, *see* (Chen J, Cold Spring Harb Perspect Med 6:a026104, 2016)). The uncertainty makes the studies on the long-term effects of p53 in cells challenging. This chapter describes a method of flow cytometric analysis of ectopic expression of p53 to better quantify cell cycle distribution and apoptosis in cells treated with DNA damaging agents. The method can be easily adapted to other genes of interest to study their contributions to the fate of variety of cell types in response to endogenous or exogenous stresses.

Key words Apoptosis, Cell cycle arrest, p53, DNA damage, Green fluorescent protein, Reporter plasmid, Flow cytometry

1 Introduction

1.1 Construction of p53 Expressing Green Fluorescent Protein (GFP) Reporter Plasmids

The strategy of analyzing the outcomes of ectopic p53 expression is to identify cells that concurrently express GFP. We constructed a single expression vector that contains a multicloning region to allow the expression of p53 under the control of a strong CMV promoter, as well as independent expression of GFP driven by a moderate SV40 promoter. This design ensures that all transfected cells express both p53 and GFP at an optimal ratio, thereby providing an objective and quantitative measurement of p53-mediated cellular events [1]. This approach will also prevent the toxic effects of GFP overexpression in cells if a polycistronic expression vector was used. Furthermore, the uncertain function of a GFP-fusion protein can be ruled out. In addition to the empty vector control (the GFP-only expressing vector), we also

Ayesha B. Alvero and Gil G. Mor (eds.), *Detection of Cell Death Mechanisms: Methods and Protocols*, Methods in Molecular Biology, vol. 2255, https://doi.org/10.1007/978-1-0716-1162-3_5,

implemented a dominant-negative p53 gene as a negative control to validate the observation with wild type p53 expression in cells. The dominant-negative p53mt135 (Cys → Tyr) loses its DNA binding activity but is capable of forming complexes with wild type p53 [2, 3]. Therefore, the transcriptional activity of wild type p53 and its downstream functions are abrogated [4]. This feature is useful if a cell line expressing wild type p53 is chosen for the study. We used SKOV3 ovarian cancer cells as a host cell line for the present study. SKOV3 cells were readily transfected and exhibit no endogenous p53 protein [5].

1.2 Flow Cytometric Analysis of Cell Cycle Distribution in GFP-Positive Cell Populations

Measurement of cell cycle distribution based on DNA content with a fluorescent dye is usually conducted with a total cell population. Cells transfected with the p53 and GFP expressing vector can be identified and gated by flow cytometry and subsequently analyzed for DNA content to determine cell cycle distribution. The DNA content was measured by propidium iodide (PI) staining. GFP can be excited at 488 nm and detected at 510 nm. Without substantial overlapping in spectrum, PI can be excited at 493 nm and detected at 636 nm. The GFP positivity will allow the sorting of p53 expressing cells and provide better analysis of cell cycle distribution influenced by p53-mediated signaling events. The cell cycle analysis was conducted using FlowJo software (FlowJo). Using the univariate algorithm, mathematic and statistical modeling was used to create a fit to cell cycle data based on the DNA content of cells, assuming Gaussian distributions of the 2N (G1 phase) and 4N (G2/M phases) in the cell cycle. Furthermore, EdU (5-ethynyl-2-′-deoxyuridine)-based DNA labeling can be used in place of PI staining. Bivariate analysis of cell cycle distribution is also possible. Fluorophores that do not overlap with GFP spectrum will be needed, i.e., Alexa Fluor 647 for EdU and DAPI (4′,6-diamidino-2-phenylindole) for DNA content.

1.3 Flow Cytometric Analysis of Apoptotic and GFP-Positive Cell Populations

There are several methodologies for measurement of apoptosis following the induction of DNA damage. Apoptosis can be determined by the activation of caspase 3 in cells. Upon induction of apoptosis, proteolytic processing of the inactive form of caspase 3 into activated p17 and p12 fragments is performed [6]. The cleavage of caspase 3 occurs at Asp175. We used a monoclonal antibody that only recognizes the fragments of cleaved caspase 3. The antibody is conjugated with Alexa Fluor 647 for detection by flow cytometry to analyze GFP-positive and GFP-negative cell populations in a bivariate setting. The effects of p53 on DNA damage-induced apoptosis can be determined in GFP-positive cells. GFP-negative cells that do not express p53 can be analyzed as a negative control.

2 Materials

2.1 Equipment

1. Pipette aid.
2. Micropipettes.
3. Bench-top microcentrifuge.
4. Bench-top centrifuge.
5. High-speed floor centrifuge.
6. Bacterial shaker incubator.
7. Vacuum aspiration apparatus.
8. Biological safety cabinet.
9. CO_2 cell culture incubator.
10. LSRII flow cytometer (i.e., LSRII, BD BioSciences).

2.2 Reagents

1. Hind III and Xba I restriction enzymes.
2. T4 DNA ligase.
3. Commercially available PCR Cleanup Kit (i.e., Qiagen).
4. Commercially available Gel Extraction Kit (i.e., Qiagen).
5. Commercially available plasmid mini extraction kit (i.e., Qiagen).
6. Commercially available plasmid maxi extraction kit (i.e., Qiagen).
7. dam-/dcm-competent *E. coli* (NEB).
8. Competent *E. coli* (i.e., OneShot Top10, Thermo Fisher).
9. Appropriate microbial growth media for transformation of competent cells (i.e., SOC media).
10. Ampicillin (100 mg/ml).
11. LB agar.
12. 0.05% Trypsin-EDTA.
13. McCoy's 5A medium supplemented with 10% fetal bovine serum (FBS) and 0.5% Pen-strep [penicillin (10,000 unit/ml) and streptomycin (10,000 μg/ml)].
14. McCoy's 5A medium supplemented only with 10% FBS.
15. Serum-free media (i.e., Opti-MEM reduced serum medium).
16. Appropriate transfection reagent (Lipofectamine 2000 is used in this chapter).
17. Phosphate buffered saline (PBS) (1×).
18. Propidium iodide (PI): 1 mg/ml solution in water; 20×.
19. Cisplatin.
20. Paraformaldehyde solution: 4% in PBS.

21. Permeabilization buffer: 0.2% Tween 20 in PBS.
22. 1% Bovine serum albumin (BSA) in PBS.
23. Fluorescent-conjugated anti-caspase 3 antibody/cleaved caspase-3 (Asp175) (D3E9) antibody (i.e., Alexa Fluor 647 Conjugate).

3 Methods

3.1 Preparation of GFP-p53 Expression Plasmids

3.1.1 Digestion of p53 cDNA Inserts

1. Run a restriction digest of demethylated pCMV-p53 and pCMV-p53mt135 plasmids (*see* **Note 1**) containing wild type and mutant p53 cDNA inserts, using Hind III and Xba I: 2 μl of NEB Buffer 2, 1 μl of Hind III, 1 μl of Xba I, 1 μg of plasmid DNA, and balance to 50 μl total with ddH_2O. Incubate at 37 °C for 1 h.
2. Run digest product on 1.2% agarose gel until well separated. Excise p53 fragments with a clean blade and place in a 1.5 ml microfuge tube. Perform gel extraction of DNA using a commercially available gel extraction kit, following the manufacturer's protocol.

3.1.2 Digestion of Destination Vector

The p53 cDNA fragments will be cloned into pcDNA3.1-EGFP (Fig. 1), a pcDNA3.1 derivative vector in which the hygromycin selection marker has been previously replaced with EGFP cDNA by our laboratory.

1. Digest demethylated pcDNA3.1-EGFP with Hind III and Xba I as described above.
2. Run digestion reaction cleanup using a PCR Cleanup Kit. This will yield the linearized pcDNA3.1-EGFP.

3.2 Ligation and Production of Finished Plasmids

1. Determine concentrations of inserts and linearized vector. Calculate optimal ligation reaction mix. The total reaction volume is 10 μl, including 1 μl of T4 DNA ligase and 1 μl of 10× T4 DNA Ligase Buffer. The remaining 8 μl should be divided between insert and vector such that there is approximately a tenfold molar excess of insert.
2. Set up ligation reactions for each p53 insert and incubate at room temperature for 1 h.
3. Transform one vial of competent *E. coli* with each of the ligation reactions. Incubate bacteria mixed with the ligation reaction for 30 min on ice, heat shock at 42 °C for 30 s, and return to the ice for 2 min. Add 950 μl of SOC media to the vials and incubate at 37 °C and 250 RPM for 1 h, and then plate 150 μl of each transformation mix to LB-agar plates with 100 μg/ml ampicillin.

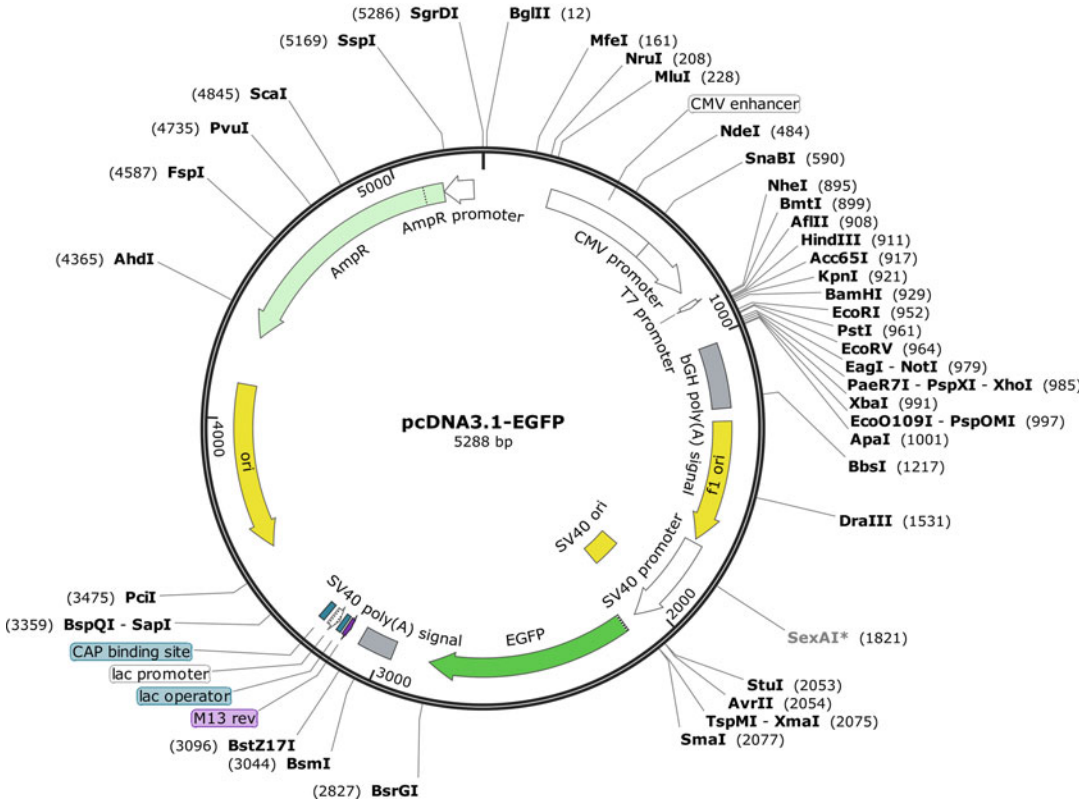

Fig. 1 Map of the pcDNA3.1-EGFP plasmid for expression of wild type and mutant p53. p53 and p53mt135 cDNAs were cloned into the multiple cloning region between HindIII and XbaI restriction sites

4. Pick a single colony from each plate and inoculate a 5 ml bacterial culture in LB plus 100 μg/ml ampicillin and grow overnight, 37 °C and 250 RPM.
5. Extract plasmid according to manufacturer's protocol. Use 1.5 ml of overnight culture as starting material. Also, make a glycerol stock of each plasmid in the bacteria by mixing 500 μl of overnight culture with 500 μl of 50% glycerol. Freeze stocks at −80 °C.
6. Confirm plasmids by sequencing.
7. Once sequencing is confirmed, perform plasmid extraction from larger volume of bacterial culture according to the manufacturer's protocol. Use 100 ml of bacterial culture in LB plus 100 μg/ml ampicillin.

3.3 Growing and Plating SKOV3 Cells

Grow SKOV3 cells in McCoy's 5A medium supplemented with 10% FBS and 0.5% Pen Strep. Upon confluency, trypsinize SKOV3 cells from a flask using 0.05% trypsin-EDTA. The splitting and plating of SKOV3 cells were based on the doubling time of 48 h.

Plate cells into 6-well plates with 1.5 ml of McCoy's 5A medium supplemented with 10% FBS without Pen-strep (*see* **Note 2**) for 16–24 h before transfection. Estimate the density of vehicle-treated control cells that will reach about 100% after 72-h growth prior to harvesting (*see* **Note 3**).

3.4 Transfection

Prepare the transfection mixture containing a plasmid and transfection reagent in serum-free media or Opti-MEM for each well. Work in a biological safety cabinet to keep transfection mix sterile.

1. Add 250 μl of serum-free media or Opti-MEM to each of two 15-ml conical tubes.
2. Add 1 μg of plasmid to the first tube and 6 μl of Lipofectamine 2000 to the second tube and vortex. Incubate at room temperature for 5 min.
3. Combine the first tube with the second tube and vortex. Incubate for 15–20 min at room temperature. The total volume of the transfection mixture is 500 μl.
4. Vortex the tubes and then add the transfection mixture to each well dropwise. Swirl the 6-well plate to mix well. The final volume in each well is 2 ml.
5. Incubate for 2 h in an incubator.
6. Replace the medium with fresh growth medium (*see* **Note 4**). Then, treat cells with cisplatin at desired concentrations.
7. Incubate for 48 h in an incubator until harvesting.

3.5 Harvesting Cells

Trypsinize cells using 0.5 ml of 0.05% Trypsin, and after 3 min, add 0.5 ml of McCoy's 5A medium with FBS and Pen-strep. Transfer cells to 15 ml conical tubes. Provided below is the methodology of flow cytometry to measure cell cycle distribution and apoptosis.

3.6 Flow Cytometric Analysis

3.6.1 Cell Cycle Distribution

1. Centrifuge trypsinized cells at 1000 rpm (100 × *g*) for 5 min.
2. Aspirate the supernatant (be careful not to disturb the pellet).
3. Add 0.5 ml of PBS, vortex, and centrifuge again at the same settings.
4. After the centrifuge, aspirate supernatant. Then, add 250 μl of PBS and 250 μl of Paraformaldehyde Solution, and vortex the tubes to mix.
5. Incubate the tubes at room temperature for 20 min to fix cells, and then centrifuge.
6. After removing the supernatant, wash cells twice using 500 μl of PBS.
7. Then, after aspirating the second wash, add 500 μl of the Permeabilization Buffer.

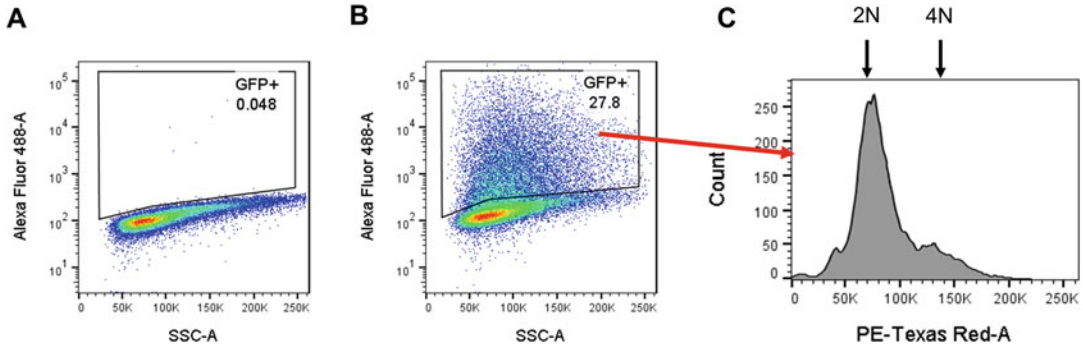

Fig. 2 Gating approach to identify GFP-positive cells for cell cycle analysis. SKOV3 cells mock-transfected (**a**) and transfected with pcDNA3.1-EGFP-p53 (**b**), followed by flow cytometric analysis of GFP-positive cells (an increase in Alexa Fluor 488 intensity; *Y*-axis). GFP-positive cells were gated and analyzed for DNA content (2N and 4N) using a histogram (PE-Texas Red; *X*-axis) (**c**)

8. Incubate the tubes 37 °C for 15 min, then add 500 μl of PBS, and vortex.
9. Centrifuge the tubes and then aspirate the supernatant.
10. Add 500 μl of PBS containing 25 μl of PI Solution.
11. Incubate for 10 min.
12. Analyze a minimum of 50,000 cells on a flow cytometer machine(*see* **Note 5**).
13. Gate cells with the bivariate dot plot (FSC vs SSC) to exclude debris and aggregates.
14. Choose the bivariate dot plot (GFP: Alexa Fluor 488 vs. SSC) to display gated cells.
15. Gate GFP-positive cells.
16. Choose the histogram plot (cell number vs. PI: PE-Texas Red) to display GFP-positive cells (Fig. 2).
17. Record the data.
18. Analyze the data using an analysis software such as FlowJo software as **steps 13–16**.
19. Use the cell cycle tool in FlowJo to model cell cycle distribution and calculate the percentage of cells in each cell cycle phase (Fig. 3).

3.6.2 Apoptosis Measurement

1. Centrifuge cells at 1000 rpm (100 × *g*) for 5 min.
2. Wash cells by adding 500 μl of PBS and centrifuge again.
3. Aspirate the supernatant.
4. Add 250 μl of PBS and 250 μl of 4% Paraformaldehyde solution.
5. Vortex the tubes and incubate for 20 min at room temperature.

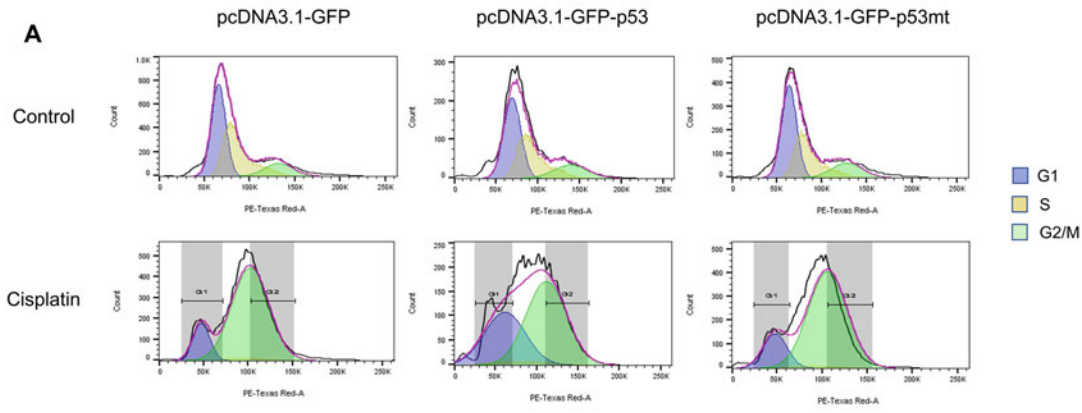

B

Treatment	Transfection	G1	S	G2M
Vehicle	pcDNA-GFP	43.7%	37.9%	12.3%
	pcDNA-GFP-p53	45.6%	35.6%	15.4%
	pcDNA-GFP-p53mt	45.8%	33.0%	15.0%
Cisplatin	pcDNA-GFP	14.8%	1.7%	80.4%
	pcDNA-GFP-p53	38.2%	3.9%	59.3%
	pcDNA-GFP-p53mt	17.5%	2.0%	78.5%

Fig. 3 Cell cycle phase analysis of cells expressing p53 in response to cisplatin-induced DNA damage. SKOV3 cells transfected with pcDNA3.1-EGFP, pcDNA3.1-EGFP-p53, or pcDNA3.1-EGFP-p53mt were treated with vehicle or cisplatin and subsequently analyzed for cell cycle distribution in GFP-positive cells by flow cytometry. GFP positivity is indicative of p53 expression. For vehicle-treated control cells, the Watson pragmatic model of the FlowJo software was used to fit the data. For cisplatin-treated cells, the Dean-Jett-Fox model of the FlowJo software was used to fit the data (**a**). The percentage of cells in each cell cycle phase was calculated according to the models (**b**)

6. After the incubation period, centrifuge again.
7. Remove the buffer and wash cells twice using 500 µl of PBS.
8. Add 500 µl of the permeabilization buffer to the pellet.
9. Incubate cells for 15 min at 37 °C. After incubation, add 500 µl of PBS and vortex.
10. Centrifuge and wash twice using 500 µl of 1% BSA in PBS.
11. After decanting the supernatant, add anticaspase 3-Alexa Fluor 647 conjugated antibody diluted at 1:50 in 1% BSA in PBS.
12. Incubate cells at 4 °C for 45 min to 1 h.
13. Wash the cells twice in 500 µl of 1% BSA in PBS.
14. Analyze a minimum of 50,000 cells on a flow cytometer machine (*see* **Note 5**).
15. Gate cells with the bivariate dot plot (FSC vs. SSC) to exclude debris and aggregates.
16. Choose the bivariate dot plot (GFP: Alexa Fluor 488 vs. Caspase 3: APC) to display gated cells.

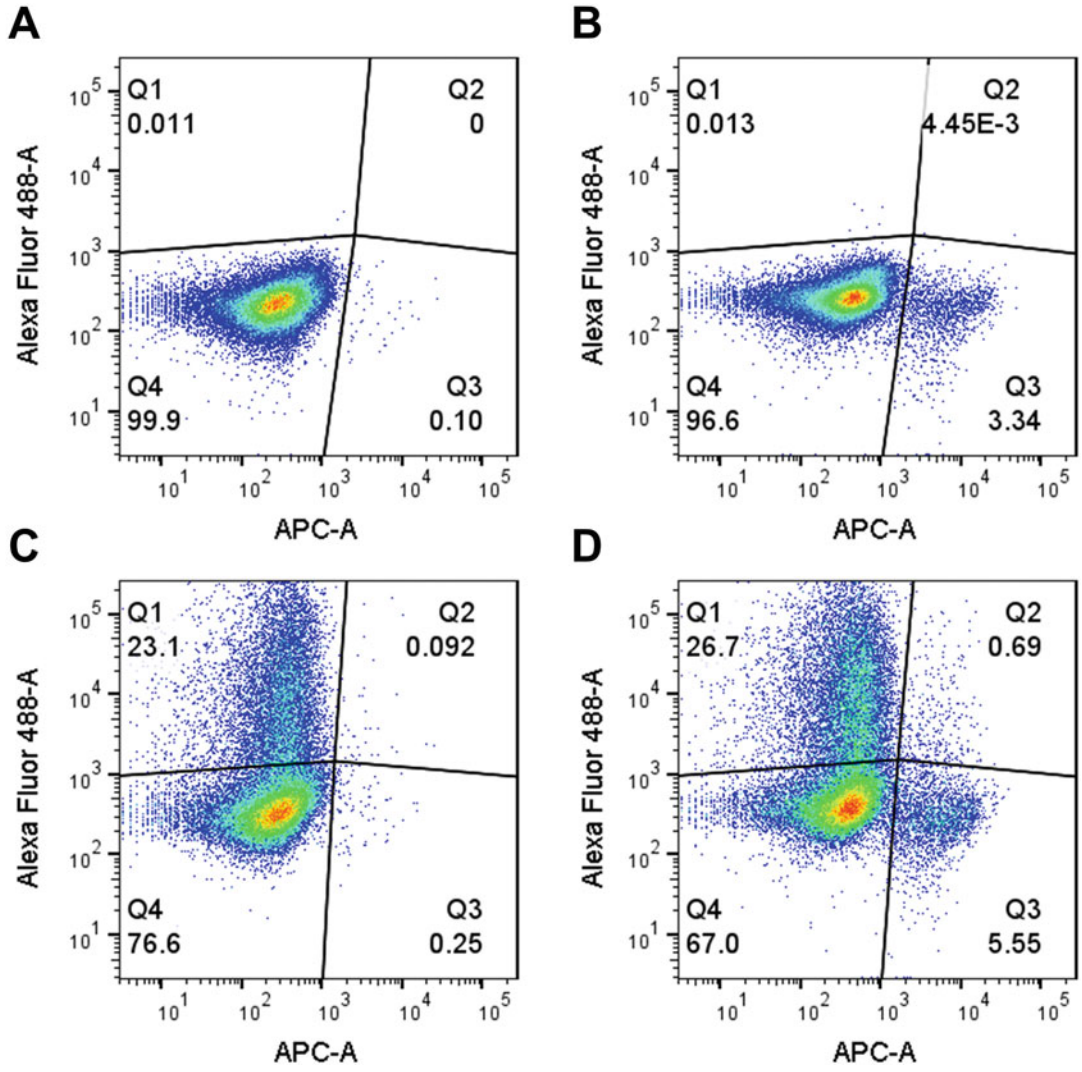

Fig. 4 Gating scheme for bivariate analysis of p53/GFP and caspase 3-positive cells (GFP: Alexa Fluor 488 vs caspase 3: APC). SKOV3 cells mock-transfected (**a** and **b**) and transfected with pcDNA3.1-EGFP-p53 (**c** and **d**) was treated with cisplatin (**b** and **d**) and analyzed for bivariate distribution of GFP^+/caspase 3^- (Q1), GFP^+/caspase 3^+ (Q2), GFP^-/caspase 3^+ (Q3), and GFP^-/caspase 3^- (Q4) cell populations, using flow cytometry

17. Use quadrant gate to identify GFP^+/caspase 3^-, GFP^+/caspase 3^+, GFP^-/caspase 3^+, and GFP^-/caspase 3^- cell populations (Fig. 4).
18. Record the data.
19. Analyze the data by FlowJo software as **steps 15–17**.
20. Calculate the percentage of caspase 3^+ cells in GFP^+ and GFP^- cells (Fig. 5) as described in the below formulas:

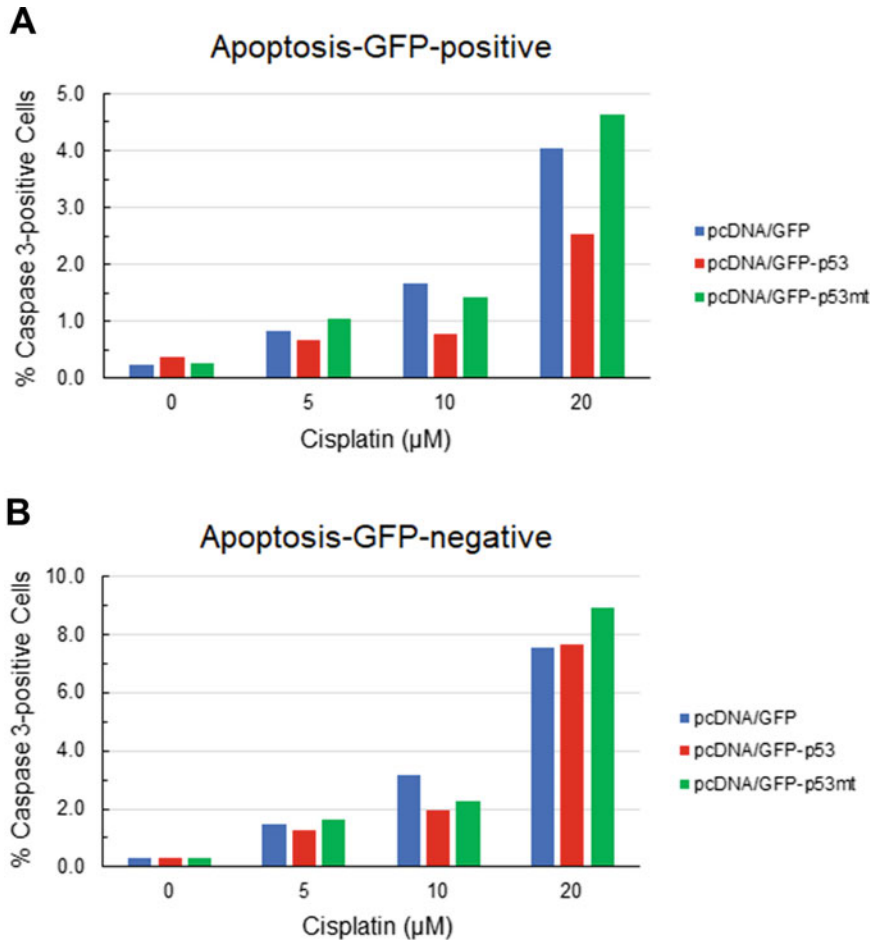

Fig. 5 Quantification of apoptosis in p53/GFP-positive cell populations. SKOV3 cells transfected with pcDNA3.1-EGFP, pcDNA3.1-EGFP-p53, or pcDNA3.1-EGFP-p53mt was treated with various concentrations of cisplatin and subsequently analyzed by flow cytometry. The percentage of caspase 3-positive populations in GFP-positive and GFP-negative cells was calculated and is presented

$$\%\text{Caspase } 3^{+} \text{ in } \text{GFP}^{+} \text{ cells} = (\text{GFP}^{+}/\text{caspase } 3^{+})/[(\text{GFP} + /\text{caspase } 3^{+}) + (\text{GFP}^{+}/\text{caspase } 3^{-})] \times 100\%$$

$$\%\text{Caspase } 3^{+} \text{ in } \text{GFP}^{-} \text{ cells} = (\text{GFP}^{-}/\text{caspase } 3^{+})/[(\text{GFP}^{-}/\text{caspase } 3^{+}) + (\text{GFP}^{-}/\text{caspase } 3^{-})] \times 100\%$$

4 Notes

1. Because the activity of the Xba I restriction enzyme is inhibited by methylation of plasmid DNA originating from dam^{+} *E. coli* bacteria, a nonmethylated version of the plasmid must be produced. dam^{-}-competent *E. coli* is required for production of

plasmids used for cloning in this study. dam+—competent *E. coli*, i.e., OneShot Top10, can be used for the final plasmid products.

2. For transfection, cells should be plated in the medium without Pen-strep according to manufacturer's instructions.
3. In contrast to the manufacturer's instructions, we recommend that cell plating density does not achieve 90% at the time of transfection (after 24 h of plating). Overgrown cells might undergo growth arrest and have a reduced responsiveness to cisplatin-induced DNA damage.
4. Changing the medium after 2-h transfection will minimize the toxicity of plasmid DNA-Lipofectamine 2000 complex.
5. Because the transfection efficiency (based on GFP positivity) was about 25–40%, acquiring 50,000 or more cells is necessary to obtain a sufficient number of cells to allow more accurate cell cycle phase modeling.

References

1. Chen J (2016) The cell-cycle arrest and apoptotic functions of p53 in tumor initiation and progression. Cold Spring Harb Perspect Med 6(3): a026104. https://doi.org/10.1101/cshperspect.a026104
2. Jordan JJ, Inga A, Conway K, Edmiston S, Carey LA, Wu L, Resnick MA (2010) Altered-function p53 missense mutations identified in breast cancers can have subtle effects on transactivation. Mol Cancer Res 8(5):701–716. https://doi.org/10.1158/1541-7786.MCR-09-0442
3. Nie L, Sasaki M, Maki CG (2007) Regulation of p53 nuclear export through sequential changes in conformation and ubiquitination. J Biol Chem 282(19):14616–14625. https://doi.org/10.1074/jbc.M610515200
4. Vogelstein B, Kinzler KW (1992) p53 function and dysfunction. Cell 70(4):523–526. https://doi.org/10.1016/0092-8674(92)90421-8
5. Yaginuma Y, Westphal H (1992) Abnormal structure and expression of the p53 gene in human ovarian carcinoma cell lines. Cancer Res 52(15):4196–4199
6. Nicholson DW, Ali A, Thornberry NA, Vaillancourt JP, Ding CK, Gallant M, Gareau Y, Griffin PR, Labelle M, Lazebnik YA et al (1995) Identification and inhibition of the ICE/CED-3 protease necessary for mammalian apoptosis. Nature 376(6535):37–43. https://doi.org/10.1038/376037a0

Chapter 6

A Real-Time, Bioluminescent Apoptosis Assay

Kevin R. Kupcho and Andrew L. Niles

Abstract

This chapter describes a real-time, bioluminescent apoptosis assay technique, which circumvents the well-documented "timing condundrum" encountered when employing traditional apoptosis detection chemistries after exposures with inducers of unknown potential. The assay continuously reports the translocation of phosphatidylserine (PS) from the inner membrane leaflet of a cell to the exofacial surface during apoptosis. This homogenous, no-wash, plate-based assay is made possible by two different annexin V fusion proteins, which contain complementing NanoBiT™ luciferase enzyme subunits, a time-released luciferase substrate, and a fluorescent membrane integrity reagent. During apoptosis, luminescence signal is proportional to PS exposure and fluorescence intensity correlated with the degree of secondary necrosis. Altogether, the measures provide exquisite kinetic resolution of dose- and agent-dependent apoptotic responses, from early through late phases. At exposure termination, other compatible reagents can be applied to measure additional orthogonal correlates of cell health.

Key words Apoptosis, Phosphatidylserine, Annexin V, Bioluminescent, Real-time, Homogenous, No-wash, Multiplexed, NanoBiT™, Necrosis

1 Introduction

The apoptotic cascade involves an ordered series of enzymatic events, which begin and progress at a rate that is dependent upon the potency and mechanism of action of the stimuli [1]. Because chemical and biological inducers vary greatly with respect to induction potential, it is exceptionally difficult to predict a priori the optimal exposure period for accurate characterization of the apoptotic phenotype [2–4]. Furthermore, the enzymatic biomarkers (caspases) responsible for executing the apoptotic program are transient and subject to decay after completing their effector function [5, 6]. Therefore, the accuracy and/or quality of any endpoint in vitro apoptosis assay dataset is dependent upon when apoptotic induction begins and when the assay measure is collected.

To overcome the experimental challenges created by unpredictable induction rates, conscientious researchers have historically examined induction potential by two primary means. First, their

Ayesha B. Alvero and Gil G. Mor (eds.), *Detection of Cell Death Mechanisms: Methods and Protocols*, Methods in Molecular Biology, vol. 2255, https://doi.org/10.1007/978-1-0716-1162-3_6,

studies are conducted utilizing parallel plates dosed with the agents in staggered additions over a multipoint time course. At study termination, multiple exposure times with the agent are represented. Second, a real-time cytotoxicity probe is introduced at dosing and cytotoxicity is continually evaluated during the exposure. When loss of membrane integrity first becomes detectable, it is assumed that a cell death program is fully initiated and the samples can be evaluated for the presence of apoptotic biomarkers. These approaches enhance data quality and remedy much of the uncertainty associated with arbitrary endpoints, but deliver coarse profiles and require significant duplication of effort, increased expense, and depleted resources.

Assay methodologies that utilize nonenzymatic, biophysical biomarkers of apoptosis are typically more kinetically forgiving than caspase activity assays. Koop et al. first recognized the potential of phosphatidylserine (PS) exposure detected via annexin V for establishing an apoptotic profile [7]. The assay concept is predicated upon the fact that PS is normally maintained in healthy cells in a cytosolic orientation by ATP-dependent flippases [8, 9]. During apoptosis, however, flippases and scramblases mediate the translocation of PS to the cell surface where they are utilized in vivo as "eat me" signals for macrophage-mediated clearance [10]. Once externalized, PS can be detected using a calcium-dependent, annexin V affinity reagent, chemically conjugated to a fluorophore. Further, admixed membrane integrity dyes with affinity for DNA can help establish the maturity of the apoptotic response.

Recently, a real-time annexin V apoptosis assay was described by Kupcho et al., which overcomes the traditional limitations of annexin assay formats that employ high-content imaging or flow cytometric analysis [11]. This single addition assay is fully homogenous and is conducted directly in a standard opaque assay plate. Notably, the assay requires no postexposure cell harvests, no cell monodispersion, and no onerous labeling, handling, and washing steps. Once applied, the reagent delivers a continuous accounting of the progression of the apoptotic program through measurement of PS exposure and loss of membrane integrity. The luminescent annexin V measure is achieved using two distinct annexin V-NanoBiT™ fusion proteins, which reconstitute a luciferase enzyme when brought into proximity on PS rafts at the apoptotic cell surface. The complemented enzyme produces luminescence in the presence of a time-released substrate, which is proportional to PS over a sustained period of up to 48 h. The profluorescent membrane integrity probe component of the reagent produces fluorescence proportional to cytotoxicity as cells progress to the secondary necrosis phenotype. Altogether, the temporal data from the assay can be used to either establish standard apoptotic mechanisms and potencies or flag nonapoptotic subroutines associated with alternative cell death programs. The methods described below outline

experimental examples of (a) a real-time annexin V apoptosis and necrosis assay and (b) a real-time annexin V apoptosis and necrosis assay multiplexed with a spectrally distinct viability assay and a luminogenic caspase 3/7 activity assay.

2 Materials

2.1 Equipment

1. 15 ml conical tubes.
2. 1.5 ml microfuge tubes.
3. 75 cm^2 tissue culture flasks.
4. Reagent reservoirs.
5. Sterile pipette tips.
6. Single and multichannel micro-pipettors.
7. Hemocytometer and coverslip.
8. Bright-field microscope.
9. Table-top centrifuge.
10. White, 96-well, tissue-culture grade plate.
11. Multimodal Luminometer/Fluorometer equipped with the following filter pairs:
    400_{ex} 505_{em}.
    $485–500_{ex}$ $520–535_{em}$.
12. CO_2 incubator.

2.2 Cells and Reagents

1. Cell lines for induction of apoptosis: adherent human breast cancer cell line, SK-BR-3 and nonadherent human myelogenous leukemia cell line, K562, are used in the methods below.
2. Cell culture medium for SK-BR-3: McCoy's 5a Modified Medium + 10% fetal bovine serum (FBS); cell culture medium for K562: RPMI 1640 + 10%.
3. 0.25% Trypsin.
4. 0.4% Trypan blue solution.
5. Apoptotic inducing agent, for this chapter, we used trastuzumab emtansine (T-DM1), bortezomib, or staurosporine.
6. Dimethyl sulfoxide or appropriate solvent for apoptotic inducing agent.
7. RealTime-Glo™ Annexin V Apoptosis and Necrosis Assay (Promega).
8. Caspase-Glo® 3/7 Assay (Promega).
9. CellTiter-Fluor™ Cell Viability Assay (Promega).

3 Methods

3.1 A Real-Time Annexin V Apoptosis and Necrosis Induction Time Course

The following protocol produces dose-dependent induction of PS exposure, which leads to time-dependent changes in membrane integrity by apoptosis. The antibody drug conjugate (ADC), trastuzumab emtansine, and the proteasome inhibitor, bortezomib, are used to induce apoptosis in the SK-BR-3 cell line. This protocol is written for cells that are attachment-dependent and allowed to recover/equilibrate for at least 2–16 h prior to dosing but can be amended to explore the kinetics of PS exposure using nearly any cell line, 3D spheroid model, treatment, or test article.

To avoid culture contamination by microorganisms, conduct cell-based assay experiments are carried out in a laminar flow hood or clean-room environment using aseptic technique with sterile reagents and consumables.

1. Harvest SK-BR-3 cells from a 75 cm^2 culture flask with the addition of 3 ml of 0.25% v/v trypsin solution. After the cells have detached, gently aspirate and dispense cell solution with a 5 ml pipette to monodisperse. Neutralize residual trypsin activity with the addition of 1 ml of FBS. Add 10 ml of additional complete medium to facilitate trypsin removal during subsequent wash. Remove a representative volume (500 μl or less) for trypan blue counting and viability analysis. Gently pellet the remaining pool by centrifugation at 200 × *g* for 8–10 min at room temperature (RT).
2. Examine a dilution of the representative cell sample by trypan blue exclusion to determine the population viability and cell count. If viability is greater than 90%, add complete medium (with serum and nutrient/cofactor adjuncts) so that the cells are at a density of 100,000 viable cells/ml.
3. Plate the cells in 50 μl volumes to all wells of a white, 96-well plate except for column 12 and allow them to attach for at least 2 h (up to 16 h) at 37 °C and 5% CO_2.
4. Solubilize the apoptotic inducing agent or test compound if needed. For example, dilute bortezomib to a 10 mM stock solution in sterile DMSO. T-DM1 is already supplied in an aqueous form at 20 mg/ml.
5. Next, prepare an intermediate 4× dilution of the apoptotic inducing agent or test compound in complete medium in a sterile Eppendorf tube. For example, for bortezomib with a desired top dose of 10 μM, dilute bortezomib to 40 μM.
6. In a separate microtiter plate, use a multichannel pipettor to add 100 μl dilution volumes of complete medium to all wells of columns 2–12 of a sterile, white 96 well plate. Add 150 μl of 4× apoptosis inducer or test compound agent to column 1, rows

A–D. In this example, 4× of T-DM1 is added to column 1 rows A–D and 4× of bortezomib is added to column 1 rows E–H. Threefold serially dilute each compound by transferring 50 µl from column 1 rows A–D to column 2 rows A–D. Similarly, transfer 50 µl from column 1 rows E–H to column 2 rows E–H. Gently mix compound/dilution medium in column 2 by aspirating and dispensing 50 µl volumes at least five times. Avoid generating bubbles. After mixing, remove 50 µl from each well in column 2 and transfer to column 3 to continue the serial dilution process through column 10, discarding 50 µl from the final dilution. Columns 11 and 12 will ultimately serve as untreated control and reagent background control, respectively.

7. Starting at column 12, transfer 50 µl replicates of test agent dilutions to the white plate containing attached cells using a multichannel pipettor. Continue to transfer volumes in columns 11, 10, 9, etc., until the entire dilution series is transferred to the plate containing cells. At this point, each well in the plate with attached cells would have a total volume of 100 µl.
8. Prepare the 2× RealTime-Glo™ Annexin V Apoptosis and Necrosis Assay Detection Reagent by first adding 12 ml of prewarmed, complete medium to a sterile 15 ml conical tube (*see* **Note 1**). Next, add 24 µl each of 1000× Annexin V-LgBiT, Annexin V-SmBiT, $CaCl_2$, Annexin V NanoBiT® Substrate, and Necrosis Detection Reagent. Mix by manual inversion until homogeneous *(see* **Notes 1** and **2**).
9. Add 100 µl of 2× RealTime-Glo™ Annexin V Apoptosis and Necrosis Assay Detection Reagent prepared from **step 8** above, to all wells of the plate containing cells and apoptosis test agents and cells. Mix the plate by orbital shaking at 500–700 RPM for 1 min to insure homogeneity and reagent dispersion.
10. Collect the luminescence and fluorescence signals generated by the RealTime-Glo™ Annexin V Apoptosis and Necrosis Assay by placing the plate in an environmentally regulated multimodal plate reader (such as BMG CLARIOstar® with Atmospheric Control Unit) prewarmed to 37 °C. Program the plate reader to sequentially collect luminescence and fluorescence (at $485–500_{ex}/520–535_{em}$) signals at desired intervals (e.g., 10–15 min) over the course of a 48 h exposure. Initiate data collection. Alternatively, the plate can be placed in a standard cell culture incubator and manually transferred to a multimodal plate reader at desired time points.
11. At exposure completion, calculate the average luminescence signal from replicates in column 12 (no-cell background controls) and subtract this value from every sample well in the

luminescent channel to obtain background-subtracted relative luminescent units (RLU) (*see* **Note 3**). Calculate the average fluorescence signal from column 12 (no-cell background controls) and subtract this value from every sample well in the fluorescence channel to obtain background-subtracted relative fluorescent units (RFUs). Next, graph background-subtracted luminescence values and background-subtracted RFU (membrane integrity) versus compound concentration and untreated control for each time point using curve-fit software (GraphPad™ Prism, SigmaPlot™, etc.) as shown in Fig. 1. It is also useful to graph background-subtracted RLU and background-subtracted RFU versus time at a fixed concentration of compound as illustrated in Fig. 2 (*see* **Note 3**).

12. Cell death mechanism of action can be tentatively assigned based on graphed datasets for PS exposure and loss of membrane integrity. In general, apoptosis inducers will produce time- and dose-dependent increases in luminescence, which occur prior to increases in fluorescence (*see* **Note 2**). The temporal lag between PS exposure and loss of membrane integrity varies with inducer but typically ranges between 2 and 12 h and is considered the hallmark of the apoptotic phenotype. Conversely, nonapoptotic, alternative cell death mechanisms, such as primary necrosis or necroptosis, produce annexin V and necrosis assay signal profiles that are largely concurrent with respect to emergence and magnitude. Any dataset ambiguity can be resolved in subsequent experimentation with a multiplexed caspase activation assay (*see* **Note 2**).

3.2 A Multiplexed Annexin V, Necrosis, Viability, and Caspase Activation Assay

As established in Subheading 3.1, the RealTime-Glo™ Annexin V Apoptosis and Necrosis Assay can be indispensable for establishing the kinetics and magnitude of biomarkers associated with an apoptotic response. However, orthogonal measures of apoptosis and viable cell number can also provide greater confidence regarding proposed mechanism of action and provide valuable insight into a treatment's efficacy (*see* **Note 4**). The CellTiter-Fluor Cell Viability Assay, which is multiplexed in the following protocol, measures a constitutive and conserved proteolytic activity resident only in viable mammalian cells and is notably unaffected by metabolic rate or status of a cell. This "live-cell protease activity" is measured using a fluorogenic, cell-permeable, peptide substrate. The substrate enters intact cells where it is cleaved to generate a fluorescence signal proportional to the number of living cells. This live cell protease activity marker becomes inactive upon loss of membrane integrity and leakage into the surrounding culture medium. This biomarker defines the relative number of viable cells in a well after treatment and can be compared with the necrosis assay data to define both cytotoxic and cytostatic effects produced during an exposure.

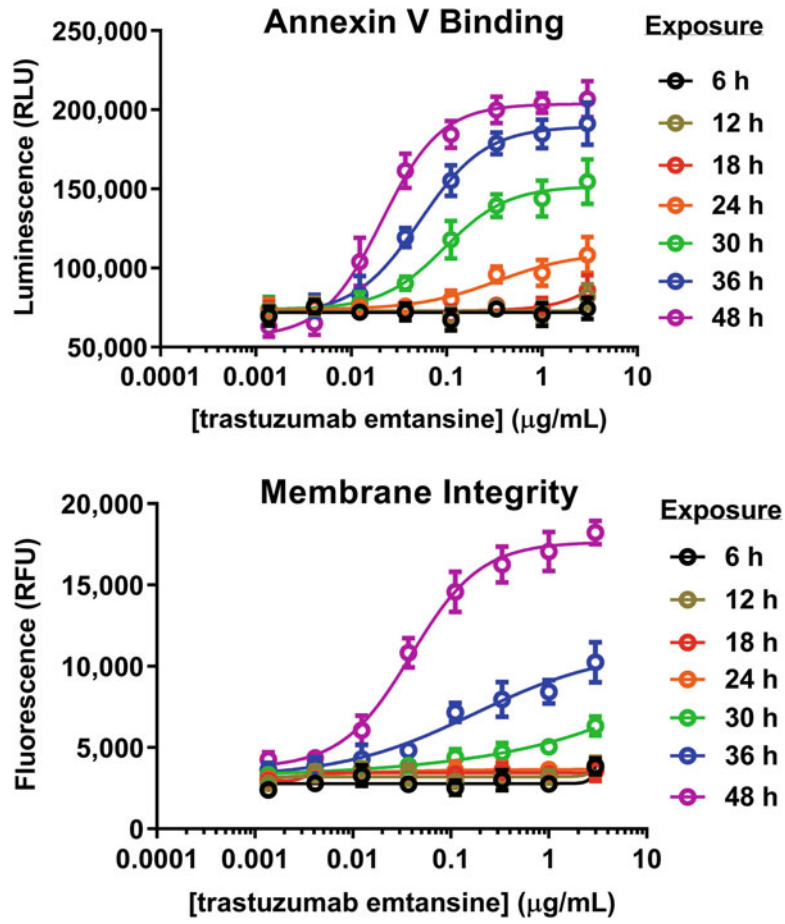

Fig. 1 PS exposure and loss of membrane integrity are dose- and time-dependent during the apoptotic cascade. SK-BR-3 cells were harvested, resuspended in McCoy's + 10% FBS, and seeded in an white plate at a density of 5000 cells per well in 50 μl volumes. After the cells had attached, serial dilutions of trastuzamab emtansine were added at 4× the desired treatment concentration in 50 μl volumes. Finally, 2× RealTime-Glo™ Annexin V Apoptosis and Necrosis Assay Detection Reagent was added. The plate was placed in a BMG CLARIOstar® multimodal plate reader equipped with atmospheric and temperature controls and luminescence and fluorescence were collected every 15 min for 48 h (only select time points shown). PS-directed, annexin V fusion binding and productive luminescence was first detectible at the highest dose (3.3 μg/ml) at 18 h and increased in magnitude (RLU) and potency to 48 h. Loss of membrane integrity owing to progression of the apoptotic program to secondary necrosis was first detectible at 30 h and progressed in signal intensity and potency throughout the 48 h endpoint

Caspase activation is an early and definitive hallmark of apoptosis. Evidence of caspase activation in addition to PS exposure prior to loss of membrane integrity provides strong support for the conclusion of programmed cell death by apoptosis. The ability to

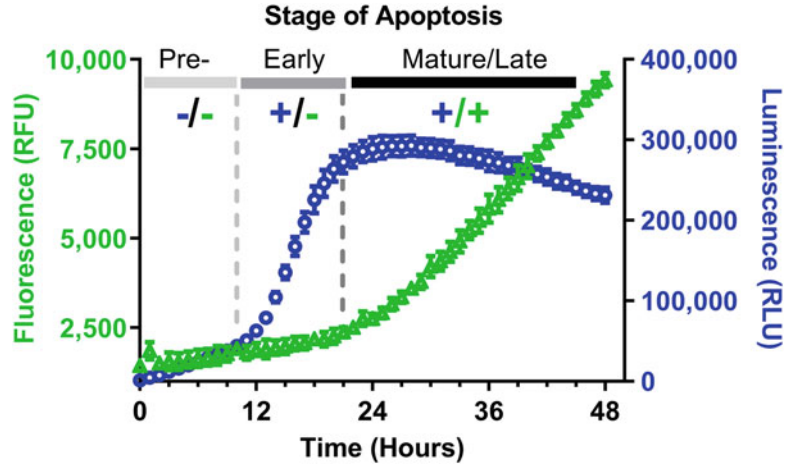

Fig. 2 Luminescence signal as a result of PS exposure precedes increases in fluorescence owing to loss of membrane integrity during apoptosis. Bortezomib was serially diluted in RPMI 1640 + 10% FBS in 50 μl volumes. K562 was added to each well of the drug dilution series at 5000 cells per well in 50 μl volumes. 2× RealTime-Glo™ Annexin V Apoptosis and Necrosis Assay Detection Reagent was added, and the plate was placed in a BMG CLARIOstar® equipped with atmospheric and temperature controls. Luminescence and fluorescence signals were collected every hour for 48 h. Standard apoptosis induction profiles segregate into pre-, early, and mature/late phases of apoptosis. These stages are marked by no increases in either signal, increases in luminescence but not fluorescence, or increases in both luminescence and fluorescence, respectively

distinguish between caspase-induced PS exposure and PS exposed by simple necrosis or alternative cell death programs is often relevant from a drug development perspective. In this protocol, caspase activation is measured by a bioluminescence chemistry utilizing an aminoluciferin consensus peptide substrate optimized for caspase-3/7 cleavage and a thermostable luciferase, which reports released product (Caspase-Glo® 3/7 Assay).

The methods described below use staurosporine as an apoptotic inducer in the K562 cell line.

1. Solubilize the apoptotic inducing agent or test compound. For example, dilute Staurosporine to a 50 mM stock solution in sterile DMSO.
2. Prepare an intermediate 4× dilution of the apoptotic inducing agent or test compound in complete medium in a sterile microfuge tube.
3. In a white 96-well microtiter plate, use a multichannel pipettor to add 25 μl dilution volumes of complete medium to all wells of columns 2–12. Add 50 μl of 4× apoptosis inducer or test compound agent to column 1, rows A–D. Twofold serially

dilute apoptosis inducer and test compound by transferring 25 µl from column 1, rows A–D to column 2. Gently mix compound/dilution medium in column 2 by aspirating and dispensing 25 µl volumes at least five times. Avoid generating bubbles. After mixing, remove 25 µl from each well in column 2 and transfer to column 3 to continue the serial dilution process. Repeat through column 10 but remove 25 µl from that final dilution. Columns 11 and 12 will ultimately serve as untreated control and reagent background control, respectively.

4. Harvest K562 cells from a 75 cm^2 culture flask by transferring the volume to a 15 ml sterile centrifuge. Remove a representative volume (500 µl or less) for trypan blue counting and viability analysis. Gently pellet the remaining pool by centrifugation at 200 × *g* for 8–10 min at RT.
5. Examine the cell sample by trypan blue exclusion to determine the population viability and cell count. If viability is greater than 90%, add complete medium (with serum and nutrient/cofactor adjuncts) so that the cells are at a density of 200,000 viable cells/ml.
6. Add 25 µl volumes of the cell solution to all wells of the plate except for column 12. Add 25 µl volumes of medium only to wells in column 12.
7. Prepare the 2× RealTime-Glo™ Annexin V Apoptosis and Necrosis Assay Detection Reagent by first adding 6 ml of prewarmed, complete medium to a sterile 15 ml conical tube. Next, add 12 µl each of 1000× Annexin V-LgBiT, Annexin V-SmBiT, $CaCl_2$, Annexin V NanoBiT® Substrate, and Necrosis Detection Reagent. Mix by manual inversion until homogeneous.
8. Add 50 µl of 2× RealTime-Glo™ Annexin V Apoptosis and Necrosis Assay reagent prepared above in **step 7** to all wells of the plate containing cells and apoptosis test agents. Mix the plate by orbital shaking at 500–700 RPM for 1 min to insure homogeneity and reagent dispersion.
9. Collect the luminescence and fluorescence signals generated by the RealTime-Glo™ Annexin V Apoptosis and Necrosis Assay by placing the plate in an environmentally regulated multimodal plate reader (such as BMG CLARIOstar® with Atmospheric Control Unit) prewarmed to 37 °C. Program the plate reader to sequentially collect luminescence and fluorescence (at 485–500_{ex}/520–535_{em}) signals at desired intervals (e.g., 10–15 min) over the course of an 18–24 h exposure. Initiate data collection. Alternatively, the plate can be placed in a standard cell culture incubator and manually transferred to a multimodal plate reader at desired time points.

10. An hour prior to RealTime-Glo™ Annexin V Apoptosis and Necrosis Assay completion, thaw frozen CellTiter-Fluor™ Cell Viability Assay and Caspase-Glo® 3/7 substrates and buffers by placement at room temperature. Vortex buffers after thawing to insure homogeneity.
11. Create a 5× CellTiter-Fluor Reagent by adding 10 µl of the GF-AFC substrate to 2.0 ml of CellTiter-Fluor Buffer. The solution may appear "milky" upon addition of the substrate but will quickly become clear with vortexing.
12. Add 20 µl of the 5× CellTiter-Fluor Reagent to all wells of the 96 well plate of cells. Mix by orbital shaking at 500–700 RPM for 1 min and then return to a 37 °C incubator for at least 30 min.
13. Measure fluorescence at 400_{ex} 505_{em}. The fluorescent product of this assay is reasonably stable, allowing for multiple reads to optimize signal acquisition. Additional incubation (up to 3 h) may improve the dynamic range. After a satisfactory signal is obtained, proceed to the luminescent caspase portion of the multiplex.
14. Transfer the Caspase-Glo®-3/7 Buffer to the lyophilized Caspase-Glo®-3/7 Substrate to create the Reagent. Mix by swirling or by inverting the contents until the substrate is completely dissolved.
15. Add 100 µl of Caspase-Glo®-3/7 Reagent to each well of columns 1–12. Mix briefly using an orbital shaker. After 30 min of incubation at RT, measure the luminescence signal associated with caspase 3/7 activity.
16. Calculate the average luminescence signal from replicates in column 12 (no-cell background controls) and subtract this value from every sample well in the luminescent channel to obtain background-subtracted relative luminescent units (RLUs) for the annexin V and caspase assays. Calculate the average fluorescence signal from column 12 (no-cell background controls) and subtract this value from every sample well in the fluorescent channel to obtain background-subtracted relative fluorescent units (RFUs) for the necrosis and cell viability assays. Next, convert the data to "percent of untreated background" and graph these values versus compound concentration using curve-fit software (GraphPad™ Prism, SigmaPlot™, etc.) as shown in Fig. 3 (*see* **Note 4**).
17. Determine whether caspase activity correlates positively with PS exposure. Apoptosis inducers will produce time- and dose-dependent increases in annexin V luminescence and caspase assay luminescence. Conversely, nonapoptotic, alternative cell death mechanisms, such as primary necrosis or necroptosis, produce annexin V and necrosis assay signal profiles that are

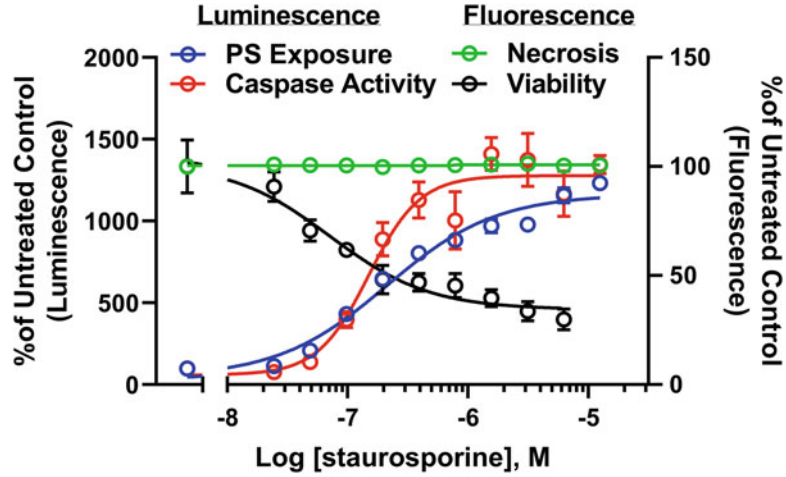

Fig. 3 The RealTime-Glo™ Annexin V Apoptosis and Necrosis Assay can be multiplexed with endpoint measures of viability and caspase activation. Staurosporine was serially diluted in RPMI 1640 + 10% FBS and transferred in 25 µl replicate volumes to an white plate containing 5000 cells per well in 25 µl. 2× RealTime-Glo™ Annexin V Apoptosis and Necrosis Assay Detection Reagent was added in an additional 50 µl volume. The plate was mixed briefly by orbital shaking and placed at 37 °C and 5% CO_2 in a humidified incubator for 18 h. Luminescence and fluorescence signals were collected using a BMG POLARstar® multimodal plate reader. 20 µl of 5× CellTiter-Fluor was added and incubated for 30 min at 37 °C. Fluorescence was collected at 400_{ex} and 505_{em}. Finally, Caspase-Glo® 3/7 Reagent was added, mixed briefly by orbital shaking, and luminescence collected after 30 min at room temperature. The resulting profile shows PS exposure and caspase activation, both indicators of apoptosis, with a dose-dependent decrease in cell number (antiproliferative effect) without loss of membrane integrity. Therefore, an 18 h exposure with staurosporine produces an early apoptotic phenotype. Note: Multiple signals can be collected in the same assay well because the fluorescence signals are spectrally distinct and because the Caspase-Glo® 3/7 Reagent quenches the annexin V signal

largely concurrent with respect to emergence and magnitude without caspase activation. The cell viability data define the potency of a response and can also define efficacy by the percentage of signal remaining versus untreated control.

4 Notes

1. The 2× RealTime-Glo™ Annexin V Apoptosis and Necrosis Assay Detection Reagent should be created in prewarmed medium containing serum (2–10% v/v fetal bovine or horse serum) for optimal solubility (Subheading 3.1, **step 8**). If

serum-free or defined medium is required, protein supplements (cytokines, growth factors, albumin, etc.) are highly recommended to promote solubility.

2. Annexin V affinity reagents bind to PS in a Ca^{2+}-dependent manner. The Ca^{2+} concentration of the 2× RealTime-Glo™ Annexin V Apoptosis and Necrosis Assay Detection Reagent has been carefully calibrated to support optimal assay performance without adversely affecting normal cell biology or signaling functions. In rare cases, the Ca^{2+} added as part of the Reagent may stimulate transient PS exposure without loss of membrane integrity. These signal profiles may complicate dataset interpretation (Subheading 3.1, **step 12**). Fortunately, this transient exposure typically begins and resolves within the first 4 h of Reagent exposure and is kinetically dissimilar to the majority of known cell death program signatures. Because common media are formulated to contain sufficient (but suboptimal) Ca^{2+} to support PS binding, cell line-specific Ca^{2+} sensitivity studies can be confirmed by omitting $CaCl_2$ during Reagent preparation (Subheading 3.1, **step 8**.)
3. Luminescence signal intensity and sustainability are cell number and cell type specific. The RealTime-Glo™ Annexin V Apoptosis and Necrosis Assay has been configured to produce luminescence signal intensities proportional to the magnitude of the PS-inducing stimulus. The assay system utilizes a time-released luciferase substrate that is dependent upon inherent cellular esterase activity. In most cell types, steady-state generation of the luciferase substrate (from the prosubstrate) persists at a constant rate for exposures up to 48 h. Extremely efficacious inducers that provoke cell death in short time frames (<3–6 h) may substantially limit the luminescence signal intensity at 48 h. For inducers that mediate PS exposure near or after 48 h, it may be necessary to normalize the data collected at each time point to the untreated control (Subheading 3.1, **step 11**).
4. Although statistically rare, all viability, cytotoxicity, and caspase activity assay chemistries are subject to both specific and nonspecific interferences. Compounds with fluorescence properties or intense absorption in the visible spectrum may complicate assay measures or cause optical quenching. Unusually rich medium (20% or more animal serum) or complex support matrices (collagen or Matrigel) may also limit the availability of assay reactants and, therefore, sensitivity. For instance, the Necrosis Detection Reagent demonstrates high background in the presence of Matrigel, which greatly limits the probe's utility to report the presence of dead cells.

References

1. Elmore S (2007) Apoptosis: a review of programmed cell death. Toxicol Pathol 35 (4):495–516
2. Riss T, Moravec R (2004) Use of multiple assay endpoints to investigate the effects of incubation time, dose of toxin, and plating density in cell-based assays. Assay Drug Dev Technol 2:51–62
3. Niles A, Moravec R, Riss T (2009) In vitro viability and cytotoxicity testing and same-well multiparametric combinations for high throughput screening. Curr Chem Genomics 3:31–41
4. Jessel R, Haertel S, Socaciu C et al (2002) Kinetics of apoptotic markers in exogenously induced apoptosis of EL4 cells. J Cell Mol 6 (1):82–92
5. Niles A, Moravec R, Riss T (2008) Update on in vitro cytotoxicity assays for drug development. Expert Opin Drug Discov 3:655–669
6. Niles A, Riss T (2014) Multiplexed viability, cytotoxicity, and caspase activity assays. Methods Mol Biol 1219:21–33
7. Koopman G, Reutelinsperger C, Kuijten G, Keehnen R, Pals S, van Oers MH (1994) Annexin V for flow cytometric detection of phosphatidyl serine expression on B cells undergoing apoptosis. Blood 84:1415–1420
8. van Meer G, Voelker DR, Feigenson GW (2008) Membrane lipids: where they are and how they behave. Nat Rev Mol Cell Biol 9:112–124
9. van der Mark VA, Elferink R, Paulusma CC (2013) P4 ATPases: flippases in health and disease. Int J Mol Sci 14:7897–7922
10. Segawa K, Nagata S (2015) An apoptotic 'eat me' signal: phosphatidylserine exposure. Trends Cell Biol 25(11):639–650
11. Kupcho K, Schultz J, Hurst R et al (2019) A real-time, bioluminescent annexin V assay for the assessment of apoptosis. Apoptosis 24 (1–2):184–197

Chapter 7

Detection of Anoikis Using Cell Viability Dye and Quantitation of Caspase Activity

Roslyn Tedja, Alexandra Fox, and Ayesha B. Alvero

Abstract

Anoikis is a type of programmed cell death triggered by the loss of cellular interaction with the extracellular matrix (ECM) and culminates in the activation of caspases. Specific interaction between cellular receptors such as integrins and the ECM is important to maintain cellular homeostasis in normal tissues through multiple cascades. This interaction provides not only physical attachment, but more importantly, vital interaction with the actin cytoskeleton and growth factors. Normal epithelial and endothelial cells require this interaction with ECM to survive. In cancer, the acquisition of anoikis resistance is a hallmark of malignant transformation and is required in the process of metastasis formation. As such, strategies to inhibit and/or counteract anoikis resistance are important in controlling cancer progression. In this chapter, we describe the method for detecting anoikis using cell viability and caspase activity assays.

Key words Programmed cell death, Anoikis, Apoptosis, Cell viability, Spheroid, Caspase activation

1 Introduction

1.1 Apoptosis, Anoikis, and Programmed Cell Death

Apoptosis is a type of programmed cell death characterized by membrane blebbing, cell shrinkage, condensation of the chromatin, fragmentation of DNA, and formation of apoptotic bodies [1, 2]. Anoikis is the induction of apoptosis in anchorage-dependent cells and occurs upon the loss of attachment to the extracellular matrix (ECM) [3, 4]. Anoikis is elicited by the lack of interaction between integrin receptors and the correct ECM. The ECM is therefore not only required as a scaffold to promote physical attachment but is also fundamentally important in the activation of signaling cascades that support prosurvival signals through adaptor proteins and kinases [5, 6]. Similar to apoptosis, anoikis leads to the activation of caspases, which are cysteine proteases that cleave substrate protein at specific aspartic acid residues [2]. Caspases serve as primary effectors during anoikis to proteolytically dismantle most cellular components.

Ayesha B. Alvero and Gil G. Mor (eds.), *Detection of Cell Death Mechanisms: Methods and Protocols*, Methods in Molecular Biology, vol. 2255, https://doi.org/10.1007/978-1-0716-1162-3_7,

Integrins, cadherins, selectins, and cell adhesion molecules of the immunoglobulin superfamily (IgCAMs) are cellular receptors with integral functions in the sensing and stabilization of inherent interactions such as cell-to-cell and cell-to-ECM. These interactions strengthen the cellular commitment for survival, and their loss can lead to cell death [7]. Upon the disengagement of integrin receptors to the appropriate ECM, caspases are activated either through the intrinsic or extrinsic apoptotic pathways. Dynamic changes in the Bcl-2 family of proteins result in the activation of the apoptosome (intrinsic apoptotic pathway). Alternatively, the extrinsic apoptotic pathway may be activated through ligand binding to death receptors such as the Fas receptor and TNF-related apoptosis including ligand (TRAIL) receptor-1 and -2, [3, 8] resulting in the formation of the death-inducing signaling complex and caspase activation. Although the intrinsic and extrinsic pathways are initiated differently, these pathways converge to the same effector caspase, Caspase-3 [3]. Therefore, the quantification of Caspase-3 activity can serve as a marker of the anoikis cell death process.

The term anoikis originated from the Greek word that means "homelessness". The anoikis process was first reported by Steven M. Frisch and Hunter Francis in 1994, when they observed cell death in epithelial cells, but not fibroblast cells [9] upon detachment. Anoikis is an important cell death process that prevents inappropriate migration of cells, which can result in an abnormal growth in an ectopic environment. This is exemplified during the initiation and progression of cancer, wherein cells acquire resistance to cell death induced by detachment to ECM or neighboring adjacent cells [3, 10]. Anoikis resistance is an essential prerequisite to metastasis formation and is acquired through the process of epithelial-mesenchymal transition (EMT) [4]. Molecular mechanisms that support anoikis resistance in cancer cells include integrin and ECM rearrangement and reprograming as well as kinase-mediated inhibition of Bcl-2 proteins [3].

1.2 Assays for Detecting Anoikis and Spheroid Formation

The detection and quantification of anoikis as well as spheroid formation (i.e., anoikis resistance) are important components of studies that aim to understand how cancer cells gain migratory capacity and metastatic potential. Several kits are commercially available to detect and quantify anoikis. These kits are usually a combination of a colorimetric cell viability assay (MTT) with fluorescent dye such as ethidium homodimer, which is permeable only in cells that have lost cell membrane integrity. In this chapter, we describe an approach to quantify and detect anoikis in vitro using a commonly used cell viability assay (MTS) in combination with quantification of caspase activity as a readout of anoikis. Other cell viability assays such as ATP based, Live-cell protease based, and MTT cell viability assays may be used in place of MTS assay.

2 Materials

2.1 Equipment and Disposables

1. Microplate reader (Abs at 490 nm).
2. Luminometer.
3. Tissue culture incubator.
4. Centrifuge.
5. Microcentrifuge.
6. Pipettes.
7. 6-well Ultra-low attachment plates.
8. 6-well tissue culture treated plates.
9. 15 mL conical tubes.
10. Microcentrifuge tubes.

2.2 Cell Lines and Reagents

1. Anoikis resistant cells (i.e., A2780 human ovarian cancer cells or THP-1 human monocytic leukemia cells); these cells can be used as positive control for anoikis resistance.
2. Anoikis sensitive cells (i.e., OVCA433 human ovarian cancer cells are generally more sensitive to anoikis than A2780 and can be used as a positive control for anoikis sensitive cells; alternatively, normal epithelial cells can be used although these are usually less available).
3. Appropriate Growth media for cells.
4. 0.05% Trypsin-EDTA.
5. Fetal bovine serum (FBS).
6. Cell viability dye (in this chapter, we used CellTiter 96® AQ_{ueous} One Solution Reagent from Promega).
7. Caspase activity assay (in this chapter, we used Caspase-Glo 3/7 Assay from Promega).
8. Protease Inhibitor Cocktail: 25×.
9. 25 mM Phenylmethylsulfonyl fluoride (PMSF): 4.36 mg of lyophilized PMSF + 1 mL ethanol.
10. 10× Cell Lysis Buffer: 20 mM Tris–HCl pH 7.5, 150 mM NaCl, 1 mM Na_2EDTA, 1 mM EGTA, 1% Triton, 2.5 mM Sodium pyrophosphate, 1 mM β-glycerophosphate, 1 mM Na_3VO_4, 1 μg/mL Leupeptin.
11. Commercially available protein quantitation kit (i.e., Bradford or BCA assay).

3 Methods

3.1 Cell Viability Assay

1. Grow the cells of interest in appropriate growth media to around 80% confluency. It is never recommended to use over confluent cells.
2. Seed the cells in a concentration range of 2×10^5 to 5×10^5 cells/well of a 6-well ultralow attachment plate (ULA plate) with 2 mL of complete growth media at 37 °C in a humidified 5% carbon dioxide atmosphere. We recommend to start with 4×10^5 cells/well. Make sure that the cells are in single cell suspension (*see* **Note 1**). The number of wells seeded depends on the number of timepoints desired. We recommend having at least three timepoints.
3. Keep the cells growing in monolayer cultures. These will be used as "Control" or Time 0.
4. Incubate the cells at 37 °C in a humidified 5% carbon dioxide atmosphere. Timepoints depend on the cell lines used. We recommend an early timepoint of 8 h and a late timepoint of 72 h. Several other timepoints in between may be useful. In our human epithelial ovarian cancer model, the reduction in percentage of viable cells has been detected as early as 8 h and progressed up to 72 h.
5. At the end of the timepoints, collect cells in conical tubes. Also, collect the cells grown in monolayer by trypsinization and collect in conical tubes.
6. Centrifuge for 5 min at ~700 × *g* at room temperature.
7. Remove the supernatant and resuspend the cells in 500 μL of 0.05% Trypsin-EDTA to break any spheroid aggregates (*see* **Note 2**).
8. Incubate at 37 °C for 5 min. Neutralize the trypsin by adding FBS to a final concentration of 5%.
9. Centrifuge at ~700 × *g* for 5 min at room temperature. Remove the supernatant.
10. Add 240 μL of complete growth media to the cell pellet and mix by pipetting. Additionally, prepare in a separate tube a blank or negative control by adding 240 μL of complete growth media with no cell pellet.
11. Add 60 μL of Cell Viability dye to each sample.
12. Incubate the plate at 37 °C for 1 h in a humidified, 5% CO_2 atmosphere.
13. Mix the samples by pipetting. Then, transfer 90 μL of the sample to one well of a 96-well plate. Distribute each sample to three separate wells to have three independent readings.

14. Record the absorbance at 490 nm using a 96-well plate reader (*see* **Note 3**).

3.2 Caspase Activity Assays

The Caspase-Glo® 3/7 activity assay is to be performed together with the cell viability assay to detect anoikis. The protocol is as follows:

1. Grow the cells of interest in their complete growth media to around 80% confluency at 37 °C in a humidified 5% carbon dioxide atmosphere.
2. Seed the cells in a concentration range of 2×10^5 to 5×10^5 cells/well of a 6-well ultralow attachment plate (ULA plate) with 2 mL of complete growth media at 37 °C in a humidified 5% carbon dioxide atmosphere. (We recommend to start with 4×10^5 cells/well. Make sure that the cells are in single cell suspension (*see* **Note 4**).). The number of wells seeded depends on the number of timepoints desired. We recommend having at least three timepoints.
3. Keep the cells growing in monolayer cultures. These will be used as "Control" or Time 0.
4. Incubate the cells at 37 °C in a humidified 5% carbon dioxide atmosphere. Timepoints may depend on the cell line used. We recommend an early timepoint of 8 h and a late timepoint of 72 h. Several other timepoints in between may be helpful.
5. At the end of the timepoints, collect cells in conical tubes. Also, collect the cells grown in monolayer by trypsinization and collect in conical tubes.
6. Centrifuge for 5 min at ~700 × *g* at room temperature.
7. Remove the supernatant and add 2 mL of PBS to wash. Centrifuge at 700 × *g* for 10 min.
8. Remove supernatant, add 60 μL of cell lysis buffer to the cell pellet, and incubate for 15 min on ice with intermittent vortexing.
9. Centrifuge at ~8000 × *g* for 15 min at 4 °C. Transfer the cell lysate to a fresh microcentrifuge tube.
10. Quantify protein concentration using commercially available assay.
11. Prepare the Caspase-Glo® 3/7 Reagent as per manufacturer's instructions. Allow the reagent to equilibrate to room temperature and mix well.
12. Transfer 10 μg of cell lysate to fresh microcentrifuge tubes and add enough water for a final volume of 25 μL.
13. Prepare positive control (*see* **Note 4**) and negative control (25 μL of water).

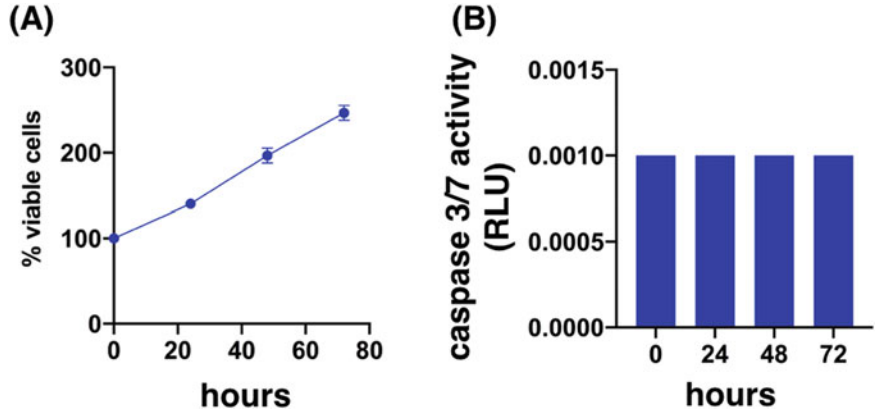

Fig. 1 Percentage of viable cells (**a**) and caspase-3/7 activity (**b**) in anoikis-resistant ovarian cancer cells cultured in ultralow attachment plate; *RLU* relative luminescence unit

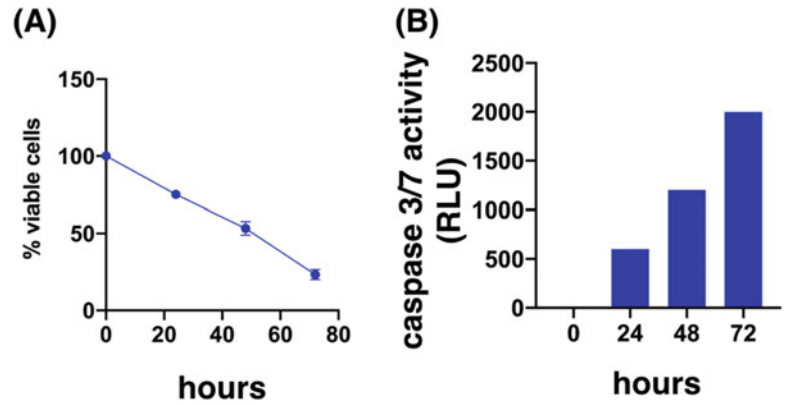

Fig. 2 Percentage of viable cells (**a**) and caspase-3/7 activity (**b**) in anoikis-sensitive ovarian cancer cells cultured in ultralow attachment plate; *RLU* relative luminescence unit

14. Add 25 μL of Caspase-Glo® 3/7 Reagent to each tube and incubate at room temperature for 1 h in the dark.
15. Measure the luminescence for each sample using luminometer (*see* **Note 5**).

Figures 1 and 2 show typical results obtained from anoikis-resistant and anoikis-sensitive cells, respectively.

4 Notes

1. Alternatively, cells can be seeded in ultralow 96-well plates.
2. If the spheroids are hard to break, perform repeated vortexing to aid the detachment of cells from the spheres and obtain single cells. If the cell-to-cell attachment is too strong to

break with trypsin treatment, there are alternative assays available to quantify the cell viability in cultures of spheroids (i.e., CellTiter-Glo® 3D Cell viability assay from Promega). This assay does not require the trypsinization step to break the spheroid, as the assay reagent is able to penetrate the spheroids.

3. The absorbance reading is the quantitation of a colored formazan product resulting from the conversion of MTS tetrazolium compound accomplished by NADPH or NADH produced by dehydrogenase enzymes in metabolically active cells. Typical absorbance at 490 nm of blank (complete growth media with 10% FBS) after 1 h of incubation at 37 °C is 0.001. The absorbance reading can be converted to the percent of viable cells at a particular timepoint, using the following formula:

$$\%\ \text{of viable cells} = \frac{\left(\text{Average Abs}_{490\text{nm}}\text{sample}_{T_1} - \text{Average Abs}_{490\text{nm}}\text{blank}\right)}{\left(\text{Average Abs}_{490\text{nm}}\text{sample}_{T_0} - \text{Average Abs}_{490\text{nm}}\text{blank}\right)} \times 100\%,$$

$$\text{Average Abs}_{490\text{nm}}\text{sample}_{T_1} = \text{average of the absorbance reading at 490 nm of cells cultured in ULA for particular time point,}$$

$$\text{Average Abs}_{490\text{nm}}\text{sample}_{T_0} = \text{average of the absorbance reading at 490 nm of cells cultured at time 0 (time of cell seeding)}$$

4. We suggest including a positive control for the caspase activity assay. If using A2780, caspase 3 activation can be observed by treating the cells with 0.2 μM Paclitaxel for 24 h.
5. The increase in the luminescence reading from Caspase-Glo® 3/7 assay indicates the increase in caspase 3/7 activity, which demonstrates the induction of anoikis. In our system, Paclitaxel treatment (described in **Note 4** for A2780) results in luminescence of 1500 to 2500 relative luminescence units (RLUs). Caspase 3/7 activation secondary to anoikis results in lower RLU although a decrease in cell viability (observed with the colorimetric assay) is typically associated with at least twofold increase in RLU when compared to Control.

References

1. Elmore S (2007) Apoptosis: a review of programmed cell death. Toxicol Pathol 35 (4):495–516. https://doi.org/10.1080/01926230701320337
2. McIlwain DR, Berger T, Mak TW (2013) Caspase functions in cell death and disease. Cold Spring Harb Perspect Biol 5:a008656
3. Paoli P, Giannoni E, Chiarugi P (2013) Anoikis molecular pathways and its role in cancer progression. Biochim Biophys Acta 1833 (12):3481–3498. https://doi.org/10.1016/j.bbamcr.2013.06.026
4. Kim Y-N, Koo KH, Sung JY, Yun U-J, Kim H (2012) Anoikis resistance: an essential prerequisite for tumor metastasis. Int J Cell Biol 2012:306879. https://doi.org/10.1155/2012/306879
5. Gilmore AP (2005) Anoikis. Cell Death Differ 12(2):1473–1477. https://doi.org/10.1038/sj.cdd.4401723

6. Reddig PJ, Juliano RL (2005) Clinging to life: cell to matrix adhesion and cell survival. Cancer Metastasis Rev 24(3):425–439. https://doi.org/10.1007/s10555-005-5134-3
7. Nagaprashantha LD, Vatsyayan R, Lelsani PCR, Awasthi S, Singhal SS (2011) The sensors and regulators of cell-matrix surveillance in anoikis resistance of tumors. Int J Cancer 128(4):743–752. https://doi.org/10.1002/ijc.25725
8. Wang P, Valentijn AJ, Gilmore AP, Streuli CH (2003) Early events in the Anoikis program occur in the absence of caspase activation. J Biol Chem 278(22):19918–19925
9. Frisch SM, Francis H (1994) Disruption of epithelial cell-matrix interactions induces apoptosis. J Cell Biol 124(4):619–626. https://doi.org/10.1083/jcb.124.4.619
10. Simpson CD, Anyiwe K, Schimmer AD (2008) Anoikis resistance and tumor metastasis. Cancer Lett 272(2):177–185. https://doi.org/10.1016/j.canlet.2008.05.029

Chapter 8

Time- and Dose-Dependent Toxicity Studies in 3D Cultures Using a Luminescent Lactate Dehydrogenase Assay

Natasha Karassina, Peter Hofsteen, James J. Cali, and Jolanta Vidugiriene

Abstract

Three-dimensional (3D) in vitro systems closely resemble tissue microenvironments and provide predictive models for studying cytotoxic drug responses. The ability to capture the kinetic profiles of such responses in a dynamic and noninvasive way can further advance the utility of 3D cell cultures. Here, we describe the use of a luminescent lactate dehydrogenase (LDH) toxicity assay for monitoring time- and dose-dependent effects of drug treatment in 3D cancer spheroids. HCT116 spheroids formed in 96-well ultralow attachment plates were treated with increasing drug concentrations. Medium samples were collected at different timepoints, frozen, stored, and analyzed at the end of experiments using the luminescent LDH-Glo™ Assay. High assay sensitivity and low volume sampling enabled drug-induced toxicity profiling in a time- and dose-dependent manner.

Key words 3D spheroids, Time-dependent cytotoxicity, LDH, LDH-Glo, 96-well ultralow attachment plates

1 Introduction

An ongoing challenge for in vitro cytotoxicity screening is the search for simple and robust assays that are predictive of in vivo responses. This is partly due to the diverse array of cell death mechanisms and the numerous assays developed to measure such specific responses [1, 2]. It is also due to the in vitro environment itself. Monolayer cell cultures (2D) are routinely used as initial model systems for evaluating safety and efficacy of drug molecules. However, 2D models do not adequately resemble the complexity of the tissue microenvironment in vivo [3, 4]. To better predict in vivo responses and compound efficacy, three-dimensional (3D) cell culture models have been developed [3]. It has been shown that 3D cell models represent a more biological relevant in vitro cell culture system that better predicts in vivo responses [3, 5, 6]. Thus, selecting the appropriate cytotoxicity assay as well as the culturing

Ayesha B. Alvero and Gil G. Mor (eds.), *Detection of Cell Death Mechanisms: Methods and Protocols*, Methods in Molecular Biology, vol. 2255, https://doi.org/10.1007/978-1-0716-1162-3_8,

environment should be considered in order to obtain prognostic and physiologically relevant data.

Lactate dehydrogenase (LDH) is a soluble stable cytosolic enzyme that is present in most cell types and is a widely used marker in cytotoxicity studies [7–9]. Upon cell membrane damage, LDH is rapidly released into the cell culture medium and can be detected by measuring the enzymatic activity by colorimetric, fluorometric, or as we describe here, luminescence methods (LDH-Glo™ Cytotoxicity Assay). We show that the LDH-Glo™ assay is applicable to cells in 3D cultures and offers an additional advantage for time-dependent toxicity testing over standard LDH assays.

1.1 Principal of Bioluminescent LDH Assay

The LDH-Glo™ assay is based on coupling LDH activity to activation of a reductase substrate that drives light output by luciferase (Fig. 1a). An LDH Detection Reagent is added to a sample of diluted cell culture medium at a 1:1 ratio. Upon reagent addition, the enzyme-coupled reaction begins and by approximately 30 min, the coupled enzyme reaction reaches equilibrium. Light generated at equilibrium is directly proportional to the amount of LDH present in the sample. Luminescence signal increases until all the reductase substrate is converted to luciferin, and the reaction is no longer in the linear range of the assay.

The important practical considerations for using LDH-Glo™ are (1) assay sensitivity and linearity, (2) sample collection, dilution, and storage, and (3) stability of LDH released from dead cells.

1.2 Assay Sensitivity and Linearity

Luminescent LDH detection provides high sensitivity and wide dynamic range. As shown in Fig. 1b, LDH released from ten A549 cells lysed in 50 µL is detected with a 32-fold signal above background. The signal remains linear up to 1000 cells/well reaching greater than 1000-fold increase above assay background. LDH-Glo™ is not homogeneous in that media samples are removed and placed into a new assay plate for measurement. However, the high sensitivity of the assay provides the unique advantage of collecting samples at different timepoints. For example, if 10,000 cells are cultured in 100 µL of media, less than 2 µL of sample will be required for each measurement. This corresponds to less than 2% of the total medium volume, enabling sampling at multiple timepoints without a significant impact on cell growth or treatment response.

1.3 Sample Collection, Dilution, and Storage

Collecting samples at different times for freezing and storage without compromising LDH activity is desirable for time-dependent toxicity studies. Freezing LDH in medium or PBS results in rapid loss of LDH activity. In contrast, LDH is stabilized when samples are diluted in the LDH Storage Buffer described below. As shown in Fig. 1c, samples collected from A549 cells treated with digitonin to release LDH showed similar light output and EC_{50} values regardless if they were analyzed immediately or after freezing and thawing.

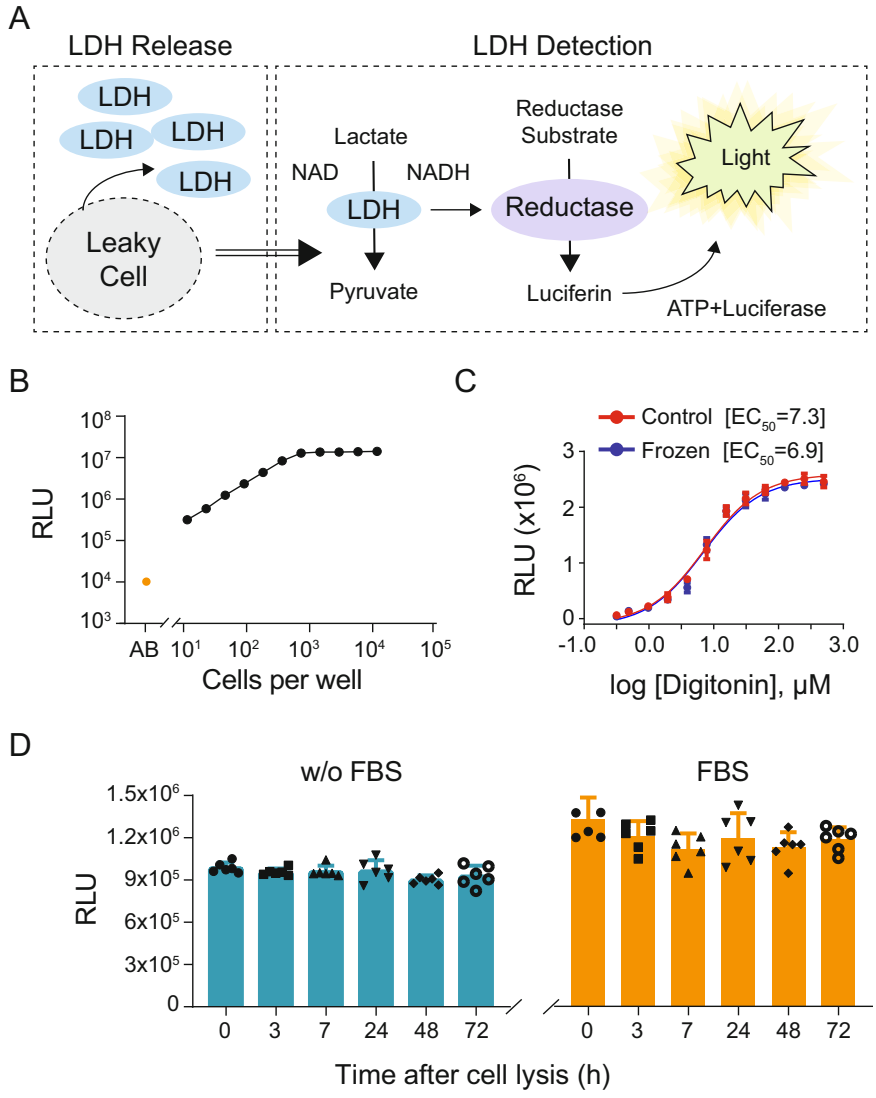

Fig. 1 Measuring time-dependent cytotoxicity with LDH-Glo Assay. (**a**) Schematic of the assay mechanism. Lactate dehydrogenase (LDH) is released in the medium from dying cells that is then removed from the well and mixed with LDH detection reagents. LDH facilitates lactate oxidation that simultaneously reduces NAD to NADH. Reductase reacts with NADH and the reductase substrate to form luciferin, which generates light when in the presence of ATP and luciferase. (**b**) A549 cell lysates were serially diluted in LDH storage buffer constituting the cell numbers indicated. Medium only wells were included for assay background (AB; orange dot). (**c**) A549 cells were incubated with increasing concentrations of digitonin. Data in C compare samples that have undergone a freeze–thaw to those that were not frozen. Data indicated that LDH is stable and can be collected and stored at −20 °C. (**d**) LDH released into the medium after cell death retains activity for at least 72 h. HepG2 cells cultured with medium in the absence (**left**) or presence (**right**) of serum were sonicated and dispensed in a 24-well plate and incubated for 72 h. A small amount of culture medium was removed at the indicated times and LDH was measured. *RLU* Relative Luminescence Units

1.4 LDH Stability

An important consideration for time-dependent toxicity studies is the stability of the released toxicity marker in cell culture medium. Serum, a common component of cell culture medium, contains a significant amount of active LDH, suggesting that it is relatively stable under cell culture conditions. We examined the stability of LDH released from dead cells by monitoring LDH activity at different timepoints after cell lysis. HepG2 cell lysates prepared in medium with and without serum were incubated under cell culture conditions. No decrease in LDH activity was measured for up to 72 h in either group (Fig. 1d). These data indicate that LDH released from dying cells is stable in cell culture medium, making the assay amendable for time-dependent toxicity studies by sampling from the same well over time.

2 Materials

The materials and methods described below outline a general protocol for forming 3D cancer spheroids in 96-well ultralow adherence plates and using the luminescent LDH assay for monitoring time- and dose-dependent toxicity (Figs. 2 and 3). Standard cell culture procedures, used for cell growth and preparation, are not described in detail.

2.1 Equipment

1. Single- and Multi-channel pipettors and reagent reservoirs.
2. Ultra-low 96 well microplates, black-walled/clear round-bottom.
3. White, opaque-walled 96-well plates for sample collection and LDH assay.
4. Centrifuge.
5. Plate-reading luminometer.
6. Thermal Adhesive Sealing Film.

2.2 Reagents

1. Spheroid forming cells such HCT 116 cancer cells.
2. Complete medium: DMEM supplemented with 10% heat-inactivated fetal bovine serum, 4.5 g/L D-Glucose, L-Glutamine, 100 mg/L sodium pyruvate.
3. 0.25% Trypsin.
4. LDH Storage Buffer: 200 mM Tris–HCl (pH 7.3), 10% glycerol, 1% BSA.
5. Cytotoxic agent such as bortezomib: 10 mM stock in dimethyl sulfoxide (DMSO).
6. DMSO for vehicle control.
7. Triton X100.
8. LDH-Glo™ Cytotoxicity Assay (Promega).

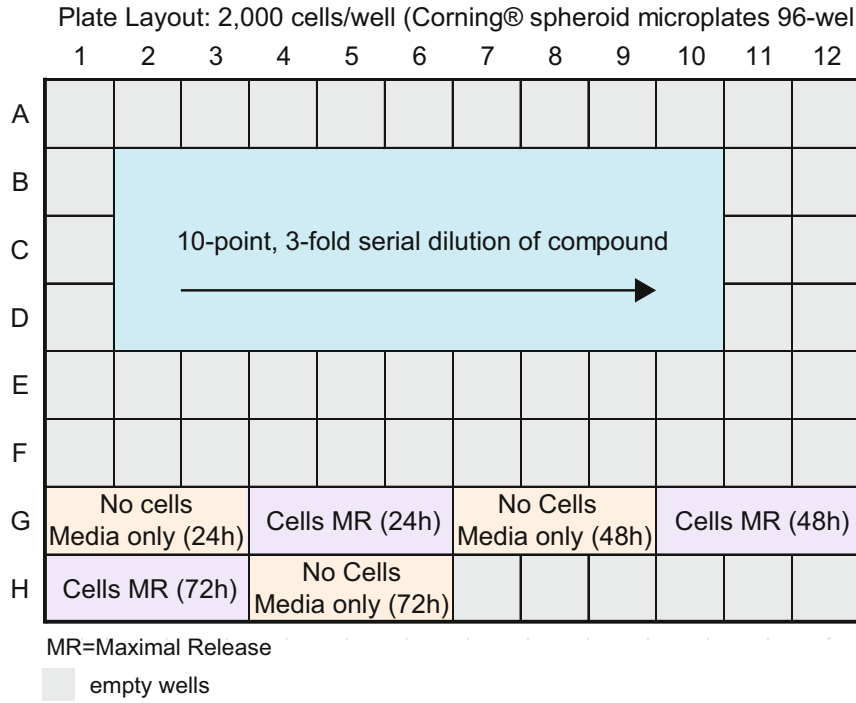

Fig. 2 Example of a 96-well assay plate set-up for spheroid formation and LDH detection

3 Methods

Here, we provide an example protocol for measuring time- and dose-dependent LDH release in 3D cancer spheroids. The experimental plate layout is shown in Fig. 2, and the data are summarized in Fig. 3.

3.1 3D Spheroid Formation

1. Set up experiment in Ultralow 96-well Black-walled/Clear Round-Bottom Microplate. An example plate layout is illustrated in Fig. 2.
2. Trypsinize cells, collect, spin down, and resuspend in complete DMEM medium at 2×10^4 viable cells/mL (*see* **Note 1**).
3. Add 100 µL to wells B2-10, C2-10, and D2-10 for 10-point, three-fold serial dilution of test agent. For this chapter, we use bortezomib treatment in triplicates (*see* Fig. 2).
4. Add 100 µL to wells G4-6, G10-12, and H1-3 for maximum LDH Release Control at 24 h, 48 h, and 72 h (*see* **Note 2** and Fig. 2).
5. Add 100 µL of complete DMEM medium without cells to wells G1-3, G7-9, and H4-6 to serve as a negative control for culture medium background (*see* Fig. 2).

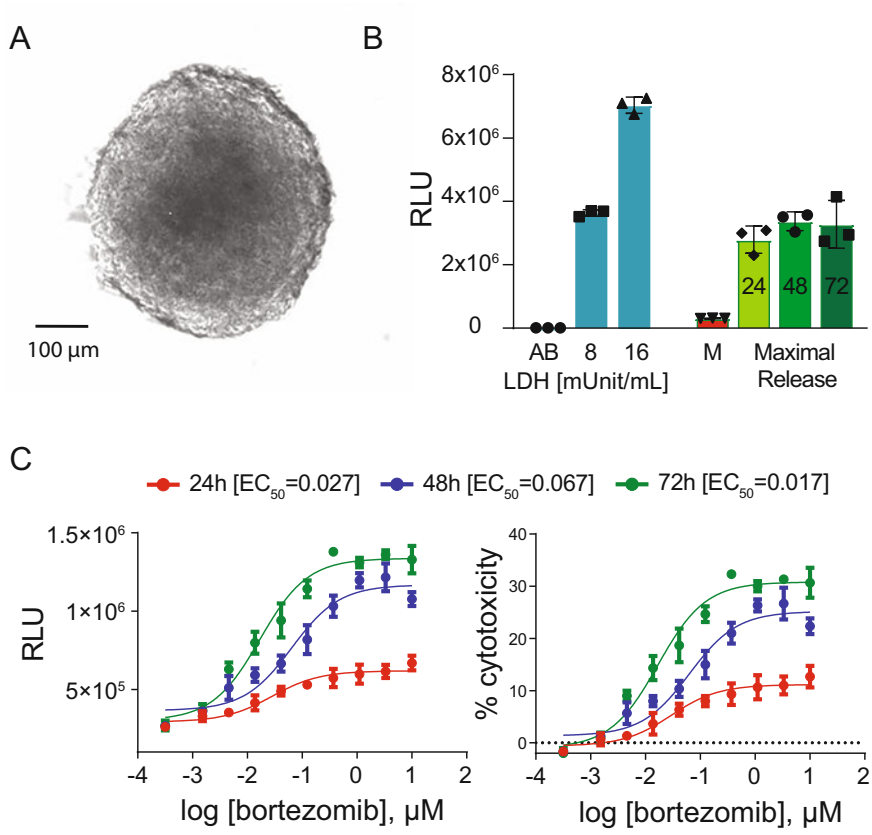

Fig. 3 Sequential LDH release from the same well of 3D spheroids. Representative data obtained using the methods described in this chapter. (**a**) Phase contrast image of formed spheroid from 2000 HCT116 cells after 72 h. (**b**) LDH standards and Maximal LDH release measurements at 24, 48, and 72 h. Purified rabbit Lactate Dehydrogenase (LDH) was added to assay wells at 8 and 16 mUnit/mL and detected using the LDH-Glo detection reagents. No LDH standard was added to the LDH detection reagents for assay background (AB) control. Maximal release from lysed spheroids was measured and compared with the LDH standards to determine linear range (*see* **Note 15**). Of note, nonspecific background levels of LDH are measured in the medium (M) due to the LDH presence in fetal bovine serum. (**c**) Time- and concentration-dependent cytotoxicity measurements using HCT116 spheroids treated with Bortezomib at indicated times (24, 48, and 72 h). LDH release increased as a result of increasing concentrations of Bortezomib and extended incubation times. Percent cytotoxicity was calculated using the equation described in the protocol. Data were fitted to a 3-parameter logistic curve, and EC_{50} was calculated using GraphPad Prism® software. *RLU* Relative Luminescence Units, *h* hour

6. Centrifuge plate at 300 × *g* for 2 min at room temperature (*see* **Note 3**).
7. Culture the plate at 37 °C in a 5% CO_2 tissue culture incubator for 72 h to form spheroids.
8. Examine spheroid formation under the microscope (*see* **Note 4**).

3.2 Drug Treatment

1. Make 20 μM bortezomib solution (2× final) in DMEM medium without serum (*see* **Note 5**).
2. Perform 10-point, three-fold serial dilutions in DMEM containing 0.1% DMSO (*see* Fig. 2). Do not transfer to the last point. It will serve as a vehicle control (*see* **Note 6**).
3. Remove plate with the cells from the incubator and briefly centrifuge at 300 × *g* for 2 min at room temperature (*see* **Note 7**).
4. Remove 50 μL of medium from each well (*see* **Note 8**).
5. Add 50 μL of prepared bortezomib dilutions to B2-10, C2-10, and D2-10 wells (*see* Fig. 2).
6. Add 50 μL of media without serum to control wells (G4-6, G10-12, and E7-10 and G1-3, G7-9, and F10-12).
7. Put the plate back into tissue culture incubator.

3.3 Media Sample Collection

1. Prepare LDH Storage Buffer (recipe described in Subheading 2.2, **item 4**; *see* **Note 9**).
2. At each timepoint (24, 48, and 72 h), prepare sample collection plate by adding 95 μL of LDH storage buffer to the white, opaque-walled 96-well plate (*see* **Note 10**).
3. Remove plate with the cells from the incubator and briefly centrifuge at 300 × *g* for 2 min at room temperature (*see* **Note 7**).
4. Add 2 μL of 10% Triton X100 to maximum LDH Release Control wells, put back into incubator, and incubate for 10–15 min (*see* **Note 11**).
5. Transfer 5 μL of cell culture medium from each experimental and control well into the plate containing LDH Storage Buffer.
6. Cover assay plate with adhesive sealing film and store the samples below −20 °C (*see* **Note 12**).

3.4 Measuring LDH Activity

1. Prepare the required amount of LDH Detection Reagent by adding 5 μL of Reductase Substrate to 1 mL of LDH Detection Enzyme Mix (*see* **Note 13**).
2. Thaw frozen samples and equilibrate them to room temperature.
3. Transfer 10 μL of samples into a new 96-well white opaque-walled assay plate.
4. Dilute the samples further by adding 40 μL of LDH Storage Buffer (*see* **Note 14**).
5. If needed for determining assay linearity, include wells containing 50 μL of LDH positive control diluted in LDH Storage Buffer at the concentrations within the linear range of the assay, for example, 8 and 16 mUnit/mL (*see* **Note 15** and Fig. 3b).

6. Add 50 μL of LDH Detection Reagent to each well.
7. Incubate for 60 min at room temperature (*see* **Note 16**).
8. Record luminescence (*see* **Note 17**).
9. Calculate % cytotoxicity if needed using the formula below:

$$\%\text{Cytotoxicity} = 100 \times [(\text{LDH Release} - \text{MB})/(\text{MR} - \text{MB})]$$

where MB = medium background and MR = Maximal LDH Release.

4 Notes

1. For experiment shown in Fig. 3, 10^5 HCT116 cells were collected and resuspended in 5 mL of complete DMEM media. The cells were transferred into reagent reservoir and dispensed into the low attachment assay plate using a multichannel pipettor. Prepare at least 10% more volume of cell suspension to account for loss during dispensing and mix before dispensing as the cells start to settle with time. The size of the spheroids can be controlled by initial cell seeding density.
2. It is important to understand Maximum LDH Release and cell growth at each timepoint when interpreting toxicity data. To this end, consider the contrasting examples of high versus low test compound treatments applied to proliferating cells. To the extent that treatments do not completely inhibit proliferation over the experimental time course, a low concentration may permit a greater growth rate than a high concentration, leading to a greater cell number and greater total LDH at low versus high concentration. In this scenario, low concentration-induced LDH release may be less than, similar to, or even greater than high concentration-induced release. However, as a percentage of total LDH, high concentration-induced release is likely greater than low concentration-induced release. When setting up maximum LDH release controls at different timepoints during an experiment, it is recommended to separate TritonX-100 treated with experimental wells to avoid cross contamination.
3. *Critical step*: briefly, centrifuge the plate at 300 × *g* for 5 min at room temperature in order to bring cells together at the bottom of the microplate. This step facilitates quick cell congregation and spheroid formation.
4. Formed spheroids appear as a single uniform multicellular globule (*see* image in Fig. 3a).
5. LDH is present in serum and increases the assay background. To avoid marked increases in assay background, we

recommend decreasing the serum concentrations to 2.5–5% if possible. Performing treatments at the lower FBS concentration does not significantly affect cell health and will lower the assay background while improving sensitivity. In this experiment, since the spheroids were plated in medium containing 10% FBS and to avoid medium exchanges that may lead to loss of the spheroids, we removed only 50% of the medium before adding drug treatment. Making drug dilutions in serum free medium reduced the final FBS concentration to 5%.

6. A vehicle control (no treatment DMSO control) should be included for measuring basal LDH levels. This control is one of the nine points of the compound titration illustrated in Fig. 2.
7. A quick plate spin helps to keep formed spheroids at the bottom of the plate before removing or adding medium.
8. Medium removal or addition can be done with an automated system or manually. Critical step: use only sides of the well to remove or add medium to minimize disturbing or inadvertently discarding spheroids. To decrease the risk of dislodging the spheroids, we removed 50 μL (50%) of spent media and added 50 μL of bortezomib solution prepared at 2× final concentration.
9. LDH Storage Buffer can be prepared and stored at +4 °C for a few months. Equilibrate LDH Storage Buffer to room temperature before use.
10. It is possible to use the same plate for freezing the samples at different timepoints if only a few samples need to be analyzed.
11. After adding Triton X100 for LDH maximal release, gently mix up and down a few times. This helps disrupt the spheroid to facilitate maximal LDH release.
12. Adhesive sealing film prevents accidental spilling of samples in a plate as well as reducing evaporation during freezing.
13. Calculate and prepare the necessary volume of LDH Detection Reagent and mix gently by inverting. The reagent should be used within 5 h. Discard any remaining reagent (do not freeze).
14. Collected samples can be further diluted if more cells are used for spheroid formation, and serum is present in order to keep signals with the linear range of the assay. In Fig. 3, 5 μL of each sample were collected at each timepoint from HCT116 cancer spheroids formed using 2000 cells/well and were diluted 40-fold for LDH detection. Using those conditions, the measured luminescence signal was within the linear range and maximum LDH release was measured with 12-fold signal above the background (Fig. 3b, c), providing a robust assay window for toxicity studies.

15. LDH positive control included in the LDH-Glo™ kit can be used for establishing the linear range of the assay. In general, LDH controls below 32 mU/mL are within the linear range of the assay. As shown in Fig. 3, increasing LDH concentration by twofold (from 8 mU/mL to 16 mU/mL) resulted in twofold increase in light output and the light output from all the samples was below LDH control, indicating that the measurements were taken within the linear range of the assay.
16. After an initial 30-min incubation with LDH Detection Reagent, luminescence can be read multiple times, for example, 30 and 60 min. Reading the plate several times will also help to determine if the measurements are in the linear range for luminescence. This is an enzymatic assay, and linearity is dependent on reaction time and released LDH.
17. We recommend using a 0.5 s integration time for 96-well plate.

References

1. Méry B, Guy JB, Vallard A, Espenel S, Ardail D, Rodriguez-Lafrasse C, Rancoule C, Madne N (2017) In vitro cell death determination for drug discovery: a landscape review of real issues. J Cell Death 10:1–8. https://doi.org/10.1177/1179670717691251
2. Riss T, Niles A, Moravec R, Karassina N, Vidugiriene J (2004) Cytotoxicity assays: in vitro methods to measure dead cells. In: Sittampalam GS, Grossman A, Brimacombe K et al (eds) Assay guidance manual. Eli Lilly and the National Center for Advancing Translational Sciences, Bethesda (MD)
3. Kapalczynska M, Kolenda T, Przybyla W, Zajaczkowska M, Teresiak A, Filas V, Ibbs M, Blizniak R, Luczewski L, Lamperska K (2018) 2D and 3D cell cultures—a comparison of different types of cancer cell cultures. Arch Med Sci 14(4):910–919. https://doi.org/10.5114/aoms.2016.63743
4. Langhans SA (2018) Three-dimensional in vitro cell culture models in drug discovery and drug repositioning. Front Pharmacol 9:6. https://doi.org/10.3389/fphar.2018.00006
5. Duval K, Grover H, Han LH, Mou Y, Pegoraro AF, Fredberg J, Chen Z (2017) Modeling physiological events in 2D vs. 3D cell culture. Physiology (Bethesda) 32(4):266–277. https://doi.org/10.1152/physiol.00036.2016
6. Lv D, Hu Z, Lu L, Lu H, Xu X (2017) Three-dimensional cell culture: a powerful tool in tumor research and drug discovery. Oncol Lett 14(6):6999–7010. https://doi.org/10.3892/ol.2017.7134
7. Fotakis G, Timbrell JA (2006) In vitro cytotoxicity assays: comparison of LDH, neutral red, MTT and protein assay in hepatoma cell lines following exposure to cadmium chloride. Toxicol Lett 160(2):171–177. https://doi.org/10.1016/j.toxlet.2005.07.001
8. Kumar P, Nagarajan A, Uchil PD (2018) Analysis of cell viability by the lactate dehydrogenase assay. Cold Spring Harb Protoc 2018(6). https://doi.org/10.1101/pdb.prot095497
9. Decker T, Lohmann-Matthes ML (1988) A quick and simple method for the quantitation of lactate dehydrogenase release in measurements of cellular cytotoxicity and tumor necrosis factor (TNF) activity. J Immunol Methods 115 (1):61–69. https://doi.org/10.1016/0022-1759(88)90310-9

Chapter 9

Visualization and Quantification of Neutrophil Extracellular Traps

Mancy Tong and Vikki M. Abrahams

Abstract

Neutrophils are innate immune cells that play important roles in many physiological and pathological processes, including immune defense and cancer metastasis. In addition to the release of proinflammatory cytokines, chemokines, and cytoplasmic granules containing digestive proteins, in recent years, neutrophils have been observed to release neutrophil extracellular traps (NETs) that consist of extracellular DNA associated with antimicrobial proteins, such as histones and myeloperoxidase. These NETs are increasingly being recognized as an important mechanism of neutrophil host defense and function. This chapter will summarize the current literature on the known processes of NET formation and describe in detail an immunofluorescence approach that can be employed to visualize and quantify NETs in vitro.

Key words NETs, Extracellular DNA, Activation, Myeloperoxidase, Sytox, PicoGreen, Citrullination

1 Introduction

Neutrophils are the body's first line of defense against pathogens. They rapidly migrate to sites of infection by following gradients of chemoattractants such as endogenous interleukin (IL)-8 or bacterial *N*-formyl peptides where they can neutralize pathogens through several mechanisms. Neutrophils can eliminate pathogens by phagocytosis, release of destructive reactive oxygen species (ROS), and secretion of chemokines and cytokines that can propagate inflammation and recruit and activate additional immune cells [1, 2]. Furthermore, neutrophils can exocytose cytoplasmic granules containing degradative enzymes and antimicrobial proteins that can neutralize pathogens extracellularly; this process is termed degranulation [1, 2]. More recently, a novel mode of extracellular killing has been observed: the release of neutrophil extracellular traps (NETs), which are DNA webs, decorated with antimicrobial proteins and enzymes, can entrap and neutralize pathogens close to the neutrophil [3, 4]. In addition to the antimicrobial effect of NETs, recent studies have also reported their involvement in the

Ayesha B. Alvero and Gil G. Mor (eds.), *Detection of Cell Death Mechanisms: Methods and Protocols*, Methods in Molecular Biology, vol. 2255, https://doi.org/10.1007/978-1-0716-1162-3_9,

propagation of inflammation and in noninfectious disease settings such as autoimmunity, thrombosis, and cancer metastasis [2, 5–7]. Thus, a better understanding of the triggers and mechanisms of NET formation and their downstream effects may be relevant to many biomedical fields.

1.1 Composition of NETs and Their Formation

NET formation is commonly induced in vitro by chemicals such as phorbol myristate acetate (PMA) or calcium ionophores (A23187). PMA-induced NET release requires ROS production mediated by NADPH oxidase, while A23187-induced NET release occurs independent of NADPH oxidase activity and instead relies on mitochondrial-derived ROS [8]. Likewise, physiologically, *E. coli* lipopolysaccharide (LPS)-induced NETs require NADPH oxidase activity, while *S. aureus* and Leishmania induce NETs independent of NADPH oxidase activity [9, 10]. Using PMA as the classic inducer of NETs, the intracellular processes involved in NET release have been investigated in detail. It has been observed that around 2 h poststimulation, there is breakdown of the nuclear envelop, which allows enzymes such as myeloperoxidase (MPO) and neutrophil elastase (NE) to migrate from cytoplasmic granules into the nucleus where they help facilitate chromatin decondensation [4]. There is also activation of protein arginine deiminase (PAD)4, which citrullinates histones 3 and 4 to aid chromatin decondensation. Around 4 h poststimulation, neutrophils burst to release NETs consisting of nuclear DNA and associated antimicrobial enzymes and proteins [4]. Recent proteomic studies have revealed that depending upon the stimulus, different proteins will be associated with the NET structures and their posttranslational modifications may also differ [11, 12]. Thus, NETs induced under different conditions may have different biological effects. Typically, during NET release, neutrophil membrane integrity is compromised and neutrophil death results, leading to the process being named "suicidal NETosis". However, other more rapid pathways have also been reported, including "vital" NET release, where neutrophil viability and function are not compromised after NET release [7, 13, 14], and the release of NETs that are composed of mitochondrial DNA [14–16].

1.2 Visualizing NETs

NETs are commonly visualized ex vivo or in vitro by fluorescence microscopy after staining with a DNA-binding dye and/or immunofluorescence using antibodies against MPO, NE, and/or citrullinated histones that are specific to NET formation. Several groups have also examined NETs by electron microscopy, reporting that NETs are made up of 15–26 nm wide filaments with 25–60 nm globular domains [3, 17]. NET release can also be visualized in real time using intravital microscopy or live-cell imaging [18–21]. In culture, NETs typically appear spread out and filamentous; however, in vivo, NETs appear round and aggregated, likely to indicate spatial restrictions of the tissue.

1.3 Quantifying NETs

In addition to qualitatively visualizing NETs, NET release can also be quantified. The most common methods include quantification of the area covered by extracellular DNA after staining, [22] fluorescence spectroscopy of the culture media after adding DNA-binding dyes, or a modified ELISA against MPO-DNA or NE-DNA complexes characteristic of NETs [23]. More recently, a new method of quantification using multispectral imaging flow cytometry was reported [24] and algorithms for automated quantification of fluorescence images have been made available [25, 26]. However, for all of these methods, in particular, when detecting NETs in vivo, care should be taken to conclude the formation of NETs as opposed to ETs derived from other innate immune cells since monocyte and macrophage-derived ETs have also been reported to be associated with MPO and elastase that were first thought to be neutrophil-specific [27, 28]. Quantification of extracellular DNA using DNA-binding dyes may also be confounded by cell-free DNA. Thus, the appropriate controls must be included to rule out cell death, such as necrosis, which would lead to the release of cell-free DNA.

2 Materials

2.1 Equipment

1. Sodium heparin-coated vacutainers.
2. 50 ml Conical tubes.
3. Plastic 1.5 ml Pasteur pipettes.
4. 12-Well flat-bottom culture plates.
5. 24-Well flat-bottom culture plates.
6. Black flat bottom 96-well plates.
7. Large volume centrifuge.
8. Centrifuge.
9. Tissue Culture Hood.
10. Tissue Culture Incubator.
11. Inverted confocal fluorescence microscope.
12. Fluorescence plate reader (excitation: ~480 nm; emission: ~520 nm).

2.2 Reagents

1. Hank's balanced salt solution (HBSS) without Ca^{2+} and Mg^{2+} (*see* **Note 1**).
2. 12% Dextran solution: v/v, diluted with HBSS without Ca^{2+} and Mg^{2+}.
3. Histopaque® 1077 and 1119.
4. 1.8% saline solution: 1.8 g NaCl in 1 L distilled water and sterile filter.

5. OptiMEM medium.
6. RPMI1640 medium.
7. Fetal bovine serum (FBS).
8. Goat serum.
9. Phosphate-buffered saline (PBS).
10. 0.05% PBS-T: Tween-20 in PBS v/v.
11. 4% paraformaldehyde w/v (PFA) (*see* **Note 2**).
12. Blocking solution for staining: 5% goat serum v/v in PBS.
13. Phorbol myristate acetate (PMA) as a positive control for NET release.
14. SYTOX® Green Nucleic Acid Stain.
15. Quant-iT™ PicoGreen® dsDNA Kit.
16. Antibody reactive against human neutrophil elastase.
17. Antibody reactive against citrullinated histone 3.
18. Antibody reactive against myeloperoxidase.
19. Secondary antibody solution: 1:500 v/v Alexa Fluor® 564-labelled antibody in blocking solution.

3 Methods

The methods described below outline the process for (1) human neutrophil isolation from peripheral blood; (2) neutrophil culture; (3) immunostaining of NETs; and (4) spectroscopic quantification of NETs.

3.1 Isolating Human Neutrophils from the Peripheral Blood

1. Collect blood by venepuncture into heparin-coated vacutainers. Proceed with the subsequent steps using sterile reagents in a tissue culture hood.
2. Pool blood into a 50 ml conical tube and add dextran to form a 1.2% solution. For example, for 30 ml of whole blood, add 3 ml of 12% dextran.
3. Invert 5–10× gently to mix and leave at room temperature for 20 min for red blood cells (RBCs) to settle.
4. While RBCs are settling, set up 15 ml conical tubes with 3 ml of Histopaque® 1119 at the bottom and carefully overlay this with 3 ml of Histopaque® 1077. If the interface is prepared properly, there should be a sharply demarcated line between the two Histopaque® layers. If not, discard and prepare again.
5. After RBCs have settled, the top layer of plasma should be transferred to the top of the Histopaque® layers using plastic Pasteur pipettes.

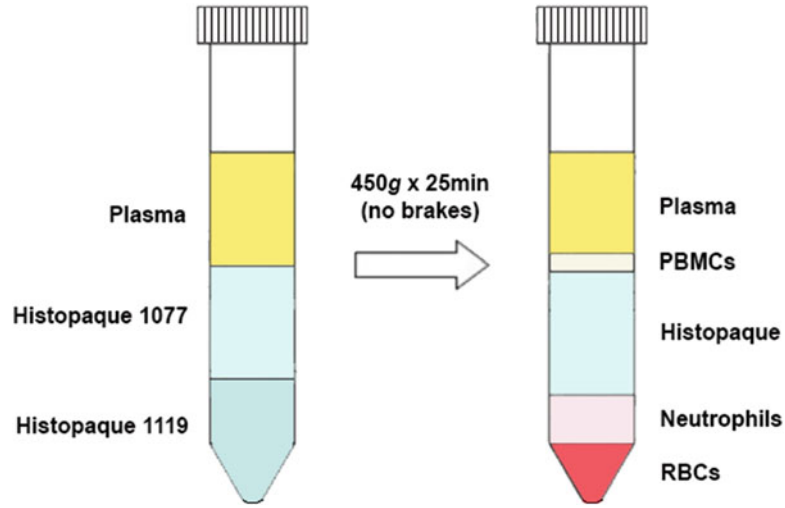

Fig. 1 Isolation of neutrophils using Histopaque®. Neutrophils can be separated from peripheral blood mononuclear cells (PBMCs) and red blood cells (RBCs) by centrifuging blood plasma on layers of Histopaque® 1077 and 1119

6. Centrifuge the Histopaque/Plasma layers at 450 × *g* for 25 min without brakes at room temperature to separate out the neutrophils from mononuclear cells (*see* Fig. 1).
7. Carefully suction off the top three layers and dispose before collecting the neutrophil layer into a new 50 ml tube.
8. Add HBSS (with no Ca^{2+} or Mg^{2+}) up to 50 ml and centrifuge at 450 × *g* for 10 min at room temperature with brakes.
9. Remove the HBSS and resuspend the cell pellet.
10. To remove contaminating RBCs, resuspend the cell pellet, add 25 ml of sterile distilled water to the tube, invert to mix, and immediately add 25 ml of sterile 1.8% saline solution to restore tonicity.
11. Centrifuge at 450 × *g* for 10 min at room temperature to pellet the neutrophils.
12. Remove the supernatant and resuspend the neutrophil pellet in OptiMEM media supplemented with 2% FBS (*see* **Note 3**).
13. Cells can be counted, checked for purity by flow cytometry for neutrophil markers such as CD16b, and plated for experiments.

3.2 Preparation of Neutrophil Cultures

1. Neutrophils are seeded into sterile culture plates for NET visualization and quantification experiments. For visualization experiments, 2×10^5 neutrophils are seeded per well of a 24-well plate, and for quantification, 1×10^6 neutrophils are seeded per well of a 12-well plate.

2. The stimulus of interest is added to neutrophils. As a positive control, 50 nM PMA should be added to the cells.
3. Culture neutrophils in 37 °C/5% CO_2 for an optimized time-point before analysis (*see* **Note 4**).

3.3 Immunostaining of NETs

1. Prepare a 167 nM SYTOX® Green solution just before use by diluting 1 μl of the dye in 30 μl HBSS and then using 1 μl of this for every ml of HBSS. Store in the dark until ready for use. SYTOX® Green is a cell membrane-impermeable DNA-binding dye.
2. After the optimized treatment timepoint, take the plate of neutrophils out of the incubator, aspirate the medium, and gently wash (*see* **Note 5**) the wells with 1 ml of HBSS twice.
3. Gently add 0.5 ml of SYTOX® Green solution to each well for 15 min at room temperature in the dark.
4. Aspirate the dye and gently wash twice with HBSS. From this point onward, perform all incubations in the dark.
5. Gently add 0.5 ml of 4% PFA to each well for 10 min at room temperature in the dark.
6. Aspirate PFA and wash twice with HBSS.
7. Block each well with 0.5 ml of blocking solution for 1 h at room temperature in the dark.
8. Prepare 0.5 ml of primary antibody solution for each well (1:100 citrullinated histone 3 or MPO or NE in blocking solution). Be sure to include an isotype-matched IgG control (*see* **Note 6**).
9. Incubate overnight at 4 °C and wash twice with PBS-T.
10. Add 0.5 ml of secondary antibody solution to each well.
11. Incubate for 1 h at room temperature in the dark.
12. After washing twice with PBS-T, NETs are ready to be viewed using an inverted confocal fluorescence microscope.

3.4 Semi-Quantification of NETs

1. Collect the neutrophil conditioned media after treatment for the optimized timepoint (Subheading 3.2).
2. Centrifuge the conditioned media at 2000 × *g* for 5 min at 4 °C and collect the supernatant (*see* **Note 7**).
3. While samples are being prepared, the Quant-iT™ PicoGreen® kit can be thawed and 1× TE buffer is made according to the manufacturer's instructions using sterile, distilled, DNase-free water.
4. After the supplied 100 μg/ml phage lambda DNA standard has been thawed and thoroughly vortexed, the standard curve can be prepared following the manufacturer's instructions in

nucleic acid- and DNAse-free Eppendorf tubes using TE buffer. The standard curve typically ranges from 1 ng/ml to 1 μg/ml, but can be diluted down to 25 pg/ml with accuracy.

5. In black flat-bottom 96-well plates, prepare different dilutions of each conditioned media using TE buffer to determine the optimal dilution required for downstream analysis. From our experience, culture of 1×10^6 neutrophils in 1 ml of media with 50 nM PMA for 4 h requires a 1:4 dilution of the conditioned media prior to analysis for the sample fluorescence to fit within the fluorescence levels of the standard curve. (Once the optimized dilution has been determined, samples can be diluted in each well, i.e., First pipette 75 μl of TE buffer into all wells, followed by 25 μl of each sample).
6. Standards should be analyzed in duplicate, and each sample should be analyzed in triplicate.
7. Once all standards and samples have been pipetted into the plate, prepare the PicoGreen® dye by diluting the provided dye stock in TE buffer 200-fold in a plastic container. This solution is susceptible to photodegradation, and so prepare just before use and store in the dark.
8. Vortex the dye solution thoroughly and pipette 10 μl of the dye to the side of each well. The dye droplet will fall and mix with the sample over time.
9. After the dye has been added to all wells, ensure that the dye droplet has mixed with each sample by tapping the plate side to side gently. From this point onward, the plate is light-sensitive and should be covered.
10. Incubate the plate at room temperature for 5 min and then read using a fluorescent plate reader (excitation: 480 nm; emission: 520 nm).
11. Using the fluorescence levels from the standard curve, the total amount of extracellular DNA in each conditioned media can be calculated (*see* **Note 8**).

4 Notes

1. HBSS without calcium and magnesium is used throughout the experiment to minimize neutrophil activation during the purification and staining steps.
2. Care should be taken when handling PFA due to known toxicity.
3. Neutrophils appear to form NETs spontaneously when exposed to serum-free conditions, and so media supplemented with 2% FBS are used throughout the experiments.

4. It is well-established that PMA induces optimal NET formation after 3–4 h of stimulation, but a time course study may be needed for the stimulus of interest to ensure analysis at the right timepoint.
5. To minimize disruptions to the NET structures, wash plates gently by pipetting gently down the side of each well and aspirating from the wall of the well.
6. If dual staining with both citrullinated histone 3 and MPO or elastase antibodies is desired, DAPI or Hoechst 33342 will need to be used as the DNA stain.
7. At this point, the supernatant can be stored at −80 °C until analysis.
8. Make sure that any dilution factors prior to analysis are taken into account.

Acknowledgments

Conflicts of interest: The authors have no conflicts of interest.
Funding: Supported by grant R01AI121183 (to VMA) from *The National Institute of Allergy and Infectious Diseases* (*NIAID*), the National Institutes of Health (NIH).

References

1. Kolaczkowska E, Kubes P (2013) Neutrophil recruitment and function in health and inflammation. Nat Rev Immunol 13(3):159–175. https://doi.org/10.1038/nri3399
2. Nathan C (2006) Neutrophils and immunity: challenges and opportunities. Nat Rev Immunol 6(3):173–182. https://doi.org/10.1038/nri1785
3. Brinkmann V, Reichard U, Goosmann C, Fauler B, Uhlemann Y, Weiss DS, Weinrauch Y, Zychlinsky A (2004) Neutrophil extracellular traps kill bacteria. Science 303 (5663):1532–1535. https://doi.org/10.1126/science.1092385
4. Fuchs TA, Abed U, Goosmann C, Hurwitz R, Schulze I, Wahn V, Weinrauch Y, Brinkmann V, Zychlinsky A (2007) Novel cell death program leads to neutrophil extracellular traps. J Cell Biol 176(2):231–241. https://doi.org/10.1083/jcb.200606027
5. Mayadas TN, Cullere X, Lowell CA (2014) The multifaceted functions of neutrophils. Annu Rev Pathol 9:181–218. https://doi.org/10.1146/annurev-pathol-020712-164023
6. Tong M, Abrahams VM (2019) Neutrophils in preterm birth: friend or foe? Placenta 495 (1):60–63. https://doi.org/10.1016/j.placenta.2019.12.010
7. Yipp BG, Kubes P (2013) NETosis: how vital is it? Blood 122(16):2784–2794. https://doi.org/10.1182/blood-2013-04-457671
8. Douda DN, Khan MA, Grasemann H, Palaniyar N (2015) SK3 channel and mitochondrial ROS mediate NADPH oxidase-independent NETosis induced by calcium influx. Proc Natl Acad Sci U S A 112(9):2817–2822. https://doi.org/10.1073/pnas.1414055112
9. Pilsczek FH, Salina D, Poon KK, Fahey C, Yipp BG, Sibley CD, Robbins SM, Green FH, Surette MG, Sugai M, Bowden MG, Hussain M, Zhang K, Kubes P (2010) A novel mechanism of rapid nuclear neutrophil extracellular trap formation in response to *Staphylococcus aureus*. J Immunol 185(12):7413–7425. https://doi.org/10.4049/jimmunol.1000675
10. Rochael NC, Guimaraes-Costa AB, Nascimento MT, DeSouza-Vieira TS, Oliveira MP, Garcia e Souza LF, Oliveira MF, Saraiva EM (2015) Classical ROS-dependent and early/rapid ROS-independent release of neutrophil

extracellular traps triggered by Leishmania parasites. Sci Rep 5:18302. https://doi.org/10.1038/srep18302

11. Chapman EA, Lyon M, Simpson D, Mason D, Beynon RJ, Moots RJ, Wright HL (2019) Caught in a trap? Proteomic analysis of neutrophil extracellular traps in rheumatoid arthritis and systemic lupus erythematosus. Front Immunol 10:423. https://doi.org/10.3389/fimmu.2019.00423
12. Petretto A, Bruschi M, Pratesi F, Croia C, Candiano G, Ghiggeri G, Migliorini P (2019) Neutrophil extracellular traps (NET) induced by different stimuli: a comparative proteomic analysis. PLoS One 14(7):e0218946. https://doi.org/10.1371/journal.pone.0218946
13. Tong M, Potter JA, Mor G, Abrahams VM (2019) Lipopolysaccharide-stimulated human fetal membranes induce neutrophil activation and release of vital neutrophil extracellular traps. J Immunol 203(2):500–510. https://doi.org/10.4049/jimmunol.1900262
14. Yousefi S, Mihalache C, Kozlowski E, Schmid I, Simon HU (2009) Viable neutrophils release mitochondrial DNA to form neutrophil extracellular traps. Cell Death Differ 16 (11):1438–1444. https://doi.org/10.1038/cdd.2009.96
15. McIlroy DJ, Jarnicki AG, Au GG, Lott N, Smith DW, Hansbro PM, Balogh ZJ (2014) Mitochondrial DNA neutrophil extracellular traps are formed after trauma and subsequent surgery. J Crit Care 29(6):1133 e1131–1133 e1135. https://doi.org/10.1016/j.jcrc.2014.07.013
16. Wang H, Li T, Chen S, Gu Y, Ye S (2015) Neutrophil extracellular trap mitochondrial DNA and its autoantibody in systemic lupus erythematosus and a proof-of-concept trial of metformin. Arthritis Rheumatol 67 (12):3190–3200. https://doi.org/10.1002/art.39296
17. Onouchi T, Shiogama K, Mizutani Y, Takaki T, Tsutsumi Y (2016) Visualization of neutrophil extracellular traps and fibrin meshwork in human Fibrinopurulent inflammatory lesions: III. Correlative light and electron microscopic study. Acta Histochem Cytochem 49 (5):141–147. https://doi.org/10.1267/ahc.16028
18. Yipp BG, Petri B, Salina D, Jenne CN, Scott BN, Zbytnuik LD, Pittman K, Asaduzzaman M, Wu K, Meijndert HC, Malawista SE, de Boisfleury CA, Zhang K, Conly J, Kubes P (2012) Infection-induced NETosis is a dynamic process involving neutrophil multitasking in vivo. Nat Med 18(9):1386–1393. https://doi.org/10.1038/nm.2847
19. de Buhr N, von Kockritz-Blickwede M (2016) How neutrophil extracellular traps become visible. J Immunol Res 2016:4604713. https://doi.org/10.1155/2016/4604713
20. Clark SR, Ma AC, Tavener SA, McDonald B, Goodarzi Z, Kelly MM, Patel KD, Chakrabarti S, McAvoy E, Sinclair GD, Keys EM, Allen-Vercoe E, Devinney R, Doig CJ, Green FH, Kubes P (2007) Platelet TLR4 activates neutrophil extracellular traps to ensnare bacteria in septic blood. Nat Med 13 (4):463–469. https://doi.org/10.1038/nm1565
21. Barr FD, Ochsenbauer C, Wira CR, Rodriguez-Garcia M (2018) Neutrophil extracellular traps prevent HIV infection in the female genital tract. Mucosal Immunol 11 (5):1420–1428. https://doi.org/10.1038/s41385-018-0045-0
22. Gonzalez AS, Bardoel BW, Harbort CJ, Zychlinsky A (2014) Induction and quantification of neutrophil extracellular traps. Methods Mol Biol 1124:307–318. https://doi.org/10.1007/978-1-62703-845-4_20
23. Sil P, Yoo DG, Floyd M, Gingerich A, Rada B (2016) High throughput measurement of extracellular DNA release and quantitative NET formation in human neutrophils in vitro. J Vis Exp 112:52779. https://doi.org/10.3791/52779
24. Zhao W, Fogg DK, Kaplan MJ (2015) A novel image-based quantitative method for the characterization of NETosis. J Immunol Methods 423:104–110. https://doi.org/10.1016/j.jim.2015.04.027
25. Mohanty T, Sorensen OE, Nordenfelt P (2017) NETQUANT: automated quantification of neutrophil extracellular traps. Front Immunol 8:1999. https://doi.org/10.3389/fimmu.2017.01999
26. van Breda SV, Vokalova L, Neugebauer C, Rossi SW, Hahn S, Hasler P (2019) Computational methodologies for the in vitro and in situ quantification of neutrophil extracellular traps. Front Immunol 10:1562. https://doi.org/10.3389/fimmu.2019.01562
27. Granger V, Faille D, Marani V, Noel B, Gallais Y, Szely N, Flament H, Pallardy M, Chollet-Martin S, de Chaisemartin L (2017) Human blood monocytes are able to form extracellular traps. J Leukoc Biol 102 (3):775–781. https://doi.org/10.1189/jlb.3MA0916-411R
28. Doster RS, Rogers LM, Gaddy JA, Aronoff DM (2018) Macrophage extracellular traps: a scoping review. J Innate Immun 10(1):3–13. https://doi.org/10.1159/000480373

Chapter 10

In Vitro Identification and Isolation of Human Neutrophil Extracellular Traps

Guillermina Calo, Analia Silvina Trevani, Esteban Grasso, Irene Angelica Keitelman, Rosanna Ramhorst, Claudia Pérez Leirós, and Florencia Sabbione

Abstract

Neutrophils release web like-structures known as neutrophil extracellular traps (NETs) that ensnare and kill microorganisms. These networks are constituted of a DNA scaffold with associated antimicrobial proteins, which are released to the extracellular space as an effective mechanism to fight against invading microorganisms. In parallel with this beneficial role to avoid microbial dissemination and wall off infections, accumulating evidence supports that under certain circumstances, NETs can exert deleterious effects in inflammatory, autoimmune, and thrombotic pathologies. Research on NET properties and their role in pathophysiological processes is a rapidly evolving and expanding field. Here, we describe a combination of methods to achieve a successful in vitro NET visualization, semiquantification, and isolation.

Key words Neutrophil extracellular traps, NETosis, Myeloperoxidase, Elastase, Cell death

1 Introduction

1.1 NET Definition

Neutrophils constitute the most abundant immune cell population in the peripheral blood and are a critical component of the innate immune response against bacterial and fungal infections. One of the antimicrobial mechanisms that these cells employ to control infections is the release of extracellular structures called Neutrophil Extracellular Traps (NETs). Neutrophil extracellular traps are filamentous structures formed by a DNA scaffold, which can be either of nuclear or mitochondrial origin with associated antimicrobial proteins [1–3].

1.2 NET Implication in Health and Disease

The primary role of NETs is to prevent microbial dissemination, avoiding overwhelming infections. However, the importance of NETs in infections is not limited to trapping microbes. These structures contain multiple molecules like alarmins and histones

Ayesha B. Alvero and Gil G. Mor (eds.), *Detection of Cell Death Mechanisms: Methods and Protocols*, Methods in Molecular Biology, vol. 2255, https://doi.org/10.1007/978-1-0716-1162-3_10,

that have antimicrobial and immunostimulatory functions [4]. NETs entrap a broad spectrum of microbes like *Staphylococcus aureus*, *Dengue virus*, and *Aspergillus fumigatus*, among many others and promote the interaction of these pathogens with granule-derived proteins followed by their subsequent disposal [5, 6]. The importance of NETs in host defense is exemplified by their conserved nature in various vertebrates, insects, and even plants [7]. Beyond their beneficial roles, the high concentrations of antimicrobial molecules make NETs potentially detrimental to the host under certain circumstances. Indeed, inappropriate NET formation, or a failure in resolving NET disposal have been described in many human diseases of infectious and noninfectious origin. The mechanisms through which NETs cause pathology are very diverse [8, 9]. On one hand, NETs have been reported to induce epithelial and endothelial cell death [10] and hepatic damage [11], affect the function of trophoblast cells [12] and platelets [13], and stimulate proinflammatory responses by airway epithelial cells [14]. Furthermore, it has been vastly documented that NETs in circulation promote coagulation, vascular occlusion, and thrombosis [13, 15, 16]. In preeclampsia, a pregnancy complication associated with vascular dysfunction and hypertension, NETs are abundantly found in the placenta and spread through the entire intervillous space in certain instances [17] although their pathogenic relevance is still unclear [17, 18]. NETs are suspected to play a pathogenic role in autoimmune diseases since the persistent presence of NET-derived products represents a source of self-antigens that enhance the autoimmune and inflammatory process [8]. In fact, antibodies against NETs' components are a hallmark of some autoimmune diseases. Systemic Erythematosus Lupus patients were found to develop autoantibodies to both the DNA and antimicrobial peptide component of NETs [19, 20]. Neutrophils have also been involved in cancer-related processes. Tumor-associated neutrophils (TAN) and NETs were found in Ewing sarcoma's biopsies [21]. Moreover, neutrophils from mice with Chronic Myelogenous Leukemia are prone to release NETs and a high expression of NETs has also been reported in murine models of malignant forms of cancer [22]. NETs also play a role in tumor-associated thrombosis [23]. It has also been proposed that NETs both capture circulating tumor cells and promote their migration to new sites [24] and favor cancer cell adhesion, proliferation, migration, and invasion [25, 26]. On the other hand, it was proposed that NETs and proteases may degrade the extracellular matrix and promote metastasis of neoplastic cells [23].

1.3 Mechanism of NET Formation

Neutrophil extracellular trap extrusion induced by many stimuli commonly results in cell death. For this reason, the process that leads to NET formation has been called NETosis [5, 27]. However, a nonlytic form of NET release has also been described. In this

pathway, NETs are delivered out of the cell without rupture of the plasma membrane. As neutrophils survive this DNA discharging, the process was called vital NETosis [28, 29]. However, in order to avoid a misleading term, as not always cell death occurs as a consequence of NET release, recent consensus has suggested to avoid the use of the term NETosis as a synonymous of the NET formation [3].

The cell death process that leads to NET extrusion known as NETosis is different from other forms of cell death like canonical apoptosis, necroptosis, and necrosis. In fact, chromatin decondensation and nuclear delobulation and expansion are unique features of NETosis [5]. As this mechanism of NET formation has been the best characterized, in this chapter, we outline a combination of tools that allow us to identify different steps of this process in order to demonstrate in vitro NET formation.

1.4 Hallmarks of the NETosis Process Useful for NET Detection and Quantification

During the NETosis process, chromatin undergoes decondensation as a consequence of digestion of nucleosome histones by the action of both neutrophil elastase that translocates from granules to nuclei and late binding of myeloperoxidase (MPO) to chromatin [3, 30]. Then, the nuclear envelope disassembles and the granule membranes disintegrate, allowing nuclear chromatin association to certain cytoplasmic and granule components. This process continues with plasma membrane rupture and NET expansion into the extracellular space 3–8 h after neutrophil activation, mainly depending on the concentration and the type of stimulus [8, 30]. Since under resting conditions, proteins like elastase or myeloperoxidase are located inside azurophil granules, the detection of colocalization of these proteins and DNA can be regarded as indicator of NET formation either inside the cell before their release or once they are extruded to the extracellular space (Fig. 1).

1.5 Neutrophil Stimulation to Induce NET Formation

Phorbol 12-myristate 13-acetate (PMA) is the most commonly used and most reproducible stimulus to induce NET formation and, employed at 50 nM, serves as a good positive control. However, several other NET inducers both natural and synthetic have been described, such as bacterial components, fungi, protozoa, viruses, activated platelets, complement-derived peptides, autoantibodies, CXCL8, monosodium urate (MSU) crystals, and cigarette smoke, among others [31].

1.6 NET Assessment

The accumulating data showing the variety of pathophysiologic effects of NETs or NET-derived products reinforce the importance to fully characterize them and the necessity to quantify them.

NET formation can be evaluated both in vivo by employing animal models, in paraffin-embedded tissue sections, and by means of in vitro assays. These in vitro approaches are usually used to test the ability of certain agonists or pathogens to induce NET

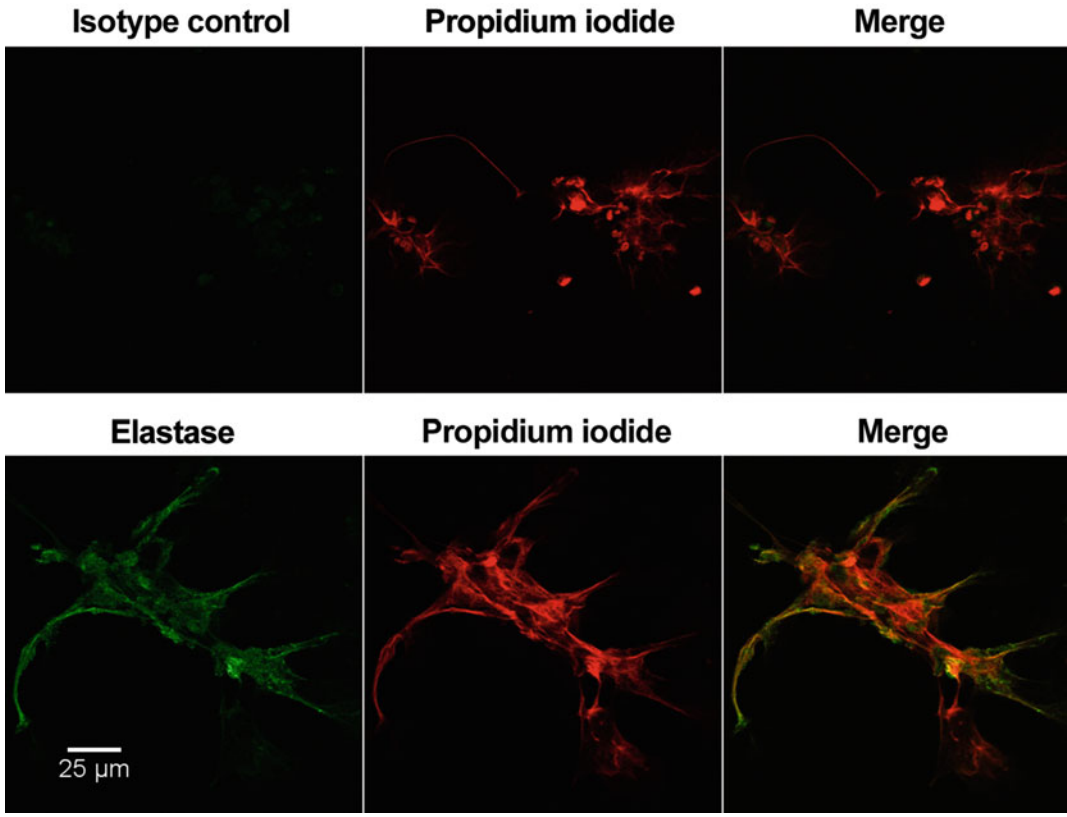

Fig. 1 Representative images of neutrophils stimulated with PMA (50 ng/mL) for 4 h at 37 °C. Cells were fixed, permeabilized, and stained with a rabbit IgG antielastase antibody or an isotype control antibody and a DyLight488-conjugated goat antirabbit IgG antibody. DNA was stained with propidium iodide (1 μg/mL). Images were acquired by using a FluoView FV1000 confocal microscope (Olympus, Tokyo, Japan) equipped with a Plapon 60×/NA1.42 objective

formation or to study mechanisms that modulate this process or the impact of NETs on different cell types. It should be mentioned that the amount of NETs released varies with the degree of stimulation, which depends on the type and concentration of the employed stimulus. Likewise, the kinetics of the process relies upon each type of stimulus and also considerably varies between donors [32].

For in vitro assays of NET formation by human neutrophils, these cells are isolated from freshly drawn peripheral blood of donors. Different protocols can be used to this end. However, the main guiding criteria for the selection of the isolation method should be to choose the one that results in a highly pure population and a diminished neutrophil spontaneous activation with minimal NET formation. Since monocytes produce large amounts of cytokines and chemokines upon stimulation, special care should be taken in order to obtain a highly pure population of neutrophils to avoid a priming effect by monocyte-derived factors on

neutrophil propensity to release NETs. Furthermore, to avoid neutrophil spontaneous activation, cells should be used immediately after isolation.

1.7 Parameters to Be Evaluated for In Vitro NET Appraisal

Even though DNA represents the main component of NETs, its solely quantification does not represent a reliable measurement of NET formation. This results from the fact that other forms of lytic cell death also lead to the release of extracellular DNA. However, when DNA quantification is performed alongside with detection of elastase or myeloperoxidase activity, it can provide a dimension of the extent of the process. Nevertheless, it should be noted that detection of these enzymatic activities might also be a consequence of neutrophil degranulation. Thus, confirmation of identity of NETs has to be done by detection of colocalization of DNA and MPO or elastase by confocal microscopy, which is commonly an accessible and rather inexpensive technology. Using this methodology, NETosis can be identified at different timepoints after stimulation by immunostaining in fixed and permeabilized specimens.

On the other hand, when NET formation is a consequence of the canonical NETosis process, an additional assay to quantify the number of cells with expanded nuclei at earlier timepoints post-stimulation, by DNA staining with a DNA intercalating fluorescent dye, is another approach that, when performed together with the above-mentioned measurements, contributes to a reliable quantification of NET formation. Although the last determination is easy to be accomplished in PMA-stimulated neutrophils, due to the kinetics of the NETosis process and the cell morphology induced by this stimulus being well known, it is not simple when other stimuli are employed, as it is usually difficult to identify the precise moment in which nuclear chromatin expands before DNA is released. Alternatively, to overcome this inconvenient, antichromatin antibodies and DNA-intercalating dyes like Hoechst 33342 can be used together to detect cells undergoing NETosis taking advantage of the fact that chromatin decondensation during NETosis exposes the epitopes, increasing the antibody-dependent fluorescence signal while reducing the DNA-signal, as reported by Brinkmann and Zychlinsky [32].

Supplementing the studies with ex vivo time-lapse microscopy and by using cell permeable—together with cell impermeable—DNA intercalating fluorescent dyes, provides additional insight into the characteristic of the NET formation process.

1.8 NET Isolation

For studies focused to evaluate the impact of NETs on other cell types, cell-free NETs can be isolated from neutrophil-stimulated cultures [14, 33] and then used in various types of assays including migration, proliferation assays, and cytotoxicity evaluation, amongst others. The main hindrance of these assays is to assure that the NETosis inducer does not affect the target cells. To avoid

this from happening, depending on the stimulus, it can be removed from neutrophil cultures by washing it out after stimulation and before NET release takes place. However, some stimuli like PMA are difficult to be eliminated in culture supernatants. Thus, controls should be performed to assure that traces of this compound that could remain after neutrophil wash out do not affect the functionality of the target cell to be studied.

Since the gold standard method for NET quantification has not been yet established, researchers should choose the most appropriate method based on the knowledge of the respective virtues and drawbacks of the different approaches [34]. Under this premise, we consider that demonstration of NET formation requires the combination of multiple assays: DNA quantification in culture supernatants of stimulated neutrophils (Subheading 3.3) and elastase or myeloperoxidase activity measurement (Subheadings 3.4 and 3.5 respectively) together with visualization of colocalization of DNA and MPO or elastase by confocal microscopy (Subheading 3.6) and, when possible, the identification of nuclear cell expansion at early timepoints poststimulation (Subheading 3.7).

2 Materials

2.1 Equipment

1. Biological safety cabinet.
2. Refrigerated centrifuge.
3. Tissue culture Incubator.
4. Neubauer chamber, hemocytometer, or cell counter.
5. Fluorometer.
6. Confocal laser scanning microscope with appropriate illumination lines and detectors.
7. Utrasonic bath.

2.2 Disposables and Reagents

1. Polypropylene tubes with heparin (final concentration of 20 U/mL in the blood sample).
2. Ficoll-Paque PLUS.
3. 50 mL conical polypropylene tube.
4. Plastic Pasteur pipette.
5. 1× and 10× Phosphate buffered saline (PBS).
6. Dextran: 6% in PBS.
7. Complete medium: RPMI 1640 without phenol red, supplemented with 10% fetal calf serum previously heated 30 min at 65 °C to inactivate endogenous DNases, 25 mM Hepes, penicillin (100 U/mL), and streptomycin (100 μg/mL) (except when stimulating with bacteria).

8. Sterile saline solution.
9. Iced-cold deionized H_2O.
10. Polypropylene microtubes.
11. Phorbol 12-myristate 13-acetate (PMA): final concentration 25–50 mM.
12. Micrococcal nuclease (MNase): stock concentration at 20× and final concentration of 1 U/mL; alternatively, DNase I can be used instead (2 U/mL).
13. EDTA: stock concentration at 20× and final concentration of 5 mM.
14. SYTOX Green.
15. Calf thymus DNA.
16. 96-well flat bottom microplate suitable for fluorescence-based assays.
17. Triton X-100: 1% in PBS.
18. MPO standard (e.g., Human polymorphonuclear leukocytes myeloperoxidase).
19. Elastase substrate: 1 nM N-Methoxysuccinyl-Ala-Ala-Pro-Val *p*-nitroanilide in PBS.
20. 3,3′,5,5′-Tetramethylbenzidine (TMB) reagent A and B.
21. ELISA Stop solution: 2 N sulfuric acid.
22. 12 mm glass coverslips.
23. 24-well plate.
24. Ethanol: 70% in water.
25. Poly-L-lysine: 0.01% (w/v) in PBS.
26. 4% paraformaldehyde (PFA).
27. Blocking buffer: PBS supplemented with 5% serum from animal species in which secondary antibodies have been produced.
28. Petri dish.
29. Permeabilization buffer: 0.5% Triton X-100 in blocking buffer.
30. Primary antibodies: unconjugated antihuman elastase or unconjugated antiMPO; alternatively fluorochrome conjugated antibodies can be used; these antibodies should be used at concentration recommended by manufacturer.
31. Flourescent-labeled secondary antibody if using unconjugated primary antibodies.
32. IgG isotype control.
33. TO-PRO-3: 1 μM working solution; or propidium iodide (PI): 1 μg/mL in PBS working solution.
34. Non-fluorescing coverslipping medium.

35. Confocal microscopy visualization chambers or dishes.
36. Glycine: 0.1 M in PBS.
37. Acetone.

3 Methods

Procedures should be done following the institution's biosafety guidelines.

3.1 Isolation of Peripheral Blood Neutrophils Using Ficoll Density Gradient and Dextran Sedimentation

1. Collect fresh blood in polypropylene tubes with heparin as anticoagulant and dilute to 1:1 with saline at room temperature (*see* **Notes 1** and **2**).
2. Carefully layer 33 mL of diluted blood on 15 mL of Ficoll-Paque PLUS at room temperature in a sterile 50 mL conical polypropylene tube (*see* **Note 3**).
3. Centrifuge 30 min at 483 × *g* at room temperature, without brake and with minimal acceleration.
4. After centrifugation, start cooling the centrifuge at 4 °C.
5. Meanwhile, discard the plasma fraction (above the interphase), the band containing peripheral blood mononuclear cells, basophils, and platelets (interphase), and the Ficoll-Histopaque fraction (below the interphase) as much as you can, leaving just a thin layer on top of the pellet containing the granulocytes and erythrocytes.
6. Using a new plastic Pasteur pipette, transfer the pellet containing granulocytes and erythrocytes to a new polypropylene tube (*see* **Note 4**).
7. Add to the pellet the same volume of Dextran 6% and two volumes of PBS (Dextran final concentration will be 1.5%) (*see* **Note 5**). Mix the content by repeated gentle inversion of the tube. Then, set the tube upright, loosen its lid so that the liquid of the inner surface of the lid falls down, and let red cells sediment at room temperature for 20 min.
8. Aspirate the erythrocyte poor, granulocyte enriched-upper layer in another sterile conical polypropylene tube. Add saline solution to top off the tube volume, and centrifuge for 10 min at 483 × *g* at 4 °C.
9. Aspirate and discard the supernatant (*see* **Note 6**) and gently move the tube to dismantle the pellet. Add 18 mL of iced-cold deionized H_2O and gently resuspend the cells for 30 s (with timer control) to lyse red cells.
10. To restore isotonicity immediately, add 2 mL of 10× PBS and then top off the tube volume with PBS.

11. Centrifuge for 10 min at 215 × *g* at 4 °C.
12. Aspirate and discard the supernatant and resuspend the cell pellet in complete medium with or without phenol red depending on the experiment to be performed (*see* **Note 7**).
13. Count the number of cells, adjust the number to the corresponding experiment, and use immediately after isolation (*see* **Note 8**).

3.2 Cell Stimulation for NET Formation

1. Mix the stock neutrophil suspension obtained at Subheading 3.1 very gently by either circular movements of the tubes or pipetting up and down to homogenize the distribution of the cells. Repeat this procedure frequently while pipetting into the tubes taking care to do this very gently because neutrophils can be easily activated if treated vigorously. Do not ever vortex the cells.
2. Pipette 100 μL (1×10^6) of the neutrophil suspension in 1.5 mL of polypropylene microtubes.
3. Add 100 μL of the appropriate 2× solution of the NET-inducer reagent to attain a final volume of 200 μL (e.g., PMA 50–100 nM to get a final concentration or 25–50 nM). Carry out all conditions in duplicates (*see* **Note 9**). Reserve one tube with unstimulated cells to be employed as positive control in future elastase and MPO activity measurements (*).
4. Incubate the tubes for 240 min at 37 °C in an incubator with a humidified atmosphere with 5% CO_2. Alternatively, for kinetic analysis, incubate individual tubes for 60, 120, 180, and 240 min.
5. Add to the samples 10.5 μL of 20× MNase for a final concentration of 1 U/mL. Alternatively, DNase I can be used instead at final concentration of 2 U/mL.
6. Incubate the samples for 30 min (15 min if DNase I is used) to detach DNA from cell debris.
7. Add 11 μL of 20× EDTA to attain a final concentration of 5 mM to stop MNase or DNAse I activity.
8. Centrifuge the samples in a microfuge by a 12-s spin down and collect the supernatants (*see* **Notes 10** and **11**).

3.3 DNA Measurement

1. Prepare a standard DNA concentration curve in the same medium in which samples were obtained using commercial thymus DNA by twofold serial dilution of DNA, starting from 10 μg/mL to 0.15 μg/mL in a final volume of 150–200 μL depending on the fluorometer to be used.
2. Pipette 50 μL of the supernatants collected in Subheading 3.2 in 96-well microplate.

3. Add 50 μL of 5 μM SYTOX green dilution (final concentration 2.5 μM) and protect from light.
4. Set the fluorometer to illuminate with 488 nm and record emission at 523 nm.
5. Measure and record the fluorescence of the standard curve tubes and make the curve.
6. Measure and record the fluorescence of the individual samples.
7. Interpolate the value in the standard curve to determine the DNA concentration of the sample.

3.4 Elastase Activity Measurement

1. Prepare the positive control of the reaction by adding to the sample reserved in Subheading 3.2 (*) 100 μL of Triton X-100 to attain 0.5% final concentration and mix by up- and down pipetting to lyse the neutrophils. This condition will give a measure of total elastase activity.
2. Pipette 20 μL of the supernatants collected in Subheading 3.2 in a 96-well microplate or 20 μL of the positive control prepared in the previous step.
3. Add to each well 100 μL of elastase substrate.
4. Incubate for 4 h at 37 °C or 18 h at room temperature.
5. Measure absorbance at 405 and subtract measurement at 505 nm. This reaction does not need to be stopped.

3.5 Myeloperoxidase Activity Measurement

Prepare a standard curve with commercially available MPO (*see* **Note 12**).

1. Pipette 50 μL of the supernatants collected in Subheading 3.2 or 50 μL of the positive control prepared in Subheading 3.4, **step 1** or the samples corresponding to each standard curve point in each well of a 96-well microplate.
2. Mix enough equal volumes of the TMB substrate reagents A and B so that 50 μL can be added per well, considering the number of samples to be analyzed.
3. Pipette 50 μL of the mix in each well.
4. Incubate 10 min at room temperature.
5. Add 100 μL of ELISA stop solution.
6. Immediately measure the absorbance at 450 nm and 570 nm by spectrophotometry and subtract the values of 570 nm from those of 450 nm.
7. Graph the standard calibration curve values to get the linear equation.
8. Interpolate the values obtained for each sample from the standard MPO curve to determine their MPO activity.

3.6 Neutrophil Stimulation and Immunostaining to Visualize NETs by Immunofluorescence

This protocol has been adapted from Ref. 35.

The procedure can be done with glass coverslips in plates or with microscope chamber slides.

3.6.1 By Using Coverslips

1. Place clean 12 mm glass coverslips into wells of a 24-well plate (*see* **Note 13**).
2. Add 300 μL of ethanol 70% to sterilize coverslips for 10 min. Do the same for each side of the coverslip aided by tweezers and a curved needle to rotate it.
3. Wash with 300 μL of PBS twice.
4. Coat the coverslips with 300 μL 0.01% (w/v) poly-L-lysine in PBS for 30 min at room temperature.
5. Aspirate the poly-l-lysine and wash the coverslips with PBS twice.
6. Seed 150 μL of cell suspension obtained in Subheading 3.1 containing 1×10^6 cells in complete RPMI media over the coverslips of the 24-well plate.
7. Add 150 μL of the stimuli to be evaluated or 150 μL of 2× PMA in complete medium to attain a final concentration of 25–50 nM as positive control.
8. Mix by gentle circular movements of the plate and incubate for 240 min at 37 °C in a humidified 5% CO_2 atmosphere. Alternatively, for kinetic analysis, incubate separate plates for 60, 120, 180, or 240 min to stop the assays and continue the staining procedure for each separate timepoint.
9. Aspirate very carefully the supernatants and add 300 μL of 4% PFA.
10. Incubate the plate for 30 min at room temperature.
11. Carefully aspirate the supernatants and wash the wells containing the coverslips by adding 300 μL of PBS. Perform the procedure twice (*see* **Note 14**).
12. Aspirate the PBS and add 300 μL of 0.5% Triton X-100 in PBS for 1 min to permeabilize the cells.
13. Repeat the washing step with 300 μL of PBS twice.
14. Aspirate the PBS and add 300 μL of blocking buffer.
15. Incubate for 60 min at 37 °C or overnight at 4 °C to block nonspecific binding of antibodies.
16. Aspirate the blocking buffer and wash twice with 300 μL of PBS.
17. Prepare a humidified chamber in a Petri dish with wet tissue and place over it a microscope slide wrapped in Parafilm.

18. Seed over the parafilm a 20 μL-drop of antihuman elastase or antihuman MPO antibody dilution in blocking buffer at concentration suggested by manufacturer or a 20 μL-drop of the corresponding isotype control at the same concentration. Alternatively, 20 μL of a dilution of a fluorochrome-conjugated antibody at a concentration suggested by the manufacturer can be used (e.g., FITC-conjugated mouse antihuman MPO antibody) (*see* **Note 15**).
19. Carefully remove the glass coverslips from the plate aided with a curved needle and tweezers and put the coverslip upside down on the drop of primary antibody (the coverslip face containing the cells should be in contact with the antibody solution); cap the Petri dish to maintain the samples humidified (*see* **Note 16**).
20. Incubate for 60 min at room temperature (in the dark in the case a fluorochrome-conjugated antiMPO antibody is being used).
21. Extend a piece of Parafilm on a flat surface and seed 30 μL drops of PBS with space between them to avoid their fusion (*see* **Note 17**).
22. Transfer each coverslip onto a clean drop of PBS. Be careful while putting in contact the coverslip face that contains the cells with the PBS solution. Repeat the procedure twice.
23. If a fluorochrome-conjugated antibody is used, proceed to **step 27**.
24. Transfer the coverslip onto a 20 μL drop of a dilution of a fluorochrome-conjugated secondary antibody at a concentration suggested by the manufacturer laid over a slide wrapped in Parafilm.
25. Incubate the slide inside the humidified chamber for 30 min at room temperature in the dark. From this point, keep the coverslips away from the light as much as possible.
26. Wash the coverslip twice by placing it upside-down onto a drop of PBS as indicated in **step 22**.
27. Transfer the coverslip upside-down onto a 20 μL drop laid over a slide wrapped in Parafilm containing 1 μM TO-PRO-3 solution or 1 μg/mL of PI to stain DNA. Maintain the slide inside the humidified chamber for 15 min in the dark (*see* **Notes 18** and **19**).
28. Transfer coverslip onto a drop of PBS over a slide wrapped in Parafilm twice.
29. Remove coverslips from the PBS solution aided by forceps and a curved needle, and after quickly draining the excess of PBS by maintaining the coverslip perpendicular to the wipe, mount

(cells facing down) on a drop of coverslipping medium laid over a clean microscope slide.

30. Store overnight at 4 °C, inside a Petri dish wrapped with aluminum foil to protect from light, in horizontal position to let the hardening of the mounting medium.
31. Acquire the images in a confocal scanning microscope with 488-laser illumination set at the minimal potency that brings adequate fluorescence to avoid bleaching and sequential 633 nm excitation for TO-PRO-3 or 543 nm excitation in case PI has been used to stain DNA (*see* **Note 20**).

3.6.2 By Using Chamber Slides

1. Pipette 100 μL of 0.01% (w/v) poly-L-lysine in PBS in each chamber well and incubate for 30 min at room temperature.
2. Aspirate poly-L-lysine and then wash the wells with 200 μL of PBS twice.
3. Seed 100 μL of the cell suspension obtained in Subheading 3.1 containing 1×10^6 cells in complete RPMI media in each chamber well.
4. Add 100 μL of the stimuli to be evaluated or 100 μL of 2× PMA solution in complete medium to attain a final concentration of 25–50 nM as positive control.
5. Mix by gentle circular movements of the chamber, put it inside a Petri dish with wet paper employed as a humidified chamber, and insert the capped Petri dish in an incubator at 37 °C in a humidified 5% CO_2 atmosphere for 240 min (*see* **Note 21**). Alternatively, for kinetic analysis, incubate separate chambers for 60, 120, 180, or 240 min.
6. Aspirate very carefully the supernatants and add 200 μL of 4% PFA.
7. Incubate the chamber for 30 min at room temperature.
8. Carefully aspirate the supernatants and wash the wells by adding 200 μL of PBS. Perform the procedure twice (*see* **Note 22**).
9. Aspirate PBS and add 200 μL of glycine and incubate for 15 min.
10. Aspirate glycine and add 200 μL of cold acetone (−20 °C) and incubate for 7 min to permeabilize the cells (*see* **Note 23**).
11. Aspirate acetone and add 200 μL of PBS drop-by-drop to rehydrate the cells and incubate at room temperature for 7 min.
12. Aspirate PBS and repeat the washing step with 200 μL of PBS.
13. Aspirate PBS and add 200 μL of blocking buffer.
14. Incubate for 60 min at 37 °C or overnight at 4 °C to block nonspecific binding of antibodies.

15. Aspirate the blocking buffer and wash twice with 200 μL of PBS.
16. Add 70 μL of a dilution of an antihuman elastase or antihuman MPO antibody in blocking buffer or the corresponding isotype control at the same concentration. Alternatively, a dilution of a fluorochrome-conjugated antibody can be used (*see* **Note 15**).
17. Incubate for 60 min at room temperature with very gentle shaking in a rocking platform (protected from light in the case a fluorochrome conjugated antibody is being used).
18. Aspirate the antibody solution and add 200 μL of PBS to wash the sample. Repeat the procedure twice.
19. If a fluorochrome-conjugated antibody is used, proceed to **step 23**.
20. Aspirate PBS and add 70 μL of a dilution of a fluorochrome-conjugated secondary antibody at a concentration suggested by manufacturer.
21. Incubate for 30 min at room temperature with very gentle shaking in the dark. From this point, keep the microscope chamber away from the light.
22. Aspirate the antibody solution and add 200 μL of PBS to wash the sample. Repeat the procedure twice.
23. Aspirate PBS and add 70 μL of 1 μM TO-PRO-3 solution or PI (1 μg/mL) to stain DNA (*see* **Notes 18** and **19**).
24. Incubate the chamber for 15 min with very gentle shaking in the dark.
25. Aspirate the dye solution and wash twice with 200 μL of PBS.
26. Remove the PBS solution and add 3 drops of coverslipping medium.
27. Keep overnight at 4 °C inside a Petri dish wrapped with aluminum foil to protect from light and in horizontal position.
28. Acquire the images in a confocal scanning microscope with the appropriate laser illumination set at the minimal potency that brings adequate fluorescence to reduce photobleaching and with sequential excitation.

The procedure is described to be done with microscope chambered slides, but it can also be done with glass coverslips in plates.

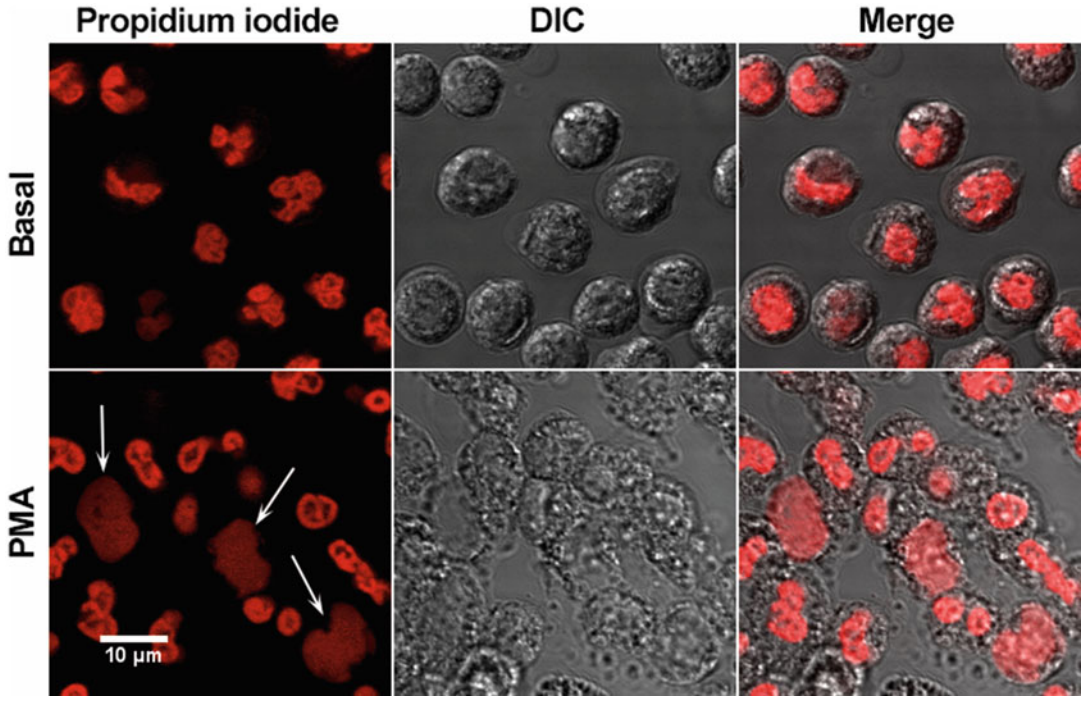

Fig. 2 Representative images of neutrophils undergoing NETosis. Neutrophils were stimulated with PMA (25 ng/mL) for 120 min at 37 °C. Cells were fixed, and DNA was stained with propidium iodide (1 μg/mL). Images were acquired by using a FluoView FV1000 confocal microscope (Olympus, Tokyo, Japan) equipped with a Plapon 60×/NA1.42 objective. White arrows indicate cells with decondensed DNA characteristic of those undergoing NETosis. DIC: Differential interference contrast

3.7 Quantification of Cells Undergoing Nuclear DNA Decondensation by Propidium Iodide Staining

1. Follow **steps 1–8** from Subheading 3.6.2 with the exception that the incubation time with the stimuli (**step 5**) should be 120–150 min (*see* **Note 24**).
2. Aspirate PBS and carefully add 70 μL of 1 μg/mL PI staining solution in PBS.
3. Incubate the chambered slides at room temperature in the dark for 30 min.
4. Aspirate the dye solution and wash twice with 300 μL of PBS.
5. Remove the PBS solution and add 3 drops of coverslipping medium.
6. Keep the chamber overnight at 4 °C inside a Petri dish wrapped with aluminum foil to protect from light, in horizontal position.
7. Acquire multiple images in a confocal scanning microscope with the appropriate laser illumination to visualize PI fluorescence (e.g., 543 nm) taking into account the PI maximum excitation/emission wavelengths (535/617 nm).
8. Cells undergoing NETosis can be identified as swallowed cells with decondensed DNA that occupies almost the entire volume

of the cell (Fig. 2). For quantification, count the number of cells with these characteristics and the total cell number and calculate the percentage.

3.8 NET Isolation for Functional Studies

1. Mix the neutrophil suspension obtained in Subheading 3.1 very gently by either circular movements of the tubes or pipetting up and down to homogenize the distribution of the cells. Repeat this procedure frequently while pipetting into the tubes taking care to do this gently because neutrophils can be easily activated if treated vigorously.
2. Pipette 100 μL (1×10^6) of the neutrophil suspension in 1.5 mL of polypropylene microtubes.
3. Add 100 μL of the appropriate 2× solution of the NET-inducer reagent to attain a final volume of 200 μL (e.g., final concentrations: MSU 300 μg/mL, UA 8 mg/dL; or PMA 50 nM) (*see* **Note 25**). For control conditions, culture neutrophils in the absence of stimuli with the vehicle employed with each stimulus.
4. Incubate the tubes for 60 min at 37 °C in an incubator with a humidified atmosphere with 5% CO_2.
5. Centrifuge in a microfuge by a 12-s spin down (*see* **Note 10**).
6. Carefully aspirate the medium without removing the pellet, loosen the cell pellet by gentle agitation of the tube or lightly tapping the tube walls, and add 200 μL of complete warm fresh medium.
7. Incubate for 180 additional min at 37 °C in a humidified atmosphere with 5% CO_2.
8. Detach NETs from cell debris by a gentle ultrasonic pulse of 60 s; 40 Hz; W200 in an ultrasonic bath (e.g., Branson) (*see* **Note 26**).
9. Centrifuge the tubes in a microfuge by a 12-s spin down.
10. Collect the supernatants.
11. Separate aliquots of these supernatants to quantify the concentrations of DNA and MPO activity as previously described.
12. Immediately after isolation, seed the rest of the supernatants containing NETs over target cell cultures on which the effect of NETs is to be evaluated (*see* **Note 27**).

4 Notes

1. Neutrophils are short-lived cells. Thus, always use fresh blood, preferably immediately after being drawn. Always employ polypropylene tubes to avoid neutrophil activation by other

materials. Use sterile materials and buffers and endotoxin-free reagents to avoid neutrophil priming.

2. Anticoagulant Citrate Dextrose (ACD) can be used as alternative anticoagulant.
3. If you are using smaller samples, adapt the volumes with respect to the proportions.
4. If pellet containing granulocytes is not transferred to another tube, there will be a greater chance for monocyte contamination of the granulocyte population to be isolated.
5. Be careful with the quality of Dextran and Ficoll-Histopaque you employ, as contaminants could result in undesirable neutrophil activation or death. Clinical grade Dextran should be used.
6. If supernatant is discarded by tube inversion, be careful because the pellet might be lost.
7. For fluorometric measurements, use medium without phenol red because this compound increases background fluorescence and interferes in the measurement. Always check the pH of the medium before using, as alkaline pH affects neutrophil viability.
8. After suspending neutrophils and while counting them, leave the tube inclined at 45° until cells are used to avoid cell accumulation in the bottom of the tube that could result in neutrophil aggregation and priming. Also avoid suspending neutrophils at concentrations higher than 10^7/mL. A working concentration of 5×10^6 neutrophils/mL is appropriate.
9. Considering that neutrophil elastase is required for NET formation induced by the majority of stimuli, it is always advisable to include in the experimental protocol, control conditions in which an elastase inhibitor is added 30 min before cells are stimulated to prevent NET formation. This condition will allow us to confirm that the measurements performed as surrogate of the presence of NETs (i.e., DNA and MPO activity) correspond to these structures.
10. Do not spin the cells for longer times because this could damage the ones that have not undergone NETosis.
11. For DNA measurements, supernatants can be frozen maintained at −20 °C and measurements can be performed within 48 h. However, MPO and elastase activities have to be evaluated the same day the supernatants are collected.
12. Suggested standard MPO curve: 1, 2.5, 5, and 10 μg/mL.
13. It is advisable to acid-wash coverslips before using them to remove manufacturing residues, oils, and other contaminants like LPS that might prime or activate neutrophils and cause

nonspecific background fluorescence after antibody staining. Coverslips can be prepared in advance and used when needed. Many different protocols are available in the web, such as https://microscopy.duke.edu/guides/glass-coverslip-cleaning.

14. Add the buffer carefully, one drop at the time, so that NETs do not detach.
15. A fluorochrome-conjugated antiMPO antibody can be used because MPO is highly expressed in neutrophils, and the sensitivity will be enough to detect the staining. However, if FITC antiMPO antibodies are used, the fast photobleaching of FITC fluorochrome should also be taken into account (also *see* **Note 20**).
16. Coverslips can easily break, and so be extra careful when taking them from the plate. Use tweezers and a thin curved needle. Also, keep special attention to recognize which side of the coverslip has the cells facing up. This coverslip side should be put in contact with the antibody.
17. Instead of using a parafilm extended on a flat surface, a parafilm extended on a tube rack can be employed as was reported in Ref. 35.
18. The selection of the DNA dye will depend on the illumination lines and the detectors of the microscope to be used as well as the fluorochrome to which antibodies antielastase or antiMPO are conjugated. TO-PRO-3 has a fast photobleaching behavior upon illumination, and thus, the use of PI, which is more photostable, is recommended when the immunostaining of elastase or myeloperoxidase is evidenced with an antibody conjugated to a fluorochrome, which does not emit at wavelengths that superpose with that of the PI spectrum. Besides, the fast photobleaching of TO-PRO-3 does not allow z-stack acquisitions to be performed. Alternatively, DNA labeling with other dyes like Draq5 has been extensively reported in literature.
19. If using TO-PRO-3, be extremely careful to perform the procedures protected of ambient light. When capturing images, always use sequential illumination and take care to first capture the TO-PRO-3 emission to avoid photobleaching.
20. Staining DNA with PI is advisable when FITC-conjugated antiMPO antibody is used, because it will allow us to set the microscopic field and focal plane by turning on only the laser to illuminate PI while turning off the 488-illumination without perceptible PI-photobleaching. Once the focal plane is selected, the 488 laser is turned on and image can be captured without being the FITC signal previously affected by photobleaching. Always use the lower laser potency as possible.

21. Inserting the chamber inside a Petri dish with wet paper is important not only to maintain the humidity but also to protect the glass coverslip of the bottom of the chamber from scratches and damage because it is very fragile. For this reason, it is convenient that all steps are performed by maintaining the coverslip chamber lying in the Petri dish even while performing the washing steps and re-capping the Petri dish during incubations. This will also help to avoid the chamber content from spill out in the case of chamber coverslips' breakage.
22. Always avoid drying out of the chamber wells in each step to prevent artifacts.
23. The addition of acetone will turn dull the chamber walls in contact with it, but this will not affect the ulterior staining procedure.
24. The proper incubation time upon PMA stimulation to detect NETosis cell changes can be determined when performing the assay in chambered coverslips by observing periodically the cells in a light inverted microscope; as before membrane rupture, cells undergoing NETosis appear swollen, nuclei cannot be distinguished, and only a reduced amount of granules persists appearing marginated in a part of the cell.
25. For experiments involving isolated NETs, it is relevant that the target cells that will be employed to evaluate the impact of NETs are not sensitive to the NET inducer. This will avoid traces of the agonist that might persist in NETs' containing supernatants even after the washing steps performed after neutrophil stimulation and before NETs are collected, affect the target cells.
26. Avoid increasing the time or potency of the ultrasonic pulse because this could cause membrane cell damage of intact cells, leading to artifactual release of DNA. Control cell integrity after the ultrasonic pulse by LDH release and/or staining with PI and flow cytometry.
27. Always include in the experimental setting a control with unstimulated cells and a control in which NETosis has been inhibited to confirm that the observed effect corresponds to the NETs present in the supernatant and not to other components. Since elastase activity appears to be required for human NET formation with the majority of the inducers, this control can be performed by adding elastase inhibitor (e.g., Sigma Aldrich) 30 min before neutrophil stimulation taking care to resupplement the inhibitor after the washing step of cells (Subheading 3.8, **steps 5** and **6**).

References

1. Brinkmann V (2004) Neutrophil extracellular traps kill bacteria. Science 303:1532–1535. https://doi.org/10.1126/science.1092385
2. Yousefi S, Mihalache C, Kozlowski E et al (2009) Viable neutrophils release mitochondrial DNA to form neutrophil extracellular traps. Cell Death Differ 16:1438–1444. https://doi.org/10.1038/cdd.2009.96
3. Boeltz S, Amini P, Anders HJ et al (2019) To NET or not to NET:current opinions and state of the science regarding the formation of neutrophil extracellular traps. Cell Death Differ 26:395–408. https://doi.org/10.1038/s41418-018-0261-x
4. Knight JS, Carmona-Rivera C, Kaplan MJ (2012) Proteins derived from neutrophil extracellular traps may serve as self-antigens and mediate organ damage in autoimmune diseases. Front Immunol 3:1–12. https://doi.org/10.3389/fimmu.2012.00380
5. Fuchs TA, Abed U, Goosmann C et al (2007) Novel cell death program leads to neutrophil extracellular traps. J Cell Biol 176:231–241. https://doi.org/10.1083/jcb.200606027
6. Papayannopoulos V, Zychlinsky A (2009) NETs: a new strategy for using old weapons. Trends Immunol 30:513–521. https://doi.org/10.1016/j.it.2009.07.011
7. Kaplan MJ, Radic M (2012) Neutrophil extracellular traps: double-edged swords of innate immunity. J Immunol 189:2689–2695. https://doi.org/10.4049/jimmunol.1201719
8. Papayannopoulos V (2017) Neutrophil extracellular traps in immunity and disease. Nat Rev Immunol 18:134–147. https://doi.org/10.1038/nri.2017.105
9. Niedźwiedzka-Rystwej P, Repka W, Tokarz-Deptuła B, Deptuła W (2019) "In sickness and in health"—how neutrophil extracellular trap (NET) works in infections, selected diseases and pregnancy. J Inflamm 16:15. https://doi.org/10.1186/s12950-019-0222-2
10. Saffarzadeh M, Juenemann C, Queisser MA et al (2012) Neutrophil extracellular traps directly induce epithelial and endothelial cell death: a predominant role of histones. PLoS One 7:e32366. https://doi.org/10.1371/journal.pone.0032366
11. Huang H, Tohme S, Al-Khafaji AB et al (2015) Damage-associated molecular pattern-activated neutrophil extracellular trap exacerbates sterile inflammatory liver injury. Hepatology 62:600–614. https://doi.org/10.1002/hep.27841
12. Calo G, Sabbione F, Pascuali N et al (2020) Interplay between neutrophils and trophoblast cells conditions trophoblast function and triggers vascular transformation signals. J Cell Physiol 235(4):3592–3603. https://doi.org/10.1002/jcp.29247
13. Zucoloto AZ, Jenne CN (2019) Platelet-neutrophil interplay: insights into neutrophil extracellular trap (NET)-driven coagulation in infection. Front Cardiovasc Med 6:85. https://doi.org/10.3389/fcvm.2019.00085
14. Sabbione F, Keitelman IA, Iula L et al (2017) Neutrophil extracellular traps stimulate Proinflammatory responses in human airway epithelial cells. J Innate Immun 9:387–402. https://doi.org/10.1159/000460293
15. Fuchs TA, Brill A, Duerschmied D et al (2010) Extracellular DNA traps promote thrombosis. Proc Natl Acad Sci U S A 107:15880–15885. https://doi.org/10.1073/pnas.1005743107
16. McDonald B, Davis RP, Kim S-J et al (2017) Platelets and neutrophil extracellular traps collaborate to promote intravascular coagulation during sepsis in mice. Blood 129:1357–1367. https://doi.org/10.1182/blood-2016-09-741298
17. Hahn S, Giaglis S, Hoesli I, Hasler P (2012) Neutrophil NETs in reproduction: from infertility to preeclampsia and the possibility of fetal loss. Front Immunol 3:1–8. https://doi.org/10.3389/fimmu.2012.00362
18. Calo G, Sabbione F, Vota D, et al (2017) Trophoblast cells inhibit neutrophil extracellular trap formation and enhance apoptosis through vasoactive intestinal peptide-mediated pathways. Hum Reprod 32(1):55–64. https://doi.org/10.1093/humrep/dew292
19. Lande R, Ganguly D, Facchinetti V et al (2011) Neutrophils activate Plasmacytoid dendritic cells by releasing self-DNA-peptide complexes in systemic lupus erythematosus. Sci Transl Med 3:73ra19. https://doi.org/10.1126/scitranslmed.3001180
20. Farrera C, Fadeel B (2013) Macrophage clearance of neutrophil extracellular traps is a silent process. J Immunol 191:2647–2656. https://doi.org/10.4049/jimmunol.1300436
21. Berger-Achituv S, Brinkmann V, Abed UA et al (2013) A proposed role for neutrophil extracellular traps in cancer immunoediting. Front Immunol 4:48. https://doi.org/10.3389/fimmu.2013.00048

22. Demers M, Krause DS, Schatzberg D et al (2012) Cancers predispose neutrophils to release extracellular DNA traps that contribute to cancer-associated thrombosis. Proc Natl Acad Sci U S A 109:13076–13081. https://doi.org/10.1073/pnas.1200419109
23. Erpenbeck L, Schön MP (2017) Neutrophil extracellular traps: protagonists of cancer progression? Oncogene 36:2483–2490. https://doi.org/10.1038/onc.2016.406
24. Cools-Lartigue J, Spicer J, McDonald B et al (2013) Neutrophil extracellular traps sequester circulating tumor cells and promote metastasis. J Clin Invest 123:3446–3458. https://doi.org/10.1172/JCI67484
25. Tohme S, Yazdani HO, Al-Khafaji AB et al (2016) Neutrophil extracellular traps promote the development and progression of liver metastases after surgical stress. Cancer Res 76:1367–1380. https://doi.org/10.1158/0008-5472.CAN-15-1591
26. Souto JC, Vila L, Brú A (2011) Polymorphonuclear neutrophils and cancer: intense and sustained neutrophilia as a treatment against solid tumors. Med Res Rev 31:311–363. https://doi.org/10.1002/med.20185
27. Steinberg BE, Grinstein S (2007) Unconventional roles of the NADPH oxidase: signaling, ion homeostasis, and cell death. Sci STKE 2007:pe11. https://doi.org/10.1126/stke.3792007pe11
28. Pilsczek FH, Salina D, Poon KKH et al (2010) A novel mechanism of rapid nuclear neutrophil extracellular trap formation in response to *Staphylococcus aureus*. J Immunol 185:7413–7425. https://doi.org/10.4049/jimmunol.1000675
29. Tong M, Potter JA, Mor G, Abrahams VM (2019) Lipopolysaccharide-stimulated human fetal membranes induce neutrophil activation and release of vital neutrophil extracellular traps. J Immunol 203(2):500–510. https://doi.org/10.4049/jimmunol.1900262
30. Papayannopoulos V, Metzler KD, Hakkim A, Zychlinsky A (2010) Neutrophil elastase and myeloperoxidase regulate the formation of neutrophil extracellular traps. J Cell Biol 191:677–691. https://doi.org/10.1083/jcb.201006052
31. Brinkmann V (2018) Neutrophil extracellular traps in the second decade. J Innate Immun 10:414–421. https://doi.org/10.1159/000489829
32. Brinkmann V, Goosmann C, Kühn LI, Zychlinsky A (2013) Automatic quantification of in vitro NET formation. Front Immunol 3:1–8. https://doi.org/10.3389/fimmu.2012.00413
33. Barrientos L, Marin-Esteban V, de Chaisemartin L et al (2013) An improved strategy to recover large fragments of functional human neutrophil extracellular traps. Front Immunol 4:166. https://doi.org/10.3389/fimmu.2013.00166
34. Masuda S, Nakazawa D, Shida H et al (2016) NETosis markers: quest for specific, objective, and quantitative markers. Clin Chim Acta 459:89–93. https://doi.org/10.1016/j.cca.2016.05.029
35. Brinkmann V, Laube B, Abu Abed U et al (2010) Neutrophil extracellular traps: how to generate and visualize them. J Vis Exp 36:1724. https://doi.org/10.3791/1724

Chapter 11

Induction and Detection of Necroptotic Cell Death in Mammalian Cell Culture

Mikhail Chesnokov, Imran Khan, and Ilana Chefetz

Abstract

The study of necroptosis is a rapidly growing field in current research of cell death mechanisms and cancer treatment strategies. While apoptotic cells can be reliably identified via annexin V assay, necroptosis is not associated with exposure of easily detectable markers. The most reliable way to identify necroptotic events is immunochemical detection of active phosphorylated RIPK1, RIPK3, and MLKL proteins facilitating necroptosis execution. This chapter describes a detailed protocol on necroptosis induction in human colon adenocarcinoma HT-29 cells, preparation of various positive and negative controls, detection of necroptosis mediator proteins via Western Blot analysis, and interpretation of results. This protocol allows reliable and specific detection of necroptosis in cell culture or tissue samples, and it provides a well-established model suitable for detailed studies of necroptosis molecular mechanisms in vitro.

Key words Necroptosis, Necroptosis induction, Necroptosis inhibitors, Necroptosis markers, TNFα, Caspase inhibitors, Western Blot

1 Introduction

1.1 Differences Between Necroptosis and Apoptosis

For many decades, apoptosis was considered the only mechanism of programmed cell death (PCD). However, that paradigm shifted with the discovery of stimuli inducing necrosis-like cell death upon caspase inhibition [1–4]. This new PCD mechanism was termed cell programmed necrosis, or "necroptosis," and has been shown to be controlled by its own distinctive cell signaling pathway [5, 6]. Other PCD pathways have been characterized recently, but apoptosis and necroptosis remain the most common and well-characterized cell death types [7]. Accordingly, research investigating cell death must reliably identify and differentiate apoptotic and necroptotic events.

The first fundamental difference between apoptosis and necroptosis is the morphology of dying cells. Apoptotic cells display chromatin condensation, shrinkage in size, and formation of small apoptotic bodies. On the other hand, necroptosis results in

Ayesha B. Alvero and Gil G. Mor (eds.), *Detection of Cell Death Mechanisms: Methods and Protocols*, Methods in Molecular Biology, vol. 2255, https://doi.org/10.1007/978-1-0716-1162-3_11,

mitochondrial membrane damage, cell swelling, vacuolization, and membrane rupture [1]. Morphological changes provide a precise way to identify necroptosis; however, their observation requires the usage of transmission electron microscopy, which is often inaccessible or cost prohibitive. Instead, molecular and biochemical markers can provide convenient and easily interpretable approach to cell death detection without the need for specialized equipment and training. An example of this approach is labeling apoptotic cells with Annexin V protein, which selectively binds phosphatidylserine after its translocation to the outer leaflet of the cell membrane. The utilization of Annexin V fluorescent conjugates in microscopy and flow cytometry allows simple and reliable detection of apoptotic events [8]. Unfortunately, no extracellular markers specific for necroptosis are described at this time; therefore, existing methodologies utilize the detection of intracellular proteins involved in necroptosis progression.

1.2 Molecular Markers of Necroptosis

Necroptosis is executed through a defined cellular regulatory circuit. While necroptosis-inducing factors may vary, the signal transduction is eventually facilitated through three major proteins: receptor interacting serine/threonine-protein kinase 1 (RIPK1), receptor interacting serine/threonine-protein kinase 3 (RIPK3), and mixed lineage kinase ligand (MLKL) [9]. RIPK1 and RIPK3 are protein kinases, while MLKL lacks enzyme activity and disrupts cell membrane integrity by forming transmembrane channels [10–13]. The necroptosis signaling pathway shows clear hierarchy: RIPK1 activation and phosphorylation at Ser166 stimulate the assembly of protein-protein complex with RIPK3 and RIPK3 autophosphorylation at Ser227 [6, 12, 14, 15]. Active RIPK3 binds MLKL and phosphorylates it at Ser358, inducing conformational changes, oligomerization, and channeling MLKL toward the cellular membrane where it executes the last phase of necroptosis through membrane permeabilization [16–18]. In some cases, RIPK3 can be activated as a result of autophosphorylation or interaction with TIR-domain-containing adapter-inducing interferon-β (TRIF) and Z-DNA Binding Protein 1 (ZBP1), rendering RIPK1 nonessential for necroptosis execution [19–21].

Activation of RIPK1, RIPK3, and MLKL through phosphorylation can be used to reliably identify necroptosis in cell culture and tissue samples via immunochemical methods like Western Blot or immunohistochemistry. Use of antibodies against phosphorylated or total proteins allows for the evaluation of RIPK1, RIPK3, and MLKL activity levels. However, conclusions based on phosphoprotein detection require several considerations. For example, RIPK1 was also shown to stimulate apoptosis in apoptosis-competent cells through activation of caspase-8; consequently, RIPK1 cannot be used alone as a necroptosis indicator [4, 22, 23]. The autophosphorylation capability of RIPK3 can also

produce detectable background signal in non-necroptotic samples, thus reducing its specificity. MLKL phosphorylation appears to be the most reliable indicator of necroptosis; however, the size and structural complexity of MLKL-containing protein complexes can cause technical difficulties during detection in nondenaturing conditions. Therefore, all three proteins should be used simultaneously to improve the efficacy of necroptosis identification.

Many manuscripts use inhibitors targeting RIPK1, RIPK3, or MLKL to discern necroptosis from other cell death types. Cell death rescued by these inhibitors serves as strong evidence for RIPK1, RIPK3, and MLKL-mediated necroptosis. The most common inhibitors are necrostatin-1 (NEC-1) for RIPK1, GSK'872 for RIPK3, and necrosulfonamide (NSA) for MLKL [6, 24–27]. However, the determination of cell death type should never be made based on inhibitor-induced rescue alone. RIPK1 kinase activity is involved in both apoptosis and necroptosis progression; therefore, NEC-1 cannot reliably discern between the two [4]. GSK'872 and other RIPK3 inhibitors can rescue necroptotic cell death and in certain conditions also trigger RIPK1-dependent apoptotic cell death [28]. NSA disrupts MLKL oligomerization and should likely be considered the most efficient necroptosis inhibitor [12]. On the other hand, NSA has additional side effects that can interfere with other detection methods. Our data indicate that NSA treatment causes pronounced phosphatidylserine exposure on the outer side of cell membrane and is therefore incompatible with Annexin V assays (data not shown). Additionally, unlike NEC-1 and GSK'872, NSA does not prevent phosphorylation of its target. As a result, we propose that NSA should be preferred for viability tests and necroptosis rescue studies, while NEC-1 and GSK'872 should be used for specific inhibition of RIPK1 and RIPK3 phosphorylation and activity, but not for determination of cell death type.

1.3 Necroptosis Induction

While necroptosis naturally occurs during a variety of physiological and pathological processes, detailed studies of its molecular mechanisms require well-characterized model systems. Such systems also allow generation of positive and negative controls that should be used in every experiment evaluating necroptosis initiation and progression. This chapter describes common necroptosis induction conditions and cell line-based models currently used in necroptosis studies.

Necroptosis is induced by various stimuli, including tumor necrosis factor α (TNFα), CD95 receptor/Fas ligand complex, other members of TNF superfamily [2, 5], and small molecules causing prominent cell stress (staurosporine [3], etoposide [4], shikonin [29], ALDH1A inhibitors, [30] and viral infections [31]). The most studied mechanism is facilitated through TNF-α-activated TNF receptor 1 (TNFR1), which binds and activates RIPK1 [32]. However, TNFα exposure alone primarily stimulates

cell survival through nuclear factor kappa B (NFκB) signaling, while necroptosis requires additional conditions including disruption of RIPK1 ubiquitination (required for NFκB activation) and inactivation of caspases (to prevent RIPK1-dependent apoptosis). The first condition can be achieved by using second mitochondrial-derived activator of caspase (SMAC) mimetics or translation inhibitor cycloheximide (CHX). SMAC mimetics antagonize cellular inhibitors of apoptosis (cIAPs) [33, 34]; CHX prevents accumulation of NFκB mediators and caspase-8 inhibitor cellular FLICE-like inhibitory protein (cFLIP) [35]. Both treatments result in apoptosis stimulation. Simultaneous inhibition of caspases with a pan-caspase inhibitor Z-VAD-FMK prevents apoptosis activation, triggering necroptosis facilitated through RIPK1-RIPK3-MLKL cascade as the preferred way of cell death [2].

HT-29 human colorectal adenocarcinoma cells and L929 murine fibroblasts are the most common cell lines reported to undergo necroptosis upon treatment with TNFα, SMAC mimetics/CHX, and Z-VAD-FMK [33, 36, 37]. A distinctive feature of L929 cells is their ability to initiate necroptosis when treated with TNFα alone—without additional factors. This effect is further promoted by caspase inhibitors [2]. Despite requirements for SMAC mimetics of CHX, HT-29 cells represent an important model for necroptosis studies due to their human origin and well-characterized downstream events.

2 Materials

2.1 Equipment

1. Hemocytometer or automated cell counter.
2. Centrifuge for 15 mL tubes.
3. Refrigerated centrifuge for 1.5 mL tubes capable of reaching at least 12,000 × *g*.
4. Western Blot apparatus of choice.

2.2 Cell Lines

1. HT-29 human colorectal adenocarcinoma cell line; alternatively, L929 murine fibroblasts (*see* **Note 1**).

2.3 Materials and Reagents

1. Sterile 60 or 100 mm tissue culture dishes.
2. Plastic cell scrapers.
3. Growth medium for HT-29: McCoy's 5A (Iwakata & Grace Modification) growth medium supplemented with 10% fetal bovine serum (FBS), 100 units/mL penicillin, 100 μg/mL streptomycin; Growth medium for L929 murine fibroblasts: DMEM +2 mM Glutamine +10% FBS.
4. Hank's Balanced Salt Solution (HBSS) without calcium and magnesium, sterile.

5. 0.25% Trypsin, in HBSS.
6. 0.4% Trypan Blue solution.
7. Dimethyl sulfoxide (DMSO), cell culture grade.
8. Sterile water, cell culture grade.
9. Human TNFα, 20 μg/mL in water.
10. Cycloheximide (CHX), 10 mg/mL in DMSO.
11. 20 mM Z-VAD-FMK, in DMSO.
12. 20 mM Necrostatin-1 (NEC-1), in DMSO.
13. 3 mM GSK'872, in DMSO.
14. 10 mM Necrosulfonamide (NSA), in DMSO.
15. Phosphate-buffered Saline (PBS): 10 mM Na_2HPO_4, 1.8 mM KH_2PO_4, 2.7 mM KCl, 137 mM NaCl, pH 7.4.
16. Radioimmunoprecipitation assay (RIPA) protein extraction buffer: 25 mM Tris–HCl, 150 mM NaCl, 1% NP-40, 1% sodium deoxycholate, 0.1% sodium dodecyl sulfate, pH 7.6.
17. Protease and phosphatase inhibitor cocktail of choice, used at concentrations suggested by manufacturer.
18. Bicinchoninic acid (BCA) protein quantification assay.
19. Conventional Western Blot reagents and solutions of choice.
20. Tris-buffered saline with Tween-20 (TBST): 20 mM Tris, 150 mM NaCl, 0.1% Tween-20, pH 7.6.
21. Bovine Serum Albumin, Fraction V (BSA), suitable for immunochemical assays.
22. Commercially available stripping buffer for Western Blot.
23. Enhanced chemiluminescent (ECL) substrate for Western Blot membrane development.
24. Antibodies against total and phosphorylated RIPK1, RIPK3 and MLKL.
25. Antibodies against reference protein of choice: glyceraldehyde 3-phosphate dehydrogenase (GAPDH) and vinculin recommended.
26. Appropriate HRP-conjugated secondary antibodies.

3 Methods

This section provides instructions on cell seeding (*see* Subheading 3.1), treatment (*see* Subheading 3.2), protein purification (*see* Subheading 3.3), and Western Blot analysis of major protein regulators of necroptosis (*see* Subheading 3.4).

3.1 Cell Seeding for Treatment

HT-29 cells are used as a model for necroptosis induction in this protocol; therefore, cell numbers were optimized in regard to their size and proliferation rate. If other cell lines are used, seeding numbers must be adjusted to achieve 50–60% confluence the day after seeding.

1. Cultivate HT-29 cells in complete growth medium to the final amount of at least 30 million cells in total (two 100 mm tissue culture dishes or 75 cm^2 tissue culture flasks with cell confluence of 80% or higher);
2. Aspirate growth media and wash the cells with HBSS;
3. Aspirate HBSS and add enough volume of trypsin to cover the vessel;
4. Observe the trypsinization process under the microscope and proceed when the cells start detaching from the vessel surface;
5. Add complete growth medium to the vessel in volume equal to trypsin volume and detach the cells from surface by repeated pipetting;
6. Collect the cell suspension into sterile centrifuge tube and spin at 300 × *g* for 5 min;
7. Aspirate the supernatant and thoroughly resuspend cells in full growth medium (*see* **Note 2**);
8. Mix 10 μL of cell suspension with 10 μL of Trypan Blue solution;
9. Estimate the number of viable cells per mL of suspension using a hemocytometer or automated cell counter;
10. Seed three million viable cells into 60 mm tissue culture dishes in 5 mL of complete growth media, 9 dishes in total;
11. Thoroughly mix the cell suspension in dishes and incubate them overnight at 37 °C in a CO_2 incubator.

3.2 Cell Treatment for Necroptosis Induction

Cell treatment should begin when cultures are around 60% confluent (*see* **Note 3**). This protocol uses nine different conditions that include necroptosis-inducing treatment, various controls, and necroptosis-inducing treatments with addition of known necroptosis inhibitors. The following labels are used below for treatment conditions:

- Control—treatment with vehicle only (0.3% DMSO);
- T—treatment with 20 ng/mL TNFα;
- C—treatment with 10 μg/mL CHX;
- Z—treatment with 20 μM Z-VAD-FMK;
- TC—treatment with 20 ng/mL TNFα and 10 μg/mL CHX;

- TCZ—treatment with 20 ng/mL TNFα, 10 μg/mL CHX, and 20 μM Z-VAD-FMK;
- TCZ + NEC-1—treatment with 20 ng/mL TNFα, 10 μg/mL CHX, 20 μM Z-VAD-FMK, and 20 μM NEC-1;
- TCZ + GSK—treatment with 20 ng/mL TNFα, 10 μg/mL CHX, 20 μM Z-VAD-FMK, and 3 μM GSK'872;
- TCZ + NSA—treatment with 20 ng/mL TNFα, 10 μg/mL CHX, 20 μM Z-VAD-FMK, and 10 μM NSA;

1. Prepare and label 15 mL tubes according to the scheme shown above, 9 tubes in total;
2. Put 5.5 mL of complete growth medium into each of the 15 mL tubes (*see* **Note 4**);
3. Add 5.5 μL of 20 mM Z-VAD-FMK to the following tubes: Z, TCZ, TCZ + NEC-1, TCZ + GSK, and TCZ + NSA;
4. Add 5.5 μL of 20 mM NEC-1 to TCZ + NEC-1 tube;
5. Add 5.5 μL of 3 mM GSK'872 to TCZ + GSK tube;
6. Add 5.5 μL of 10 mM NSA to TCZ + NSA tube;
7. Add 5.5 μL of DMSO to the following tubes: Z and TCZ;
8. Add 11 μL of DMSO to the following tubes: Control, T, C, and TC;
9. Thoroughly mix treatment media by vortexing or pipetting;
10. Label the dishes with HT-29 cells according to the treatment scheme shown above;
11. Aspirate growth media from the dishes and add 4 mL of corresponding treatment media (*see* **Note 5**). Keep the remaining treatment media;
12. Incubate the dishes at 37 °C in a CO_2 incubator for 60 min;
13. Prepare and label a new set of 9 tubes according to the scheme shown above;
14. Put 1.1 mL of treatment media left after cell pretreatment into corresponding tubes;
15. Add 5.5 μL of 20 μg/mL TNFα to the following tubes: T, CT, TCZ, TCZ + NEC-1, TCZ + GSK, and TCZ + NSA (*see* **Note 6**);
16. Add 5.5 μL of 10 mg/mL CHX to the following tubes: C, CT, TCZ, TCZ + NEC-1, TCZ + GSK, and TCZ + NSA;
17. Add 5.5 μL of DMSO to the following tubes: Control, T, and Z;
18. Add 5.5 μL of sterile water to the following tubes: Control, C, and Z;

19. Thoroughly mix treatment media by vortexing or pipetting;
20. Add 1 mL of treatment media from the second set of tubes into corresponding dishes with pretreated cells, spreading it over the whole dish in a dropwise manner (*see* **Notes 7** and **8**);
21. Mix the treatment media in the dishes by gentle swirling and rocking;
22. Incubate the dishes at 37 °C in a CO_2 incubator for 7–10 h (*see* **Note 9**).

3.3 Protein Purification

1. Chill PBS on ice prior to protein extraction;
2. Prepare 2 mL of complete RIPA lysis buffer with protease and phosphatase inhibitors and keep it on ice (*see* **Note 10**);
3. Put the dishes with treated HT-29 cells on ice and keep them on ice during all steps of protein extraction;
4. Aspirate growth media from the dishes and add 5 mL of ice-cold PBS;
5. Carefully wash the cells by gently rocking the dishes back and forth, avoid abrupt movements to prevent cell detaching;
6. Aspirate PBS as thorough as possible and put 200 μL of cold RIPA buffer to each dish;
7. Spread RIPA buffer across whole area of the dish using a cell scraper;
8. Incubate on ice for 15–20 min;
9. Scrape the cells from the surface with a scraper and transfer cells and RIPA buffer into prechilled 1.5 mL tubes;
10. Disrupt any cell clumps by pipetting the lysates 5–7 times with 200 μL pipette tip;
11. Incubate the lysates on ice for 5–10 more minutes;
12. Centrifuge the tubes at 12,000 × *g* for 15 min at 4 °C;
13. Transfer the protein extracts into clean prechilled tubes (*see* **Note 11**);
14. Store purified protein samples at −80 °C.

3.4 Western Blot Analysis of Proteins Involved in Necroptosis

Cell death facilitated through necroptotic mechanisms is distinguished by specific changes in activity and phosphorylation of RIPK1, RIPK3, and MLKL proteins. Western Blot is one of the easiest ways to monitor these changes and confirm necroptosis induction. At the same time, necroptosis inhibitors should prevent signal transduction through RIPK1-RIPK3-MLKL cascade, causing specific changes of protein phosphorylation. As a result, HT-29 cells subjected to necroptosis-inducing stimuli should be rescued by addition of RIPK1, RIPK3, and MLKL inhibitors. These changes in cell viability and protein phosphorylation are depicted in Fig. 1 and are explained in detail within the Figure Caption.

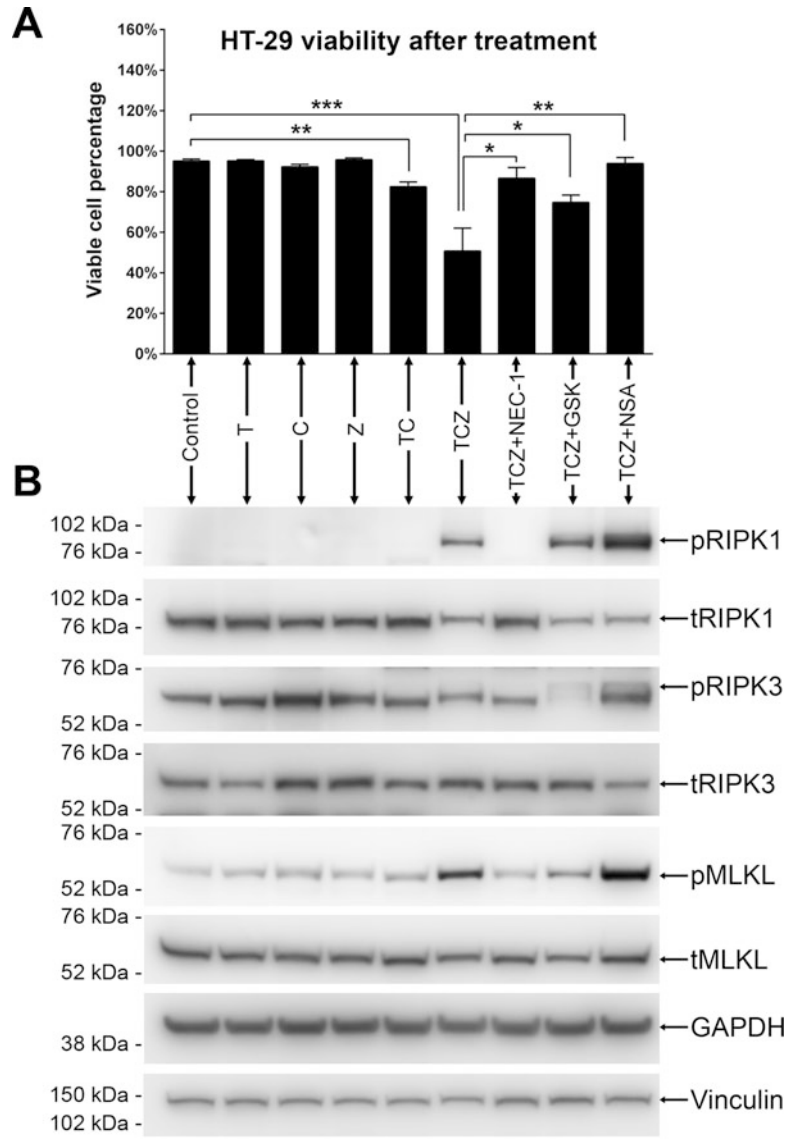

Fig. 1 Induction and detection of TNFα-induced necroptosis in HT-29 cells. (**a**) Effects of TNFα, CHX, Z-VAD-FMK, NEC-1, GSK'872, and NSA treatment on viability of HT-29 cells. Cells were treated according to the aforementioned protocol, but the length of treatment was extended to 72 h. Cell viability was determined based on Trypan Blue exclusion assay. TNFα+CHX + Z-VAD-FMK treatment induces prominent cell death that is prevented by addition of NEC-1, GSK'872, or NSA. * $-p < 0.05$, ** $-p < 0.01$, *** $-p < 0.001$ based on Mann-Whitney U test. (**b**) Phosphorylation state of major necroptosis mediators in HT-29 cells treated with TNFα, CHX, Z-VAD-FMK, NEC-1, GSK'872, and NSA. Phosphorylated proteins are denoted as pRIPK1, pRIPK3 (*see* **Note 14**), and pMLKL; total proteins are denoted as tRIPK1, tRIPK3, and tMLKL, respectively. Treatment with single drugs or TNFα+CHX combination (lanes T, C, Z, and TC) does not result in any significant activation of RIPK1, RIPK3, or MLKL in

1. Evaluate total protein concentration in the purified extracts using standard protein quantification assay; BCA protein assay is highly recommended (*see* **Note 12**);
2. Prepare samples for SDS-polyacrylamide gel electrophoresis according to protocol of choice;
3. Load 40 μg or more of total protein per lane;
4. Run protein gel electrophoresis and transfer to a PVDF membrane according to protocol of choice;
5. Block the membranes with 5% BSA diluted in TBST for 1 h;
6. Probe the membranes with antibodies against phospho-RIPK1, phospho-RIPK3, or phospho-MLKL diluted in TBST with 5% BSA overnight at 4 °C (*see* **Notes 13** and **14**);
7. Develop the membranes with ECL substrate (*see* **Note 15**);
8. Strip membranes with stripping buffer and block the membranes with 5% BSA diluted in TBST for 1 h;
9. Reprobe the same membranes with antibodies against total RIPK1, total RIPK3, or total MLKL diluted in TBST with 5% BSA overnight at 4 °C (*see* **Note 16**);
10. Develop the membranes with ECL substrate for Western Blot;
11. Strip membranes with stripping buffer and block the membranes with 5% BSA diluted in TBST for 1 h;
12. Reprobe the same membranes with antibodies against GAPDH or vinculin diluted in TBST with 5% BSA (*see* **Note 17**);
13. Develop the membranes with ECL substrate for Western Blot;
14. Compare the levels of phosphorylated and total proteins in the samples to evaluate the necroptosis-associated changes. Use Fig. 1 as a reference.

Fig. 1 (continued) comparison to Control. Treatment with necroptosis-inducing TCZ combination results in prominent phosphorylation of RIPK1 and MLKL and weak phosphorylation of RIPK3 (indicated by a faint band appearing right above the bright band present in all samples including Control). Addition of NEC-1 completely inhibits phosphorylation of RIPK1 and therefore prevents subsequent activation of RIPK3 and MLKL. Addition of GSK'872 significantly reduces RIPK3 phosphorylation and MLKL activation, but it does not affect RIPK1 phosphorylation since RIPK1 is an upstream element of the cascade. Addition of NSA, while preventing MLKL-dependent cell death, does not prevent phosphorylation of RIPK1, RIPK3, or MLKL itself

4 Notes

This section provides additional explanations and suggestions for the instructions outlined in the main protocol.

1. HT-29 human colorectal adenocarcinoma cells and L929 murine fibroblasts are the most common cell lines reported to undergo necroptosis upon treatment with TNFα, SMAC mimetics/CHX, and Z-VAD-FMK.
2. HT-29 cells are predisposed to forming cell-cell contacts; therefore, thorough resuspension is required. Failing to fulfill this requirement may result in highly heterogeneous cell distribution across the dish surface and reduced assay efficacy due to notable resistance of tight HT-29 cell clusters to drug treatment. Do not leave resuspended cells in tubes for prolonged periods of time, since this will result in their aggregation;
3. The efficiency and specificity of necroptosis induction in cells are significantly affected by cell conditions prior to treatment. For optimal results, the cells should be at 60% confluence and spread homogeneously across the surface of the culture dish. If the cells form tight clumps and clusters, they will be less sensitive to the treatment. If the cells appear stressed, damaged, or dying, they are likely to demonstrate high background activity of necroptosis mediators, making the experiment less specific.
4. Treatment media volumes provided in this step and subsequent steps suggest preparation of 10% extra volume. This prevents accidental media loss due to pipetting errors and foaming.
5. To minimize cell stress during media replacement, it is recommended to proceed by replacing medium in one dish at a time;
6. **Steps 15–18** describe preparation of treatment media with 5× concentrations of TNFα (100 ng/mL), CHX (50 μg/mL), and DMSO (0.5%). These solutions are diluted fivefold in **step 20** by adding 1 mL of 5× treatment media to 4 mL of media already present in each dish;
7. If desired, the preparation of 5× treatment media may be substituted by preparation of 5 mL of 1× treatment media (working drug concentrations are 20 ng/mL TNFα, 10 μg/mL CHX, 20 μM Z-VAD-FMK, 20 μM NEC-1, 3 μM GSK'872, and 10 μM NSA) and complete replacement of pretreatment media with fresh treatment media after 60 min. However, this approach will use twice as much Z-VAD-FMK, NEC-1, GSK'872, and NSA and will subject cells to additional stress due to an extra cycle of media aspiration and replacement;

8. Some protocols suggest using Z-VAD-FMK, NEC-1, GSK'872, and NSA only for pretreatment and not for a full treatment duration. However, our tests demonstrate that keeping these inhibitors throughout the entire treatment results in more efficient RIPK1, RIPK3, and MLKL inhibition and cell death rescue;
9. Seven hours of treatment is usually enough to induce prominent activation of RIPK1, RIPK3, and MLKL in HT-29 cells. Treatment for more than 10 h stimulates protein degradation and results in less total protein yield, plus reduced sensitivity and increased background in Western Blot assays. Treatment times should be experimentally optimized if different cell cultures are used;
10. Extracting proteins from HT-29 cells can be challenging; therefore, this protocol uses RIPA buffer due to its high protein extraction efficiency. If preservation of protein-protein complexes is important for subsequent experiments, mild lysis buffers that do not contain sodium dodecyl sulfate should be used; however, the expected protein yield will be lower.
11. If the protein-containing supernatants have nonpelleted debris or turbidity, an additional centrifugation at 12,000 × *g* or higher for 20 min at 4 °C should be performed to clear the lysates;
12. Bradford protein assays are not recommended for samples purified using RIPA buffer because SDS increases background signal. Bradford assays are acceptable if the lysis buffer does not contain SDS;
13. In the case of antibodies targeting phosphorylated proteins, it is recommended to use 5% BSA solution in TBST instead of 5% skim milk to improve assay sensitivity. Casein from skim milk can nonspecifically bind phospho-specific antibodies, resulting in higher background. Secondary antibodies, however, should be always diluted with 5% skim milk in TBST to achieve better blocking efficiency and to avoid detection of nonspecific bands;
14. Phospho-RIPK3 (Ser227) antibody included in the Cell Signaling Technology Necroptosis Antibody Sampler Kit (Cat. No. 98110) has low specificity and detects a visible band around 60 kDa even in normal conditions. This band most likely represents nonactive RIPK3 protein. Activated phosphorylated RIPK3 has lower electrophoretic mobility and is therefore detected as a second band slightly higher than the nonspecific one. This band upshift was reported in published research papers [12, 33, 38], but reliable detection of upshifted band requires optimization of electrophoresis condition (e.g., higher acrylamide percentage and prolonged run time). Substitution of Cell Signaling Technology phospho-RIPK3

antibodies with antibodies from other manufacturers can improve detection specificity. Nevertheless, the Cell Signaling Technology Necroptosis Antibody Sampler Kit is recommended for initial experiments because it provides all antibodies required for necroptosis detection in one package;

15. Present protocols suggest the stripping and reprobing of Western Blot membranes if the bands were detected using ECL technique. Diaminobenzidine staining cannot be stripped from the membrane, and it requires the use of a new membrane for each antibody and is therefore not recommended;
16. There are two strategies in reprobing membranes with antibodies against total proteins:
    - Detecting the same protein (e.g., probing the membrane previously stained for phospho-RIPK1 with total RIPK1 antibodies) allows more direct comparison of phospho- and total protein levels, but it can be affected by inefficient stripping of phospho-protein bands. Usually, this is not a problem because total proteins typically produce bands of much higher intensity than phosphorylated ones. Nevertheless, it is recommended to test stripping efficiency and optimize the protocol prior to use;
    - Detecting protein of different molecular weight (e.g., probing membrane previously stained for phospho-RIPK1 with total MLKL antibodies) avoids the risk of band overlap even if the stripping process was not efficient enough. However, use of different membranes for phospho- and total protein detection makes comparison of protein levels trickier (band intensity may be affected by gel defects, protein transfer efficiency, and other handling factors);
17. Housekeeping reference proteins like GAPDH and vinculin are expressed at very high levels and should be detected last. Based on our experience, β-actin and α-tubulin should be avoided, since their levels can be significantly altered by necroptosis induction;

References

1. Hirsch T, Marchetti P, Susin SA, Dallaporta B, Zamzami N, Marzo I, Geuskens M, Kroemer G (1997) The apoptosis-necrosis paradox. Apoptogenic proteases activated after mitochondrial permeability transition determine the mode of cell death. Oncogene 15 (13):1573–1581. https://doi.org/10.1038/sj.onc.1201324
2. Vercammen D, Beyaert R, Denecker G, Goossens V, Van Loo G, Declercq W, Grooten J, Fiers W, Vandenabeele P (1998) Inhibition of caspases increases the sensitivity of L929 cells to necrosis mediated by tumor necrosis factor. J Exp Med 187(9):1477–1485. https://doi.org/10.1084/jem.187.9.1477
3. Dunai ZA, Imre G, Barna G, Korcsmaros T, Petak I, Bauer PI, Mihalik R (2012) Staurosporine induces necroptotic cell death under caspase-compromised conditions in U937 cells. PLoS One 7(7):e41945. https://doi.org/10.1371/journal.pone.0041945

4. Tenev T, Bianchi K, Darding M, Broemer M, Langlais C, Wallberg F, Zachariou A, Lopez J, MacFarlane M, Cain K, Meier P (2011) The Ripoptosome, a signaling platform that assembles in response to genotoxic stress and loss of IAPs. Mol Cell 43(3):432–448. https://doi.org/10.1016/j.molcel.2011.06.006
5. Degterev A, Huang Z, Boyce M, Li Y, Jagtap P, Mizushima N, Cuny GD, Mitchison TJ, Moskowitz MA, Yuan J (2005) Chemical inhibitor of nonapoptotic cell death with therapeutic potential for ischemic brain injury. Nat Chem Biol 1(2):112–119. https://doi.org/10.1038/nchembio711
6. Degterev A, Hitomi J, Germscheid M, Ch'en IL, Korkina O, Teng X, Abbott D, Cuny GD, Yuan C, Wagner G, Hedrick SM, Gerber SA, Lugovskoy A, Yuan J (2008) Identification of RIP1 kinase as a specific cellular target of necrostatins. Nat Chem Biol 4(5):313–321. https://doi.org/10.1038/nchembio.83
7. Galluzzi L, Vitale I, Aaronson SA, Abrams JM, Adam D, Agostinis P, Alnemri ES, Altucci L, Amelio I, Andrews DW, Annicchiarico-Petruzzelli M, Antonov AV, Arama E, Baehrecke EH, Barlev NA, Bazan NG, Bernassola F, Bertrand MJM, Bianchi K, Blagosklonny MV, Blomgren K, Borner C, Boya P, Brenner C, Campanella M, Candi E, Carmona-Gutierrez D, Cecconi F, Chan FK, Chandel NS, Cheng EH, Chipuk JE, Cidlowski JA, Ciechanover A, Cohen GM, Conrad M, Cubillos-Ruiz JR, Czabotar PE, D'Angiolella V, Dawson TM, Dawson VL, De Laurenzi V, De Maria R, Debatin KM, DeBerardinis RJ, Deshmukh M, Di Daniele N, Di Virgilio F, Dixit VM, Dixon SJ, Duckett CS, Dynlacht BD, El-Deiry WS, Elrod JW, Fimia GM, Fulda S, Garcia-Saez AJ, Garg AD, Garrido C, Gavathiotis E, Golstein P, Gottlieb E, Green DR, Greene LA, Gronemeyer H, Gross A, Hajnoczky G, Hardwick JM, Harris IS, Hengartner MO, Hetz C, Ichijo H, Jaattela M, Joseph B, Jost PJ, Juin PP, Kaiser WJ, Karin M, Kaufmann T, Kepp O, Kimchi A, Kitsis RN, Klionsky DJ, Knight RA, Kumar S, Lee SW, Lemasters JJ, Levine B, Linkermann A, Lipton SA, Lockshin RA, Lopez-Otin C, Lowe SW, Luedde T, Lugli E, MacFarlane M, Madeo F, Malewicz M, Malorni W, Manic G, Marine JC, Martin SJ, Martinou JC, Medema JP, Mehlen P, Meier P, Melino S, Miao EA, Molkentin JD, Moll UM, Munoz-Pinedo C, Nagata S, Nunez G, Oberst A, Oren M, Overholtzer M, Pagano M, Panaretakis T, Pasparakis M, Penninger JM, Pereira DM, Pervaiz S, Peter ME, Piacentini M, Pinton P, Prehn JHM, Puthalakath H, Rabinovich GA, Rehm M, Rizzuto R, Rodrigues CMP, Rubinsztein DC, Rudel T, Ryan KM, Sayan E, Scorrano L, Shao F, Shi Y, Silke J, Simon HU, Sistigu A, Stockwell BR, Strasser A, Szabadkai G, Tait SWG, Tang D, Tavernarakis N, Thorburn A, Tsujimoto Y, Turk B, Vanden Berghe T, Vandenabeele P, Vander Heiden MG, Villunger A, Virgin HW, Vousden KH, Vucic D, Wagner EF, Walczak H, Wallach D, Wang Y, Wells JA, Wood W, Yuan J, Zakeri Z, Zhivotovsky B, Zitvogel L, Melino G, Kroemer G (2018) Molecular mechanisms of cell death: recommendations of the Nomenclature Committee on Cell Death 2018. Cell Death Differ 25(3):486–541. https://doi.org/10.1038/s41418-017-0012-4
8. van Engeland M, Nieland LJ, Ramaekers FC, Schutte B, Reutelingsperger CP (1998) Annexin V-affinity assay: a review on an apoptosis detection system based on phosphatidylserine exposure. Cytometry 31(1):1–9. https://doi.org/10.1002/(sici)1097-0320(19980101)31:1<1::aid-cyto1>3.0.co;2-r
9. Grootjans S, Vanden Berghe T, Vandenabeele P (2017) Initiation and execution mechanisms of necroptosis: an overview. Cell Death Differ 24(7):1184–1195. https://doi.org/10.1038/cdd.2017.65
10. Holler N, Zaru R, Micheau O, Thome M, Attinger A, Valitutti S, Bodmer JL, Schneider P, Seed B, Tschopp J (2000) Fas triggers an alternative, caspase-8-independent cell death pathway using the kinase RIP as effector molecule. Nat Immunol 1(6):489–495. https://doi.org/10.1038/82732
11. Zhang J, Zhang H, Li J, Rosenberg S, Zhang EC, Zhou X, Qin F, Farabaugh M (2011) RIP1-mediated regulation of lymphocyte survival and death responses. Immunol Res 51(2–3):227–236. https://doi.org/10.1007/s12026-011-8249-3
12. Sun L, Wang H, Wang Z, He S, Chen S, Liao D, Wang L, Yan J, Liu W, Lei X, Wang X (2012) Mixed lineage kinase domain-like protein mediates necrosis signaling downstream of RIP3 kinase. Cell 148(1–2):213–227. https://doi.org/10.1016/j.cell.2011.11.031
13. Dondelinger Y, Declercq W, Montessuit S, Roelandt R, Goncalves A, Bruggeman I, Hulpiau P, Weber K, Sehon CA, Marquis RW, Bertin J, Gough PJ, Savvides S, Martinou JC, Bertrand MJ, Vandenabeele P (2014) MLKL compromises plasma membrane integrity by binding to phosphatidylinositol phosphates. Cell Rep 7(4):971–981. https://doi.org/10.1016/j.celrep.2014.04.026

14. Zhang Y, Su SS, Zhao S, Yang Z, Zhong C-Q, Chen X, Cai Q, Yang Z-H, Huang D, Wu R, Han J (2017) RIP1 autophosphorylation is promoted by mitochondrial ROS and is essential for RIP3 recruitment into necrosome. Nat Commun 8:14329–14329. https://doi.org/10.1038/ncomms14329
15. Cho Y, Challa S, Moquin D, Genga R, Ray TD, Guildford M, Chan FK-M (2009) Phosphorylation-driven assembly of the RIP1-RIP3 complex regulates programmed necrosis and virus-induced inflammation. Cell 137 (6):1112–1123. https://doi.org/10.1016/j.cell.2009.05.037
16. Murphy JM, Czabotar PE, Hildebrand JM, Lucet IS, Zhang JG, Alvarez-Diaz S, Lewis R, Lalaoui N, Metcalf D, Webb AI, Young SN, Varghese LN, Tannahill GM, Hatchell EC, Majewski IJ, Okamoto T, Dobson RC, Hilton DJ, Babon JJ, Nicola NA, Strasser A, Silke J, Alexander WS (2013) The pseudokinase MLKL mediates necroptosis via a molecular switch mechanism. Immunity 39(3):443–453. https://doi.org/10.1016/j.immuni.2013.06.018
17. Liu S, Liu H, Johnston A, Hanna-Addams S, Reynoso E, Xiang Y, Wang Z (2017) MLKL forms disulfide bond-dependent amyloid-like polymers to induce necroptosis. Proc Natl Acad Sci U S A 114(36):E7450–E7459. https://doi.org/10.1073/pnas.1707531114
18. Wang H, Sun L, Su L, Rizo J, Liu L, Wang LF, Wang FS, Wang X (2014) Mixed lineage kinase domain-like protein MLKL causes necrotic membrane disruption upon phosphorylation by RIP3. Mol Cell 54(1):133–146. https://doi.org/10.1016/j.molcel.2014.03.003
19. Orozco S, Yatim N, Werner MR, Tran H, Gunja SY, Tait SW, Albert ML, Green DR, Oberst A (2014) RIPK1 both positively and negatively regulates RIPK3 oligomerization and necroptosis. Cell Death Differ 21 (10):1511–1521. https://doi.org/10.1038/cdd.2014.76
20. Kaiser WJ, Sridharan H, Huang C, Mandal P, Upton JW, Gough PJ, Sehon CA, Marquis RW, Bertin J, Mocarski ES (2013) Toll-like receptor 3-mediated necrosis via TRIF, RIP3, and MLKL. J Biol Chem 288(43):31268–31279. https://doi.org/10.1074/jbc.M113.462341
21. Newton K, Wickliffe KE, Maltzman A, Dugger DL, Strasser A, Pham VC, Lill JR, Roose-Girma M, Warming S, Solon M, Ngu H, Webster JD, Dixit VM (2016) RIPK1 inhibits ZBP1-driven necroptosis during development. Nature 540(7631):129–133. https://doi.org/10.1038/nature20559
22. Feoktistova M, Geserick P, Kellert B, Dimitrova DP, Langlais C, Hupe M, Cain K, MacFarlane M, Hacker G, Leverkus M (2011) cIAPs block Ripoptosome formation, a RIP1/caspase-8 containing intracellular cell death complex differentially regulated by cFLIP isoforms. Mol Cell 43(3):449–463. https://doi.org/10.1016/j.molcel.2011.06.011
23. Dondelinger Y, Jouan-Lanhouet S, Divert T, Theatre E, Bertin J, Gough PJ, Giansanti P, Heck AJ, Dejardin E, Vandenabeele P, Bertrand MJ (2015) NF-kappaB-independent role of IKKalpha/IKKbeta in preventing RIPK1 kinase-dependent apoptotic and necroptotic cell death during TNF signaling. Mol Cell 60(1):63–76. https://doi.org/10.1016/j.molcel.2015.07.032
24. Chen S, Lv X, Hu B, Shao Z, Wang B, Ma K, Lin H, Cui M (2017) RIPK1/RIPK3/MLKL-mediated necroptosis contributes to compression-induced rat nucleus pulposus cells death. Apoptosis 22(5):626–638. https://doi.org/10.1007/s10495-017-1358-2
25. Chen T, Pan H, Li J, Xu H, Jin H, Qian C, Yan F, Chen J, Wang C, Chen J, Wang L, Chen G (2018) Inhibiting of RIPK3 attenuates early brain injury following subarachnoid hemorrhage: possibly through alleviating necroptosis. Biomed Pharmacother 107:563–570. https://doi.org/10.1016/j.biopha.2018.08.056
26. Arora D, Siddiqui MH, Sharma PK, Shukla Y (2016) Deltamethrin induced RIPK3-mediated caspase-independent non-apoptotic cell death in rat primary hepatocytes. Biochem Biophys Res Commun 479(2):217–223. https://doi.org/10.1016/j.bbrc.2016.09.042
27. Jing L, Song F, Liu Z, Li J, Wu B, Fu Z, Jiang J, Chen Z (2018) MLKL-PITPalpha signaling-mediated necroptosis contributes to cisplatin-triggered cell death in lung cancer A549 cells. Cancer Lett 414:136–146. https://doi.org/10.1016/j.canlet.2017.10.047
28. Mandal P, Berger SB, Pillay S, Moriwaki K, Huang C, Guo H, Lich JD, Finger J, Kasparcova V, Votta B, Ouellette M, King BW, Wisnoski D, Lakdawala AS, DeMartino MP, Casillas LN, Haile PA, Sehon CA, Marquis RW, Upton J, Daley-Bauer LP, Roback L, Ramia N, Dovey CM, Carette JE, Chan FK, Bertin J, Gough PJ, Mocarski ES, Kaiser WJ (2014) RIP3 induces apoptosis independent of pronecrotic kinase activity. Mol Cell 56 (4):481–495. https://doi.org/10.1016/j.molcel.2014.10.021
29. Piao JL, Cui ZG, Furusawa Y, Ahmed K, Rehman MU, Tabuchi Y, Kadowaki M, Kondo T

(2013) The molecular mechanisms and gene expression profiling for shikonin-induced apoptotic and necroptotic cell death in U937 cells. Chem Biol Interact 205(2):119–127. https://doi.org/10.1016/j.cbi.2013.06.011

30. Chefetz I, Grimley E, Yang K, Hong L, Vinogradova EV, Suciu R, Kovalenko I, Karnak D, Morgan CA, Chtcherbinine M, Buchman C, Huddle B, Barraza S, Morgan M, Bernstein KA, Yoon E, Lombard DB, Bild A, Mehta G, Romero I, Chiang CY, Landen C, Cravatt B, Hurley TD, Larsen SD, Buckanovich RJ (2019) A pan-ALDH1A inhibitor induces Necroptosis in ovarian cancer stem-like cells. Cell Rep 26(11):3061–3075.e3066. https://doi.org/10.1016/j.celrep.2019.02.032
31. Upton JW, Kaiser WJ, Mocarski ES (2012) DAI/ZBP1/DLM-1 complexes with RIP3 to mediate virus-induced programmed necrosis that is targeted by murine cytomegalovirus vIRA. Cell Host Microbe 11(3):290–297. https://doi.org/10.1016/j.chom.2012.01.016
32. Micheau O, Tschopp J (2003) Induction of TNF receptor I-mediated apoptosis via two sequential signaling complexes. Cell 114 (2):181–190. https://doi.org/10.1016/s0092-8674(03)00521-x
33. He S, Wang L, Miao L, Wang T, Du F, Zhao L, Wang X (2009) Receptor interacting protein kinase-3 determines cellular necrotic response to TNF-alpha. Cell 137(6):1100–1111. https://doi.org/10.1016/j.cell.2009.05.021
34. Bai L, Smith DC, Wang S (2014) Small-molecule SMAC mimetics as new cancer therapeutics. Pharmacol Ther 144(1):82–95. https://doi.org/10.1016/j.pharmthera.2014.05.007
35. Kreuz S, Siegmund D, Scheurich P, Wajant H (2001) NF-kappaB inducers upregulate cFLIP, a cycloheximide-sensitive inhibitor of death receptor signaling. Mol Cell Biol 21 (12):3964–3973. https://doi.org/10.1128/mcb.21.12.3964-3973.2001
36. Seo J, Lee EW, Sung H, Seong D, Dondelinger Y, Shin J, Jeong M, Lee HK, Kim JH, Han SY, Lee C, Seong JK, Vandenabeele P, Song J (2016) CHIP controls necroptosis through ubiquitylation- and lysosome-dependent degradation of RIPK3. Nat Cell Biol 18(3):291–302. https://doi.org/10.1038/ncb3314
37. Ros U, Pena-Blanco A, Hanggi K, Kunzendorf U, Krautwald S, Wong WW, Garcia-Saez AJ (2017) Necroptosis execution is mediated by plasma membrane nanopores independent of calcium. Cell Rep 19 (1):175–187. https://doi.org/10.1016/j.celrep.2017.03.024
38. Weber K, Roelandt R, Bruggeman I, Estornes Y, Vandenabeele P (2018) Nuclear RIPK3 and MLKL contribute to cytosolic necrosome formation and necroptosis. Commun Biol 1(1):6. https://doi.org/10.1038/s42003-017-0007-1

Chapter 12

Visualization of Necroptotic Cell Death through Transmission Electron Microscopy

Naresh Golla, Linda J. Hong, and Ilana Chefetz

Abstract

Transmission electron microscopy (TEM) is an all-in-one tool to visualize the complex systems of any specimen that is 1 nm in size or smaller. The current chapter provides detailed guidelines for imaging morphological changes during programmed cell necrosis using TEM as a single-step methodology. In this protocol, a novel aldehyde dehydrogenase inhibitor is used to induce cell programmed necrosis in ovarian cancer cell lines (A2780 and SKOV3). This process is followed by gradient dehydration with ethanol, chemical fixation, sampled grid preparation, and staining with 0.75% uranyl formate. Following fixation and grid preparation, cells are imaged using TEM. The resulting images reveal morphological changes consistent with necrotic morphology, including swelling of cells and organelles, appearance of vacuoles, and plasma membrane rupture followed by leakage of cellular contents. The current approach allows a single-step methodology for characterization of cell-programmed necrosis in cells based on morphology.

Key words Transmission electron microscopy (TEM), Negative staining, Aldehyde dehydrogenase inhibition, Cellular morphology, Necroptosis

1 Introduction

1.1 Transmission Electron Microscopy

Transmission Electron Microscopy (TEM) was invented by Ernst Ruska and Max Knoll [1]. TEM is a powerful imaging tool of scanning electron microscopy (SEM) in transmission mode. The downstream application of TEM is focused on detecting and visualizing particles smaller than 1 nm from any specimen [2]. Keith Porter was the first person to use TEM to visualize and capture eukaryotic cell images [3]. In fact, using TEM, preparation of samples in their native state and capture of high resolution images allow cellular visualization and characterization [4, 5]. Depending on the preparation and resolution requirements, TEM has evolved to include variations like cryo-electronic microscopy (CEM), cryo-electron tomography (CET), and cryo-electron microscopy of vitreous sections (CEMOVIS) [6, 7]. Currently, due to the maximal resolution of TEM and its relatively simple methodology, TEM is

Ayesha B. Alvero and Gil G. Mor (eds.), *Detection of Cell Death Mechanisms: Methods and Protocols*, Methods in Molecular Biology, vol. 2255, https://doi.org/10.1007/978-1-0716-1162-3_12,

used as an alternative to X-ray crystallography and nuclear magnetic resonance (NMR) to capture macromolecules in their native form [4, 5, 8]. TEM has a simple preparation methodology, good signal-to-noise ratio, and high resolution [9].

Various cell morphological changes can be detected by TEM to distinguish between normal and pathological conditions. For example, during oxidative stress, spherical mitochondria transform into spheroid forms, and this alteration can be observed directly by TEM [10]. Also, in clinical medicine, TEM imaging can confirm cardiomyopathy diagnosis by observing the presence of giant mitochondria—a morphological signature for mitochondrial cardiomyopathy [11]. Further, ultraimaging of kidneys allows for visualization of all five layers of the glomerular filtration barrier, assisting characterization of kidney physiology [12]. By using TEM, distinguishing platelet types is possible; mature platelets contain limited or reduced canalicular systems, rough endoplasmic reticulum (ER), and Golgi apparatus, whereas immature platelets contain well-developed ER and Golgi apparatus [13]. TEM also represents the gold standard for diagnosis of phospholipidosis, because its images indicate abundant myelin/myeloid bodies or lamellar inclusions in various organ samples such as lungs, lymph nodes, liver, kidney, spleen, and retina [14]. TEM is also utilized for low resolution structure determination of macromolecular complexes, such as the double helical array of actin subunits, elongated strands of tropomyosin, and actin-tropomyosin interactions [8, 9].

Negative staining is the most preferred TEM method, due to its high resolution, native form of specimen, and its easy performance. In negative staining, the background is stained and the unstained specimen is highly visible. Negative staining involves the addition of a heavy metal salt solution to an electron microscopy (EM) grid that contains a sample, forming electron-dense-shapes around individual macromolecular complexes [15]. In TEM, these shapes are formed by air-drying and produce high contrast images without the radiation damage that occurs in EM grids [9, 15]. Uranyl stain is one of the most commonly used negative stains for the preparation of biological samples due to its unique properties: uranyl stains are cationic and, as such, interact less with positively charged phospholipids. As a result, this stain does not produce Rouleaux formations in samples containing lipids [16]. In addition, a dry layer of uranyl stain possesses a granularity of 0.3 nm in comparison to other stains such as phosphotungstate (PTA), which has a diameter of 0.8–0.9 nm [17]. Among uranyl stains, uranyl formate (UF) has the finest grain size, which provides the best staining for structural detail. This advantage is important in the visualization of protein molecules smaller than 100 kDa or 3.5 nm [18]. While TEM allows visualization of organs and tissues, quantitative parameters such as distances, sizes, shapes, and number of particles are difficult to obtain. In contrast, other techniques accurately represent three-

dimensional (3-D) structures of biological specimens [19]. The CEM, CET, and CEMOVIS not only predict shape but also represent interior density variations, allowing 3-D images of the respective biological object. The newly established 3-D TEM methodology allows quantification of complex morphologies and inner structures [8–16]. Undoubtedly, TEM has become an exceptional tool to depict morphological changes, including changes in cellular morphology during programmed cell death [20, 21].

1.2 Programmed Cell Death

Programmed Cell Death (PCD) is a cascade of signaling pathways that regulate death in living systems. In previous decades, apoptosis was considered the only type of PCD. However, recent technologies have revealed clear and distinctive differences within PCD. As a result, the Nomenclature Committee on Cell Death (NCCD) has classified PCD into various cell death types (e.g., apoptosis, anoikis, ferroptosis, pyroptosis, and necroptosis) based on differences in morphology and signaling mechanisms. Among PCD, apoptosis and programmed cell necrosis (necroptosis) are the most well-characterized cell death types [22]. Advances in TEM have helped to further distinguish between apoptosis and necroptosis based on cell morphology: [21] apoptotic cells shrink in size and form apoptotic bodies, while necroptotic cells swell in size and exhibit vacuolization of cytoplasmic organelles followed by membrane rupture and release of cellular contents [21–23]. Tumor necrosis factor α (TNFα) and other members of the TNF superfamily, such as the CD95 receptor/Fas ligand complex, are widely studied necroptotic activators [24–28]. Most studies demonstrate necroptotic PCD through TNFα-based receptor interacting serine/threonine-protein kinase 1 (RIPK1) activation upon caspase inhibition. Accordingly, necroptotic cascade events solely depend on the specificity of activators (e.g., TNFα) or stimuli (e.g., caspase inhibition) [22, 25, 29–38]. In addition to RIPK1, receptor interacting serine/threonine-protein kinase 3 (RIPK3) and mixed lineage kinase ligand (MLKL) are required to execute necroptosis [29]. RIPK1 activation (Ser166 phosphorylation) stimulates the formation of RIPK1-RIPK3 (Ser227 autophosphorylation) assembly. This assembly leads to RIPK3 activation and MLKL phosphorylation (Ser358), ultimately causing membrane permeabilization [30, 31].

Many scientific studies inhibit key proteins of necroptosis like RIPK1, RIPK3, and MLKL to distinguish necroptosis from other types of PCD. Reported inhibitors of RIPK1, RIPK3, and MLKL include necrostatin-1 (NEC-1), GSK'872, and necrosulfonamide (NSA), respectively. However, RIPK1 kinase activity is not only involved in necroptosis but also in apoptosis wherein RIPK1 induces apoptosis through caspase-8 activation in apoptosis-competent in vitro models [32]. Further confounding, RIPK3 inhibitors like GSK'872 induce RIPK1-dependent apoptosis

instead of necroptosis [39]. As a result, rescue of cell death following RIPK1, RIPK3, and MLKL inhibition is not sufficient for confirmation of necroptosis. Immunochemical strategies that reveal phosphorylation of RIPK1, RIPK3, and MLKL require TEM morphological imaging to validate necroptotic cascade findings [25, 32–35].

1.3 Cancer Stem Cells and a Novel Targeted Therapy

Cancer stem cells (CSCs) are cells within tumor masses that possess the ability to self-renew as well as to differentiate to produce heterogeneous subpopulations of cancer cells, which are able to form whole tumors [40]. The existence of CSCs was first revealed in leukemia and later identified in various types of solid tumors. CSCs comprise a minor part of heterogeneous tumor cells and can be enriched following chemotherapy and during wound repair [41]. Chemoresistant CSCs are identified by constitutive NFκB activity, slower proliferation rates, and cell-to-cell contact inhibition [41]. Additionally, stemness-associated marker genes, such as Nanog, Oct-4, SOX2, and KLF4, are highly expressed in chemoresistant CSCs in comparison to chemosensitive nonCSCs. Ovarian CSCs act as putative mediators for tumor initiation and chemoresistance in ovarian cancer patients. Consequently, targeting ovarian CSCs is a novel strategy for addressing the resistance of recurrent ovarian cancer to chemotherapy. For example, inhibition of Aurora A kinase by a chemical inhibitor, MK-5108, in ovarian CSCs decreased the cancer cell proliferation rate as a result of cell cycle arrest and was mediated by inhibition of the NFκB pathway. This outcome suggests that inhibition of signaling pathways overexpressed in CSCs is a novel approach to overcome cancer [40].

Ovarian CSCs can be identified by their aldehyde dehydrogenase (ALDH)-positive activity [42]. Recently, our lab reported that ALDH1A inhibition causes induction of necroptotic cell death by inhibiting oxidative phosphorylation in $CD133^{+}$ ovarian CSCs [20]. TEM is well-suited to further study this phenomenon, particularly validating the morphological changes involved. The current protocol describes morphological changes occurring during necroptosis as observed by TEM. These changes include swelling of cells, swelling of mitochondria and other organelles, appearance of vacuoles, and plasma membrane rupture followed by leakage of cellular contents (Fig. 1). All of these morphological changes are observed following ALDH1A inhibition in ovarian cancer primary cells and cell lines [20]. Following berberine treatment in combination with cisplatin, a similar pattern of necroptotic cell death morphology was observed using TEM, suggesting necroptosis relevance following a variety of treatments [21]. In total, this chapter provides detailed information for visualizing cellular morphology by using TEM in order to identify and confirm necroptosis.

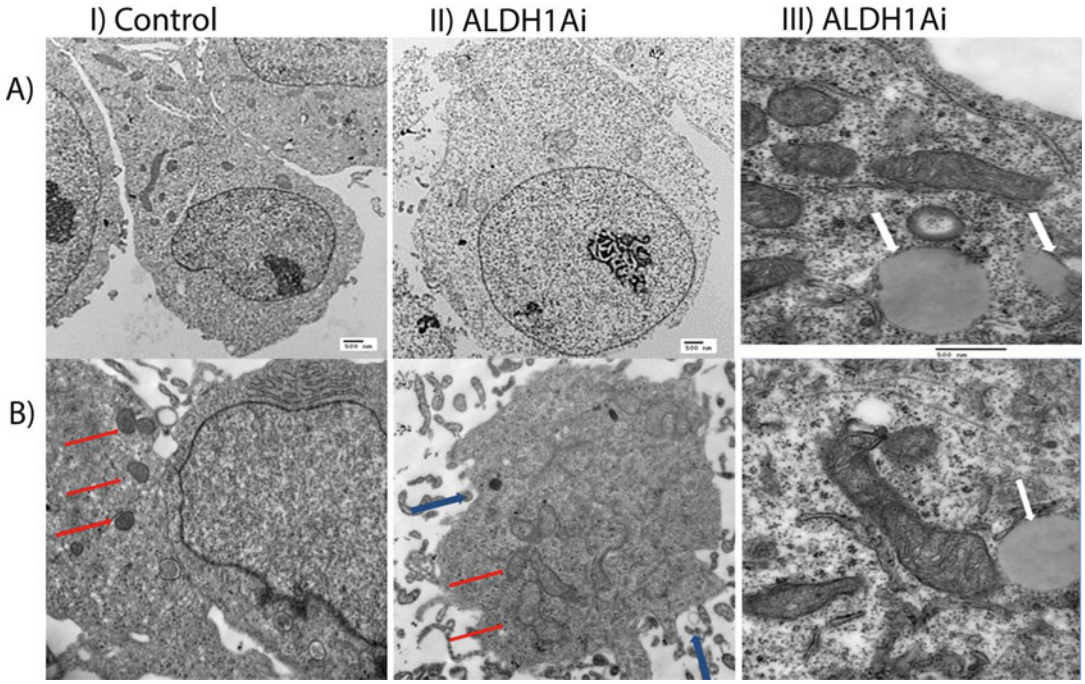

Fig. 1 Transmission electron microscopy (TEM) imaging-based necroptosis identification: (**a**) (I) A2780 and (**b**) (I) SKOV3 cell morphology visualized by TEM in a control group; no disruptive structure was noticed. (**a**) (II), (III) A2780 and (**b**) (II), (III) SKOV3 cells with ALDH1i (673A) treatment revealed precise morphological changes within the cell as visualized by TEM after 20 h (II and III are 6000× and 23,000× of TEM magnification, respectively). A typical visual pattern of necroptosis was clearly identified in the TEM images, including swollen cells, enlarged mitochondria, appearance of globular vacuoles, rupture of plasma membrane, and leakage of cellular contents. (Red arrows indicate mitochondria; blue arrows indicate rupture of plasma membrane; white arrows indicate enlarged vacuoles)

2 Materials

2.1 Equipment

1. 120 kV Lab6 electron microscope (Leica, Germany).
2. 5% CO_2 incubator.
3. Refrigerated centrifuge.
4. Automated Cell Counter.
5. Ultra-microtome.
6. Grid Storage Box.
7. Self Closing Tweezers.
8. Standard General Work Tweezers.
9. Tweezers Storage Box.
10. Formvar 400-mesh grids (i.e., Leica, Germany).
11. Whatman 41 ashless filter paper.
12. Pipets.

13. Leica ACE600.
14. Syringes.
15. 0.22 μm filter.
16. Beaker.
17. 1.5 mL Eppendorf tubes.
18. 15 mL tubes.
19. Parafilm.
20. T-75 tissue culture flasks.
21. Tissue culture dishes (60 mm).

2.2 Cell Lines

1. A2780 human ovarian endometrioid cancer cell line.
2. SKOV-3 human ovarian cancer cell line.

2.3 Reagents

1. RPMI 1640 medium (Roswell Park Memorial Institute1640; Corning Life Sciences, USA); with 5% fetal bovine serum (FBS; Gibco, Carlsbad, CA, USA), 100 units/mL penicillin, 100 μg/mL streptomycin.
2. Hank's Balanced Salt Solution (HBSS) without calcium and magnesium, sterile.
3. 0.25% Trypsin in HBSS.
4. 0.4% Trypan Blue solution.
5. Dimethyl sulfoxide (DMSO, cell culture grade).
6. Sterile water (cell culture grade).
7. 673A (4-(1,3-dihydro-2H-isoindol-2-yl) benzaldehyde): 25 μM in DMSO.
8. Ethanol, 25%, 50%, 75%, 95% prepared by diluting with sterile water.
9. Eposy resin.
10. 12.5 mM NaOH.
11. Uranyl formate (UF): 0.75% prepared in 12.5 mM NaOH then adjusted to pH 4.5 with tris HCL.
12. Dulbecco's Phosphate-Buffered Salt Solution (DPBS, 1×), Cat. No. MT21030CV Corning™ cell culture grade.
13. 2% Glutaraldehyde.

3 Methods

This section provides instructions on cell seeding (*see* Subheading 3.1), treatment (*see* Subheading 3.2), sample preparation (*see* Subheading 3.3), and TEM visualization (*see* Subheading 3.4).

3.1 Cell Seeding for Treatment

The ovarian cancer cell lines (A2780 and SKOV3) were used as the ex vivo models for the current TEM studies. Depending on the growth ability and proliferation rate, the cell culture conditions need to be optimized.

1. Both cell lines are cultured separately in RPMI1640 medium supplemented with 5% FBS and 1% strep/penicillin in T-75 tissue culture flasks, kept at 37 °C and in a 5% CO_2 incubator, allowing them to reach nearly 80% confluence.
2. After achieving the desired confluence, remove the medium and wash the cells 3× with molecular grade HPBS (*see* **Note 1**).
3. Remove the HPBS and then add nearly 4 mL of 0.25% trypsin; then, incubate solution in a 5% CO_2 incubator until all cells are detached (*see* **Note 2**).
4. Add an equal volume of FBS containing medium followed by repeated pipetting to neutralize the trypsin (*see* **Note 3**).
5. Transfer the cell suspension into sterile 15 mL centrifuge tubes. Pellet by centrifuging at 1500 × *g* for 5 min (fixed rotor).
6. Remove the supernatant fraction and suspend the cell pellets in RPMI1640 medium (*see* **Note 4**).
7. Take a 1:1 ratio dilution of cell suspension with 0.4% Trypan Blue solution. Total number of cells in suspension is estimated by using the Countess II FL Automated Cell Counter according to the manual instructions.
8. In the present study, three million viable cells are seeded in 5 mL of medium per dish (60-mm) and kept in a 5% CO_2 incubator until they reach 60% confluence by the time of treatment.

3.2 ALDH1A Inhibition to Induce Necroptosis

The condition of cells plays a crucial role in order to effectively induce necroptosis. We have conducted trials to optimize a specific drug concentration and incubation time for inducing necroptosis by using a novel drug (673A) [21]. To achieve reproducible results, the cells must be at nearly 60% confluence, equally distributed on the surface of 60-mm dishes with no morphologic stress is required. A2780 and SKOV3 cells that reached 60% confluence were used for treatment studies (*see* **Note 5**).

The current protocol proceeds with two different treatment conditions, which are ALDH1A inhibitor (673A) treatment to induce necroptosis and vehicle-added RPMI medium as a control in both cell lines separately. The following labels are used throughout the protocol for the treatment conditions:

- Control—treatment with DMSO-added RPMI medium only (0.3% DMSO);
- T—treatment with 25 μM 673A.

1. For drug treatments, a 1× solution of the 673A drug was prepared by adding 4.5 μL of 25 μM 673A to 4.5 mL of RPMI1640 medium in 15 mL tubes and labeled as T.
2. Similarly, 4.5 μL of DMSO was added to 4.5 mL of RPMI1640 medium to act as control cells and labeled as C.
3. Slightly vortex and mix tubes by pipetting to achieve rapid solubility.
4. Label the 60-mm dishes of both cell lines as C and T.
5. Aspirate the medium and then add 4 mL of medium C (only DMSO) and T (only 25 μM 673A) to corresponding dishes in the corner using the side by dropwise method (*see* **Note 6**).
6. Mix the dishes by gentle swirling and rocking to different sides a few times.
7. Keep dishes at the above mentioned incubation conditions (at 37 °C in a 5% CO_2 incubator) for 20 h before proceeding for TEM preparation.

At least 3–5 biological replicates with 3 technical repeats were performed in the current study, to insure reproducible effects of 673A treatment on A2780 and SKOV3 cells and their morphological changes as determined by TEM.

3.3 Sample Preparation

For effective visualization of samples under TEM, the researcher must optimize the conditions required for sample preparation, grid activation, stain selection, and microscopic conditions accordingly (*see* **Note 7**).

3.3.1 Preparation of Ultrathin Cell Samples

1. Both cell lines treated with 25 μM 673A and DMSO (control) for 20 h were washed 3× with DPBS for about 10 min.
2. Cells were fixed by adding 2% glutaraldehyde for 2 h followed by washing three times with DPBS for 10 min (*see* **Note 8**).
3. The fixed samples were gradually dehydrated with a 25, 50, 75, 95, and 100% ethanol solution, each for 15 min at RT.
4. Following dehydration, cells were embedded into epoxy resin.
5. Using an ultramicrotome (Leica EM UC7), the samples were sliced into nearly 100 nm thin sections.
6. The resulting ultrasliced sections were used as grids to observe under TEM.

3.3.2 Stain Selection

1. A 0.75% of UF (pH = 4.2–4.5) was used for negative staining in this current protocol.
2. Weigh 0.0047 g of UF powder into a sterile 1.5 mL Eppendorf tube and add 627 μL of 12.5 mM NaOH.
3. Vortex the tube and place into a boiling beaker of water.

4. Repeat the vortex/heating/mixing again until the powder is dissolved in solution (*see* **Note 9**).
5. Filter the heated solution into another Eppendorf tube by using syringe filtration.
6. Label the tube and use it for negative staining (*see* **Note 10**).

3.3.3 Preparation of Sample Grids

Carbon supports of grids are inherently hydrophobic in chemical nature. Leica ACE600 was used for X-ray glow discharge (1 mm for 15 s) on carbon-coated formvar 400-mesh grids (Leica, Germany) (*see* **Note 11**). As a result of this procedure, the grids gain a hydrophilic nature (negative charge), which allows appropriate sample spreading on the grid surface (*see* **Note 12**).

1. Carefully hold the grids by using self-closing tweezers and then drop the ultrathin sample sections with the help of standard tweezers on the 400 mesh grids (*see* **Note 13**).
2. Add 6 μL of 0.75% UF solution to the sample-containing side of the grids and incubate at RT for 10 min.
3. Following incubation, remove the excess stain by filter paper and leave it to dry.
4. Store grids in a special grid box until TEM visualization.

3.4 TEM Visualization

Fixed grid specimens are observed under a 120 kV Lab6 electron microscope (Leica, Germany) to capture the morphological visualization. The built-in software parameters are slightly optimized for processing, visualizing, and converting the data.

1. Initially, fill the LN2 cold trap and turn on the High Tension 120 kV and filament (yellow means on and gray means off).
2. Once the instrument is ready, load the sample grid into the holder (*see* **Note 14**).
3. Insert the holder into the chamber to line up the pin on the sample holder with the 5 o'clock position on the goniometer of the instrument (*see* **Note 15**).
4. The airlock begins pumping the compustage with the red light on and immediately select a single tilt as a specimen holder type (*see* **Note 16**).
5. Once the vacuum reaches 6 (optimized to current protocol), open the column valves (yellow means on and gray means off).
6. The stage trackball of the instrument was used to find the grid square and adjust the beam intensity.
7. Next adjust the magnification to 1050× to view overall sample grid integrity (*see* **Note 17**).

8. Once grid integrity is confirmed, increase magnification to 13,000× to find a point of interest on the sample grid with the help of the stage trackball.
9. Further, the instrument eucentric achieves to the point of interest by combined operation of the alpha stage wobbler (LC button L2) and "Z-axis" control buttons (Z ±).
10. The "Alpha stage wobbler" (L2) is activated by pressing L2 causing rocking specimen movement through the tilt range of ± 15°.
11. Later the "Z-axis" control buttons (RC) are used to minimize the specimen grid movement to the already decided point of interest.
12. Alpha stage wobbler is deactivated once the visualizing point is confirmed on sample grid.
13. Finally, insert the objective aperture of scope for X and Y alignment to visualize and capture the images.
14. Default digital micrograph software is used to adjust intensity with brightness on scope until the indicator is in green range (*see* **Note 18**).
15. Clear images of area of interest are acquired by 1 s exposure in sample grid.
16. Set the scale bar 200 nm on image and use the batch convert option to save all the images in TIFF format (*see* **Note 19**).
17. Finally, analyze and interpret the images of samples C and T comparatively.
18. Our results showed a normal morphology in control images and necroptotic morphology in treated images (Fig. 1).

After taking enough images, close the column valves, neutralize the stage by resetting the holder, lower digital micrograph screen, turn off filament, remove objective aperture, lower the magnification to 2400× (*see* **Note 20**), remove the sample holder, recover the sample grid, and store them in the grid box.

4 Notes

This section provides additional instructions and suggestions for trouble shooting purposes.

1. In the process of addition and removal of PBS, make sure that cells are not disturbed by pipet tips, as this will cause stress. In addition, cells should never be left without medium or fixatives.
2. Use microscope or just slightly half-tilt the T-75 flask to observe the detached cells.

3. Few cells are very sensitive to trypsin; use 0.05% trypsin followed by FBS for neutralization.
4. To maintain accuracy in cell counting, the cell pellets must be diluted to nearly 5 mL, taking into consideration suggested detection limit range of 1×10^4 to 1×10^7 cells/mL.
5. Always use microscopic visualization to the desired confluence (avoid the cells being over confluent in the center of the dish); strive for even distribution of cells with no contamination.
6. Adding medium at the center of the dish by the dropwise method may cause stress to cells and detachment from the dish surface, which would affect the experimental results.
7. In order to visualize a sample by TEM, the sample (a) must be ultrathin so that a beam of electrons can penetrate it (ideally $\leq$100 nm), (b) must be evenly deposited onto the EM grids (circular at 3 mm in diameter), and (c) must bear high vacuum and electron radiation inside the TEM column.
8. Glutaraldehyde is volatile and should be used in a fume hood to avoid exposure.
9. UF does not solubilize unless heated.
10. UF solution is best for 1 week. Make fresh stain after 1-week usage or if the old solution shows precipitation.
11. Dark side of grid is the carbon containing portion. The dark side must be used for glow discharge and for dropping the samples.
12. Adding water drop on the dark side of grid is a simple way to confirm the glow discharge. If water is dispersed, this indicates a discharged grid.
13. Hold the grid by self-closing tweezers at the corner sides to avoid damaging the carbon coat.
14. First, insert the opening tool into the hole in the holder clamp and gently raise the clamp straight up until it stops. Then, place the sample grid, carbon side up, at the end of the holder and then lower the clamp straight down to hold the grid securely.
15. Be careful while gently inserting the holder until it stops and do not scrape the tip.
16. Do not move the holder while the red stage LED is lit and be sure to select single tilt.
17. This observation step is very important to identify any damage occurring in the grid carbon coat and sample uniformity spread.
18. Be careful not to overexpose camera to a too bright beam, because this can damage the charge-coupled device.

19. Numerous formats can be used to save the images. We prefer TIFF for high quality.
20. This is essential to maintain stable objective lens current and prevent thermal drift for usage next time.

References

1. Knoll MAER, Ruska E (1932) The electron microscope. Z Phys 78(5-6):318–339
2. Van der Pol E, Coumans FAW, Grootemaat AE, Gardiner C, Sargent IL, Harrison P, Sturk A, Van Leeuwen TG, Nieuwland R (2014) Particle size distribution of exosomes and microvesicles determined by transmission electron microscopy, flow cytometry, nanoparticle tracking analysis, and resistive pulse sensing. J Thromb Haemost 12(7):1182–1192
3. Porter KR, Claude A, Fullam EF (1945) A study of tissue culture cells by electron microscopy: methods and preliminary observations. J Exp Med 81(3):233–246
4. Mielańczyk Ł, Matysiak N, Klymenko O, Wojnicz R (2015) Transmission electron microscopy of biological samples. Trans Electron Microsc Theory Appl 1
5. Zewail AH (2010) Micrographia of the twenty-first century: from camera obscura to 4D microscopy. Philos Trans R Soc A Math Phys Eng Sci 368(1914):1191–1204
6. Cavalier A, Spehner D, Humbel BM (2008) Handbook of cryo-preparation methods for electron microscopy. CRC Press, Boca Raton, FL
7. Steinbrecht RA, Müller M (1987) Freeze-substitution and freeze-drying. In: Cryotechniques in biological electron microscopy. Springer, Berlin, pp 149–172
8. Lehman W, Vibert P, Uman P, Craig R (1995) Steric-blocking by tropomyosin visualized in relaxed vertebrate muscle thin filaments. J Mol Biol 251(2):191–196
9. Hayat MA (1981) Principles and techniques of electron microscopy. Biological applications. Edward Arnold, London
10. Ding WX, Li M, Biazik JM, Morgan DG, Guo F, Ni HM, Goheen M, Eskelinen EL, Yin XM (2012) Electron microscopic analysis of a spherical mitochondrial structure. J Biol Chem 287(50):42373–42378
11. Kanzaki Y, Terasaki F, Okabe M, Otsuka K, Katashima T, Fujita S, Ito T, Kitaura Y (2010) Giant mitochondria in the myocardium of a patient with mitochondrial cardiomyopathy: transmission and 3-dimensional scanning electron microscopy. Circulation 121(6):831–832
12. Arkill KP, Qvortrup K, Starborg T, Mantell JM, Knupp C, Michel CC, Harper SJ, Salmon AH, Squire JM, Bates DO, Neal CR (2014) Resolution of the three dimensional structure of components of the glomerular filtration barrier. BMC Nephrol 15(1):24
13. Williams WJ (1990) Hematology in the aged. Hematology, 4th edn. McGraw Hill, New York
14. Fagerland JA, Wall HG, Pandher K, LeRoy BE, Gagne GD (2012) Ultrastructural analysis in preclinical safety evaluation. Toxicol Pathol 40 (2):391–402
15. Ohi M, Li Y, Cheng Y, Walz T (2004) Negative staining and image classification—powerful tools in modern electron microscopy. Biol Proc Online 6(1):23
16. Glauert AM, Lewis PR (1998) Biological specimen preparation for transmission electron microscopy. Princeton University Press, Princeton, NJ
17. Estis LF, Haschemeyer RH, Wall JS (1981) Uranyl sulphate: a new negative stain for electron microscopy. J Microsc 124(3):313–318
18. Erickson HP (2009) Size and shape of protein molecules at the nanometer level determined by sedimentation, gel filtration, and electron microscopy. Biol Proc Online 11(1):32
19. Frank J (2006) Three-dimensional electron microscopy of macromolecular assemblies: visualization of biological molecules in their native state. Oxford University Press
20. Chefetz I, Grimley E, Yang K, Hong L, Vinogradova EV, Suciu R, Kovalenko I, Karnak D, Morgan CA, Chtcherbinine M, Buchman C (2019) A Pan-ALDH1A inhibitor induces necroptosis in ovarian cancer stem-like cells. Cell Rep 26(11):3061–3075
21. Liu L, Fan J, Ai G, Liu J, Luo N, Li C, Cheng Z (2019) Berberine in combination with cisplatin induces necroptosis and apoptosis in ovarian cancer cells. Biol Res 52(1):37
22. Li X, Guo M, Shao Y (2013) Ultrastructural observations of programmed cell death during metanephric development in mouse. Microsc Res Tech 76(5):467–475
23. Galluzzi L, Vitale I, Aaronson SA, Abrams JM, Adam D, Agostinis P, Alnemri ES, Altucci L, Amelio I, Andrews DW, Annicchiarico-

Petruzzelli M (2018) Molecular mechanisms of cell death: recommendations of the Nomenclature Committee on Cell Death 2018. Cell Death Differentiation 25(3):486

24. Degterev A, Huang Z, Boyce M, Li Y, Jagtap P, Mizushima N, Cuny GD, Mitchison TJ, Moskowitz MA, Yuan J (2005) Chemical inhibitor of nonapoptotic cell death with therapeutic potential for ischemic brain injury. Nat Chem Biol 1(2):112
25. Vercammen D, Beyaert R, Denecker G, Goossens V, Van Loo G, Declercq W, Grooten J, Fiers W, Vandenabeele P (1998) Inhibition of caspases increases the sensitivity of L929 cells to necrosis mediated by tumor necrosis factor. J Exp Med 187(9):1477–1485
26. Dunai ZA, Imre G, Barna G, Korcsmaros T, Petak I, Bauer PI, Mihalik R (2012) Staurosporine induces necroptotic cell death under caspase-compromised conditions in U937 cells. PLoS One 7(7):e41945
27. Tenev T, Bianchi K, Darding M, Broemer M, Langlais C, Wallberg F, Zachariou A, Lopez J, MacFarlane M, Cain K, Meier P (2011) The Ripoptosome, a signaling platform that assembles in response to genotoxic stress and loss of IAPs. Mol Cell 43(3):432–448
28. Piao JL, Cui ZG, Furusawa Y, Ahmed K, Rehman MU, Tabuchi Y, Kadowaki M, Kondo T (2013) The molecular mechanisms and gene expression profiling for shikonin-induced apoptotic and necroptotic cell death in U937 cells. Chem Biol Interact 205(2):119–127
29. Micheau O, Tschopp J (2003) Induction of TNF receptor I-mediated apoptosis via two sequential signaling complexes. Cell 114 (2):181–190
30. Murphy JM, Czabotar PE, Hildebrand JM, Lucet IS, Zhang JG, Alvarez-Diaz S, Lewis R, Lalaoui N, Metcalf D, Webb AI, Young SN (2013) The pseudokinase MLKL mediates necroptosis via a molecular switch mechanism. Immunity 39(3):443–453
31. Liu S, Liu H, Johnston A, Hanna-Addams S, Reynoso E, Xiang Y, Wang Z (2017) MLKL forms disulfide bond-dependent amyloid-like polymers to induce necroptosis. Proc Natl Acad Sci U S A 114(36):E7450–E7459
32. Degterev A, Hitomi J, Germscheid M, Ch'en IL, Korkina O, Teng X, Abbott D, Cuny GD, Yuan C, Wagner G, Hedrick SM (2008) Identification of RIP1 kinase as a specific cellular target of necrostatins. Nat Chem Biol 4(5):313
33. Chen S, Lv X, Hu B, Shao Z, Wang B, Ma K, Lin H, Cui M (2017) RIPK1/RIPK3/MLKL-mediated necroptosis contributes to compression-induced rat nucleus pulposus cells death. Apoptosis 22(5):626–638
34. Chen T, Pan H, Li J, Xu H, Jin H, Qian C, Yan F, Chen J, Wang C, Chen J, Wang L (2018) Inhibiting of RIPK3 attenuates early brain injury following subarachnoid hemorrhage: possibly through alleviating necroptosis. Biomed Pharmacother 107:563–570
35. Arora D, Siddiqui MH, Sharma PK, Shukla Y (2016) Deltamethrin induced RIPK3-mediated caspase-independent non-apoptotic cell death in rat primary hepatocytes. Biochem Biophys Res Commun 479(2):217–223
36. Jing L, Song F, Liu Z, Li J, Wu B, Fu Z, Jiang J, Chen Z (2018) MLKL-PITPα signaling-mediated necroptosis contributes to cisplatin-triggered cell death in lung cancer A549 cells. Cancer Lett 414:136–146
37. Dondelinger Y, Jouan-Lanhouet S, Divert T, Theatre E, Bertin J, Gough PJ, Giansanti P, Heck AJ, Dejardin E, Vandenabeele P, Bertrand MJ (2015) NF-κB-independent role of IKKα/IKKβ in preventing RIPK1 kinase-dependent apoptotic and necroptotic cell death during TNF signaling. Mol Cell 60(1):63–76
38. Feoktistova M, Geserick P, Kellert B, Dimitrova DP, Langlais C, Hupe M, Cain K, MacFarlane M, Häcker G, Leverkus M (2011) cIAPs block Ripoptosome formation, a RIP1/caspase-8 containing intracellular cell death complex differentially regulated by cFLIP isoforms. Mol Cell 43(3):449–463
39. Mandal P, Berger SB, Pillay S, Moriwaki K, Huang C, Guo H, Lich JD, Finger J, Kasparcova V, Votta B, Ouellette M (2014) RIP3 induces apoptosis independent of pronecrotic kinase activity. Mol Cell 56(4):481–495
40. Chefetz I, Holmberg JC, Alvero AB, Visintin I, Mor G (2011) Inhibition of Aurora-A kinase induces cell cycle arrest in epithelial ovarian cancer stem cells by affecting NFκB pathway. Cell Cycle 10(13):2206–2214
41. Mor G, Yin G, Chefetz I, Yang Y, Alvero A (2011) Ovarian cancer stem cells and inflammation. Cancer Biol Ther 11(8):708–713
42. Deng S, Yang X, Lassus H, Liang S, Kaur S, Ye Q, Li C, Wang LP, Roby KF, Orsulic S, Connolly DC (2010) Distinct expression levels and patterns of stem cell marker, aldehyde dehydrogenase isoform 1 (ALDH1), in human epithelial cancers. PLoS One 5(4): e10277

Chapter 13

Methodology for Comprehensive Detection of Pyroptosis

Yang Feng and Xiaoli Huang

Abstract

Pyroptosis is a new type of programmed cell death identified in recent years, which destroys the integrity of cell membranes by punching pores on them, resulting in cell lysis. Light- and dark-colored vesicles/pore-like structures on the membranes of pyroptotic cells are generally observed using light microscope, accompanied by cell swelling and cytoplasmic release. However, due to the release of the cell contents in both pyroptosis and necrosis, it is difficult to distinguish them solely by morphological characteristics. The mechanism of pyroptosis involves three major signaling pathways, all activating downstream gasdermin (GSDM) D and E, which results in the formation of pores (10–15 nm) on the cell membrane, while small cytoplasmic molecules such as interleukin (IL)-1 and IL-18 flow out from the pores and cause inflammation. The occurrence of pyroptosis can be determined by a combination of markers. These include cleavage of GSDM D and E, activation and release of IL-1β and IL-18, and activation of cysteinyl aspartate specific proteinase (caspase-1, -3, -4, -5, and -11). This chapter discusses several common methods to assist researchers in detecting pyroptosis.

Key words Pyroptosis, Gasdermin D/E, Interleukin-1β/-18, Caspase

1 Introduction

Pyroptosis is a new type of programmed cell death identified in recent years. Different from apoptosis, pyroptosis presents a series of morphological and physiological changes related to the inflammatory response in innate immune cells (such as macrophages and dendritic cells) [1]. Morphologically, small pores (10–14 nm) emerge on the membrane of pyroptotic cells, which change the permeability of the membrane [2]. After that, numerous pro-inflammatory cytokines in the cytoplasm are released from the pores to the extracellular space [3], promoting the cell to lyse and die. Finally, the cells burst, and an inflammatory response around the dead cell is triggered because of the released cytokines (Fig. 1) [4]. Generally, it is possible to confirm whether the cell is in the state of pyroptosis according to morphological changes, and confirmation of this state is very important to guide cellular research.

Ayesha B. Alvero and Gil G. Mor (eds.), *Detection of Cell Death Mechanisms: Methods and Protocols*, Methods in Molecular Biology, vol. 2255, https://doi.org/10.1007/978-1-0716-1162-3_13,

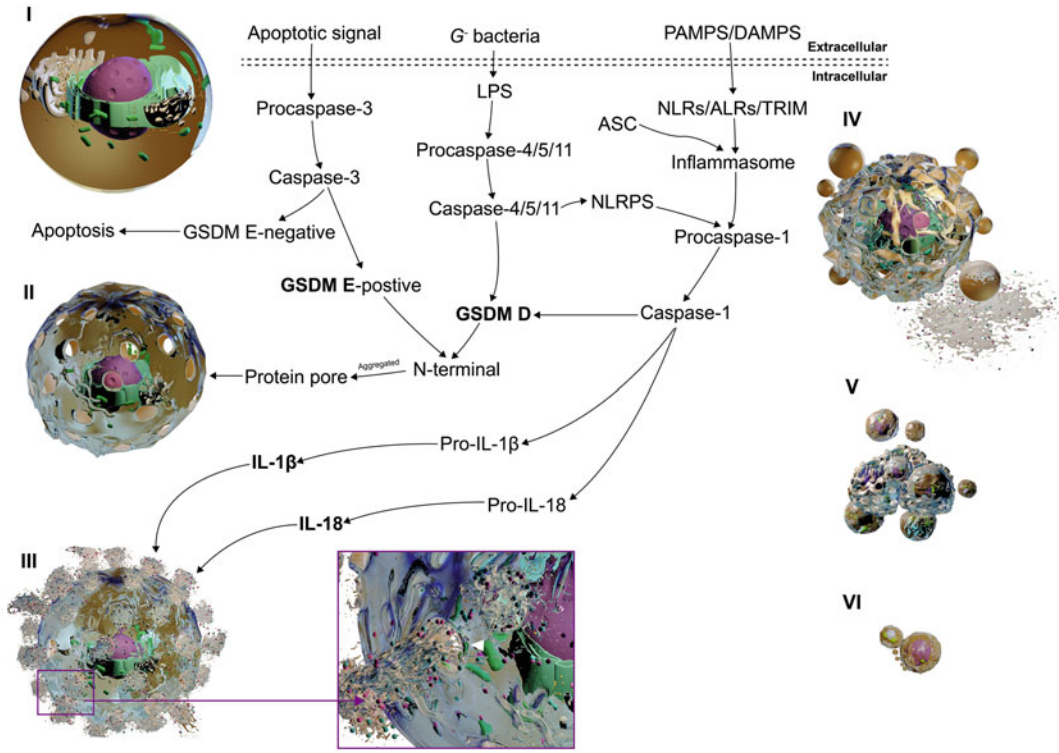

Fig. 1 Morphologic pattern of pyroptotic cells and the signaling pathways [4, 5]. I: Normal cells; II: numerous pores appear on the cell membrane, and membrane permeability increases; III: IL-1β and IL-18 along with the rest of the cytoplasm are released from the cells; IV: the cytoplasm is drained, and the cells shrink; V: the nuclei are fragmented, and the cells break into vesicles; VI: the broken cells are cleared

1.1 Cellular Events During Pyroptosis

Pyroptosis, also known as gasdermin (GSDM)-dependent necroptosis, is characterized by the cleavage of GSDM (Fig. 1). The GSDM family includes GSDM A, B, C, D, and E and DFNB 59 [6]. Among them, GSDM D and E are the most important mediators of pyroptosis, and they exhibit the homologous N-terminal pore-forming domain (PFD) and C-terminal caspase activation and recruitment domain, but with different links between the two domains [7]. The PFD of GSDM generally cleaves when it is activated, followed by 24 PFDs that polymerize and form small pores of 10–14 nm on the cell membrane [8, 9]. Finally, the pores increase the membrane permeability and can result in changes such as membrane breakage.

Also, a distinct characteristic of pyroptosis is the release of pro-inflammatory cytokines. Bauernfeind indicated that pyroptosis induces inflammation via the release of interleukin (IL)-1α, IL-1β, and IL-18 [10]. Necrosis can also induce inflammation by releasing IL-1α, IL-33, and damage-associated host factors [11]. Thus, IL-1β and IL-18 are the two most important pro-inflammatory cytokines used to distinguish the inflammatory response from

necrosis or pyroptosis (Fig. 1). Above all, the most effective way to evaluate pyroptosis is usually to detect the activation of GSDM and the release of IL-1β and -18.

1.2 The Signaling Pathway of Pyroptosis

At present, scientists have identified three signaling pathways that regulate pyroptosis: canonical pathways [12], noncanonical pathways [13], and GSDM E-dependent pathways [14], which are all mediated by the cysteinyl aspartate specific proteinase (caspase) family (Fig. 1). Canonical pyroptosis is mediated by caspase-1. When the cell is stimulated, the pathogen/damage-associated molecular patterns (P/DAMPs) promote the formation of inflammasomes, which then activate caspase-1 by recruiting it for self-cleavage [15–17]. Then, activated caspase-1 promotes the cleavage of IL-1β and IL-18 precursors to produce mature cytokines [18, 19], which simultaneously cleave and activate GSDM D (Fig. 1) [8]. Noncanonical pyroptosis is regulated by human-derived caspase-4 and -5 or mouse-derived caspase-11 (homologous to caspase-4 and -5) [20–22]. Unlike caspase-1, caspase-11 binds and is directly activated by lipopolysaccharide (LPS), in association with the stimulation of Gram-negative bacteria [23, 24]. Caspase-11 also activates GSDM D but does not activate IL-1β or -18 [25, 26]. Fortunately, *Kayagaki* found that caspase-11 could activate caspase-1 through a cascade reaction, which then promotes the cleavage of the cytokines (Fig. 1) [26].

Additionally, caspase-3 is generally considered to be an effector that mediates apoptosis [27]. However, studies have found that caspase-3 is also a key enzyme in regulating GSDM E-dependent pyroptosis [7, 14]. GSDM E is homologous to GSDM D [28, 29], and there is a natural caspase-3 cleavage site in GSDM E [30]. Rogers and Wang found that activated caspase-3 could cleave this site and cause pyroptosis (Fig. 1) [7, 14], although it is unknown how this process is inhibited in apoptotic cells. Caspase has the disadvantage of a great workload when it is used to directly detect pyroptosis, but it is suitable for detecting pyroptotic signaling pathways. Thus, the methods for detecting pyroptosis at different stages are selected according to the characteristics and regulatory mechanisms of pyroptosis.

The distinction that pyroptosis occurs can be based on the collective demonstration of distinct morphological changes, double positive staining for Annexin V and PI, release of lactate dehydrogenase, cleavage of GSDM D/E, and activation of IL-1β, IL-18, and caspases -1, -3, -4, -5, and -11. The methods to demonstrate these markers of pyroptosis are described below.

2 Materials

2.1 Equipment and Disposables

1. Biosafety cabinet.
2. Tissue culture incubator.
3. Confocal microscope.
4. Centrifuge.
5. Flow cytometer.
6. 96-well plate microplate reader.
7. Cover slips and glass-bottom culture dishes.
8. Conical tubes.
9. 12 × 75 mm flow cytometry tubes.
10. flat-bottom 96-well plate.
11. gel electrophoresis and western blot apparatus including gel imager.

2.2 Reagents and Cell Lines

1. Cell line of choice (examples of cells that have been used to demonstrate pyroptosis are macrophages and Hela cells).
2. Inducer of pyroptosis (example of an agent known to induce pyroptosis is LPS).
3. 0.25% Trypsin.
4. 1× PBS: 2 mM KH_2PO_4 2 mM, 8 mM Na_2HPO_4, 136 mM NaCl, 2.6 mM KCl; pH adjusted to 7.4.
5. bovine serum albumin (BSA).
6. Binding buffer: 10 mM 2-[4-(2-hydroxyethyl)-1-piperazinyl] ethanesulfonic acid (HEPES), 150 nM NaCl, 1 mM $MgCl_2$, 1.8 mM $CaCl_2$ and 5 mM KCl; pH adjusted to 7.4 (*see* **Note 1**).
7. FITC-conjugated Annexin V (Annexin-FITC).
8. Propidium iodide: 1 mg/mL.
9. LDH working fluid: 50 mM Sodium lactate, 0.66 mM nitrotetrazolium chloride (INT), 0.28 mM phenazine dimethyl sulfate (PMS), 1.3 mM oxidized coenzyme I (nicotinamide adenine dinucleotide, NAD), 0.2 M Tris-HCl 0.2 M (pH 8.2) (*see* **Notes 2** and **3**).
10. Western blot reagents (full list can be found in Chapter 1 of this book).
11. Primary antibodies: anti-GSDM D/E; and anti-caspase -1, -3, -4, -5, and -11.
12. HRP-conjugated secondary antibodies.

3 Methods

3.1 Methodology for Assessment of Morphological Characteristics

1. Seed cells on cover slips that have been placed in the bottom of culture dishes and allow to attach for 24 h.
2. Induce pyroptosis using agent of choice.
3. Observe cell morphology (*see* **Note 4** and **5**).

3.2 Determination of Pyroptosis by Flow Cytometry

1. Induce pyroptosis using agent of choice.
2. Trypsinize cells (if adherent). Add BSA to a final concentration of 2% during digestion to prevent overdigestion (*see* **Note 6**).
3. Centrifuge at 250 × *g* for 5 min.
4. Resuspend pellets in enough PBS to wash and centrifuge at 250 × *g* for 5 min.
5. Resuspend pellets in PBS to obtain 1×10^6/mL cell suspension.
6. Remove 500 μL of PBS containing the single-cell suspension. Centrifuge at 250 × *g* for 5 min and discard the supernatant.
7. Resuspend pellet (with about 1×10^5 cells) in 200 μL of 1× binding buffer.
8. Add Annexin V-FITC following concentration suggested by manufacturer.
9. Incubate for 10 min at room temperature and in the dark.
10. Add 1 μL of PI and stain for 5 min at room temperature and in the dark.
11. Add 400 μL of PBS.
12. Analyze the cells immediately using the flow cytometer (*see* **Note 7**).

3.3 Lactate Dehydrogenase (LDH) Assay

LDH is a glycolytic enzyme existing in the cytoplasm of cells. When there are changes in membrane permeability during pyroptosis, LDH is released from the cell and can be easily detected in the supernatant.

1. Induce pyroptosis using agent of choice.
2. Collect cell-free supernatant by centrifugation (250 × *g* for 5 min).
3. Add 50 μL of supernatant into a well of a 96-well plate.
4. Add 50 μL of LDH working fluid.
5. Incubate the plate at room temperature (approximately 25 °C) in the dark for 30 min.
6. Measure the absorbance at 490 nm (*see* **Note 8**).

3.4 Detection of Pyroptosis by Western Blot Analysis (See Note 9)

After the induction of pyroptosis in cells, the cleavage of GSDM D/E and caspase -1, -3, -4, -5, and -11 can be detected by western blot using protocols described in Chapter 1 of this book.

4 Notes

1. The binding of Annexin V to PS requires Ca^{2+}, which must be added to the binding buffer.
2. LDH oxidizes lactate to pyruvate and then, pyruvate reacts with the tetrazole salt INT to form formazan crystals. Thus, the increase in formazan crystals in the medium is directly related to the increase in pyroptotic cells.
3. The combination and application are determined according to the enzymatic activity, which is affected by pH, temperature, heavy metals, ultraviolet light, and other factors. The lactic acid solution and enzyme solution should be mixed and immediately used, as delays in usage will decrease the enzymatic activity.
4. Apoptosis, necrosis, and pyroptosis are the main forms of cell death. Apoptosis features the fragmentation of nuclei, atrophy of cells, and the eventual formation of apoptotic bodies. In contrast, necrosis features rapid plasma membrane rupture and release of enterocytes. The characteristics of pyroptosis are increased cell membrane permeability and release of cytokines, as well as a pyroptotic body that is similar to that observed in apoptosis and necrosis [5]. The action of GSDM results in the formation of pores, and under the microscope, different light- and dark-colored vesicles and pore-like structures are observed [14]. However, this is not solid evidence that can be used for evaluating pyroptosis. In general, pyroptosis can be preliminarily judged based on morphological characteristics, mainly through the following three methods to evaluate the possibility of its existence.
5. Generally, cells appear pyroptotic in approximately 20–30 min [31]. After the experimental treatment, it is often necessary to track the cells over time and observe the cellular changes. Confocal microscopy is an excellent modality that can be used to capture pyroptosis.
6. The chelation of EDTA with Ca^{2+} affects the binding of Annexin V. If digested with trypsin containing EDTA, EDTA should be thoroughly removed by washing with 1× PBS or 1× binding buffer before labeling.
7. Annexin V-FITC/PI is commonly used for the detection of cell death because different staining patterns can be displayed

depending on the type of cell death. In normal cells, neither Annexin V-FITC nor PI can penetrate the cell membrane, and therefore, the cells appear negatively stained via flow cytometry. In apoptotic cells, especially early apoptosis, because membrane integrity is not affected, PI cannot penetrate the cell membrane to stain intracellular DNA. However, phosphatidylserine (PS) is expressed extracellularly in apoptotic cells and can then be stained with Annexin V-FITC. Thus, apoptotic cells are single positive for Annexin V staining via flow cytometry. However, due to increased membrane permeability in pyroptotic cells, PI and Annexin V are free to enter the cell to stain DNA and PS, respectively. Thus, pyroptotic cells would exhibit double-positive staining for PI and Annexin V. It should be noted that necrotic cells can also be double-stained with PI and Annexin V due to the rupture of the membrane.

8. Supernatants can be further diluted if the absorbance is too high.
9. In normal cells, the signaling pathway of pyroptosis is usually blocked, and the protein precursors (GSDM, interleukin, and caspase) are not activated. The occurrence of pyroptosis is activated by caspase and is accompanied by the cleavage of GSDM as well as the release of IL-1 and -18. Therefore, relevant markers can be used for detecting pyroptosis according to the requirement of researchers: (I) to determine the existence of pyroptosis, the cleavage of GSDM D and E or the activation and release of IL-1β and -18 can be detected; (II) to determine the signaling pathway of pyroptosis, the activation of caspase-1, -3, -4, -5, and -11 can be detected. Additionally, the regulation of pyroptosis is rarely involved in transcription and translation. Thus, immunological techniques such as western blotting (WB) become the most effective methods to detect pyroptosis.

References

1. Sendler M, Mayerle J, Lerch MM (2016) Necrosis, apoptosis, necroptosis, pyroptosis: it matters how Acinar cells die during pancreatitis. Cell Mol Gastroenterol Hepatol 2 (4):407–408
2. Chen X, He WT, Hu L, Li J, Fang Y, Wang X, Xu X, Wang Z, Huang K, Han J (2016) Pyroptosis is driven by non-selective gasdermin-D pore and its morphology is different from MLKL channel-mediated necroptosis. Cell Res 26(9):1007–1020
3. Lamkanfi M, Dixit VM (2012) Inflammasomes and their roles in health and disease. Annu Rev Cell Dev Biol 28(28):138–161
4. Vincent WJB, Freisinger CM, P-y L, Huttenlocher A, Sauer J-D (2016) Macrophages mediate flagellin induced inflammasome activation and host defense in zebrafish. Cell Microbiol 18(4):591–604. https://doi.org/10.1111/cmi.12536
5. Zhang Y, Chen X, Gueydan C, Han J (2017) Plasma membrane changes during programmed cell deaths. Cell Res 28:9–21. https://doi.org/10.1038/cr.2017.133
6. Kovacs S, Miao E (2017) Gasdermins: effectors of pyroptosis. Trends Cell Biol 27:673–684. https://doi.org/10.1016/j.tcb.2017.05.005

7. Wang Y (2018) Chemotherapy drugs induce pyroptosis through caspase-3 cleavage of GSDM E. China Agricultural University, Beijing
8. Ding J, Wang K, Wang L, Yang S, Qi S, Shi J, Sun H, Wang DC, Feng S (2016) Pore-forming activity and structural autoinhibition of the gasdermin family. Nature 535 (7610):111–116
9. Aglietti RA, Estevez A, Gupta A, Ramirez MG, Liu PS, Kayagaki N, Ciferri C, Dixit VM, Dueber EC (2016) GsdmD p30 elicited by caspase-11 during pyroptosis forms pores in membranes. Proc Natl Acad Sci U S A 113 (28):7858–7863
10. Bauernfeind F, Hornung V (2013) Of inflammasomes and pathogens - sensing of microbes by the inflammasome. EMBO Mol Med 5 (6):814–826. https://doi.org/10.1002/emmm.201201771
11. Kaczmarek A, Vandenabeele P, Krysko DV (2013) Necroptosis: the release of damage-associated molecular patterns and its physiological relevance. Immunity 38(2):209–223. https://doi.org/10.1016/j.immuni.2013.02.003
12. Bergsbaken T, Fink SL, Cookson BT (2009) Pyroptosis: host cell death and inflammation. Nat Rev Microbiol 7:99–109
13. Kayagaki N, Warming S, Lamkanfi M, Walle L, Louie S, Dong J, Newton K, Qu Y, Liu J, Heldens S, Zhang J, Lee W, Dixit V (2011) Non-canonical inflammasome activation targets caspase-11. Nature 479:117–121. https://doi.org/10.1038/nature10558
14. Rogers C, Alnemri T, Mayes L, Alnemri D, Cingolani G, Alnemri E (2017) Cleavage of DFNA5 by caspase-3 during apoptosis mediates progression to secondary necrotic/pyroptotic cell death. Nat Commun 8:14128. https://doi.org/10.1038/ncomms14128
15. Latz E, Xiao T, Stutz A (2013) Activation and regulation of the inflammasomes. Nat Rev Immunol 13:397–411. https://doi.org/10.1038/nri3452
16. Martinon F, Tschopp J (2007) Inflammatory caspases and inflammasomes: master switches of inflammation. Cell Death Differ 14 (1):10–22. https://doi.org/10.1038/sj.cdd.4402038
17. Keller M, Rueegg A, Werner S, Beer H-D (2008) Active caspase-1 is a regulator of unconventional protein secretion. Cell 132 (5):818–831. https://doi.org/10.1016/j.cell.2007.12.040
18. Hilbi H, ., Chen Y, ., Thirumalai K, ., Zychlinsky A, . (1997) The interleukin 1beta-converting enzyme, caspase 1, is activated during Shigella flexneri-induced apoptosis in human monocyte-derived macrophages. Infect Immun 65 (12):5165–5170
19. Hilbi H, Moss JE, Hersh D, Chen Y, Arondel J, Banerjee S, Flavell RA, Yuan J, Sansonetti PJ, Zychlinsky A (1998) Shigella-induced apoptosis is dependent on caspase-1 which binds to IpaB. J Biol Chem 273(49):32895–32900
20. Wang S, Miura M, Yk J, Zhu H, Gagliardini V, Shi L, Greenberg AH, Yuan J (1996) Identification and characterization of Ich-3, a member of the interleukin-1beta converting enzyme (ICE)/Ced-3 family and an upstream regulator of ICE. J Biol Chem 271(34):20580–20587. https://doi.org/10.1074/jbc.271.34.20580
21. Faucheu C, Diu A, Chan AW, Blanchet AM, Miossec C, Herve F, Collard-Dutilleul V, Gu Y, Aldape RA, Lippke JA (1995) A novel human protease similar to the interleukin-1 beta converting enzyme induces apoptosis in transfected cells. EMBO J 14(9):1914–1922. https://doi.org/10.1002/j.1460-2075.1995.tb07183.x
22. Kamens J, Paskind M, Hugunin M, Talanian RV, Allen H, Banach D, Bump N, Hackett M, Johnston CG, Li P (1995) Identification and characterization of ICH-2, a novel member of the interleukin-1 beta-converting enzyme family of cysteine proteases. J Biol Chem 270 (25):15250–15256. https://doi.org/10.1074/jbc.270.25.15250
23. Broz P, Ruby T, Belhocine K, Bouley DM, Kayagaki N, Dixit VM, Monack DM (2012) Caspase-11 increases susceptibility to Salmonella infection in the absence of caspase-1. Nature 490(7419):288–291. https://doi.org/10.1038/nature11419
24. Rathinam VAK, Vanaja SK, Waggoner L, Sokolovska A, Becker C, Stuart LM, Leong JM, Fitzgerald KA (2012) TRIF licenses Caspase-11-dependent NLRP3 inflammasome activation by gram-negative bacteria. Cell 150 (3):606–619. https://doi.org/10.1016/j.cell.2012.07.007
25. Kayagaki N, Wong MT, Stowe IB, Ramani SR, Gonzalez LC, Akashi-Takamura S, Miyake K, Zhang J, Lee WP, Muszyński A, Forsberg LS, Carlson RW, Dixit VM (2013) Noncanonical inflammasome activation by intracellular LPS independent of TLR4. Science 341 (6151):1246–1249
26. Kayagaki N, Warming S, Lamkanfi M, Vande WL, Louie S, Dong J, Newton K, Qu Y, Liu J, Heldens S (2011) Non-canonical inflammasome activation targets caspase-11. Nature 479(7371):117–121

27. Wolf BB, Green DR (1999) Suicidal tendencies: apoptotic cell death by caspase family proteinases. J Biol Chem 274(29):20049–20052. https://doi.org/10.1074/jbc.274.29.20049
28. Rogers C, Fernandesalnemri T, Mayes L, Alnemri D, Cingolani G, Alnemri ES (2017) Cleavage of DFNA5 by caspase-3 during apoptosis mediates progression to secondary necrotic/pyroptotic cell death. Nat Commun 8:1–14
29. Kayagaki N, Stowe IB, Lee BL, O'Rourke K, Anderson K, Warming S, Cuellar T, Haley B, Roosegirma M, Phung QT (2015) Caspase-11 cleaves gasdermin D for non-canonical inflammasome signalling. Nature 526 (7575):666–671
30. Ruan J, Xia S, Liu X, Lieberman J, Wu H (2018) Cryo-EM structure of the gasdermin A3 membrane pore. Nature 557 (7703):62–67. https://doi.org/10.1038/s41586-018-0058-6
31. Alnemri T, Wu J, Yu J-W, Datta P, Miller B, Jankowski W, Rosenberg S, Zhang J, Alnemri E (2007) The pyroptosome: a supramolecular assembly of ASC dimers mediating inflammatory cell death via caspase-1 activation. Cell Death Differ 14:1590–1604. https://doi.org/10.1038/sj.cdd.4402194

Chapter 14

Determination and Quantitation of Cytotoxic T Cell-Mediated Cell Death

Han-Hsuan Fu and Harry Qui

Abstract

Cytotoxic T cell-induced cell death is well documented. Cytotoxic T cell releases various cytolytic proteins. The cytolytic proteins induce target cell death. T cell-induced cell death can be measured by the lytic assay. One of the well-known lytic assays uses radioactive tracer, Chromium-51 (^{51}Cr), and detects the amount of ^{51}Cr released from target cells. This assay can detect cell death and the efficiency of the T cell-induced cell death by coculture effector cells (T cells) and target cells. This assay can determine the kinetics of the cell lysis. The issue of this approach is the use of radioactive material. This chapter describes measuring T cell-induced cell death by determining the epigenetic remodeling and the release of cytolytic proteins. Determine the efficiency of T cell-induced cell death by using a flow cytometry-based detection method.

Key words $CD8^+$ T cells, Activated T cells, FACS analysis

1 Introduction

There are various types of T cells. One prominent subset is $CD8^+$ T cells. This subset of T cells expresses cytolytic proteins contained within cytotoxic granules [1, 2]. The $CD8^+$ T cells, also known as cytotoxic T lymphocyte (CTL), are mainly involved in T cell-induced cell death. $CD8^+$ T cell induces target cell death through the release of cytolytic proteins [1, 2]. The release of the cytolytic proteins is triggered after $CD8^+$ T cell encounters antigen presented by the antigen presenting cell (APC). The mechanisms that promote this are beyond the scope of this chapter but have been extensively discussed [3].

The antigen is recognized by the $CD8^+$ T cell through T Cell Receptor (TCR) engagement. TCR sends the activation signal downstream, which triggers epigenetic remodeling of the lytic genes [4, 5]. The continuous signaling allows an increased production of the cytolytic proteins, which leads to $CD8^+$ T cell-induced target cell death.

Ayesha B. Alvero and Gil G. Mor (eds.), *Detection of Cell Death Mechanisms: Methods and Protocols*, Methods in Molecular Biology, vol. 2255, https://doi.org/10.1007/978-1-0716-1162-3_14,

The cytolytic proteins that are released by the $CD8^+$ T cells are granzyme B and perforin [1, 2]. Granzyme B and perforin are contained within the cytotoxic granules (Fig. 1). Upon $CD8^+$ T cell activation, the granules will move to the surface and fuse with the cell membrane, thus allowing granzyme B and perforin to be released (Fig. 2). At this point, the T cells are within close proximity with the target cells. Perforin is a pore-forming protein [6, 7]. It creates a passage for granzyme B to gain entry into the target cell. Upon entering the target cell, granzyme B activates the caspase pathway, which leads to target cell death [6, 7].

This chapter describes the step-by-step procedure in detecting T cell-mediated cell death using three different assays: (1) Cytolytic protein expression, (2) Degranulation assay, and (3) Lytic assay. The methods described in this chapter are mainly flow cytometry. This is due to the flexibility and the versatility of the assays and the technique.

1.1 Cytolytic Protein Expression

As mentioned, the cytolytic protein expression is driven by TCR engagement. One of the epigenetic remodeling is the acetylation of K9 and K14 lysine of histone H3 [8, 9]. The acetylation of histone H3 is an indicator of transcriptional activation [8, 10]. One of the methods that can be used to demonstrate $CD8^+$ T cell activation is to measure the level of histone acetylation. Although not a part of the methods described, the measurement of histone acetylation complements the described Fluorescence-Activated Cell Sorting (FACS; flow cytometry)-based methodology and together provides strong data that can support the demonstration of T cell activation. A well-known method for measuring the degree of acetylation is by immunoprecipitation of K14 followed by quantitation of granzyme B and perforin using real-time RT-PCR [9]. Following the measurement of the chromatin acetylation, the lytic molecule mRNA expression should be determined as well. The reason for measuring the mRNA is to create a direct link where the chromatin acetylation indeed led to the transcription of mRNA. The activated $CD8^+$ T cells should have a greater cytolytic mRNA expression compared to naïve or $CD8^+$ T cells that have not been exposed to an antigen. Finally, the cytolytic protein expression can be detected and quantified by using flow cytometry. The measurement of the cytolytic proteins ensures that mRNAs are being translated into proteins. Activated CD8+ T cells will be producing and releasing the cytolytic proteins, and this can be determined by staining the cells with fluorochrome-conjugated monoclonal antibodies (mAb) that can recognize the cytolytic proteins [11]. Once stained, the presence of cytolytic proteins can be detected using flow cytometry.

1.2 Degranulation Assay

As previously mentioned, CD8+ T cells undergo degranulation and release cytolytic proteins [6]. Using flow cytometer to detect the presence of the lytic proteins shows that the cells have the potential

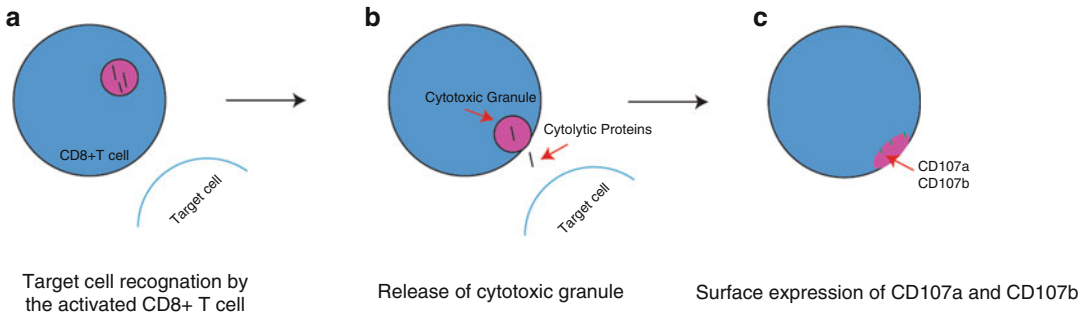

Fig. 1 Degranulation Assay. Once activated $CD8^+$ T cells recognize the target cell (**a**), they will release cytotoxic granules (**b**). As the granules reach the cell surface, CD107a and CD107b are expressed extracellularly (**c**) and can be detected by flow cytometry

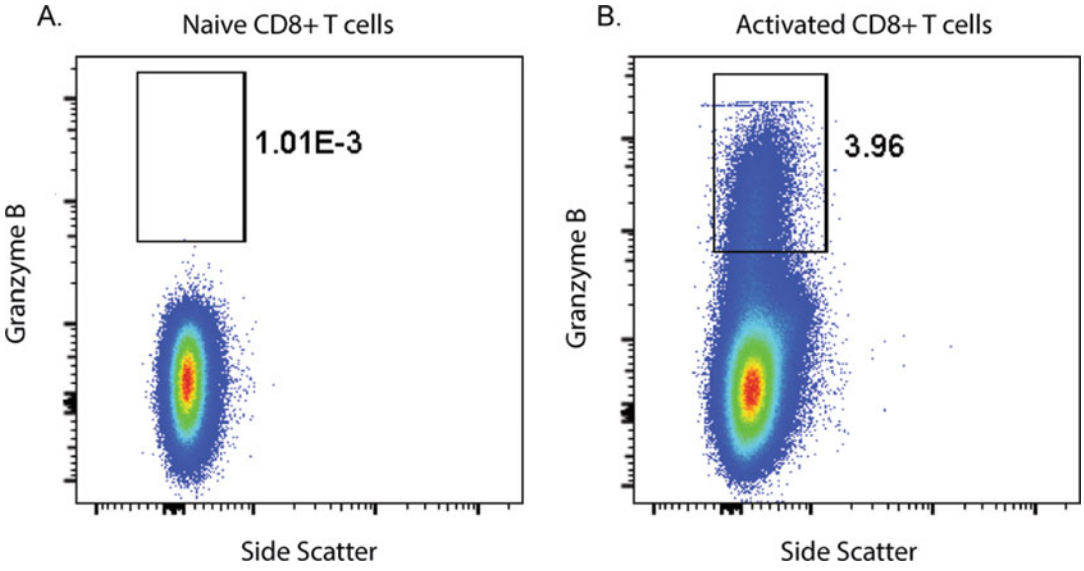

Fig. 2 Flow Cytometry Data showing Granzyme B Expression. The shift in fluorescence intensity corresponding to Granzyme B demonstrates its increased expression in activated $CD8^+$ T cells (**b**; percent Granzyme B positive cells = 3.96) compared to naive $CD8^+$ T cells (**a**; percent Granzyme B positive cells = 0.001)

to induce target cell death. The degranulation assay shows that the CD8+ T cells have released the cytotoxic granules (Fig. 1) [12]. CD107a and CD107b (LAMP-1 and LAMP-2) are found within the cytotoxic granules. When the cytotoxic granules are released, CD107a and CD107b can be detected on the cell surface. Fluorochrome-conjugated mAb is used to visualize CD107a and CD107b expression [12].

1.3 Lytic Assay

The measurement of cytolytic protein expression and the degranulation assay allow determination of the ability of $CD8^+$ T cells to induce cell death but do not directly measure target cell death. To quantify target cell death, the lytic assay can be performed.

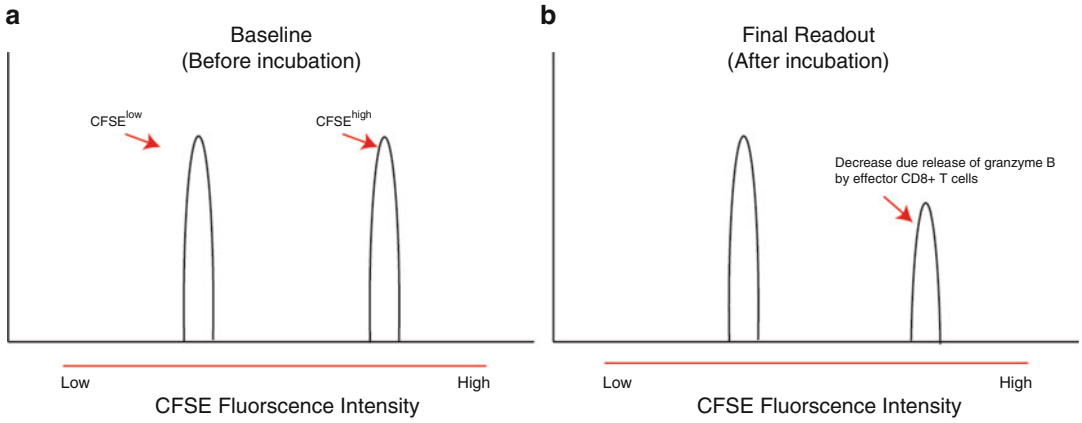

Fig. 3 Sample of flow cytometry data from lytic assay. (**a**) CFSE levels are acquired before incubation of the target cells with CD8+ T cells. This will show the fluorescence intensity of the two groups of target cells (i.e., $CFSE^{low}$ vs $CFSE^{high}$). Note that the peaks have the same height. (**b**) CFSE levels are acquired after incubation of the target cells with CD8+ T cells. Note a decrease in the peak of cells $CFSE^{high}$ cells, which illustrates that lytic activity took place during the incubation period

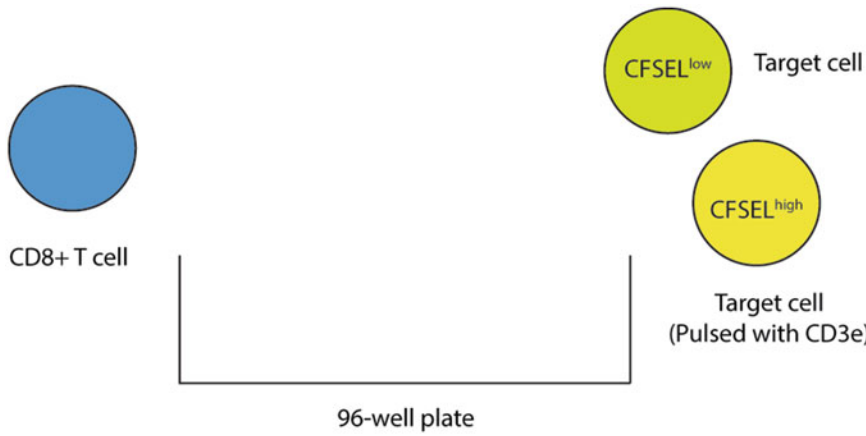

Fig. 4 Lytic Assay Plate Setup. Using a 96-well U-bottom microplate, incubate $CD8^+$ T cells with equal amounts of $CFSE^{low}$ (nonpulsed) and $CFSE^{high}$ (pulsed) target cells

Traditionally, lytic assay uses radioactive material [13]. However, a combination of fluorescent dye, Carboxyfluorescein succinimidyl ester (CFSE) and FACS, can be used for the same determination. The activated $CD8^+$ T cell is cocultured with the target cell labeled with CFSE (Figs. 3 and 4). The use of CFSE allows visualization of lytic activity. A20 mouse B-cell lymphoma cell line is routinely used as the target cells in lytic assay, and it is used here as an example. $CD8^+$ T cell lytic efficiency is determined by coculturing with target cell at various ratios [14, 15]. Effector (E) to target (T) ratio could have a wide range; an example would be from 10(E):1(T) to 1 (E):10(T). Typically, the lower the effector to target ratio, the greater the lytic ability.

2 Materials

2.1 Equipment and Disposables

1. Flow cytometer with FL1 (530 nm), FL2 (585 nm), FL3 (670 nm) and FL4 (661 nm).
2. Refrigerated centrifuge.
3. 37 °C tissue culture incubator with 5% CO_2.
4. Cell counter.
5. Scalpel and scissors.
6. 70 μM nylon cell strainer.
7. 1 mL syringe.
8. 50 mL conical tubes.
9. 5 mL round bottom polystyrene tubes.
10. microfuge tubes.
11. 12-well flat-bottom tissue culture plate.
12. 24-well flat-bottom tissue culture plate.
13. 96-well U-bottom tissue culture microplate.
14. T25 tissue culture flask.
15. Soluble functional grade CD3e (500A2).

2.2 Fluorochrome-Conjugated Monoclonal Antibodies (mAbs)

The mAb can be purchased from various companies. In this chapter, we used the specific clones enumerated below. The concentration of each mAb for staining cells needs to be determined experimentally to have the best signal to noise ratio. Most manufacturers recommend a starting point. The flow cytometer should be properly calibrated to prevent compensation issues.

1. CD8 (clone 53-6.7).
2. Granzyme B (clone NGZB).
3. Perforin (clone eBioOMAK-D).
4. CD107a (clone 1D4B).
5. CD107b (clone H4B4).

2.3 Cell Lines and Reagents

1. Lysing solution: 30 mM Tris/HCl (pH 7.4) containing 150 mM NaCl and 5 mM KCl, 10% glycerol, 2 mM EDTA.
2. Cell culture medium: RPMI 1640, supplemented with 10% v/v heat-inactivated FBS, 2 mM L-glutamine, 100 U/mL penicillin and 100 μg/mL streptomycin.
3. FACS buffer: Phosphate-Buffered Saline, 5% FBS, 0.1% NaN_3 .
4. Fixation/Permeabilization buffer: in this chapter, we used BD Fixation/Permeabilization Solution containing 4.2% formaldehyde.

5. Wash buffer: in this chapter, we used BD Perm/Wash buffer containing 10% saponin and 10% FBS.
6. Protein transport inhibitor: in the chapter, we used Golgi-Plug™ containing brefeldin A.
7. Target cell for T cell-mediated cell death: we have used A20 murine B-cell lymphoma cell line and CT26 murine colon adenocarcinoma cell line.
8. Carboxyfluorescein succinimidyl ester (CFSE).

3 Methods

3.1 Splenocyte Preparation

This section describes the general approach for murine splenocyte preparation.

1. Euthanize the animal based on your institute's guidelines and current standards as outlined in the US Department of Health and Human Services publication for humane handling and care of laboratory animals.
2. Incise the abdominal cavity and remove the spleen. Place the spleen in a 50 mL conical tube containing enough RPMI medium to cover the spleen. Use scissors to cut the excised spleen into small pieces. Keep the tubes on ice.
3. Load the contents of the tube in **step 2** onto a strainer attached to a fresh 50 mL conical tube. Use the plunger end of a 1 mL syringe to carefully press contents through the strainer.
4. Wash the cells through the strainer with RPMI medium.
5. Centrifuge the collected cell suspension at 400 $\times g$ for 5 min.
6. Aspirate the supernatant. Resuspend the cell pellet in 2 mL of lysing solution. Incubate at room temperature for 5 min.
7. Add 10 mL of RPMI medium and centrifuge the cells at 400 $\times g$ for 5 min.
8. Aspirate the supernatant and resuspend the cells in RPMI medium at 2×10^6 cells per mL. Perform the cell count using your laboratory's established cell counting protocols.

3.2 Determination of Cytolytic Protein Expression by FACS Analysis

The below methods describe the procedure for performing surface and intracellular staining. Surface staining allows the determination of different cell populations, such as $CD8^+$ T cells. The intracellular staining described below is for the detection of lytic proteins, granzyme B and perforin (Fig. 2). Alternatively, staining can be performed for transcription factors, and T-bet and Eomes Activated antigen-specific $CD8^+$ T cells have higher expression of lytic proteins and these transcription factors.

1. Collect splenocytes as described in Subheading 3.1. When performing this experiment after an in vivo study (i.e., to compare Control versus Vaccinated mice bearing colon cancer; *see* **Note 1**), proceed to **step 2** after preparation of the splenocytes. When using healthy mice to perform in vitro studies, the protocol to activate CD8+ T cells in vitro is described in **Note 2**.
2. Transfer 5×10^6 cells into a round-bottom polystyrene tube.
3. Centrifuge the cells at $400 \times g$ for 5 min.
4. Wash the cells with 2 mL of FACS buffer and centrifuge the cells at $400 \times g$ for 5 min.
5. Resuspend cells in 100 μL of FACS buffer.
6. Stain for surface markers: add CD8 mAb at a concentration recommended by the manufacturer (*see* **Note 3**; in this chapter, our focus is $CD8^+$ T cells, and therefore, we are staining for surface marker CD8; depending on the experimental design, different surface markers may be used such as CD4).
7. Incubate for 30 min at 4 °C protected from light.
8. Add 2 mL of FACS buffer and centrifuge at $400 \times g$ for 5 min.
9. Decant supernatant and fix the cells by resuspending pellets in 100 μL of fixation/permeabilization buffer.
10. Incubate in the dark for 20 min at 4 °C.
11. Add 2 mL of fixation/permeabilization buffer and centrifuge at $400 \times g$ for 5 min.
12. Decant the supernatant and resuspend pellets in 100 μL of fixation/permeabilization buffer.
13. Add granzyme B and perforin mAb at a concentration recommended by the manufacturer (*see* **Note 3**).
14. Incubate in the dark for 20 min at 4 °C.
15. Add 2 mL of wash buffer and centrifuge at $400 \times g$ for 5 min.
16. Decant the supernatant and resuspend the cells in 100 μL of FACS buffer. The samples are ready for FACS analysis.
17. In-depth guide to FACS analysis is beyond the scope of this chapter. **Notes 4** and **5** provide a general guide to flow cytometry and FACS analysis.

3.3 Determination of $CD8^+$ T Cell Degranulation Ability by FACS Analysis

The below methods describe the procedure for performing in vitro degranulation assay. This is an in vitro assay, where $CD8^+$ T cell is stimulated and cultured for a period of time with fluorochrome-conjugated mAb (*see* **Note 6**).

1. Follow the splenocyte preparation technique described in Subheading 3.1.

2. Resuspend 2 × 10^6 cells in 1 mL of RPMI culture medium. Each sample (e.g., Naïve, tumor bearing mice, and tumor bearing mice with treatments) should be plated in three wells of a 24-well plate. In well 1, add 1 μL/mL of GolgiPlug. In well 2, add 5 μg/mL of soluble functional grade CD3e mAb (positive control) plus 1 μL/mL of GolgiPlug (*see* **Note 7**). In well 3, add tumor MHC Class I peptides with 1 μL/mL of GolgiPlug.
3. Add fluorochrome-conjugated mAb CD107a and CD107b to all wells (*see* **Note 8**).
4. Incubate for 5 h in a tissue culture incubator.
5. Collect cells into 15 mL conical tubes and add 10 mL of RPMI medium.
6. Centrifuge the cell suspension at 400 × *g* for 5 min.
7. Aspirate the supernatant and resuspend the pellet in 100 μL of FACS buffer and transfer the cell suspension into a round-bottom polystyrene tube.
8. Add CD8 mAb (*see* **Note 3**) and incubate in the dark for 30 min at 4 °C.
9. Add 2 mL of FACS buffer and centrifuge at 400 × *g* for 5 min.
10. Decant the supernatant and resuspend the cells in 200 μL of FACS buffer. Analyze degranulation using flow cytometer (*see* **Note 9**).

3.4 Quantitation of T Cell-Mediated Cell Death by Lytic Assay

The below methods describe the procedure for performing CFSE labeling and quantifying T cell-mediated cell death. This is an in vitro assay where effector cells (i.e., $CD8^+$ T cells) are cocultured with target cells (i.e., A20). The target cells are separated into two settings. In the first setting, target cells are pulsed with soluble functional grade CD3e mAb and labeled with 1000 μM of CFSE ($CFSE^{high}$). In the second setting, target cells are not pulsed with CD3e mAB and will be labeled with 100 μM of CFSE ($CFSE^{low}$). The difference in CFSE concentration is for better separation and distinguishing lysis activity (Figs. 3 and 4). The effector cell:target cell ratio typically ranges from 10:1 (lower lytic ability) to 1:10 (higher lytic ability). Each setting of the target cell can be incubated with splenocytes from either Naïve mice, tumor-bearing mice but without treatment, or tumor bearing mice posttreatment.

1. In a T25 flask, pulse target cells with 5 μg/mL soluble functional grade CD3e mAb for 2 h in 5 mL of cell culture medium (*see* **Note 10**).
2. In a separate T25 flask, incubate target cells in 5 mL of cell culture medium without the CD3e mAb.

3. Label the pulsed target cells in **step 1** with 1000 μM CFSE ($CFSE^{high}$) for 5 min.
4. Label nonpulsed target cells in **step 2** with 100 μM CFSE ($CFSE^{low}$) for 5 min.
5. Collect pulsed and nonpulsed cells in conical tubes and centrifuge at 400 × *g* for 5 min.
6. Aspirate the supernatant and resuspend the cells in 1 mL of cell culture medium. Count cells.
7. In each well, combine pulsed and nonpulsed cells at a 1:1 ratio. The final target cell count per well should be 5×10^4 target cells/50 μL cell culture medium (thus, 2.5×10^4 pulsed cells in 25 μL of cell culture medium +2.5×10^4 nonpulsed cells in 25 μL of cell culture medium).
8. Add 5×10^4 splenocytes in 50 μL of cell culture medium per well.
9. Coculture for 5 h.
10. Collect the cells from each well in individual conical tubes and add 1 mL of cell culture medium.
11. Centrifuge for 5 min at 400 × *g*.
12. Aspirate the supernatant and resuspend the cells in 1 mL of FACS buffer.
13. Centrifuge at 400 × *g* for 5 min.
14. Aspirate the supernatant and resuspend the cells in 200 μL of FACS buffer.
15. Proceed to FACS analysis and analyze CFSE intensity (FL-1) as shown in Fig. 3.
16. Calculate the percentage of lysis:

$$\left(1 - \frac{\left[\%\text{pulsed } CFSE^{high}\text{cells}\right]}{\left[\%\text{of } CFSE^{low}\text{cells (non-pulsed)}\right]}\right) \times 100.$$

4 Notes

1. Naïve mice should be added to the experimental groups for negative control.
2. $CD8^+$ T cells can be activated in vitro to induce the expression of the cytolytic proteins, granzyme B and perforin. Follow the splenocyte preparation technique described in Subheading 3.1. Resuspend the cell suspension in cell culture medium. Following cell count, culture 5×10^6 cells in 1 mL of cell culture medium in a 24-well plate. As culture starts, each sample

should have 3 stimulation sets: 1 μL/mL of GolgiPlug alone (negative control); 5 μg/mL soluble functional grade CD3e mAb (positive control) with 1 μL/mL of GolgiPlug; and tumor MHC Class I peptides (such as CT26) with 1 μL/mL of GolgiPlug in the cell culture medium at the beginning of the incubation for 5 h. The GolgiPlug is applied to prevent the release of cytolytic proteins by inhibiting the transport protein inside the cell. Collect the cells at the end of the incubation period. For cell staining and processing, proceed to Subheading 3.2 beginning with **step 2**.

3. Check with the manufacturer for each antibody concentration and the recommended dilution. It is important to optimize the antibody dilution before using it in the experiment.
4. The Fluorescence Minus One Control (FMO) is suggested for the determination of proper gating strategy.
5. Depending on the number of fluorochromes, a set of compensation control should be run first. This is to ensure a proper separation of each channel (i.e., FL1 vs. FL2). Use Forward Scatter (FSC) vs. Side Scatter (SSC). Plot to visualize different population of cells in the suspension. Figure 5 illustrates the gating strategy for lymphocytes. Lymphocytes are typically smaller cells and with fewer granules, meaning that they have a lower FSC and a lower SSC, respectively.
6. The culture time needs to be determined experimentally. We suggest a minimum of 2 h.
7. For optimal results, the concentration of functional grade CD3e mAb should be determined experimentally.
8. mAb concentration needs to be determined experimentally. We suggest 4 μL per mL to start.

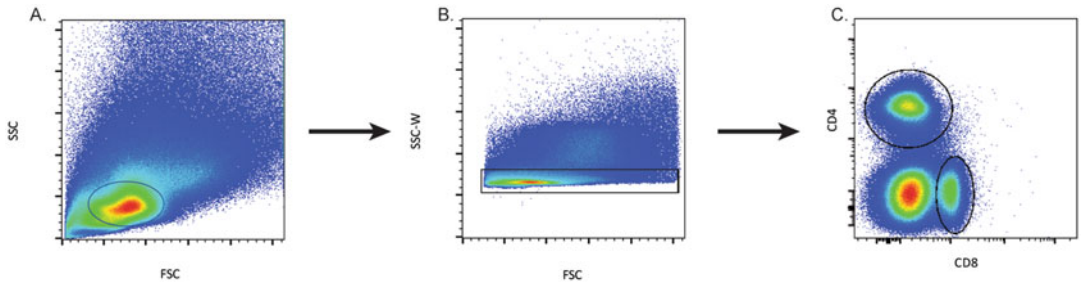

Fig. 5 Lymphocyte gating strategy. Acquire the samples and plot the data using FSC vs. SSC plot. Gate on the lymphocytes from FSC vs SSC plot (**a**). Plot the lymphocyte gate using SSC-W vs FSC to gate on singlets (**b**). Gating on singlets will eliminate cell clumps and decrease background noise. Use the singlet gate to plot the fluorescence intensity of antibody that was used, in this case, CD4 vs CD8 (**c**). Once either lymphocyte population has been selected, either gate can be used to plot data from other antibodies used

9. Naïve $CD8^+$ T cells should be used as negative control to determine the degree of degranulation in other groups.
10. We suggest 1×10^6 cells for each group. The cell number can be expanded based on the experimental design.

References

1. Podack ER, Young JD, Cohn ZA (1985) Isolation and biochemical and functional characterization of perforin 1 from cytolytic T-cell granules. Proc Natl Acad Sci U S A 82 (24):8629–8633. https://doi.org/10.1073/pnas.82.24.8629
2. Pasternack MS, Eisen HN (1985) A novel serine esterase expressed by cytotoxic T lymphocytes. Nature 314(6013):743–745. https://doi.org/10.1038/314743a0
3. Williams MA, Bevan MJ (2007) Effector and memory CTL differentiation. Annu Rev Immunol 25:171–192. https://doi.org/10.1146/annurev.immunol.25.022106.141548
4. Pearce EL, Mullen AC, Martins GA, Krawczyk CM, Hutchins AS, Zediak VP, Banica M, DiCioccio CB, Gross DA, Mao CA, Shen H, Cereb N, Yang SY, Lindsten T, Rossant J, Hunter CA, Reiner SL (2003) Control of effector CD8+ T cell function by the transcription factor eomesodermin. Science 302 (5647):1041–1043. https://doi.org/10.1126/science.1090148
5. Intlekofer AM, Takemoto N, Wherry EJ, Longworth SA, Northrup JT, Palanivel VR, Mullen AC, Gasink CR, Kaech SM, Miller JD, Gapin L, Ryan K, Russ AP, Lindsten T, Orange JS, Goldrath AW, Ahmed R, Reiner SL (2005) Effector and memory CD8+ T cell fate coupled by T-bet and eomesodermin. Nat Immunol 6 (12):1236–1244. https://doi.org/10.1038/ni1268
6. Russell JH, Ley TJ (2002) Lymphocyte-mediated cytotoxicity. Annu Rev Immunol 20:323–370. https://doi.org/10.1146/annurev.immunol.20.100201.131730
7. Henkart PA (1985) Mechanism of lymphocyte-mediated cytotoxicity. Annu Rev Immunol 3:31–58. https://doi.org/10.1146/annurev.iy.03.040185.000335
8. Araki Y, Fann M, Wersto R, Weng NP (2008) Histone acetylation facilitates rapid and robust memory CD8 T cell response through differential expression of effector molecules (eomesodermin and its targets: perforin and granzyme B). J Immunol 180 (12):8102–8108. https://doi.org/10.4049/jimmunol.180.12.8102
9. Juelich T, Sutcliffe EL, Denton A, He Y, Doherty PC, Parish CR, Turner SJ, Tremethick DJ, Rao S (2009) Interplay between chromatin remodeling and epigenetic changes during lineage-specific commitment to granzyme B expression. J Immunol 183(11):7063–7072. https://doi.org/10.4049/jimmunol.0901522
10. Koprinarova M, Schnekenburger M, Diederich M (2016) Role of histone acetylation in cell cycle regulation. Curr Top Med Chem 16 (7):732–744. https://doi.org/10.2174/1568026615666150825140822
11. Cao X, Cai SF, Fehniger TA, Song J, Collins LI, Piwnica-Worms DR, Ley TJ (2007) Granzyme B and perforin are important for regulatory T cell-mediated suppression of tumor clearance. Immunity 27(4):635–646. https://doi.org/10.1016/j.immuni.2007.08.014
12. Betts MR, Brenchley JM, Price DA, De Rosa SC, Douek DC, Roederer M, Koup RA (2003) Sensitive and viable identification of antigen-specific CD8+ T cells by a flow cytometric assay for degranulation. J Immunol Methods 281 (1–2):65–78. https://doi.org/10.1016/s0022-1759(03)00265-5
13. Cerottini JC, Nordin AA, Brunner KT (1970) In vitro cytotoxic activity of thymus cells sensitized to alloantigens. Nature 227 (5253):72–73. https://doi.org/10.1038/227072a0
14. Noto A, Ngauv P, Trautmann L (2013) Cell-based flow cytometry assay to measure cytotoxic activity. J Vis Exp (82):e51105. https://doi.org/10.3791/51105
15. Quah BJ, Wijesundara DK, Ranasinghe C, Parish CR (2013) Fluorescent target array T helper assay: a multiplex flow cytometry assay to measure antigen-specific CD4+ T cell-mediated B cell help in vivo. J Immunol Methods 387(1–2):181–190. https://doi.org/10.1016/j.jim.2012.10.013

Chapter 15

Detection of Immunogenic Cell Death in Tumor Vaccination Mouse Model

Kazuki Tatsuno, Patrick Han, Richard Edelson, and Douglas Hanlon

Abstract

Immunogenic cell death (ICD) is a form of regulated cell death that is capable of eliciting an immune response. In cancer, tumor cells undergoing ICD are known to emit damage associated molecular patterns (DAMPs) that are capable of recruiting and activating antigen presenting cells (APCs), which ultimately lead to the activation of an antitumor immune response. Surface translocation of intracellular chaperones such as calreticulin, release of TLR agonists such as high mobility box 1, and the secretion of type I IFN are some of the hallmark features seen in tumors succumbing to ICD. While detection of these molecules is suggestive of ICD induction, which alone does not certify that the treatment is an ICD inducer, an in vivo vaccination assay using injured tumor cells remains to be the gold standard method to functionally verify ICD. This chapter will discuss the necessary steps required to conduct an in vivo vaccination assay, focusing on the preparation of vaccine using treated tumor cells, and how these cells are then utilized in the animal model.

Key words Immunogenic cell death, Tumor vaccination, Clonogenic cell death, Colony formation assay, Murine tumor model, DAMPs

1 Introduction

Over the past few decades, most cancer therapies were developed to efficiently maximize the cytotoxic effect against tumor cells, based on the dogma that the efficacy of antitumor treatment is mediated mainly through their lethality against the neoplastic lesion. Most of the chemotherapeutic reagents utilized today, some designed to be as selective as possible to the neoplastic cells, are aimed to effectively kill the cells mainly by impairing cell division. However, with the development of immune-checkpoint inhibitors, the strategy for combating cancer has shifted dramatically, putting immunology in the forefront of the war against malignant neoplastic diseases. While there are still concerns over safety and efficacy with these newly developed immunotherapies, it has become apparent that partnership with the immune system is key to successful cancer treatment.

Ayesha B. Alvero and Gil G. Mor (eds.), *Detection of Cell Death Mechanisms: Methods and Protocols*, Methods in Molecular Biology, vol. 2255, https://doi.org/10.1007/978-1-0716-1162-3_15,

With this heightening expectation in the field of onco-immunotherapy, the concept of immunogenic cell death (ICD) has gained much attention since it was first proposed in 2005 by Cassares et al. [1]. Their work, which challenged the long standing conception that apoptosis is an immunoquiescence form of cell death, demonstrated that tumor cells treated with certain apoptosis-inducing chemotherapeutic reagents, when inoculated into immunocompetent animals, are capable of eliciting immuno-protection specifically against the tumors, which was used for the vaccination. Their finding became the basis for the fundamental notion of ICD that methods using which the cancer is treated, including modalities triggering the apoptotic cell death pathway, hold strong capacity to influence the ensuing antitumor immune response in the host and that cytotoxic effect may not be the only measurement to define the therapeutic efficacy of a given treatment. A variety of antitumor treatments, including traditional chemotherapeutic reagents such as anthracycline [1] and oxaliplatin [2]; targeted anticancer reagents such as cetuximab [3]; proteasome inhibitors such as bortezomib [4]; oncolytic viruses [5]; and various forms of irradiation therapies such as gamma irradiation [6], hypericin-based photodynamic therapy [7], near-infrared photoimmunotherapy, [8] and extracorporeal photochemotherapy (ECP) utilizing UVA activated psoralen [9] are some of the known methods to induce this unique form of cell death. Accumulating evidences suggesting that ICD inducers are capable of synergizing with immune checkpoint inhibitors [10], and the relevance of this immunostimulatory cell death in a clinically functioning dendritic cell-based therapy such as ECP [11] clearly highlights the essential role of ICD in immunotherapy.

While the precise mechanism of ICD is just starting to be deciphered, it is now quite unarguable that certain DAMPs that are emitted from the dying tumor cells play important role in the process of ICD. Among the several ICD-associated molecules that have been investigated thus far, detection of ecto-calreticulin (CRT) on dying cells has been one of the earliest and well-described observations [12]. Exposure to ICD-inducing treatment is often linked to the induction of endoplasmic reticulum (ER) stress [13], which is then followed by the unfolded protein response (UPR) as a means to restore the ER homeostasis. During this process, phosphorylative inactivation of eukaryotic initiation factor 2α (eIF2α) is triggered, which ultimately leads to the translocation of CRT, an ER chaperon, to the outer leaflet of the plasma membrane [14]. The surface exposure of CRT serves as a strong phagocytic signal, potentiating the uptake of the relevant antigens residing in these dying cells by antigen presenting cells (APCs) [15]. Extracellular release of adenosine 5-triphosphate (ATP) is another type of DAMP released by the dying tumor cells, acting as a “find me” signal to recruit the APCs via its interaction with the P2Y2 receptor

[16]. Additionally, ATP is also capable of interacting with the P2X7 receptor on the dendritic cells (DCs), which drives the activation of NLRP3 inflammasomes, ultimately leading to the secretion of IL-1β, a pro-inflammatory cytokine essential in the activation of cytotoxic T cells (CTLs) [17]. In the later phase of apoptosis, high mobility group box 1 (HMGB1) is released from the nucleus of a dying cell. Through its interaction with the pattern recognition receptors (PRPs) on DCs, extracellular HMGB1 promotes the maturation and the antigen processing, which is mediated mainly through its binding to RAGE and TLR4, respectively [18, 19]. In addition to DAMPs, some tumor cells dying in ICD manner are also known to secrete type I IFN, which is triggered through signaling driven by cytosolic dsDNA. This pro-inflammatory cytokine conveys potent stimulatory effects on broad spectrum of immune cells through its binding to the IFNAR1 [20].

Detection of above-mentioned DAMPs and cytokines in an in vitro setting is a valuable method to evaluate whether the choice of treatment possesses the capability to induce ICD. Flow cytometric assays evaluating the surface exposure of ER chaperons and the detection of immunostimulatory DAMPs and cytokines associated with ICD through ELISA assays are some methods that can be conveniently performed in a short period of time, provided that appropriate equipment, reagents, and protocol are in place [21]. However, while these in vitro assays are frequently applied in investigative study for ICD, it is critical to keep in mind that emission of DAMPs is not the sole factor that dictates ICD. For instance, cardiac glycosides, a compound used for the treatment of congestive heart failure, is known for its capability to induce the emission of these ICD-associated DAMPs, but cancer cells treated with this compound alone do not sufficiently lead to an in vivo immune protection phenomenon [22]. Antigenicity of the tumor cells, as well as host-related factors, is also another component that influences the intricacy of ICD, and thus, the gold standard method to truly evaluate ICD, to date, is through the in vivo vaccination model using animals injected with treated tumor cells.

This chapter describes the sequential steps required to set up in vivo tumor cell vaccination assay, which is essential for the detection of bona fide ICD. As the dosage at which a treatment is applied to the tumor cells has been shown to impact the immunogenicity in certain modalities such as gamma irradiation and ECP [9, 23], preparatory work to determine the range in which you may want to treat the cells may become quite crucial. Once this is established, treated tumor cells are injected into mice as vaccination, followed a few days later with challenge injection with live tumor cells. Protection from tumor development on the site of tumor cell challenge is a clear sign indicating the generation of a successful antitumor immunity in mice that received vaccination with tumor cells succumbing to ICD. The assay can further be

expanded for deeper investigative studies by applying genetic modifications to the tumor cells (i.e., knock-down of certain proteins), which may greatly facilitate the understanding of the mechanisms and pathways that govern ICD induction in the treatment of your choice.

2 Materials

2.1 Equipment

1. Cell culture incubator, cell culture hood, centrifuge.
2. Hemocytometer and microscope or cell counting slides and cell counter.
3. Flow cytometer.
4. Camera.
5. Anesthesia machine with oxygen flow.
6. Fur shaver.
7. Caliper for tumor measurement.
8. UVA irradiator.

2.2 Materials and Reagents

1. Murine tumor cell line.
2. Cell culture media.
3. Phosphate buffered saline.
4. 0.25% Trypsin.
5. Cell scraper.
6. Sterile conical tubes (15 ml and 50 ml).
7. Tissue culture flasks (75 cm^2 or 150 cm^2).
8. Tissue culture plates (6, 12 and 24 well plate).
9. Annexin V/PI staining kit.
10. 4% Paraformaldehyde.
11. 0.05% Crystal violet.
12. Mice (*see* **Notes 1** and **2**).
13. 1 ml syringe.
14. 26G or 27G needle.
15. 2.5% Isoflurane.
16. 8-methoxypsoralen.

3 Methods

The goal of the ICD animal vaccination assay is to evaluate whether tumor cells treated with the agent of choice, when injected into mice as vaccine, are capable of preventing tumor (the same tumor used in the vaccination) from developing in these mice. Hence, the model can be separated into two phases: the vaccination phase and the challenge phase. For the model to fully operate, it is important to optimize the model with the tumor cell line that is being implemented so that (1) treatment is sufficient enough to kill the cells so that tumors will not grow on the vaccination site and (2) the implant in the challenge phase is optimized (i.e., injected cell number) so that the tumors in the control group grow without overt variance (speed and size) and no spontaneous regression happens past a certain period of time.

To evaluate the optimal treatment dosage, we recommend that you first start treating the cells in varying dosages and assess the tumor cell viability at several different timepoints (Fig. 1). There may be a suggested dosage for the treatment of interest, but the effect may differ depending on the cell line. Therefore, titrating the dosage both ways (reduced and increased) based on the suggested amount is highly advised. As reference, a dosage that results in significant cell death at 24–48 h posttreatment is often utilized as a starting point. However, some treatment may impact more heavily the cell's proliferative capacity (strongly inducing clonogenic cell death), where cells may appear less "dead" at 24–48 h timepoint, but is on the path of "dying", and hence may require less treatment intensity than predicted. As such, preliminary studies including colony formation assay may be required depending on the mode of treatment that is being implemented [24].

3.1 Assessing Tumor Cell Viability

1. Prepare and grow the murine tumor cell line of interest. For this chapter, we use the B16 murine melanoma cell line. When testing for chemotherapeutic or chemical reagents, grow cells in 12- or 24-well tissue culture plates. If the treatment of interest requires cells to be detached from the flasks and treated in suspension (i.e., repeated freeze-thaw cycle, psoralen UVA, etc.), grow cells in large flasks instead.
2. Once adequately confluent (50–70% confluency), aspirate media off the well and then wash the wells gently with PBS. Add media containing the agent of choice. For this chapter, we use 8-MOP UVA treatment (*see* **Note 3**) to treat B16 murine melanoma cells. Cells are first harvested from culture flask and then treated with 200 ng/ml 8-MOP in conical tube for 20 min at 37C°. Subsequently, cells are irradiated with UVA ranging from 0.5 J/cm^2 to 8 J/cm^2. Plate treated cells back into culture plate (*see* **Note 4**).

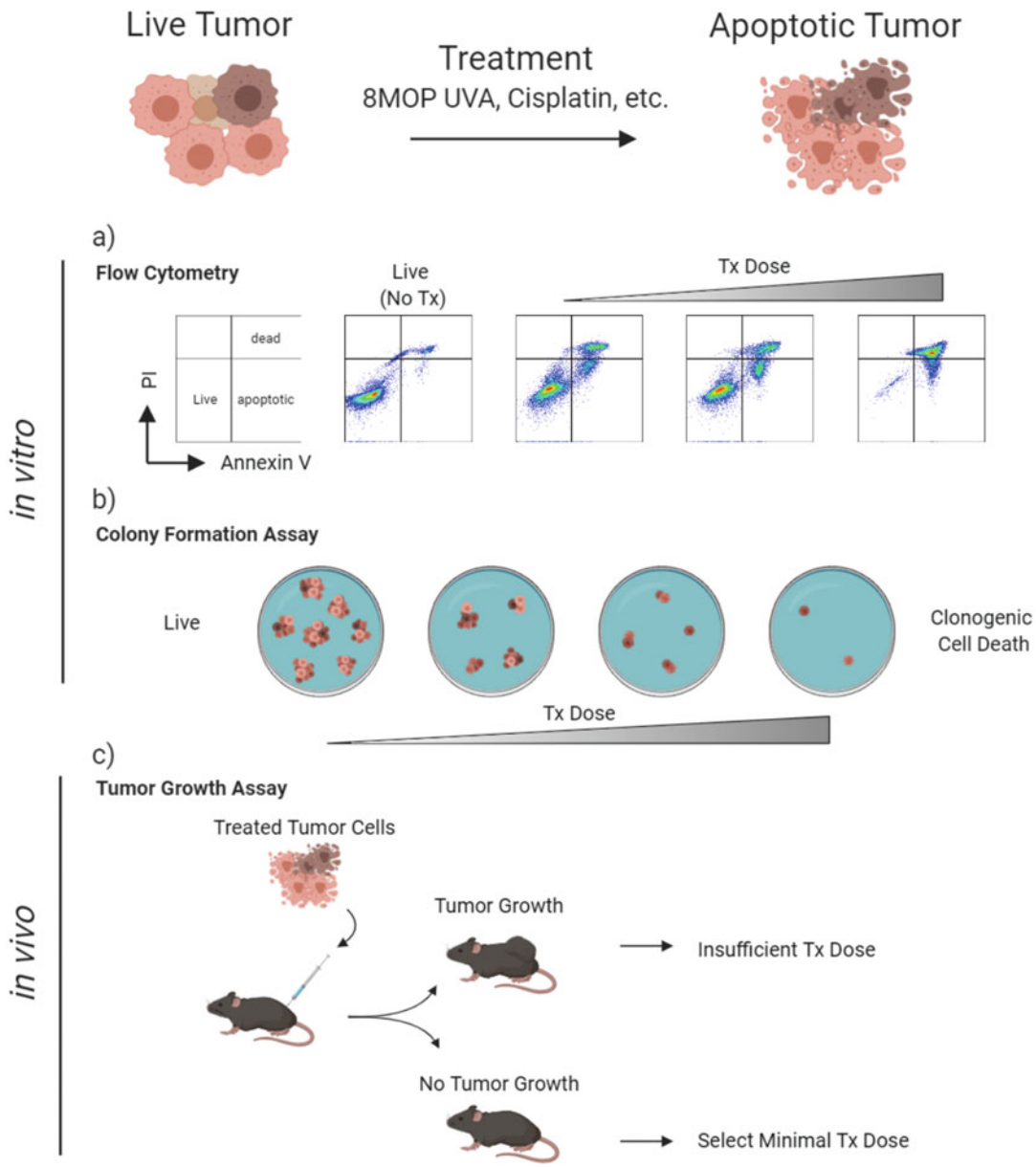

Fig. 1 Methods for assessing tumor cell viability. (**a**) After cells have been damaged by the treatment of choice, determine the viability via flow cytometry assay via PI/annexin V surface staining protocol. Live cells are PI/annexin V negative, while dead cells are positive for both stains. Cells dying through apoptosis will be PI negative, but positive for annexin V. Increase in treatment dosage will lead to stronger cell death, and treatment dose that results in 50–70% cell death 24 h posttreatment is usually the recommended dosage. (**b**) Certain treatment, such as radiation and 8-MOP UVA, which inhibits cell's proliferative capacity, induces clonogenic cell death, which can be assessed using colony formation assay. Subsequent to treatment, cells are plated sparsely on to a tissue culture plate (i.e., 100–1000 cells/well into a 6-well tissue culture plate) and then observed for 7–14 days for the formation of cell colonies. (**c**) After establishing the optimal dosage required to kill the tumor cells, proceed to testing in in vitro setting. Inject treated tumor cells into syngeneic/immunocompetent mice and evaluate tumor growth on injection site (30–60 day observation required) to select the minimal treatment dose required for the assay

3. Collect the samples at different timepoints. For 8-MOP UVA treatment, we collect and analyze the samples at 6 h, 12 h, 24 h, 48 h, and 96 h. We suggest analyzing samples at later timepoints when treating cells with 8-MOP UVA since cells tend to die slowly, but when using standard chemotherapeutic modalities, cells may die more rapidly, and in such case, later time points may be omitted.
4. When collecting, transfer culture supernatant into an adequate size centrifuge tube first, then harvest the adherent cells by either trypsinization or scraping, and transfer the detached cells into the tubes containing the collected culture supernatant (*see* **Note 5**).
5. Determine percentage of viable cells via trypan blue exclusion (*see* **Note 6**) or PI/Annexin V staining. Alternatively, assays evaluating cellular metabolism and enzymatic activities can also be implemented.

3.2 Assessing Clonogenic Cell Death

1. The treatment dose required for inducing clonogenic cell death may be lower than the dose required to elicit rapid apoptotic cell death (i.e., effective dose observed in Subheading 3.1). If the treatment of choice is known to induce clonogenic cell death, lower dosage range should be included in the assay (*see* **Note 7**). Using the best choice of dose for the agent in use, treat and wash the cells, and prepare them in single cell suspension.
2. Carefully count the cells using cytometer (include dead cells in the count), and plate cells (100–1000 cells per well) into a tissue culture plate (6-, 12-, or 24-well plate) in the optimal growing media. The size of the plate and the number of cells seeded per well should be determined depending on the anticipated number of colonies that may form (*see* **Note 8**). The aim is to achieve a range of 20–150 colonies per well. There should be enough room in the well so that growing colonies will not overlap with each other.
3. Incubate the plate for 7–14 days. Observe the wells each day under microscope to follow the formation of cell colony in the wells. A cell that has replicated at least 6 times will form a large enough colony consisting of more than 50 cells.
4. Once colonies of appropriate size have formed, aspirate off the media and wash the well with PBS.
5. Fix the cells using 4% PFA or 10% formalin for 5–10 min.
6. Aspirate off the fixation solution and stain the cells with 0.05% crystal violet for 30 min.

7. Wash with dH_2O twice and then let the plate dry overnight. You should be able to visualize multiple purple dots (colonies) on the bottom of the plate.
8. Count the colonies manually through stereomicroscope or acquire digital image using camera and count the cells using imaging software (*see* **Note 9**).
9. The plating efficiency (number of colonies counted/number of cells plated) and the surviving fraction (plating efficiency of the treated wells/plating efficiency of the untreated wells) can be calculated for evaluation (*see* **Note 10**).

As mentioned above, it is essential that tumors do not grow on the vaccination site. While the in vitro cell viability assays described above will aid in predicting the sufficient dosage to achieve this requirement, ultimate confirmation is obtained only through the actual injection of the treated tumor cells into the mice (*see* **Note 11**).

3.3 Determining the Minimal Dosage Required for In Vivo Vaccination Assay

1. Culture and treat the cells as above.
2. The number of cells to be grown depends on the number of mice that will be injected. At least 5 mice should be designated to each treatment dosage group. The baseline treatment dosage should be established based on the approximate minimal dosage required to kill the cell of interest determined by the in vitro cell viability assays described above. Include dosages below and above this baseline intensity (*see* **Note 12**). The number of treated tumor cells injected per mouse may range from 2×10^5 cells to 1×10^6 cells, but should be fixed to a certain number, so that tumor cell number used in the vaccination will be consistent throughout future experiments.
3. Once cells have grown to appropriate confluency, wash the cells gently with PBS to remove any nonviable cells.
   (a) If the treatment of your choice is a chemotherapeutic reagent, add media containing the appropriate concentration of the damaging reagent to the washed cells and continue culturing the cells for the time required to sufficiently kill the cells.
   (b) If the cells are required to be treated in suspension, harvest the washed cells and treat them in appropriate condition. If cells need to be cultured posttreatment, plate them in appropriate sized flask with optimal growing media (*see* **Note 13**).
4. After treatment, collect the culture supernatant into an appropriate size centrifuge tube. Do not discard these culture media, as they may contain died cells.

5. Harvest the adherent cells by adding warmed trypsin. Stop the reaction by adding equal volume of serum-containing media. After pipetting off the cells from the culture dish, transfer the cells into the tubes containing the culture supernatant that was collected in prior step.
6. Centrifuge the tube at 300 × *g* for 5 min at RT. Decant the supernatant, and resuspend the cells with PBS. Repeat the wash two times.
7. Resuspend the cells in PBS, and count the cells by trypan-blue exclusion method.
8. Centrifuge again, and resuspend the cells in appropriate volume of PBS, so that the final concentration will be in the range of 2×10^5 to 1×10^6 cells per 100 μl (include dead cells).
9. Prepare mice for injection by shaving the left flank (to facilitate the injection, shaving should be done the day before).
10. Anesthetize one cage at a time. While anesthetizing, fill 1 ml syringe with treated tumor cell suspension. Make sure to mix the suspension before drawing into the syringe, as tumor cells tend to settle down in the tube (*see* **Note 14**).
11. Use 26–27 G needles for injection.
12. Inject 100 μl of treated tumor cells per mouse subcutaneously.
13. While injecting, keep other cells on ice or refrigerated.
14. Monitor the vaccination site for tumor development (typically 30–60 days).
15. Monitor every 2–3 days.
16. The group receiving the lowest treatment dosage in which no mice ultimately develop tumor is the group that received the minimal dosage required for the in vivo vaccination assay (Fig. 2).
17. Optional: Time required to gather data from the in vivo vaccination model can be quite lengthy. To maximize efficiency, challenging mice 7–10 days postvaccination (as described below) in this set of screening experiment will give you a general idea on whether the treatment of your interest possess any ICD potential and also may give hint at the optimal dosage for the ICD effect, which will help in the planning of future experiments.

Once the treatment dosage is established, proceed to conduct the vaccination assay. Ideally, the vaccination assay will include mice receiving tumor cell vaccination prepared by the treatment of your choice and cells prepared by a known ICD and/or nonICD inducers.

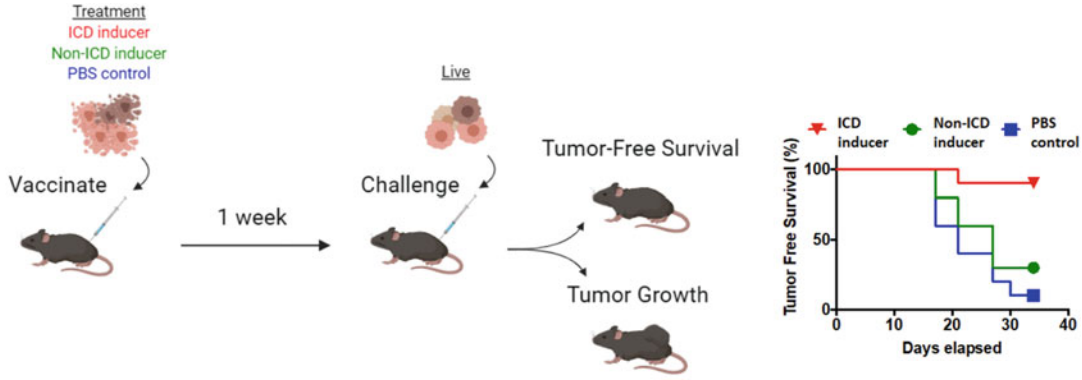

Fig. 2 In vivo vaccination assay to evaluate bona fide ICD. Vaccinate mice by injecting tumor cells, damaged via treatment of choice, subcutaneously into left flank. One week later, inject live tumor cells of the same kind, contralateral to the vaccination site. Mice that are injected with tumor cells dying via ICD will be protected from tumor development, while mice that are given PBS only or injected with tumor cells killed via nonICD inducer will succumb to tumor development

3.4 Vaccinating Mice with Treated Tumor Cells

1. Grow the murine tumor cell line of your interest in appropriate culture media. The number of cells to be grown depends on the number of mice that will be vaccinated and also on the number of cells that each mouse receives. Each experiment will contain control groups (*see* **Note 15** and **16**) and the experimental group (mice receiving tumor cells damaged with the treatment of your interest). At least 5 mice should be designated to each group in a single experiment.
2. Wash the cells gently and treat the cells as described above (*see* **Note 17**).
3. Set aside some cells for continuous cell culture. Cells will be required for challenge injection 7–10 days postvaccination.
4. After the cells have been treated and given sufficient time to be damaged, transfer the culture supernatant into an appropriate size centrifuge tube. Do not discard these culture media, as dying cells may be contained in the supernatant.
5. Harvest the adherent cells by adding warmed trypsin. Stop the reaction by adding equal volume of serum-containing media. After pipetting off the cells from the culture dish, transfer the cells into the same centrifuge with the culture media that was collected in prior step.
6. Centrifuge the tube at 300 × *g* for 5 min at RT. Decant the supernatant, and resuspend the cells with PBS. Repeat the wash two times.
7. Resuspend the cells with PBS and count the cells by trypan-blue exclusion method.

8. Centrifuge again and resuspend the cells in appropriate volume of PBS.
9. Prepare the mice for injection with the tumor cell vaccine. Both the left and right flank should be shaved (*see* **Note 18**).
10. Vaccinate mice on the left flank as described in Subheading 3.3.
11. Maintain the cells in culture for tumor challenge.

3.5 Challenging Mice with Live Tumor Cells

1. Tumor challenge is performed 7–10 days postvaccination.
2. Wash cells gently with PBS.
3. Harvest cells and wash two times with PBS.
4. Resuspend cells in PBS and count the cells using cytometer.
5. After centrifugation, bring up the cells in cold PBS at appropriate concentration (*see* **Note 19**).
6. Tumor challenge is performed on the right flank of the mice. If hair has regrown, reshave the mice (to perform the injection smoothly, shaving should be done 1 day before the challenge) (*see* **Note 18**).
7. Observe for tumor appearance on the challenge site. In mice that received no vaccination (PBS), tumors should grow on the challenge site, with close to 0% tumor-free mice by the end of the assay. If the treatment has induced ICD, large portion of the mice should be tumor-free (50–100%) by the end of the assay. While tumor-free survival is the ultimate read-out, tumor growth kinetics (size and speed) or the overall survival can also be measured for evaluation.

4 Notes

1. For a tumor cell line with C56BL/6 background, the same C56BL/6 mice should be used (i.e., when using a B16 melanoma cell line, use a C56BL/6. When using a CT26 colon cancer cell line, use BALB/c).
2. Female mice are preferable, as there are less problematic issues during the housing (i.e., fighting and biting within the cage). Age at which mice are used may affect the immune response, and so it should be kept consistent between the experiments conducted. We recommend the vaccination starting around 6–8 weeks age.
3. For 8-MOP UVA treatment, harvested cells are first incubated in FBS or FBS containing media for 20 min at 37 °C in the presence of 8-MOP. 8-MOP is used at 200 ng/ml. Subsequently, cells are transferred into a standard 12-well tissue culture plate and then irradiated with UVA dosage ranging

from 0.5 J/cm^2 to 8 J/cm^2. Dosage required to induce sufficient cell death will vary depending on cell line. With B16 murine melanoma cells, increase in apoptosis becomes recognizable 24 h post 8-MOP UVA treatment when irradiated with 4 J/cm^2 UVA, which gradually increments over time, and a majority of cells will die within 96 h. This dosage is optimal in inducing ICD in B16 melanoma cells.)

4. Adjust number of cells putting into a well, depending on the size of the well. If certain degree of cell growth is expected even after the treatment, adjust the number of cells to put back so that the cells will not over grow in the returned well.
5. After treatment, dying cells may start to detach from the plate. It is crucial to collect these dying cells for evaluating cell viability and also for downstream functional assays.
6. Although trypan blue exclusion is a crude method to evaluate cell viability, the simplicity of the method may be very attractive for initial screening.
7. When treating B16 melanoma cells with 8-MOP UVA, sufficient clonogenic cell death can be achieved with UVA irradiation ranging between 1 J/cm^2 and 4 J/cm^2. However, for rapid apoptotic cell death, higher UVA irradiation (8 J/cm^2 or more) is required. Of note, higher treatment dose may lead to insufficient ICD induction, and therefore, exploration of minimal dosage required to "kill" the cells may become essential for successful functional assays.
8. Fast growing cell line will form sufficient number of colonies even in low density. In our hands, B16 melanoma cell line plated in a 6-well plate at cell density of 100 cells per well develops 90–95 colonies on average. Cell lines that are not as vigorous may require smaller surface area and/or larger initial seeding number.
9. Only count colonies that have sufficient size. A sufficient sized colony should be composed of more than 50 cells.
10. Surviving fraction for 8-MOP UVA treatment described above is less than 0.1. In certain treatment such as 8-MOP UVA, dosage resulting in significant clonogenic cell death may be considerably lower than dosage required to induce strong apoptosis within 24–48 h. If such is the case, a dosage ranging from minimal amount required for clonogenic cell death to maximal amount leading to strong apoptotic cell death within 24–48 h should be tested for the in vivo assay described below.
11. Over-treating the tumor cells with higher dosage may negatively impact the immunogenicity of a dying tumor cell in certain treatment modality. Therefore, evaluating varying treatment dosages ranging from the minimal dosage is essential [9, 23].

12. Since the actual minimal dosage required in the actual in vivo assay may be less or more than the baseline dosage determined in the in vitro assay, we suggest including 25%, 50%, and 200% of the baseline dosage.
13. For treatment such as psoralen UVA irradiation, cells can be injected into mice right after the irradiation without further incubation in the flask.
14. When injecting the same material into several cages, aliquoting sufficient amount of cells evenly into 1.5 ml tubes, with each tube containing enough amount to inject mice in single cage, can reduce intercage variability.
15. Ideally, you should prepare (1) a control group where mice receive PBS instead of tumor cell vaccination, (2) a negative control group where mice receive tumor cells that were damaged via non-ICD method, and (3) a positive control group where tumor cells were damaged via ICD method.
16. Depending on certain experimental settings, the same ICD or nonICD treatment may demonstrate some degree of difference in the outcome. For example, mitomycin C, which is generally regarded as a nonICD inducing reagent, may in some setting show partial immune-protection. There may be varying immune-protective effect depending on the dosage or the intensity of the treatment, and therefore, running parallel groups using cells treated in varying treatment dosage is advised to optimize the experiment.
17. When treating cells with repeat freeze thaw cycle, make sure that cells are injected into the mice with the solution of which the cells were treated in. In other words, if 10 mice are planned for injection and each mouse receives 1×10^6 cells in 100 μl volume, bring up 10×10^6 cells in 1 ml of PBS (it is always better to prepare excess cells for vaccination, and so ideally, bring up $12–13 \times 10^6$ cells in 1.2–1.3 ml of PBS) and then render them to freeze thaw cycles (2–3 min in ethanol or methanol on dry ice and 2–3 min in 37 °C water bath, repeat 3 times). Do not centrifuge after the treatment. Inject 100 μl of the freeze-thawed cells per mouse, so that the cells are injected along with any cell debris that may be contained in the PBS.
18. Mice shaved at age 7–8 weeks will most likely not regrow hair for 1–2 months, and so shaving is generally required to be done once.
19. Amount of cells used for challenge injection can vary depending on the cell line used and also on the age of mice. We advise you to conduct a preliminary tumor kinetics study to figure out the optimal amount of cells required in the assay. Ideally, all mice should grow tumors, and no spontaneous regression should occur. As reference, in our hands, B16 murine

melanoma cell line injected subcutaneously into 6–7 week old mice at 2×10^5 cells results in tumor appearance 1–2 weeks postinjection and grows to significant size by 4 weeks.

References

1. Casares N, Pequignot MO, Tesniere A, Ghiringhelli F, Roux S, Chaput N, Schmitt E, Hamai A, Hervas-Stubbs S, Obeid M, Coutant F, Metivier D, Pichard E, Aucouturier P, Pierron G, Garrido C, Zitvogel L, Kroemer G (2005) Caspase-dependent immunogenicity of doxorubicin-induced tumor cell death. J Exp Med 202 (12):1691–1701. https://doi.org/10.1084/jem.20050915
2. Tesniere A, Schlemmer F, Boige V, Kepp O, Martins I, Ghiringhelli F, Aymeric L, Michaud M, Apetoh L, Barault L, Mendiboure J, Pignon JP, Jooste V, van Endert P, Ducreux M, Zitvogel L, Piard F, Kroemer G (2010) Immunogenic death of colon cancer cells treated with oxaliplatin. Oncogene 29(4):482–491. https://doi.org/10.1038/onc.2009.356
3. Pozzi C, Cuomo A, Spadoni I, Magni E, Silvola A, Conte A, Sigismund S, Ravenda PS, Bonaldi T, Zampino MG, Cancelliere C, Di Fiore PP, Bardelli A, Penna G, Rescigno M (2016) The EGFR-specific antibody cetuximab combined with chemotherapy triggers immunogenic cell death. Nat Med 22(6):624–631. https://doi.org/10.1038/nm.4078
4. Spisek R, Charalambous A, Mazumder A, Vesole DH, Jagannath S, Dhodapkar MV (2007) Bortezomib enhances dendritic cell (DC)-mediated induction of immunity to human myeloma via exposure of cell surface heat shock protein 90 on dying tumor cells: therapeutic implications. Blood 109 (11):4839–4845. https://doi.org/10.1182/blood-2006-10-054221
5. Donnelly OG, Errington-Mais F, Steele L, Hadac E, Jennings V, Scott K, Peach H, Phillips RM, Bond J, Pandha H, Harrington K, Vile R, Russell S, Selby P, Melcher AA (2013) Measles virus causes immunogenic cell death in human melanoma. Gene Ther 20(1):7–15. https://doi.org/10.1038/gt.2011.205
6. Frey B, Rubner Y, Wunderlich R, Weiss EM, Pockley AG, Fietkau R, Gaipl US (2012) Induction of abscopal anti-tumor immunity and immunogenic tumor cell death by ionizing irradiation - implications for cancer therapies. Curr Med Chem 19(12):1751–1764. https://doi.org/10.2174/092986712800099811
7. Garg AD, Krysko DV, Vandenabeele P, Agostinis P (2012) Hypericin-based photodynamic therapy induces surface exposure of damage-associated molecular patterns like HSP70 and calreticulin. Cancer Immunol Immunother 61 (2):215–221. https://doi.org/10.1007/s00262-011-1184-2
8. Ogawa M, Tomita Y, Nakamura Y, Lee MJ, Lee S, Tomita S, Nagaya T, Sato K, Yamauchi T, Iwai H, Kumar A, Haystead T, Shroff H, Choyke PL, Trepel JB, Kobayashi H (2017) Immunogenic cancer cell death selectively induced by near infrared photoimmunotherapy initiates host tumor immunity. Oncotarget 8(6):10425–10436. https://doi.org/10.18632/oncotarget.14425
9. Tatsuno K, Yamazaki T, Hanlon D, Han P, Robinson E, Sobolev O, Yurter A, Rivera-Molina F, Arshad N, Edelson RL, Galluzzi L (2019) Extracorporeal photochemotherapy induces bona fide immunogenic cell death. Cell Death Dis 10(8):578. https://doi.org/10.1038/s41419-019-1819-3
10. Pfirschke C, Engblom C, Rickelt S, Cortez-Retamozo V, Garris C, Pucci F, Yamazaki T, Poirier-Colame V, Newton A, Redouane Y, Lin YJ, Wojtkiewicz G, Iwamoto Y, Mino-Kenudson M, Huynh TG, Hynes RO, Freeman GJ, Kroemer G, Zitvogel L, Weissleder R, Pittet MJ (2016) Immunogenic chemotherapy sensitizes tumors to checkpoint blockade therapy. Immunity 44(2):343–354. https://doi.org/10.1016/j.immuni.2015.11.024
11. Ventura A, Vassall A, Robinson E, Filler R, Hanlon D, Meeth K, Ezaldein H, Girardi M, Sobolev O, Bosenberg MW, Edelson RL (2018) Extracorporeal photochemotherapy drives monocyte-to-dendritic cell maturation to induce anticancer immunity. Cancer Res 78 (14):4045–4058. https://doi.org/10.1158/0008-5472.CAN-18-0171
12. Obeid M, Tesniere A, Ghiringhelli F, Fimia GM, Apetoh L, Perfettini JL, Castedo M, Mignot G, Panaretakis T, Casares N, Metivier D, Larochette N, van Endert P, Ciccosanti F, Piacentini M, Zitvogel L, Kroemer G (2007) Calreticulin exposure dictates the immunogenicity of cancer cell death. Nat Med 13(1):54–61. https://doi.org/10.1038/nm1523

13. Garg AD, Galluzzi L, Apetoh L, Baert T, Birge RB, Bravo-San Pedro JM, Breckpot K, Brough D, Chaurio R, Cirone M, Coosemans A, Coulie PG, De Ruysscher D, Dini L, de Witte P, Dudek-Peric AM, Faggioni A, Fucikova J, Gaipl US, Golab J, Gougeon ML, Hamblin MR, Hemminki A, Herrmann M, Hodge JW, Kepp O, Kroemer G, Krysko DV, Land WG, Madeo F, Manfredi AA, Mattarollo SR, Maueroder C, Merendino N, Multhoff G, Pabst T, Ricci JE, Riganti C, Romano E, Rufo N, Smyth MJ, Sonnemann J, Spisek R, Stagg J, Vacchelli E, Vandenabeele P, Vandenberk L, Van den Eynde BJ, Van Gool S, Velotti F, Zitvogel L, Agostinis P (2015) Molecular and translational classifications of DAMPs in immunogenic cell death. Front Immunol 6:588. https://doi.org/10.3389/fimmu.2015.00588

14. Panaretakis T, Kepp O, Brockmeier U, Tesniere A, Bjorklund AC, Chapman DC, Durchschlag M, Joza N, Pierron G, van Endert P, Yuan J, Zitvogel L, Madeo F, Williams DB, Kroemer G (2009) Mechanisms of pre-apoptotic calreticulin exposure in immunogenic cell death. EMBO J 28(5):578–590. https://doi.org/10.1038/emboj.2009.1

15. Gardai SJ, McPhillips KA, Frasch SC, Janssen WJ, Starefeldt A, Murphy-Ullrich JE, Bratton DL, Oldenborg PA, Michalak M, Henson PM (2005) Cell-surface calreticulin initiates clearance of viable or apoptotic cells through transactivation of LRP on the phagocyte. Cell 123 (2):321–334. https://doi.org/10.1016/j.cell.2005.08.032

16. Elliott MR, Chekeni FB, Trampont PC, Lazarowski ER, Kadl A, Walk SF, Park D, Woodson RI, Ostankovich M, Sharma P, Lysiak JJ, Harden TK, Leitinger N, Ravichandran KS (2009) Nucleotides released by apoptotic cells act as a find-me signal to promote phagocytic clearance. Nature 461(7261):282–286. https://doi.org/10.1038/nature08296

17. Ghiringhelli F, Apetoh L, Tesniere A, Aymeric L, Ma Y, Ortiz C, Vermaelen K, Panaretakis T, Mignot G, Ullrich E, Perfettini JL, Schlemmer F, Tasdemir E, Uhl M, Genin P, Civas A, Ryffel B, Kanellopoulos J, Tschopp J, Andre F, Lidereau R, McLaughlin NM, Haynes NM, Smyth MJ, Kroemer G, Zitvogel L (2009) Activation of the NLRP3 inflammasome in dendritic cells induces IL-1beta-dependent adaptive immunity against tumors. Nat Med 15(10):1170–1178. https://doi.org/10.1038/nm.2028

18. Apetoh L, Ghiringhelli F, Tesniere A, Obeid M, Ortiz C, Criollo A, Mignot G, Maiuri MC, Ullrich E, Saulnier P, Yang H, Amigorena S, Ryffel B, Barrat FJ, Saftig P, Levi F, Lidereau R, Nogues C, Mira JP, Chompret A, Joulin V, Clavel-Chapelon F, Bourhis J, Andre F, Delaloge S, Tursz T, Kroemer G, Zitvogel L (2007) Toll-like receptor 4-dependent contribution of the immune system to anticancer chemotherapy and radiotherapy. Nat Med 13(9):1050–1059. https://doi.org/10.1038/nm1622

19. Sims GP, Rowe DC, Rietdijk ST, Herbst R, Coyle AJ (2010) HMGB1 and RAGE in inflammation and cancer. Annu Rev Immunol 28:367–388. https://doi.org/10.1146/annurev.immunol.021908.132603

20. Sistigu A, Yamazaki T, Vacchelli E, Chaba K, Enot DP, Adam J, Vitale I, Goubar A, Baracco EE, Remedios C, Fend L, Hannani D, Aymeric L, Ma Y, Niso-Santano M, Kepp O, Schultze JL, Tuting T, Belardelli F, Bracci L, La Sorsa V, Ziccheddu G, Sestili P, Urbani F, Delorenzi M, Lacroix-Triki M, Quidville V, Conforti R, Spano JP, Pusztai L, Poirier-Colame V, Delaloge S, Penault-Llorca F, Ladoire S, Arnould L, Cyrta J, Dessoliers MC, Eggermont A, Bianchi ME, Pittet M, Engblom C, Pfirschke C, Preville X, Uze G, Schreiber RD, Chow MT, Smyth MJ, Proietti E, Andre F, Kroemer G, Zitvogel L (2014) Cancer cell-autonomous contribution of type I interferon signaling to the efficacy of chemotherapy. Nat Med 20(11):1301–1309. https://doi.org/10.1038/nm.3708

21. Kepp O, Senovilla L, Vitale I, Vacchelli E, Adjemian S, Agostinis P, Apetoh L, Aranda F, Barnaba V, Bloy N, Bracci L, Breckpot K, Brough D, Buque A, Castro MG, Cirone M, Colombo MI, Cremer I, Demaria S, Dini L, Eliopoulos AG, Faggioni A, Formenti SC, Fucikova J, Gabriele L, Gaipl US, Galon J, Garg A, Ghiringhelli F, Giese NA, Guo ZS, Hemminki A, Herrmann M, Hodge JW, Holdenrieder S, Honeychurch J, Hu HM, Huang X, Illidge TM, Kono K, Korbelik M, Krysko DV, Loi S, Lowenstein PR, Lugli E, Ma Y, Madeo F, Manfredi AA, Martins I, Mavilio D, Menger L, Merendino N, Michaud M, Mignot G, Mossman KL, Multhoff G, Oehler R, Palombo F, Panaretakis T, Pol J, Proietti E, Ricci JE, Riganti C, Rovere-Querini P, Rubartelli A, Sistigu A, Smyth MJ, Sonnemann J, Spisek R, Stagg J, Sukkurwala AQ, Tartour E, Thorburn A, Thorne SH, Vandenabeele P, Velotti F, Workenhe ST, Yang H, Zong WX, Zitvogel L, Kroemer G, Galluzzi L (2014) Consensus guidelines for the detection of immunogenic cell death. Onco Targets Ther 3 (9):e955691. https://doi.org/10.4161/21624011.2014.955691

22. Menger L, Vacchelli E, Adjemian S, Martins I, Ma Y, Shen S, Yamazaki T, Sukkurwala AQ, Michaud M, Mignot G, Schlemmer F, Sulpice E, Locher C, Gidrol X, Ghiringhelli F, Modjtahedi N, Galluzzi L, Andre F, Zitvogel L, Kepp O, Kroemer G (2012) Cardiac glycosides exert anticancer effects by inducing immunogenic cell death. Sci Transl Med 4(143):143ra199. https://doi.org/10.1126/scitranslmed.3003807

23. Vanpouille-Box C, Alard A, Aryankalayil MJ, Sarfraz Y, Diamond JM, Schneider RJ, Inghirami G, Coleman CN, Formenti SC, Demaria S (2017) DNA exonuclease Trex1 regulates radiotherapy-induced tumour immunogenicity. Nat Commun 8:15618. https://doi.org/10.1038/ncomms15618

24. Rafehi H, Orlowski C, Georgiadis GT, Ververis K, El-Osta A, Karagiannis TC (2011) Clonogenic assay: adherent cells. J Vis Exp 49:2573. https://doi.org/10.3791/2573

Chapter 16

A Luminescence Assay to Quantify Cell Viability in Real Time

Peter Hofsteen, Natasha Karassina, James J. Cali, and Jolanta Vidugiriene

Abstract

Comprehensive understanding of cellular responses to changes in the cellular environment or by drug treatment requires time-dependent analysis ranging from hours to several days. Here, we describe a sensitive, nonlytic live-cell assay that allows continuous or 'real-time' monitoring of cell viability, growth, and cytotoxicity over an extended period of time. We illustrate the use of the assay for small drug molecule and antibody-dependent cytotoxicity studies using cancer cells in 384-well plates. We show that the ability to measure changes in live cells over time provides instantaneous information on the biological status of the cells, information about the mode of action of the drug, and offers an added advantage of preserving the cells for multiplexing with downstream applications.

Key words Real-time cell viability assay, Continuous viability measurements, Time-dependent cytotoxicity, Live cell viability assay, Antibody-dependent cytotoxicity, ADC

1 Introduction

1.1 Assay Principal and Background

RealTime-Glo™ MT Cell Viability Assay is a nonlytic in vitro bioluminescence method that quantifies viable cells by measuring the reducing potential of living cells (Fig. 1a). This method utilizes a prosubstrate (MT Cell Viability Substrate) that enters living cells where it is reduced to an active luciferase substrate that is released from the cell into the culture medium. The converted substrate rapidly reacts with the small, bright, and highly stable NanoLuc Luciferase enzyme to generate a quantitative luminescence signal [1–4].

Unlike other assays that utilize the reducing potential of the cell (e.g., MTT and AlamarBlue), this assay is unique in that it rapidly measures changes in viability in real time over the course of hours to days from the same sample. This is achieved through slow prosubstrate conversion by viable cells only and by rapid decrease in signal upon cell death. The converted substrate is rapidly consumed by reaction with NanoLuc luciferase, and so it does not accumulate

Ayesha B. Alvero and Gil G. Mor (eds.), *Detection of Cell Death Mechanisms: Methods and Protocols*, Methods in Molecular Biology, vol. 2255, https://doi.org/10.1007/978-1-0716-1162-3_16,

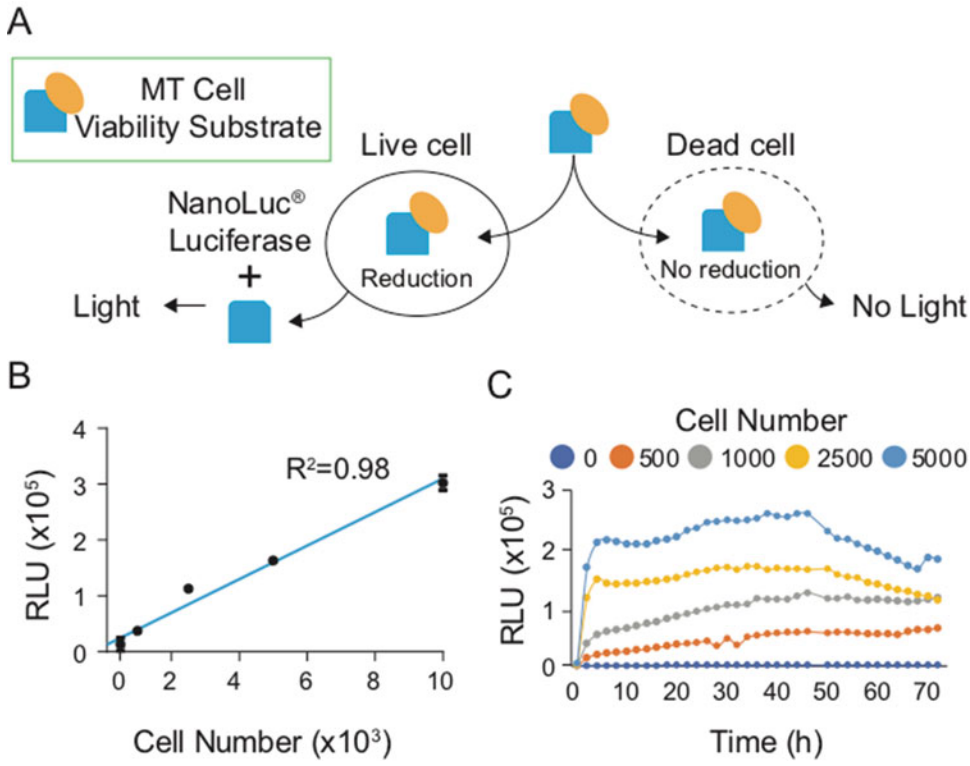

Fig. 1 Determining assay conditions for each cell line is critical for optimal assay performance. (**a**) Schematic of assay principle. A protected MT cell viability substrate (prosubstrate) enters live cells where it is reduced to an active substrate that reacts with NanoLuc Luciferase to generate luminescence. The substrate is not reduced by dead cells. (**b**) Assay linearity for end point assays. The detection reagents are added at the end of the treatment, and luminescence is read within 2 h after addition. The assay is linear from 500 to 10,000 cell per well. (**c**) Assay linearity for continuous read. The luminescence signals were measured over a 3-day time course. At the 73-h timepoint, the signals from 500 to 1000 cells per well were still increasing, indicating continuous cell growth and sustained assay performance. At higher cell densities, signals began to level off and then decrease at earlier timepoints, indicating the loss of assay linearity due to the prosubstrate depletion. SK-BR-3 cells were plated at indicated cell densities in the presence of RealTime-Glo reagents, and measurements were taken at 2 h (**b**: mean values, $N = 3$) or every 2 h (**c**: mean values, $N = 3$) for 3 days. *RLU* relative light units, *h* hours

over time. Therefore, the signal depends on the viable cells present at the time it is measured and this enables real-time viability monitoring.

The MT RealTime-Glo reagents are added directly to cells in culture. Upon addition of the reagents, the luminescence signal rapidly increases until equilibrium between substrate conversion and light generation by NanoLuc is achieved (Fig. 1c). The signal is proportional to the number of live cells (Fig. 1b, c). After luminescence is read, the reagents can be removed and live cells can be used for other end point assays, including protein, DNA and RNA analysis, or other cytotoxicity assays. The assay duration is

generally limited to 3 days as substrate availability eventually declines. For longer-term experiments (weeks to months), the reagents can be added, read, and removed multiple times with minimal reagent occupancy during the course of the experiment [5].

1.2 Identifying Optimal Cell Densities for Continuous Cell Viability Quantification

When using the assay for continuous time-dependent toxicity studies, the most important consideration is prosubstrate availability during the entire length of the experiment. This is determined not only by cell density but also by the metabolic activity of the cells because the substrate conversion rate is faster with highly active versus less metabolically active cells. As shown in Fig. 1c, the human breast cancer cell line (SK-BR-3), plated at 5000 cells per well, continue to grow and the luminescence signal continues to increase until about 48 h when the prosubstrate is depleted and luminescence starts to decline. The length of the experiment can be extended by using fewer cells. For example, with 1000 cells per well, no decrease in signal was measured for up to 73 h (Fig. 1c). While less than 1000 SK-BR-3 cells per well allow extended time-dependent toxicity measurements, different starting cell numbers may be optimal for other cell types. Thus, it is critical to optimize for each cell type to identify the linear range over the duration of the experiment.

1.3 Quantifying Cell Viability Over Time Following Drug Treatments

This assay can be used to understand drug efficacy, potency, and onset of action. In Fig. 2, SK-BR-3 cells were treated with cytotoxic drugs that induce cell death by either inhibiting topoisomerase II (doxorubicin [6]) or histone deacetylase (panobinostat [7]), while cell viability was being measured in real time over 3 days. In non-treated control cells, the luminescence signal continued to increase over time indicative of cell growth. In contrast, either doxorubicin (Fig. 2a–c) or panobinostat (Fig. 2d–f) caused the luminescence signal to decrease in a time- and concentration-dependent manner. Variations in drug potency and efficacy can be ascertained by calculating the half maximal effective concentration (EC_{50}) and percent viability over time (Fig. 2b, c, e, f), respectively. The EC_{50} value of doxorubicin continually decreased each day over the assay duration (Fig. 2c), whereas the EC_{50} value of panobinostat decreased until 47 h and then remained unchanged (Fig. 2f). These data demonstrate the utility of the assay for understanding onset of action and changes in cell viability over time, which may otherwise be missed with single-point endpoint assays.

Cells were also treated with varying concentrations of Kadcyla (trastuzumab-DM1), and cell viability was quantified over 3 days (Fig. 3). Kadcyla is an antibody-drug conjugate that inhibits cancer cell proliferation [8]. As above, the relative light units (RLUs) from nontreated SK-BR-3 cells continually increased over the duration of the assay. Cells treated with Kadcyla did not elicit marked

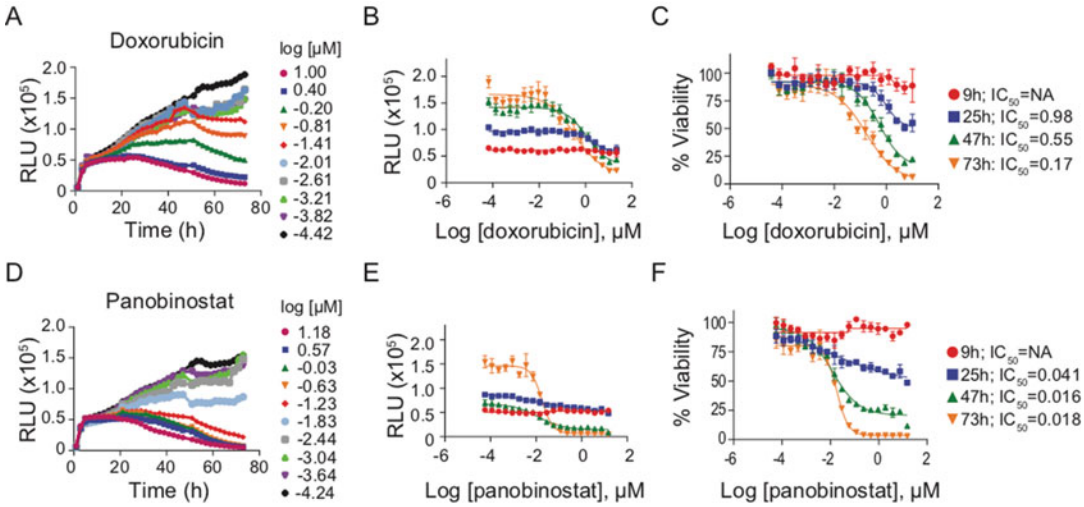

Fig. 2 Kinetic measurements of cell viability following treatment with doxorubicin (**a**–**c**) or panobinostat (**d**–**f**). Cells were plated at 1000 cells per well in the presence of RealTime-Glo reagents and indicated drug concentrations in a 384-well assay plate ($N = 3$ per drug concentration). The assay plate was placed into the Spark® multimode microplate reader (Tecan) at 37 °C with 5% CO_2, and measurements were taken every 2 h over 3 days. (**a**, **d**) Mean relative light units (RLU) are plotted for doxorubicin (**a**) or panobinostat (**d**) treatment, half maximal inhibitory concentration (EC_{50}) values (**b**, **e**), and percent changes in cell viability compared to control (**c**, **f**) were calculated at 9, 25, 47, and 73 h. Data were fitted to a 4-parameter logistic curve, and EC_{50} was calculated using GraphPad Prism® software. *h* hour

responses in luminescence signal over the first 48 hours (Fig. 3a). The RLUs continually increased in both nontreated and Kadcyla-treated cells for approximately 48 h. After 48 h, the RLUs plateaued and gradually decreased as a result of Kadcyla treatment in a concentration-dependent manner (Fig. 3a). These data are consistent with Kadcyla impeding cell growth rather than directly inducing cell death.

Some drugs, including Kadcyla, have delayed onset of action that requires longer assay duration (>72 h). For longer-term measurements, RealTime-Glo reagents can be added at later timepoints. An example of this is shown in Fig. 3b. Cells were incubated with Kadcyla for approximately 2 days without RealTime-Glo reagents. Following addition of the detection reagents, cell viability was continuously measured for an additional 3 days. Initial measurements between 48 and 72 h denote concentration-dependent differences in RLUs (Fig. 3b) that closely resemble those taken at similar time points in Fig. 3a. Furthermore, stark differences were apparent after 80 h of drug treatment (Fig. 3b) as RLUs gradually diminished in cells responsive to Kadcyla.

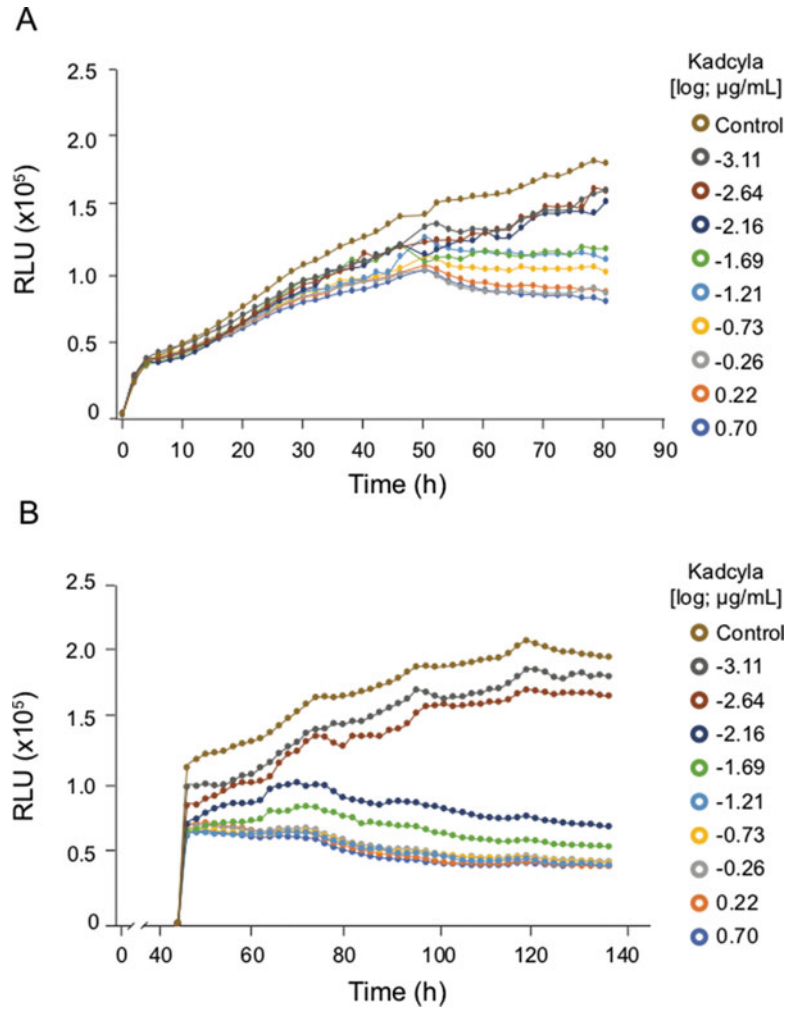

Fig. 3 Monitoring Kadcyla effect on SK-BR-3 cells in real time. SK-BR-3 cells were plated at 1000 cells per well in the presence of indicated concentrations of Kadcyla. RealTime-Glo reagents were added at cell plating (**a**) or 2 days after cell plating (**b**), and luminescence was read at indicated times. Shown are mean values representative of $N = 4$ per drug concentration. *RLU* relative light units, *h* hour

2 Materials

The materials and methods described in this chapter outline a general protocol for quantifying cell viability using the RealTime-Glo MT Cell Viability assay system. The examples shown are generated using SK-BR-3 cancer cells that are treated with titrations of panobinostat, doxorubicin, and Kadcyla in 384-well white-walled assay plates under optimized conditions.

2.1 Equipment

1. Single- and multi-channel pipettors and reagent reservoirs.
2. White, opaque-walled 384-well tissue culture treated assay plates.
3. 37 °C water bath.
4. Plate-reading luminometer capable of reading 384-well plates with or without temperature and gas control.

2.2 Cells and Reagents

1. SK-BR-3: human breast cancer cell line.
2. SK-BR-3 growth medium: McCoy's 5A Modified Medium +10% fetal bovine serum (FBS).
3. RealTime-Glo™ MT Cell Viability Assay (Promega).
4. Panobinostat: 10 mM stock solution.
5. Doxorubicin: 50 mM stock solution.
6. Kadcyla: 5 mg/mL stock solution.

3 Methods

The methods described below detail how to (1) identify the optimal cell density for the duration of the assay and how to (2) set up experiments for continuous monitoring of cell viability during drug treatments over time. All experimental procedures use sterile tissue culture treated equipment and reagents. Standard cell culture procedures are used for cell growth and preparation and are not described in detail.

3.1 Determining Optimal Cell Density for Assay Duration

As shown in Fig. 1c, it is critical to identify a cell density that is within the assay linear range that does not deplete substrate availability for the entire experimental duration. It is required to conduct a cell titration experiment for each cell type that spans the intended experimental duration prior to setting up a toxicity study. For example, here, we were interested in monitoring real-time changes in viability for an extended period of time (>70 h) with drug treatments using SK-BR-3 cells. Therefore, we first determined the cell density that is compatible with such measurements.

1. Remove the MT Cell Viability Substrate and NanoLuc Luciferase (RealTime-Glo reagent) from −20 °C and allow to equilibrate to 37 °C in a water bath (*see* **Note 1**).
2. Calculate the number of cells required for plating cell titration. Set up cell titration to cover a wide range of cell densities (*see* **Note 2**).
3. Plate the cells at various cell densities in an assay plate (*see* **Note 3**).

4. Prepare a 2× solution of RealTime-Glo reagents and add an equal volume to each well of cells (*see* **Note 4**).
5. Place the plate into a cell culture incubator or multimode reader equipped with temperature and gas control and culture the cells at 37 °C with 5% CO_2 (*see* **Note 5**).
6. When using a multimode reader with a gas control module, set up the program for reading luminescence every 1–2 h (*see* **Note 6**).
7. If the cells are cultured in a tissue culture incubator, transfer the plate to the luminometer at the desired timepoints, read luminescence, and return the plate to the incubator immediately after the measurement (*see* **Note 7**).
8. Continue measuring luminescence for the desired time course (*see* **Note 8**).
9. To determine the linear range of cell densities, plot luminescence versus cell number and determine the range within the linear curve fit (*see* **Note 9**).

3.2 Real-Time Measurement of Cell Viability Following Drug Treatments

The protocol described below details how to set up real-time cytotoxicity studies in a 384-well plate using the RealTime-Glo™ MT Cell Viability Assay. Using the protocol described in Subheading 3.1, we observed that ≤1000 SK-RB-3 cells per 80 μl (12,500/ml) per well grew for at least 73 h and produced signals within the linear range of the assay (Fig. 1c). Therefore, these conditions are optimal for a time-dependent toxicity study.

1. Thaw RealTime-Glo reagents as described in Subheading 3.1, **step 1**.
2. Prepare the required amounts of cells at 12,500/ml in complete media.
3. Add RealTime-Glo reagents to the cell suspension to a final concentration of 2× for each reagent (*see* **Note 10**).
4. Dispense the desired volume of cells into assay plate.
5. Prepare 2× working stock of drug treatments (i.e., Doxorubicin, Panobinostat, or Kadcyla as shown in Figs. 2 and 3) in cell culture medium and add equal volumes to the cells (*see* **Note 11**).
6. Follow **steps 5–8** described in Subheading 3.1.
7. Analyze the data by calculating half-maximal effective concentrations (EC50) and maximum response. The data can be calculated at multiple time points from the same sample wells (*see* **Note 12**).

4 Notes

1. It is important to prewarm RealTime-Glo reagents at 37 °C. If the reagents are not prewarmed properly, it may result in significant errors when handling reagents and increased risk of MT Cell Viability Substrate precipitation when diluted into media.
2. The rate of prosubstrate consumption differs significantly between cell types due to the differences in their metabolic activity. We recommend testing a wide range of cell densities, for example, from 2.5 K to 12.5 K per ml to determine the optimal density for your experimental set-up. In general, if the RealTime-Glo reagents are added and luminescence is read within several hours, the assay is linear from few cells to thousands of cells per well. If the reagents are present in the cell culture medium for an extended period of time, the cells will continually consume prosubstrate over time until the linear range decreases. For experiments ranging from 48–72 h, the optimal cell density is typically from 200–1000 cells/well for most cell types.
3. When using 384-well assay plates, we recommend using a final volume per well $\geq$50 µl. For the experiment in Fig. 1, cells were plated in 40 µl and an additional 40 µl of RealTime-Glo reagents diluted in cell culture medium were added (80 µl total). We do not recommend using the two outer rows or columns due to increased evaporation (edge effects). Instead, adding medium to all nonexperimental wells will help to control evaporation.
4. Both MT Cell Viability Substrate and NanoLuc Luciferase are formulated as 1000× solutions. The reagents are diluted in cell culture medium prewarmed to 37 °C. To prepare 1 ml of 2× Realtime-Glo reagent, add 2 µl of MT cell Viability Substrate and 2 µl of NanoLuc enzyme to 996 µl of cell culture medium. The RealTime-Glo substrate can be concentrated in cell culture medium up to 5× without precipitation. Mix well with a vortex mixer and check for precipitation. Do not prepare a stock concentration in excess of 5×.
5. When using a temperature- and gas-controlled multimode reader, leave the assay plate lid on during continuous measurements to avoid evaporation during the assay duration.
6. Reading luminescence every 1–2 h with an integration time of 0.25 s per well is a guideline for 48–72 h experiments. More frequent reads can be set up for shorter experiments or at the beginning of the experiment if needed. Longer integration times will improve data quality; however, when the plate is read multiple times, removal of the lid and longer reads will

increase the evaporation rate and the possibility of contamination. Reading with the lid on is another option to minimize evaporation and contamination, but this increases cross talk between the wells.

7. The NanoLuc reaction and light intensity are affected by temperature. When cells are cultured in a tissue culture incubator and transferred to the plate reader at each time point, care should be taken for temperature control. To minimize temperature changes, certain plate-reading luminometers can be set at 37 °C and we recommend reading the plate immediately after removing it from the incubator and placing it back after the read. If variations in relative light units (RLUs) between each measurement are observed due to variations in temperature, analyzing the data as percent change of untreated control will normalize the data for each time point.
8. After addition of RealTime-Glo detection reagents, the plate can be read at any timepoint. However, if the readings are not done using temperature- and gas-controlled multimode readers, we recommend keeping the plate in the tissue culture incubator for at least 30 min before reading to allow the system to reach equilibrium between prosubstrate conversion and light generation.
9. The linear range of the assay will vary at different timepoints. The cell density for a linear assay needs to be identified over the desired experimental time course (e.g., 8 h, 24 h, and 72 h). As shown in Fig. 1c, it is important to pick a density of proliferating cells that increases RLUs in a linear fashion over the time course of the assay.
10. RealTime-Glo detection reagents can be added directly to cells in suspension before dispensing. For data shown in Figs. 2 and 3a, the cells were collected and diluted into full medium at required cell density, and Realtime-Glo detection reagents were added at 2× final concentration. 40 μl of cells was dispensed into a 384-well assay plate. All the treatments were set up in triplicate. However, the Realtime-Glo detection reagents can be added to the cells at any time of the treatment. For example, in Fig. 3b, the cells were dispensed without RealTime-Glo detection reagents and the detection reagents were added after 48 h of drug treatment. To accommodate the maximum volume of 80 μl for 384-well plates, the cells were plated at 30 μl per well and 30 μl of increasing concentrations of Kadcyla prepared in complete medium were added. After 48 h of incubation, 20 μl of 4× RealTime-Glo reagents diluted in the same medium was added.
11. A zero-drug vehicle control should be included as one of the titration points for measuring basal cell viability.

12. In order to directly compare multiple time points, it may be useful to calculate the percent change in viability as shown in Fig. 2c, f by calculating [(sample/vehicle control) × 100]. This will allow for direct comparisons between numerous time-points and normalize any experimental artifacts due to swings in temperature.

References

1. Duellman SJ, Zhou W, Meisenheimer P, Vidugiris G, Cali JJ, Gautam P, Wennerberg K, Vidugiriene J (2015) Bioluminescent, nonlytic, real-time cell viability assay and use in inhibitor screening. Assay Drug Dev Technol 13 (8):456–465. https://doi.org/10.1089/adt.2015.669
2. England CG, Ehlerding EB, Cai W (2016) NanoLuc: a small luciferase is brightening up the field of bioluminescence. Bioconjug Chem 27(5):1175–1187. https://doi.org/10.1021/acs.bioconjchem.6b00112
3. Hall MP, Unch J, Binkowski BF, Valley MP, Butler BL, Wood MG, Otto P, Zimmerman K, Vidugiris G, Machleidt T, Robers MB, Benink HA, Eggers CT, Slater MR, Meisenheimer PL, Klaubert DH, Fan F, Encell LP, Wood KV (2012) Engineered luciferase reporter from a deep sea shrimp utilizing a novel imidazopyrazinone substrate. ACS Chem Biol 7 (11):1848–1857. https://doi.org/10.1021/cb3002478
4. Shimomura O, Masugi T, Johnson FH, Haneda Y (1978) Properties and reaction mechanism of the bioluminescence system of the deep-sea shrimp Oplophorus gracilorostris. Biochemistry 17(6):994–998. https://doi.org/10.1021/bi00599a008
5. Hata AN, Niederst MJ, Archibald HL, Gomez-Caraballo M, Siddiqui FM, Mulvey HE, Maruvka YE, Ji F, Bhang HE, Krishnamurthy Radhakrishna V, Siravegna G, Hu H, Raoof S, Lockerman E, Kalsy A, Lee D, Keating CL, Ruddy DA, Damon LJ, Crystal AS, Costa C, Piotrowska Z, Bardelli A, Iafrate AJ, Sadreyev RI, Stegmeier F, Getz G, Sequist LV, Faber AC, Engelman JA (2016) Tumor cells can follow distinct evolutionary paths to become resistant to epidermal growth factor receptor inhibition. Nat Med 22(3):262–269. https://doi.org/10.1038/nm.4040
6. Nitiss JL (2009) Targeting DNA topoisomerase II in cancer chemotherapy. Nat Rev Cancer 9 (5):338–350. https://doi.org/10.1038/nrc2607
7. Atadja P (2009) Development of the pan-DAC inhibitor panobinostat (LBH589): successes and challenges. Cancer Lett 280(2):233–241. https://doi.org/10.1016/j.canlet.2009.02.019
8. Barok M, Tanner M, Koninki K, Isola J (2011) Trastuzumab-DM1 causes tumour growth inhibition by mitotic catastrophe in trastuzumab-resistant breast cancer cells in vivo. Breast Cancer Res 13(2):R46. https://doi.org/10.1186/bcr2868

Chapter 17

Kinetic Measurement of Apoptosis and Immune Cell Killing Using Live-Cell Imaging and Analysis

Jill E. Granger and Daniel M. Appledorn

Abstract

The rapid, efficient detection of cell death is critical for characterizing the underlying biology of in vitro disease models and, in particular, immunotherapy products used for preclinical therapeutic research. Traditional endpoint assays are laborious to perform for mass screening of therapeutic candidates and may fail to fully capture the kinetics of events surrounding the initiation, duration, and mechanisms of cell death—important events that may affect translational relevance and impact therapeutic decision-making during development. Here, we describe simple, efficient methods to measure apoptosis and immune cell killing in both adherent and nonadherent cell populations using the Incucyte® Live-Cell Analysis system and associated nonperturbing reagents, cells, and protocols. Assays are performed in the user's own incubator with minimal disturbance and may be readily incorporated into existing workflows. Users may multiplex to maximize data collection from each sample. The integrated, user-friendly software does not require advanced technical training, enabling rapid analysis. Taken together, this method provides essential kinetic insight for greater understanding of cell death and the dynamic interactions between immune cells and their targets.

Key words Kinetic multiplex cell death assay, Apoptosis live-cell imaging, Immune cell killing

1 Introduction

Apoptosis, and immune cell killing assays, are widely used to monitor cell death in basic biology research and preclinical therapeutic development. Methods are commonly performed at a single endpoint, but key events along the experimental timeline, essential for biological understanding, may be missed. Here, we describe the use of the Incucyte® apoptosis assays and Incucyte® immune cell killing assays. These assays are easy to perform, using simple mix-and-read reagents for the real-time detection of apoptosis and cell killing in both adherent and nonadherent cell types. High-definition, phase-contrast images may also be generated, allowing examination of accompanying morphological changes throughout the cell death process.

Ayesha B. Alvero and Gil G. Mor (eds.), *Detection of Cell Death Mechanisms: Methods and Protocols*, Methods in Molecular Biology, vol. 2255, https://doi.org/10.1007/978-1-0716-1162-3_17,

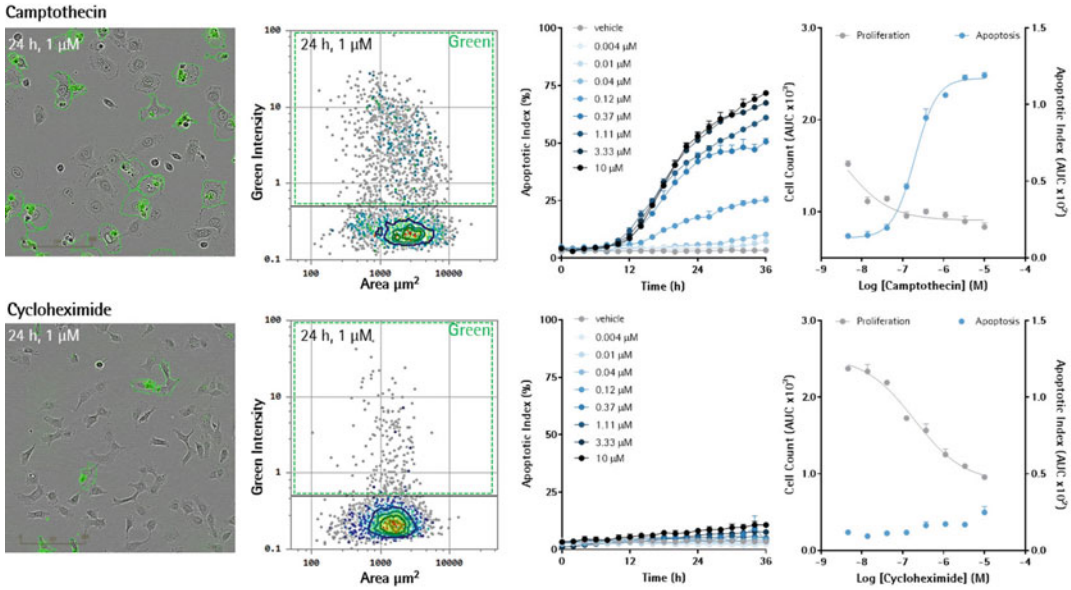

Fig. 1 Multiplex apoptosis measurements with live-cell label-free counting and quantification of time courses and concentration dependence of cytotoxicity and proliferation. Camptothecin (1 µM) or cycloheximide (1 µM)-treated HT1080 fibrosarcoma cells in the presence of the IncuCyte® Annexin V Green Reagent to detect apoptotic cells at 24 h (masking of dead cells shown). Classification plots to identify green (apoptotic) population (second column), time-course plots (third column), and concentration-response curves (forth column) show difference in effect of a cytotoxic and cytostatic compound

1.1 Kinetic Measurement of Apoptosis in Adherent and Nonadherent Cells

Apoptosis can lead to caspase-3 or caspase-7 activation. In these assays, investigators can use either Incucyte® Caspase-3/7 Green Apoptosis Reagent or Caspase-3/7 Red Apoptosis Reagent for detection of apoptosis. These inert, nonfluorescent (DEVD) substrates cross the cell membrane and are cleaved by activated caspase-3/7, releasing either a green or red DNA-binding fluorescent label, which is manifested by the appearance of fluorescently labeled nuclei within the cells.

The loss of plasma membrane phosphatidylserine (PS) symmetry is another indicator of apoptosis. Annexin V is a recombinant protein with both high affinity and selectivity for phosphatidylserine (PS) residues. The Incucyte® Annexin V reagents employ bright, photostable dyes that can emit either a red or green fluorescence signal when they bind to exposed phosphatidylserine in cells undergoing early apoptosis.

Both the Caspase-3/7 and Annexin V assays utilize mix-and-read reagents that do not require washing, fixing, or lifting for ease of use. The protocols can be performed in either 96- or 384-well formats, with a capacity as high as 6 × 384 well plates for screening at moderate throughput. They can also be combined with other Incucyte® reagents for multiplexing assays, such as proliferation with Nuclight® reagents or cytotoxicity with Cytotox® reagents,

labeled cell lines, as well as label-free detection of proliferation with Incucyte® Cell-By-Cell software. The Nuclight® regents are non-perturbing, cell permeable DNA stains that label nuclei for monitoring proliferation. The Cytotox reagents are nucleic acid dyes that are able to cross compromised, unhealthy cell plasma membranes, allowing the dye to enter and increase in fluorescence to quantify cell death. As shown in Fig. 1, Incucyte® apoptosis assays may be combined with Nuclight® or Cytotox® reagents for multiplexed, real-time measurements of apoptosis and cell proliferation, which can help provide important kinetic details of and insights into drug effects.

More information on Incucyte® Apoptosis Assays, including multiplexing capabilities, and reagents can be found at https://www.essenbioscience.com/en/applications/cell-health-viability/apoptosis/.

Link to apoptosis protocol at Essenbiosciences.com:

https://www.essenbioscience.com/media/uploads/files/8000-0492-F00%2D%2DIncucyte_Apoptosis_Assay_protocol.pdf

For answers to frequently asked questions about these apoptosis assays:

https://www.essenbioscience.com/en/applications/apoptosis-faq/

1.2 Kinetic Measurements of Immune Cell Killing in Adherent and Nonadherent Cells

Immunotherapy continues to evolve, incorporating a variety of approaches such as the development of immune checkpoint inhibitors, genetically engineered immune cells, and monoclonal antibodies [1]. To maximize translational relevance, it is important to understand the underlying biology of in vitro disease models, including the dynamic interactions between cells during the immune cell killing process, their functional and morphological changes, the influence of their microenvironment, and the resistance of the target cells to treatment. Capturing this information by traditional endpoint analysis can be quite laborious and technically time-consuming. With the ever growing demand to improve time-to-result, efficient analysis methods are needed for activities such as the assessment of T-cell killing and antibody-dependent cell-mediated cytotoxicity (ADCC assays) to study pharmacology, efficacy, and possible off-target effects of genetically engineered cells to assess efficacy and toxicity concerns.

Live cell analysis is well-suited to assist in the optimization of immunotherapy workflows. These automated, kinetic assays are technically straightforward, easy to execute, flexible, and compatible with screening workflows to enhance time to results and provide assessment of potential therapeutics and monitoring in preclinical development, as exemplified in studies of T-cell reprogramming

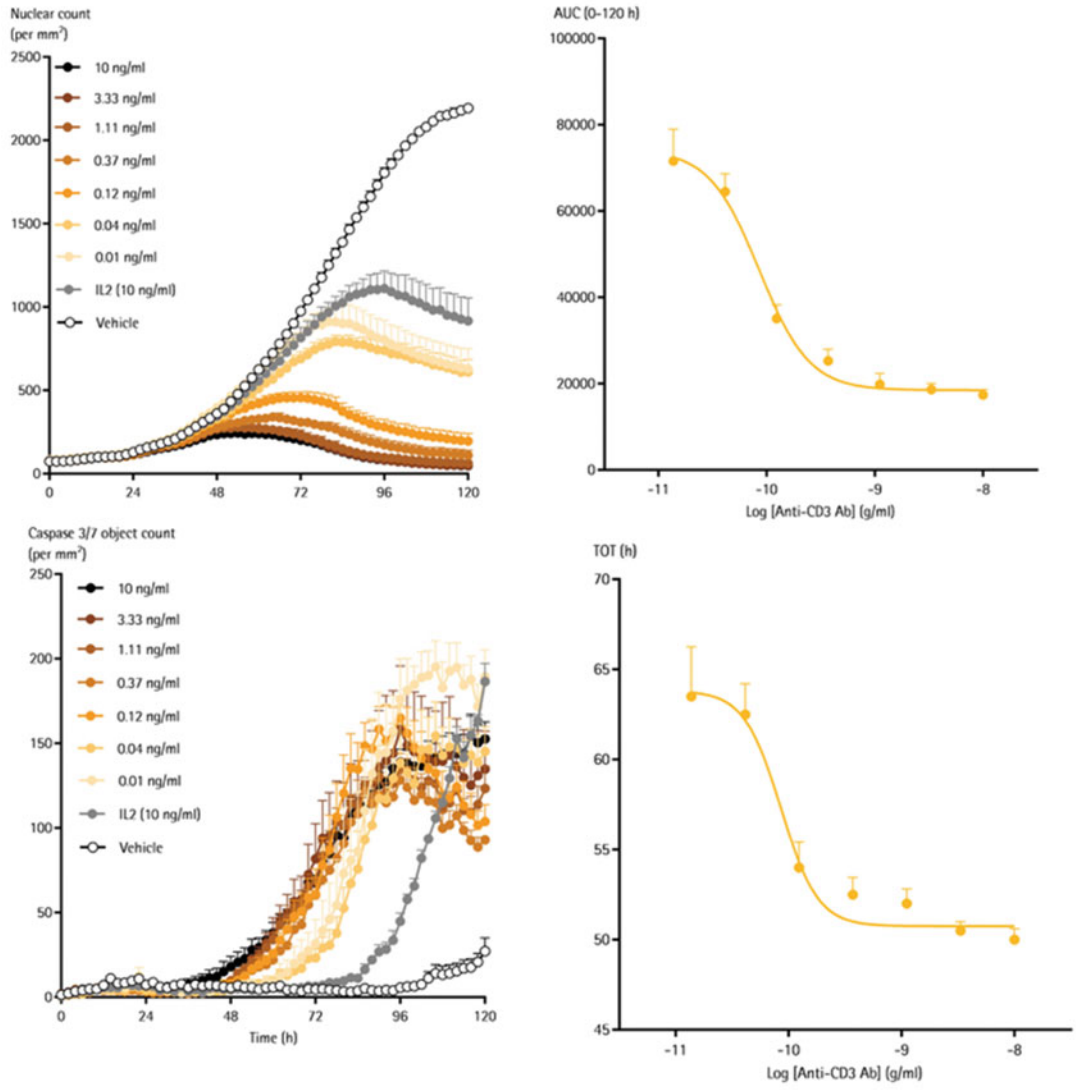

Fig. 2 Pharmacology of AntiCD3-Mediated Tumor Cell Killing. Incucyte® A549 NucLight Red cells (2 K/well) were seeded with human CD8+ T cells and activated with increasing concentrations of antiCD3 antibody (0.01–10 ng/mL) in the presence of IL-2 (10 ng/mL). Data demonstrate a concentration-dependent decrease in target tumor cell proliferation with an IC50 of 85.3 pg/mL (AUC). The data show a reduction in the time taken to induce target tumor cell apoptosis with an apoptosis threshold onset time midpoint of 85.4 pg/mL

using CRISPR technology [2], regulation of T-cell stimulation for melanoma treatment [3], as well as resistance to immunotherapy in relapsed/refractory pre-B cell acute lymphoblastic leukemia (B-ALL) [4]. Incucyte® assays also allow users to study the dynamics of T-cell killing and ADCC. As shown in Fig. 2, this can provide valuable insights for therapeutic development.

The Incucyte® immune cell killing assays and associated reagents study cell death in both nonadherent and adherent cell

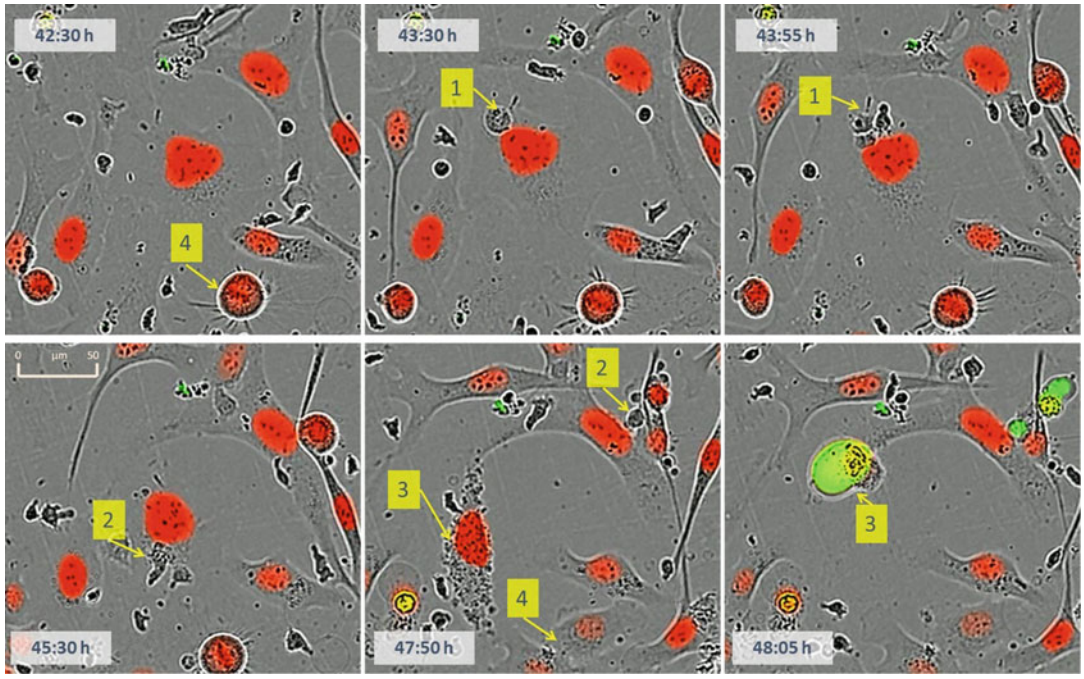

Fig. 3 Visualization of immune cell/tumor cell interplay using IncuCyte® immune cell killing assays. (1) Physical contact between a small cytotoxic T cell and a larger labeled tumor cell (red). T lymphocyte division. (2) Tumor cells under attack from a cytotoxic T lymphocyte: The "kiss of death". (3) Tumor cell cytoplasmic granulation immediately followed by caspase 3/7 labeling (green), nuclear condensation, and cell death. (4) Tumor cell mitosis: One cell becomes two

types, enabling users to coculture tumor target cells with immune cells of choice, such as T-cells and human peripheral blood mononuclear cells (PBMCs). Like the apoptosis assays, the nonperturbing Caspase-3/7 and Annexin V can be used (either red or green), along with Incucyte® Nuclight Red or Green Lentivirus Reagents for simultaneous counting of tumor cells. Further, the Incucyte® Cytolight Rapid Red or Green regents can be employed to assess T cell killing and antibody-dependent cell-mediated cytotoxicity (ADCC assays), respectively. These dyes are ideal for identifying the location of cells within a population and monitoring cellular interactions (Fig. 3). They freely pass through cell membranes and are then transformed to a cell membrane impermeant form. As daughter cells are produced, the dyes are transferred and diluted to the daughter cells, but not transferred to adjacent cells. Coculture methods combine direct measures of tumor cell death, with mix-and-read protocols for easy execution and analysis. This is facilitated by use of the Incucyte® Cell-by-Cell software, which allows label-free cell counts on both adherent and nonadherent cells and subsequent cell-by-cell classification based on shape, size, or fluorescence intensity to quantify dynamic changes in subpopulations within a mixed culture. Fosr nonadherent target cell

killing, this software enables the users to quantify features of both labeled target cells and nonlabeled effector cells (proliferation and death). Users may also track effector cell populations in the presence of adherent target cells. Following analysis, supernatants and cells can be harvested to perform additional downstream analysis of cytokines and activation states, using additional equipment such as the Intellicyt® iQue Screener, to maximize the data collected from each sample.

More information on the iQue® screener and Incucyte® Immune Cell Killing Assays and reagents can be found at https://intellicyt.com/research-areas/immuno-oncology/ and https://www.essenbioscience.com/en/applications/live-cell-assays/immune-cell-killing-assays/, respectively.

Link to Incucyte® Immune Cell Killing protocol at Essenbiosciences.com

https://www.essenbioscience.com/media/uploads/files/8000-0487-E00%2D%2DImmune_Cell_Killing_Assay_Protocol_ZCIzPuj.pdf

Watch a movie of immune cell killing using Incucyte®

https://www.essenbioscience.com/en/applications/live-cell-assays/immune-cell-killing-assays/

For answers to frequently asked questions about these immune cell killing assays:

https://www.essenbioscience.com/en/applications/incucyte-immune-cell-killing-faqs/

Watch a movie of immune cell killing using Incucyte®

https://www.essenbioscience.com/en/applications/live-cell-assays/immune-cell-killing-assays/

For more information on the Incucyte® Cell-Bby-Cell Software.

https://www.essenbioscience.com/en/products/software/cell-by-cell/

2 Materials

2.1 Equipment and Consumables

1. Incucyte® Live-Cell Analysis System (Essen BioScience, Ann Arbor, MI, USA).
2. For analysis of adherent and non-adherent tumor cell assays, Incucyte® Cell-by-Cell Analysis Software Module (9600-031) Essen BioScience, Ann Arbor, MI, USA).
3. Centrifuge.
4. 96-well microplate for setting up dilutions.

5. Sterile 96-well tissue culture-treated plate (Corning® 3595 recommended) and untreated plates for dilution.
6. Single and multichannel pipettes.
7. Consumables: sterile pipette tips, 50 mL reservoirs, 15 mL conical tubes, 1.5 mL microfuge tubes.

2.2 Cells and Cell Culture Reagents

1. Target cells for apoptosis or for immune killing (i.e., adherent epithelial cancer cells such as colon or ovarian; or non-adherent leukemic cells; for Immune killing assays, the use of nonadherent cells as target cells requires labeling with Incucyte® Nuclight live-cell labeling reagent to enable target cell counting). Immune (effector) cells of interest for immune killing assays (e.g., T cells, PBMCs).
2. Appropriate growth media for desired target cells and immune effector cells (*see* **Note 1**).
3. 0.25% Trypsin.
4. Coating matrix: 0.01% poly-L-ornithine solution or 5 μg/mL fibronectin diluted in 0.1% BSA.
5. Apoptosis inducer (i.e., TNFa, cisplatin or paclitaxel).

2.3 Reagents and Compounds

Choice of reagent will depend on preference for red/green labeling and measurement of caspase-3/7 or Annexin Red.

1. Fluorescent reporter for measurement of caspase 3/7 activity (i.e., Incucyte® Caspase-3/7 Green or Red Apoptosis Reagent.
2. Fluorescent reporter measurement of Annexin V (i.e., Incucyte® Annexin V Red Reagent or Incucyte® Annexin V Green Reagent).
3. Reagents for live-cell labeling (Incucyte® Cytolight Rapid Green or Rapid Red Reagent).
4. Reagents for labeling non-adherent target cells (i.e., Incucyte® Nuclight Red or Nuclight Green Lentivirus Reagent).

3 Methods

3.1 Apoptosis Assay, Adherent Cells (Fig. 4)

1. Seed your choice of cells (100 μL per well) at an appropriate density into a 96-well plate, such that confluence the next day is approximately 30%. The seeding density will need to be optimized for the cell line used; however, we have found that 1000–5000 cells per well (10,000–50,000 cells/mL seeding stock) are reasonable starting points (*see* **Notes 2** and **3**).
2. Monitor cell growth using the Incucyte® system to capture phase contrast images every 2 h and quantify culture confluence using the integrated confluence algorithm (*see* **Note 4**).

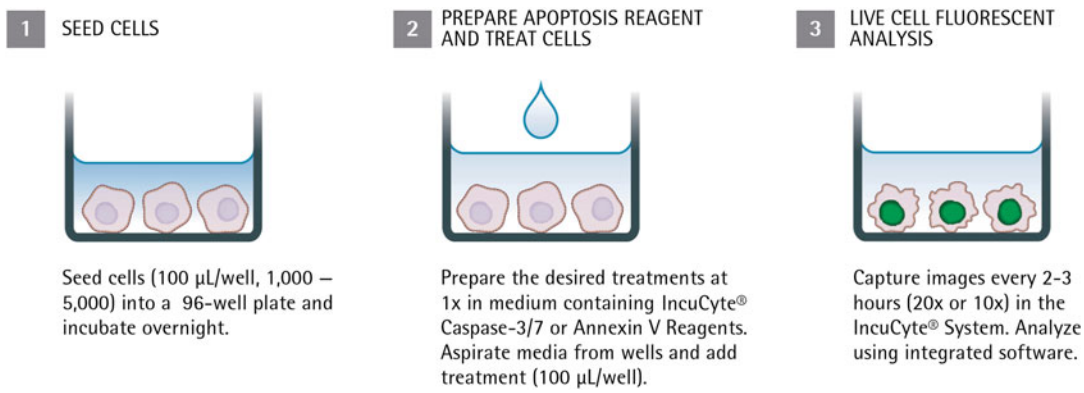

Fig. 4 Adherent cell line protocol

3. The following day, dilute apoptosis reagents in desired media formulations. When using Caspase-3/7 Green Reagent, dilute the reagent 1:1000 in complete medium (5 µM final concentration); when using Caspase-3/7 Red Reagent, evaluate optimal reagent concentration by diluting the reagent 1:200 in complete medium and then make twofold dilutions (2.5, 1.25, and 0.5 µM final concentrations); when using Annexin V reagents, solubilize Annexin V by adding 100 µL of complete medium or PBS. The reagents may then be diluted in complete medium containing at least 1 mM $CaCl_2$ for a final dilution of 1:200 of Annexin V (*see* **Notes 5** and **6**).
4. Use the medium with diluted apoptosis reagents (from **step 3**) to prepare different concentrations of test agents. The volumes/dilutions added to cells may be varying; however, a volume of 100 µL per well is generally sufficient for the duration of the assay.
5. Remove the cell plate from the incubator and aspirate off growth medium.
6. Add treatments (with test agents) and control to the appropriate wells of the 96-well plate.
7. Proceed to Subheading 3.5.1.

3.2 Apoptosis Assay, Nonadherent Cells (Fig. 5)

1. Coat a 96-well flat bottom plate with 50 µL of desired coating matrix (i.e., 0.01% poly-L-ornithine solution or 5 µg/mL fibronectin). Coat plates for 1 h at ambient temperature, remove solution from wells, and then allow plates to dry for 30–60 min prior to cell seeding.
2. While plates are drying and prior to cell seeding, dilute apoptosis reagents in desired medium formulation (*see* **Notes 6** and **7**). When using Caspase-3/7 Reagents, dilute the reagent 1:1000 in complete medium (5 µM final concentration for Caspase-3/7 Green and 0.5 µM for Caspase-3/7 Red); when

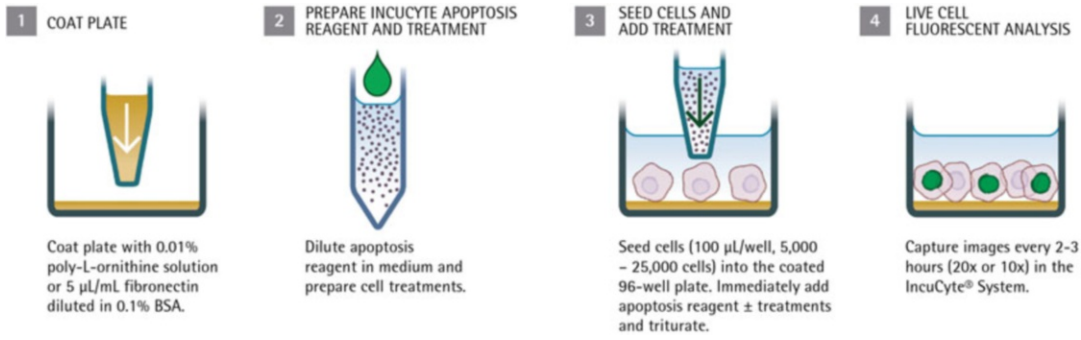

Fig. 5 Nonadherent cell line protocol

using Annexin V reagents, solubilize Annexin V by adding 100 µL of complete medium or PBS. The reagents may then be diluted in complete medium containing at least 1 mM $CaCl_2$ for a final dilution of 1:200.

3. Use the medium with diluted apoptosis reagents (from **step 2**) to prepare different doses of test agents or treatments at 2× concentration Use enough cell culture medium containing caspase-3/7 or Annexin V to achieve a volume of 100 µL per well.
4. Once plate in **step 1** is dry and treatments are set up, seed your choice of cells (100 µL per well) at your desired density into a 96-well plate. The seeding density will need to be optimized for the cell line used; however, we have found that 5000–25,000 cells per well (50,000–250,000 cells/mL seeding stock) are reasonable starting points. Use the same medium with diluted apoptosis reagents (from **step 2**) to resuspend and seed the cells (*see* **Note 2**).
5. Immediately add treatments and control to appropriate wells of the 96-well plate containing cells. Triturate wells to appropriately mix the treatment to ensure cell exposure at 1×.
6. Proceed to Subheading 3.5.1.

3.3 Immune Cell Killing Assays of Adherent Tumor Cells (Fig. 6)

1. Seed target cells (100 µL per well) at an appropriate density into a 96-well flat-bottom plate such that the cell confluency is approximately 20% the next day. The seeding density will need to be optimized for each tumor cell line used; however, we have found that 1000–3000 cells per well are reasonable starting points (*see* **Notes 2** and **3**).
2. Monitor target cell growth using the Incucyte® Live-Cell Analysis System and confluence algorithm. Target cells can be labeled with Nuclight® Lentivirus Reagent or Cytolight® Rapid Reagents to enable simultaneous real-time quantification of viable target cells.

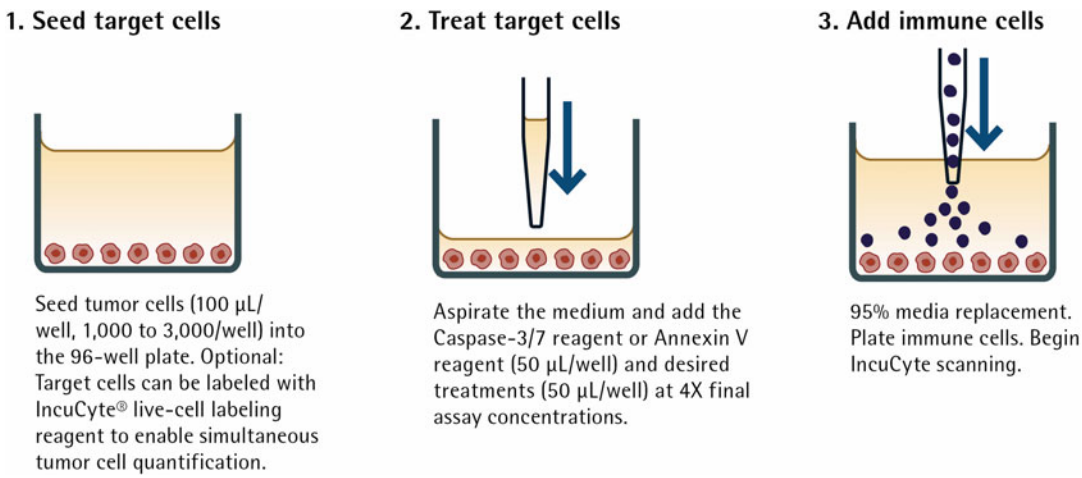

Fig. 6 Immune cell killing of adherent tumor cell protocol

3. Treat cells 24 h after seeding. Dilute apoptosis reagents, ensuring compatibility of target cell label and apoptotic marker, and treatments (e.g., T cell stimuli, antibodies, and cytokines) at 4X final assay concentration in desired assay medium. When using Caspase-3/7 green, dilute reagent to a concentration of 20 µM (1:250 dilution), sufficient for 50 µL per well. When using Caspase-3/7 Red Reagent, evaluate optimal reagent concentration by diluting the reagent to 1:50 in complete medium and then make twofold dilutions (10, 5, and 2.5 µM final concentrations), sufficient for 50 µL per well. When using Annexin V reagents, solubilize Annexin V by adding 100 µL of complete medium or PBS. The reagents may then be diluted in complete medium containing at least 1 mM $CaCl_2$ for a dilution of 1:50, sufficient for 50 µL per well.
4. Remove the cell plate from the incubator and aspirate off growth medium.
5. Add 50 µL of each of the prepared apoptosis reagent and treatments above (*see* **Note 8**).
6. Count chosen immune effector cells (e.g., T cells and PBMCs) and prepare a cell suspension at a density of 100,000–300,000 cells/mL (100 µL per well, 10,000–30,000 cells/well). It is recommended that different target-to-effector cell ratios are tested (e.g., 1:5 and 1:10). *See* **Note 9**.
7. Seed 100 µL of effector cells into the appropriate wells of the cell plate to achieve a final assay volume of 200 µL. Allow plates to settle on level surface at ambient temperature for 30 min.
8. Proceed to Subheading 3.5.2.

3.4 Immune Cell Killing Assays of Nonadherent Tumor Cells (Fig. 7)

1. Coat a 96-well flat bottom plate with coating matrix as in Subheading 3.2. Coat plates for 1 h at ambient temperature, remove solution from wells, and then allow plates to dry for 30–60 min prior to cell addition. Choice of coating will need to be determined prior to the assay for target cells of interest.
2. Prepare the following reagents in medium:
   (a) Test materials (e.g., T cell stimuli, antibodies, cytokines; 50 μL per well, prepared at 4X final assay concentration).
   (b) Incucyte® Annexin V Reagent (apoptosis detection reagent; ensure compatibility of cell label and apoptotic marker): solubilize Annexin V by adding 100 μL of complete medium or PBS. The reagents may then be diluted in complete medium containing at least 1 mM $CaCl_2$ for a dilution of 1:50 (4X final assay concentration, 50 μL per well (*see* **Note 10**).
3. Add 50 μL of each of the prepared apoptosis reagent and treatments from **step 2** for a total volume of 100 μL in appropriate wells.
4. Count labeled target cells and prepare a cell suspension at a density of 40,000–80,000 cells/mL (seed 50 μL per well, 10,000–20,000 cells/well). Target cells can be labeled with Nuclight Red or Green Lentivirus Reagent for real-time quantification of target cell viability.
5. Count chosen immune effector cells (e.g., T cells and PBMCs) and prepare a cell suspension at a density of 400,000–800,000 cells/mL (50 μL per well, 100,000–200,000 cells/well). It is recommended that different target-to-effector cell ratios are tested (e.g., 1:5 and 1:10). (*see* **Note 9**).
6. Add target cells and immune effector cells to assay plate to achieve a final assay volume of 200 μL. Allow plates to settle on level surface at ambient temperature for 30 min.
7. Proceed to Subheading 3.5.3.

3.5 Incucyte® Live Cell Analysis Setup and Image Processing

3.5.1 Apoptosis Assays (For Both Adherent and Nonadherent Cells)

1. Place the cell plate into the Incucyte® Live-Cell Analysis System and allow the plate to warm to 37 °C for 30 min prior to scanning.
   (a) Objective: 10× or 20×.
   (b) Channel selection: Phase Contrast and green or red (depending on apoptosis reagent used).
   (c) Scan type: Standard (2–4 images per well).
   (d) Scan interval: Typically, every 2 h, until your experiment is complete.

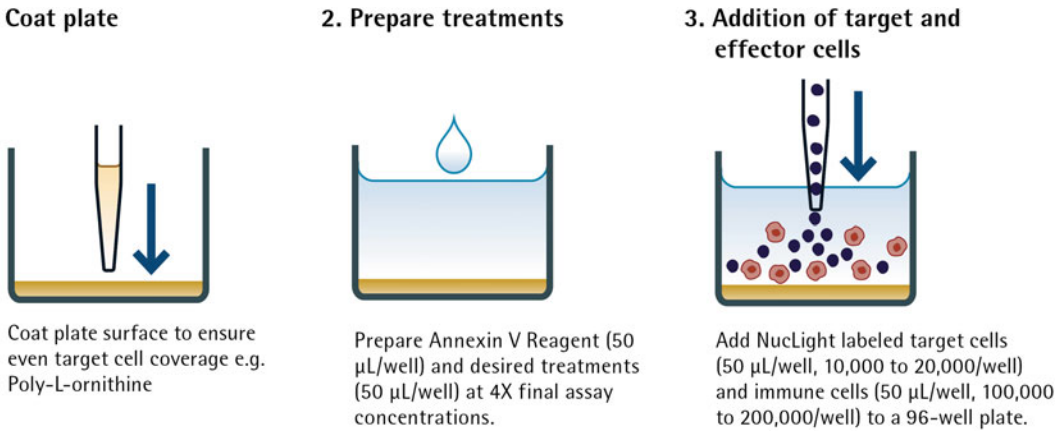

Fig. 7 Immune cell killing of nonadherent tumor cell protocol

3.5.2 Immune Cell Killing Assays, Adherent Tumor Cells

Place the assay plate into the Incucyte® Live-cell Analysis system and schedule 24 h repeat scanning (*see* **Note 4**).

(a) Objective: 10× or 20×.

(b) Channel selection: Phase Contrast + "Green" or "Red" depending on apoptosis reagent and target cell label used.

(c) Scan type: Standard (2 images per well) *see* **Note 11**.

(d) Scan interval: Every 3 h.

3.5.3 Immune Cell Killing Assays, Nonadherent Tumor Cells

Place the assay plate into the Incucyte® instrument and schedule 24 h repeat scanning:

(a) Objective: 4× or 20× with Cell-by-Cell.

(b) Channel selection: Phase Contrast + "Green" and "Red".

(c) Scan type: Standard (2 images per well) *see* **Note 11**.

(d) Scan interval: Every 2–3 h.

3.6 Analysis of Incucyte® Apoptosis and Immune Cell Killing Assays

3.6.1 Analysis with Incucyte® Basic Analyzer

- When defining your analysis definition, select "Basic Analyzer" from the list of options.
  - Select appropriate images to describe the biology in your plate across time, including example control wells.
  - Define a fluorescence mask for nuclear label cell expression to quantify cell number over time.
  - Define a fluorescence mask for the cell health indicator, if included.
- Use area and eccentricity filters to avoid masking any inappropriately labeled cells (e.g., effector cells) (*see* **Note 12**).
  - When looking at results, use cell fluorescence to quantify cell proliferation.

When using a nuclear marker with adherent cells, use Count of Objects.

When using a cytoplasmic marker with adherent cells, use Total Fluorescence Area or Fluorescence Confluence.

For nonadherent cells, use Total Fluorescence Area or Fluorescence Confluence regardless of cell labeling.

- Fluorescence of the cell health indicator will indicate apoptosis in the cell population, which can be normalized for cell number. Again, use metrics of cell Total Fluorescence Area or Fluorescence Confluence.

3.6.2 Analysis with Incucyte® Cell-by-Cell Analysis Module for Immune Cell Killing

Use above recommendations with Basic Analyzer for tracking the target cell population, but use Nonadherent Cell-by-Cell Analysis to track properties of the effector cell population (*see* **Note 13**).

For effector cell masking when defining your analysis definition, select "Nonadherent Cell-by-Cell" from the list of options (only visible if images are acquired with 20× and if license is active):

Adherent Target Cells

- Select appropriate images to describe biology in your plate across time, including example control wells. Include effector only wells if present in the plate.
- Define a phase mask to describe individual effector cells using control sliders (*see* Cell-By-Cell Analysis Guideline document for full details of software).
- When looking at total population metrics, use object count to define proliferation of cells.
- If interested in the health of effector cells, set up a classification job on the segmented cells, based on fluorescence intensity, to define live and apoptotic effector cells.—Use percentage of apoptotic cells as indicator of cell health of effector cells.

Nonadherent Target Cells

When defining your analysis definition, select "NonAdherent Cell-by-Cell" from the list of options (only visible if images are acquired with 20× and if license is active):

- Select appropriate images to describe biology in your plate across time, including example control wells.
- Define a phase mask for all true cell objects (target and effector) using control sliders (*see* Cell-By-Cell Analysis Guideline document for full details of software.)—For target cells in the image, it may not be possible to mask as individual cells due to clumping—this will not cause an issue for overall quantification of target cell biology.

- Once the segmentation job has run, set up a two metric classification job based on red and green fluorescence intensity to identify subpopulations:
  - Color 1 (e.g. Nuclight Red)—Target cells (fluorescent cells) and effector cells (nonfluorescent).
  - Color 2 (e.g. Annexin V Green)—Live and apoptotic cells.

To view results, we recommend the following metrics:

- *Target cell properties*—these will be from the high Color 1 intensity population.
  - *For proliferation*, create a metric (+) of high Color 1 (the population you are interested in) channel Color 1 integrated intensity per area (image or mm^2) or channel phase area per image. This will provide a total fluorescence area or phase area in the well for the target cell population. As it is difficult to mask individual target cells, avoid the count metric. When using Cytolight Rapid dyes, use the phase area as the fluorescence intensity may drop over time.
  - *For target cell death*, create a metric (+) of high Color 1 and 2 phase count normalized by high Color 1 to provide an apoptotic index for the target cell population.
- *Effector cell properties*—these will be from low Color 1 intensity population.
  - *For proliferation*, again, create a metric (+) of low Color 1, phase object count. Effector cells can normally be masked individually, and so a readout of count can be used.
  - *For effector cell death*, create a metric (+) of low Color 1 and high Color 2 phase count normalized by low Color 1.

4 Notes

1. We recommend medium with low levels of riboflavin to reduce the green fluorescence background. EBM, F12-K, and Eagles MEM have low riboflavin (<0.2 mg/L). DMEM and RPMI have high riboflavin (>0.2 mg/L).
2. Remove bubbles from all wells by gently squeezing a wash bottle (containing 70–100% ethanol with the inner straw removed) to blow vapor over the surface of each well.
3. Following cell seeding, place plates at ambient temperature (15 min for adherent cell lines and 45 min for nonadherent cell lines) to ensure homogenous cell settling.
4. After placing the plate in the Incucyte® live-cell analysis system, allow the plate to warm to 37 °C for 30 min prior to scanning.

5. All test agents will be diluted in this reagent-containing medium, and so prepare a volume that will accommodate all treatment conditions. The volumes/dilutions added to cells may be varied; however, a volume of 100 μL per well is generally sufficient for the duration of the assay.
6. When monitoring apoptosis in primary neuronal cultures, we recommend use of the Incucyte® Annexin V Red reagent to eliminate risk of green channel excitation issues in these sensitive cell lines.
7. All test agents will be diluted in this reagent-containing medium, and so make up a volume that will accommodate all treatment conditions. The volumes/dilutions added to cells may be varied; however, a volume of 200 μL per well is generally sufficient for the duration of the assay.
8. For treatment controls, add 50 μL of assay medium.
9. Assay duration may be reduced by preactivating the effector cells before addition to assay plate; however, this may require a higher initial seeding density of target cells.
10. Although either the Incucyte® Annexin V or Caspase-3/7 Reagents can be used to detect immune cell killing of target cells, we recommend that the Annexin V Reagent is used for nonadherent target cells. Nonadherent target and effector cell types can have very similar nuclear sizes negating the use of size filters to remove Caspase-3/7 labeled effector nuclei from the analysis. Additionally, we have observed raised levels of caspase-3/7 activity in some nonadherent cell types, particularly at higher confluency, which can interfere with the interpretation of immune cell-driven target cell death. In our experience, the Annexin V Reagent labels fewer effector cells and provides lower nonspecific background.
11. If the Incucyte® Cell-by-Cell Analysis Software Module (Cat. No. 9600-0031) is activated, use nonadherent Cell-by-Cell image acquisition, 4 images/well.
12. The phase confluence mask is of limited use as this will mask all target and effector cells in the well.
13. It is possible to use Adherent Cell-by-Cell Analysis to mask target cells, but it is very difficult to not include effector cells in the mask and is very dependent on the contrast level of the target cells.

Acknowledgement

The science presented in this chapter is a product of the sustained, multidisciplinary R&D activities of Essen BioScience/Sartorius personnel based in Ann Arbor, Michigan, USA, and Welwyn

Garden City, Hertfordshire, UK. This includes cell biologists, software engineers, optical and hardware designers as well as essential backup support functions, communications, and product development. We thank you for your hard work and dedication to move science forward. We also thank our customers for their feedback and creativity, which continues to inspire us.

References

1. Bernards R et al (2020) A roadmap for the next decade in cancer research. Nat Cancer 1:12–17
2. Roth TL et al (2018) Reprogramming human T cell function and specificity with non-viral genome targeting. Nature 559(7714):405–409
3. Shifrut E et al (2018) Genome-wide CRISPR screens in primary human T cell reveal key regulators of immune functions. Cell 175 (7):1958–1971
4. Fry TJ et al (2018) CD22-targeted CAR T cells induce remission in B=ALL that is naive or resistant to CD19-targeted CAR immunotherapy. Nat Med 24(1):20–28

Further Reading

Additional protocols available online at EssenBioscience.com. Obtain a copy of the third edition, Live-cell analysis handbook: https://www.essenbioscience.com/en/communications/live-cell-analysis-handbook-4th-edition/

Chapter 18

Two Plasmid-Based Systems for CRISPR/Cas9 Mediated Knockout of Target Genes

Cai M. Roberts and Elena S. Ratner

Abstract

CRISPR/Cas9-based gene editing is a recent advance that allows for the knockout or alteration of target genes within mammalian cells. Many variations of the technique exist, but here we describe two systems of plasmid-based CRISPR gene knockout which together allow for the selective knockout of virtually any gene target. Compared with other CRISPR-based systems, these plasmids have the advantages of delivering all the necessary components in one plasmid, choice of multiple selectable markers, and choice of route of administration into target cells. In addition, potential off-target effects from one system (dependent upon selection of target gene) can be overcome through use of the second system. Strategies for optimizing the knockout process and selection of finished cell lines are also presented.

Key words CRISPR, Cas9, sgRNA, Knockout, Nickase, Plasmids, Transfection, Selection

1 Introduction

1.1 What Is CRISPR?

CRISPR has been hailed as a revolution in gene editing technology. Standing for Clustered Regularly Interspaced Short Palindromic Repeats, the system is derived from a rudimentary immune surveillance system employed by bacteria and archaea [1]. These prokaryotes would save small fragments of DNA from pathogens they previously encountered, storing them in their own DNA as protospacers between repetitive sequences (the eponymous short palindromic repeats), in a locus referred to as CRISPR [2]. Just as humans possess a catalog of antibodies to help the immune system identify and combat infections, bacteria are able to recognize and combat those infections of which they have CRISPR memory. The bacterial equivalent of the effector immune cell is the Cas (Crispr ASsociated) family of enzymes, particularly Cas9. This enzyme is a nuclease that cleaves infectious DNA in the bacterium. The sequence specificity of the enzyme is provided by a complex comprising a CRISPR RNA transcribed from a protospacer in the CRISPR locus and a trans-activating RNA (tracrRNA). The two

Ayesha B. Alvero and Gil G. Mor (eds.), *Detection of Cell Death Mechanisms: Methods and Protocols*, Methods in Molecular Biology, vol. 2255, https://doi.org/10.1007/978-1-0716-1162-3_18,

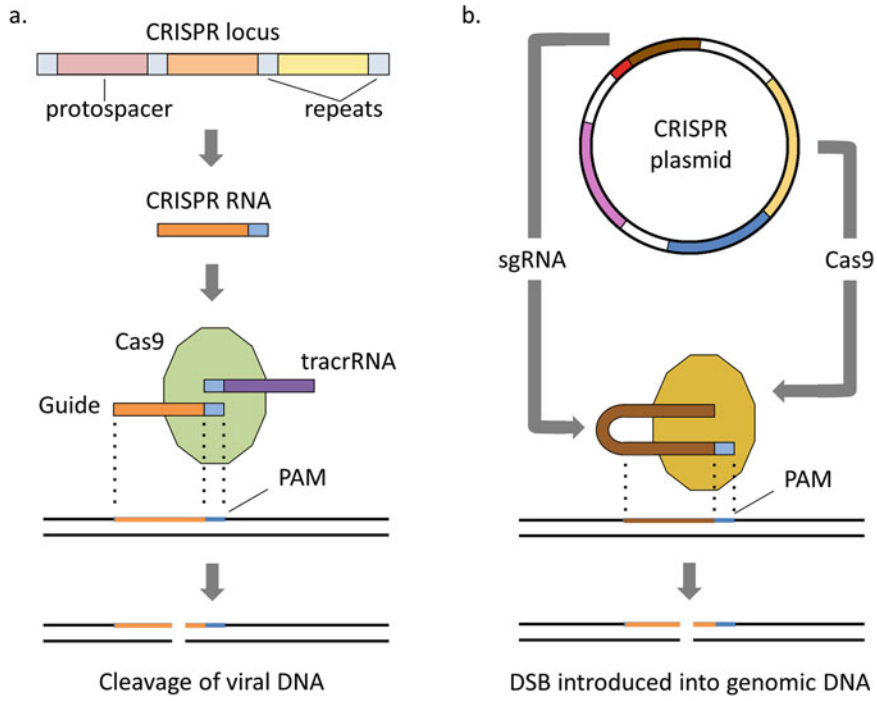

Fig. 1 Schematic of CRISPR function. (**a**) In bacteria, CRISPR guides are transcribed from the CRISPR locus, and pair with tracrRNA to recruit Cas9. Upon recognition of foreign viral DNA by the guide sequence, Cas9 cleaves both strands just upstream of the PAM sequence. (**b**) In the systems described in this chapter, a single-guide RNA and the Cas9 enzyme are encoded in a single plasmid to be delivered to target cells. The sgRNA both recognizes the target sequence and recruits Cas9, leading to a double strand break just upstream of the PAM

RNA constituents anneal and are cleaved by RNAse III, and the resulting RNA hybrid complexes with Cas9, bringing it to the target site [3]. The target sequence is followed by a protospacer adjacent motif (PAM) which is recognized by the Cas9, and the DNA is cleaved upstream from the PAM sequence (Fig. 1a).

A humanized version of the CRISPR/Cas9 system has been developed in order to leverage this system for gene editing in mammalian cells. The Cas9 protein can be expressed in human cells, where it can cleave genomic DNA at a specific point again specified by an RNA intermediary, referred to as a guide RNA. Genomic sequences targeted by guides must still neighbor a PAM (NGG, where N denotes any of the four nucleotide bases). Guides are typically transcribed as a single molecule encompassing the tracrRNA and the targeting sequence, hence their name: single-guide RNA (sgRNA). The two-part system of Cas9 and sgRNA based on the bacterium Streptococcus pyogenes was pioneered by the laboratories of Jennifer Doudna and Emmanuelle Charpentier, and first described in a 2012 publication [4]. Feng Zhang and George Church independently showed that the system could be

used to make edits in human cells the following year [5, 6]. Since that time, the system has been further fine-tuned and widespread, and remains a valuable tool for research in the biological and medical science fields (Fig. 1b).

It is important to note that the Cas9 and its sgRNA are only capable of cutting DNA. The consequences of the cut are entirely dependent upon the DNA damage response pathways activated in the target cell. The most common repair pathway employed is non-homologous end joining (NHEJ) [7]. In this process, breaks are repaired as quickly as possible, but this speed often comes at the expense of insertion or deletion mutations at the break site. Knockout of a gene relies upon these mutations to introduce a frame shift in the coding sequence of the target gene, thus rendering all sequence downstream of the break site useless. Knockout can also be accomplished by insertion of foreign DNA, such as a reporter cassette, into the break site. In this case, homology directed repair (HDR) is the pathway used. By supplying a template for HDR repair with "homology arms" with sequences identical to endogenous DNA flanking the break site and the desired insertion in the center, the target cell can be fooled into incorporating the reporter, thus disrupting the target gene. Knock-ins of reporters as fusion proteins with target genes or mutations of genes can be accomplished by the same means.

1.2 Advantage over Other Gene Knockout Approaches

The primary advantages CRISPR possesses over previous generations of gene editors are relative ease of design and use. In particular, we will focus here on zinc finger nucleases (ZFNs) and transcription activator-like effector nucleases (TALENs).

ZFNs comprise a nuclease along with zinc finger domains, each recognizing a three-nucleotide motif, combined together to recognize longer (i.e., more unique) sequences. A typical ZFN system will have two nuclease domains, each fused to three zinc fingers and arranged antiparallel to each other to cover a total of eighteen nucleotides of sequence, with the cleavage site in between the two halves [8]. The design of ZFNs is complicated; specificity to given nucleotide sequences is variable and depends on sequences flanking the site in question. Selection of tightly binding zinc fingers using phage display and pools of zinc fingers can offset this challenge [9]; however, the fact remains that for each desired gene edit, a completely new enzyme must be designed and optimized, which consumes time and resources.

TALENs rely on the nucleotide sequence specificity of particular repeated amino acid sequences within proteins called TALEs (transcription activator-like effectors). By altering two amino acids within these repeats, TALEs can be engineered to target a given nucleotide sequence [10]. Fusing a nuclease to this protein gives the N in TALEN, and confers the ability to cut DNA in a sequence-specific manner. However, the repetitive nature of the sequences

complicates their production, and may necessitate piecewise assembly of the repeated regions of the gene for the TALEN [11]. Furthermore, as with ZFNs, a new enzyme must be designed for each target site. While more straightforward than ZFN design, a great deal of work is still required in order to assemble multiple TALEN genes.

Enter CRISPR. In this system, the nuclease, Cas9, never needs to be altered. Target site specificity is conferred only by RNA, and nucleic acid oligos can be designed and synthesized cheaply and easily. Because nothing changes in the protein component of the system, no specialized knowledge in protein engineering is required to use CRISPR gene editing. All that is required is selection of the best RNA sequence for the intended edit. Indeed, once the CRISPR system is in place in a laboratory, targeting of new genes of interest requires only designing a guide, a process akin to ordering new primers for PCR. How to design and use these guides will be the focus of the remainder of this chapter.

1.3 Alternative CRISPR Systems

At this point in time, multiple strategies exist for introducing CRISPR machinery into target cells. In any strategy, one must instruct the target cell to express the Cas9 protein and the guide RNA specific to your target gene, but protocols differ on how to accomplish this. Cas9 can be introduced in its final protein form, as mRNA, or as plasmid-borne DNA. Similarly, guides can be introduced as RNA or DNA. In this protocol we describe the introduction of both components as plasmid DNA. Among plasmids, however, there is also a great deal of variety. Plasmids can be viral or non-viral, include one or both CRISPR components, and can have a variety of selectable markers, or none at all. This chapter will provide instruction on the assembly of two alternate plasmids, each of which carries genes for Cas9, sgRNA, and a selectable marker. The reason for having two plasmids to choose from is that a standard Cas9 enzyme is not always desirable.

The only thing targeting Cas9 to a specific point in the genome is a twenty-nucleotide sequence. In some cases, a guide RNA sequence can be found that matches only to the gene of interest. In other cases, the same sequence, or one very nearly identical, may be found in other parts of the genome, including the exons of one or more off-target genes. In these instances, there is a higher likelihood of unintended edits being made to the target cells, and a workaround is needed. This comes in the form of a mutation to Cas9, in which one of the two nuclease domains, HNH and RuvC, is rendered catalytically inactive. A D10A mutation inactivates the RuvC domain, while H840A inactivates HNH [12]. The resulting "nickase" enzyme (Cas9n) is capable of cleaving only one strand of the DNA duplex at the specified target site. In order to create the double strand break required for editing to take place, two guides on opposite strands and in close proximity are used, directing

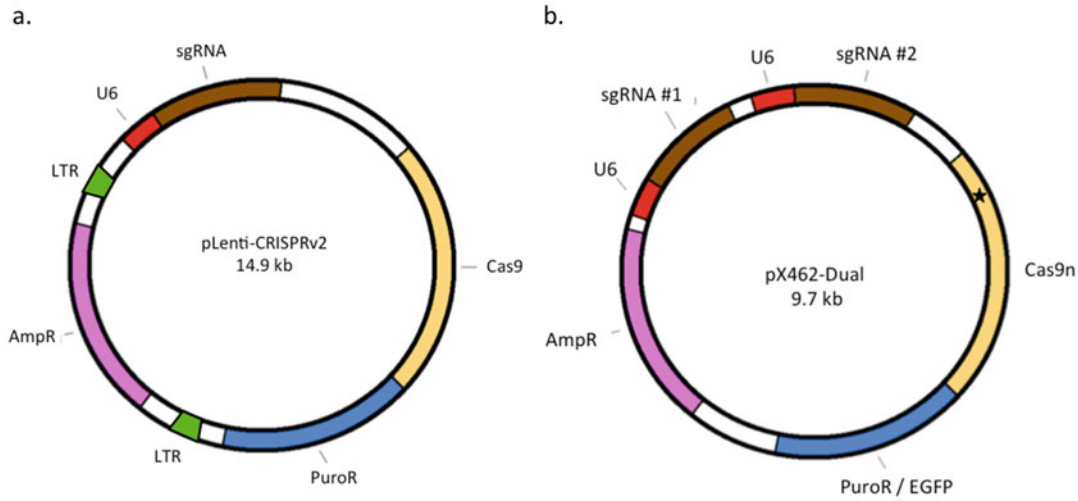

Fig. 2 Example final plasmid products of these protocols. (**a**) pLentiCRISPRv2 encodes one sgRNA, WT Cas9, puromycin resistance, and ampicillin resistance for propagation in *E. coli*. Long tandem repeats (LTR) allow for integration into the genome of a target cell. (**b**) A finished Cas9 nickase plasmid with two sgRNA cassettes, including the U6 promoter for each, the Cas9n gene (star denotes D10A mutation), ampicillin resistance and a selectable marker. pX462 is shown here, with puromycin resistance; pX461 would contain EGFP where marked

Cas9n to create two single strand breaks that in turn give rise to a double strand break (DSB).

The first plasmid system we will introduce encodes a wild type (WT) Cas9 and a single guide. It can be introduced into target cells by standard transfection or viral transduction, and contains the gene for puromycin resistance for selection (Fig. 2a). The second plasmid we describe contains the D10A Cas9n gene, has both guide RNAs required for DSB formation, and enables either puromycin or GFP selection (Fig. 2b). Regardless of transfection method, the former plasmid can give rise to cells stably expressing the CRISPR machinery; the latter plasmid is better suited to transient expression.

2 Materials

2.1 Equipment

1. 37 °C incubator/shaker.
2. 4 °C refrigerator.
3. −80 °C freezer.
4. Sterile 1.5 ml microfuge tubes.
5. Sterile 14 ml snap-cap tubes.
6. Parafilm.
7. Balance.

8. Inverted microscope.
9. 42 °C water bath or heat block.
10. Thermal cycler.
11. Nanodrop/spectrophotometer.
12. Agarose gel electrophoresis apparatus and gel imager.
13. Biological safety cabinet/cell culture hood.
14. 37 °C, 5% CO_2 cell culture incubator.
15. T25 cell culture flasks.
16. 100 mm cell culture dishes.
17. Multiwell cell culture plates (96, 24, 6-well plates).
18. Fluorescence microscope (when using GFP screening).
19. Fluorescence-activated cell sorter (when using GFP screening).
20. Ultracentrifuge (for virus production only, *see* Subheading 3.3).
21. Ultracentrifuge tubes (for virus production only, *see* Subheading 3.3).

2.2 Reagents

1. Plasmid pLentiCRISPRv2.
2. Plasmid pSpCas9n(BB)-2A-GFP (pX461).
3. Plasmid pSpCas9n(BB)-2A-Puro (pX462) V2.0 (*see* **Note 1**).
4. Plasmid pCMV-VSV-G.
5. Plasmid psPAX2.
6. Synthesized DNA oligos encoding guide RNAs specific for gene target.
7. Sequencing primer for pLentiCRISPRv2: 5′-CAGGGACAG CAGAGATCCAGTTTGG-3′.
8. Sequencing primers for pX461 and pX462: Forward: 5′-CGG CCTTTTTACGGTTCCTGGC-3′;
   Reverse: 5′-GTTGGGCGGTCAGCCAGG-3′.
9. Primers for adding restriction sites in Subheading 3.4 (stock concentration 10 μM):
   Forward: 5′-CACCGCTAGCGAGGGCCTATTTCCCAT GATTCCTTC-3′.
   Reverse: 5′-GTACCTCTAGAGCCATTTGTCTGCAG-3′.
10. Chemically competent *E. coli*.
11. Liquid Luria Broth (LB) with 100 μg/ml ampicillin.
12. LB-agar plates with 100 μg/ml ampicillin (LB-Amp).
13. Medium for growing competent cells such as SOC medium: 0.5% yeast extract + 2% Tryptone + 10 mM NaCl + 2.5 mM KCl + 10 mM $MgCl_2$ + 10 mM $MgSO_4$ + 20 mM Glucose.

14. Sterile 50% glycerol in water.
15. Hanks Balanced Salt Solution (HBSS).
16. Restriction enzymes: BbsI, BsmBI, KpnI, NheI, NotI, XbaI (*see* **Note 2**).
17. Restriction enzyme buffer: supplied with restriction enzymes (e.g., NEBuffer 3.1, CutSmart).
18. 100 mM dithiothreitol (DTT).
19. T4 DNA Ligase: at 400,000 units/ml.
20. 10× T4 DNA ligase buffer: supplied with T4 DNA ligase.
21. Nuclease-free water.
22. Calf intestinal phosphatase (CIP) OR shrimp alkaline phosphatase (rSAP): at 5000 or 1000 units/ml, respectively.
23. T4 polynucleotide kinase (PNK): commercially available at 10,000 U/ml.
24. Thermosensitive Alkaline phosphatase: stock concentration 1 U/μl.
25. Pfu Ultra II Fusion HS DNA Polymerase.
26. Pfu polymerase buffer.
27. Deoxynucleotide triphosphates (dNTPs).
28. Plasmid preparation kit such as Qiagen's QIAprep Spin Miniprep Kit.
29. PCR cleanup kit such as Qiagen's QIAquick PCR Cleanup Kit.
30. Gel extraction kit such as Qiagen's QIAquick Gel Extraction Kit.
31. Agarose.
32. TAE buffer: 40 mM Tris, 20 mM acetic acid, 1 mM EDTA.
33. OptiMEM.
34. Transfection reagent (*see* **Note 3**).
35. HEK293T cell line.
36. Cell culture media for HEK293T cells: DMEM +20% fetal bovine serum.
37. Cell culture media for target cells.
38. Trypsin-EDTA.
39. Puromycin.

3 Methods

3.1 Making Empty CRISPR Vector Stocks

Empty vectors for both the lentiviral, wild-type Cas9 and the transient, nickase variant can be obtained commercially (i.e., from Addgene). These plasmids are shipped as bacterial stabs, and prior

to use, long-term stocks of the bacteria carrying these plasmids must be made.

1. Streak LB agar plate (with ampicillin) with bacterial stab. Insert a sterile pipet tip into the void in the stab and spread across the surface of the plate. Incubate the plate upside down overnight at 37 °C.
2. The next day, wrap the plate in Parafilm, and store it at 4 °C until you are ready to pick a colony. This stops colonies growing into one another. At the end of the day, pick a single colony on the end of a sterile pipet tip and inoculate 5 ml LB with 100 μg/ml ampicillin in a snap-cap tube. The cap should be closed only to the first stop to allow air into the tube. Incubate at 37 °C, shaking at 250 RPM overnight.
3. The next day, recover plasmid using a Plasmid Miniprep kit, according to the manufacturer protocol, using 1.5 ml of each overnight culture as input. Using the remaining volume of the overnight culture, make a glycerol stock for each culture. Mix 500 μl of each culture with 500 μl 50% glycerol in water and freeze stocks at −80 °C. These stocks can be used to generate more plasmid without having to repeat transformation of bacteria.

3.2 Designing Oligos for Gene Knockout

1. Use the sequence information for the mRNA of your target gene in the NCBI Nucleotide database (or similar resource) to determine where you want your cut to be. Ideally, this should be as close as practical to the start of the coding region of the target gene (*see* **Note 4** for further guidelines). mRNA is used since mutation of exonic sequence is the goal.
2. Take the sequence of the target region and input it into a CRISPR guide design tool. Several are available, but here we will employ CRISPOR (crispr.tefor.net [13]). Name your query and input the sequence, and select the reference genome and PAM. The default genome is *Homo sapiens* hg19; if editing non-human cells, change to your target species. The Default PAM, 20 bp-NGG/eSpCas9, is correct.
3. The results page will show all potential sgRNAs in the input sequence. Those at the top have a higher quality score, which reflects specificity, and each guide has two measures of predicted editing efficiency. If there is an oligo with no (or very few) predicted off target cuts in exons and scores ~90 or above, you may wish to choose a single sgRNA and use the WT Cas9 system (to be described in Subheading 3.3). If all guides have undesired potential off-target cut sites, another region of sequence can be tried, or else two sgRNAs may be selected for use in the Cas9 Nickase system, outlined in Subheading 3.4. Annotated examples of CRISPOR outputs for the apoptosis

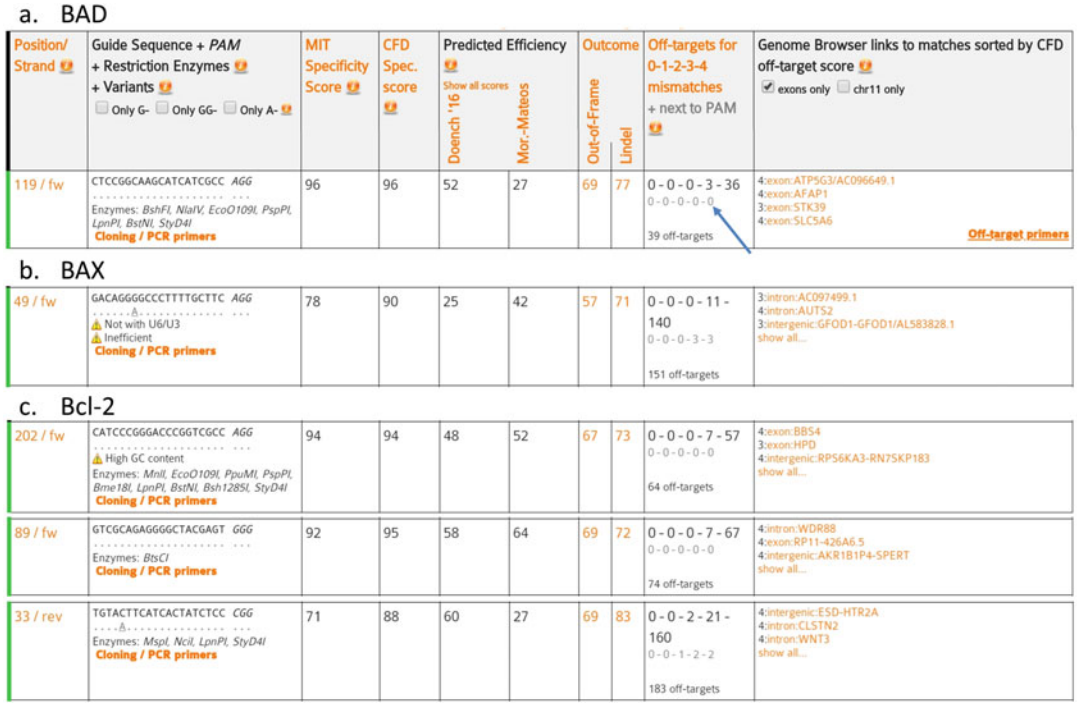

Fig. 3 Sample outputs from CRISPOR guide searches. (**a**) Top result for the gene BAD. From left to right, the position of the guide in the query sequence and which strand it is on, the guide sequence, two specificity scores (higher is better), two efficiency scores (higher is better), the predicted percentage of mutations after cutting, and the numbers and identities of potential off-target cuts. This guide has high scores for specificity, though the efficiency may be lower than ideal. However, there are only 39 off-target sites, only four of which are in exons of other genes (seen by checking the "exons only" box at right). Importantly, no off-target sites have perfect sequence match within 12 bp of the PAM site (grey numbers indicated by blue arrow), reducing the chance of cutting at those sites. This guide is acceptable for use with the WT Cas9 system. (**b**) Top CRISPOR result for the gene BAX. Guide is not compatible with U6 promoter found in all plasmids in this chapter, is inefficient, and has too many off-target sites, including some with perfect matches near the PAM. Selecting a downstream sequence produces better results for BAX. (**c**) Top result for Bcl-2 is a long way from the start codon (position 202) and has 64 off-targets. Looking through additional guides reveals two (89 fw and 33 rev) with appropriate spacing and orientation to use the nickase system. They have more off-target sites, but none in the same exon as one another, meaning no off-target double strand breaks are predicted

genes BAD, BAX, and Bcl2 are shown in Fig. 3. When selecting two guides, the 5′ guide should be in the reverse orientation, and the 3′ guide forward, what is referred to as the "PAM out" configuration, in order to maximize cutting efficiency. Also, the nick sites should be 37–68 bp apart. Nick sites are 3 bp upstream of the PAM (Fig. 3c).

4. Order or synthesize oligos. For each 20 nt target sequence, a complementary oligo must also be obtained to make a DNA duplex. In order to enable cloning into the plasmids used, additional nucleotides must also be added to the ends:

   Sense: 5′-CACC***G*** XXXXXXXXXXXXXXXXXXX-3′.

Antisense: 5′-AAAC YYYYYYYYYYYYYYYYYYY *C*-3′.

where Xs represent the 20 nt guide, and Ys represent its reverse complement. Do not include the 3 nt PAM sequence. This will leave the correct sticky ends for ligation into any of the plasmids. The additional C-G base pair (italicized) is needed for transcription from the U6 promoter.

3.3 Creation of WT Cas9 Plasmid

Once oligos have been designed, ordered, and received, the construction of a WT Cas9 plasmid is fairly rapid. The protocol below outlines the procedure to cut the empty vector and remove a filler sequence and replace it with the oligos targeting your gene of interest. The protocol is adapted from one originally published by Feng Zhang's laboratory [14, 15]. Following sequence verification, the plasmid can be used in one of two ways: production of lentiviral particles for transduction of target cells or direct transfection into target cells.

1. Prepare oligos (sense and anti-sense) for insertion: Resuspend oligos to 100 μM concentration. Run phosphorylation and annealing reaction for each oligo pair:

   1 μl sense Oligo (100 μM).
   1 μl anti-sense Oligo (100 μM).
   1 μl 10× T4 Ligase Buffer.
   6.5 μl ddH_2O.
   0.5 μl T4 PNK.

   Incubate at 37 °C for 1 h, then 95 °C for 5 min, then ramp down to 25 °C at 0.1 °C/s (*see* **Note 5**)

2. Perform restriction digestion and dephosphorylation of the pLentiCRISPRv2 vector:

   X μl pLentiCRISPRv2 plasmid (use 5 μg).
   3 μl BsmBI restriction enzyme.
   6 μl restriction enzyme buffer (e.g., NEBuffer 3.1).
   3 μl Alkaline phosphatase.
   0.6 μl DTT.
   X μl nuclease-free water to 60 μl total volume.
   Incubate at 37 °C for 1 h. *See* **Note 6**.

3. Run the digest product from **step 2** on an agarose gel (1.2% w/v agarose in TAE buffer) to separate the ~1.9 kB filler from the vector backbone. Excise only the backbone—the larger band—using a clean razor blade. Perform gel extraction using a Gel Extraction Kit according to the manufacturer protocol and elute in 30 μl water (*see* **Note 7**).

4. Ligate annealed oligos from **step 1** into vector backbone eluted in **step 3**:

   1 μl 10× T4 Ligase Buffer.
   1 μl T4 Ligase.
   1 μl annealed Oligo from **step 1** (diluted 1:100; *see* **Note 8**).

7 μl Purified digest product (eluted in **step 3**).
Incubate at room temperature for 1 h.

5. Transform competent *E. coli*. Thaw one vial per ligation on ice, add 5 μl ligation product from **step 4** to corresponding vial, and mix by gently flicking tube. Incubate 30 min on ice, heat shock at 42 °C for 30 s, then return to ice 2 min. Add 400 μl SOC medium to the vial and incubate 1 h at 250 RPM, 37 °C. Spin down at 300 × *g* for 3 min, gently resuspend in 200 μl LB and spread on LB-Amp plate. Incubate upside-down overnight at 37 °C.
6. The next day, store plates at 4 °C, wrapped in parafilm to seal. At the end of the day, pick single colonies and inoculate 5 ml overnight cultures in LB with ampicillin.
7. The next day, recover plasmid using Plasmid Miniprep kit and make glycerol stocks as described in Subheading 3.1.
8. Verify correct insertion by sequencing the completed plasmid, using the following primer: 5′- CAGGGACAGCAGAGATC CAGTTTGG-3′ (**item 7** in Subheading 2.2).

At this point, the plasmid can be used for knockout of the gene of interest in target cells. If directly transfecting target cells, use your standard transfection procedure for the line (*see* again **Note 3**) and skip to **step 13**. If using viral transduction, proceed to **step 9**.

9. Repeat plasmid miniprep in order to obtain >10 μg plasmid.
10. Plate 350,000 HEK293T cells in 100 mm cell culture dish in 10 ml growth medium. The next day, transfect 10 μg CRISPR plasmid, 4 μg pCMV-VSV-G, and 8 μg psPAX2. Wait 24 h, then change to 10 ml fresh media. Wait 48 h for virus production.
11. Working only in a biological safety cabinet, collect conditioned media from HEK293T cells containing assembled viral particles. Centrifuge for 2 h at 23,000 RPM to pellet virus (using a swinging bucket rotor, RCF is variable but should reach ~85,000 × *g* at the pellet). In the safety cabinet, carefully decant supernatant and resuspend viral pellet in HBSS. Typically, viral pellet obtained from 10 ml media is resuspended in 100 μl HBSS.
12. Optional: Add fresh media to the HEK293T cells and grow an additional 24 h to make more virus, and then repeat **step 11**.
13. Add 100 μl of resuspended viral pellet to target cells plated in T25.
14. The day after transfection/transduction, change medium and add puromycin at the predetermined selection concentration. Grow cells for six passages in puromycin. We have found that six cycles are often sufficient to produce a knockout cell

population without clonal expansion from single cells. However, not all cells will have the exact same change in sequence. If a clonal line is desired, proceed to Subheading 3.5.

3.4 Creation of Cas9 Nickase Plasmid

As mentioned in Subheading 3.2, if all guides obtained from CRISPOR have undesired potential off-target cut sites, then two sgRNAs (sgRNA 1 and sgRNA 2) should be selected for use in the Cas9 Nickase system. Construction of a nickase plasmid is more involved than a WT Cas9 plasmid. The two vectors used, referred to hereafter as pX461 and pX462, carry different selection markers—EGFP and Puromycin resistance, respectively. By the end of the procedure, one single vector will be produced, containing only one of these markers. As the nickase requires two guides to work, it is advisable to insert each guide into a different vector. Once this initial step is complete (largely similar to the WT Cas9 protocol above), one guide RNA cassette is copied and inserted into the opposite vector (Fig. 4). By having each guide in a different backbone, if at a later date a final plasmid with the opposite selection is needed, only the second half of the procedure need be repeated.

1. Prepare oligos for insertion: Resuspend oligos to 100 μM concentration. Run phosphorylation and annealing reaction for each oligo pair:

   1 μl sgRNA 1 (100 μM).
   1 μl sgRNA 2 (100 μM).
   1 μl 10× T4 Ligase Buffer.
   6.5 μl nuclease-free water.

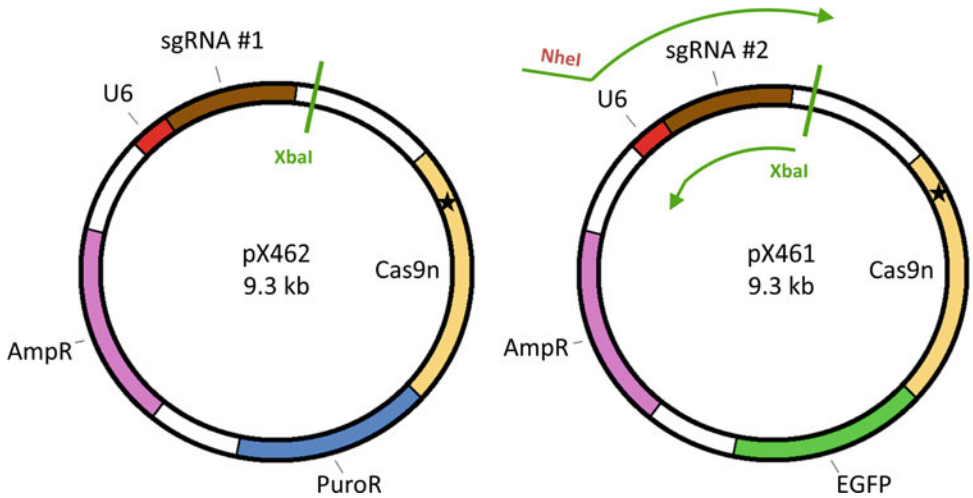

Fig. 4 Procedure for combining nickase vectors. The final backbone is selected on the basis of selectable marker—PuroR has been chosen in this example—and cut with XbaI. sgRNA #2 is PCR amplified, including the XbaI restriction site and adding a novel NheI site. These two restriction enzymes yield identical sticky ends, allowing ligation into the XbaI site in the destination vector, destroying the NheI site

0.5 μl T4 PNK.
Incubate at 37 °C for 1 h, then 95 °C for 5 min, then ramp down to 25 °C at 0.1 °C/s (*see* **Note 5**)

2. Digest pX461 and pX462 with BbsI, one reaction for each plasmid:

   5 μl Restriction enzyme Buffer.
   X μl Plasmid (2 μg).
   1 μl BbsI HF.
   X μl ddH_2O (to 50 μl total).
   Incubate at 37 °C for 1 h.

3. Perform reaction cleanup on digest products, using a PCR Purification Kit, following manufacturer protocol. The filler sequence removed is smaller than the size cutoff of the columns, and will not carry through to the elution.

4. Ligate annealed oligos into vectors—one each into pX461 and pX462:

   1 μl 10× T4 Ligase Buffer.
   1 μl T4 Ligase.
   1 μl annealed Oligo from **step 1** (diluted 1:100; *see* **Note 8**).
   7 μl Purified digest product from **step 3**.
   Incubate at room temperature for 1 h.

5. Transform competent *E. coli*. Thaw one vial per ligation on ice, add 5 μl ligation product to corresponding vial, and mix by gently flicking tube. Incubate 30 min on ice, heat shock at 42 °C for 30 s, then return to ice 2 min. Add 400 μl SOC medium to the vial and incubate 1 h at 250 RPM, 37 °C. Spin down at 300 × *g* for 3 min, gently resuspend in 200 μl LB and spread on LB-Amp plate. Incubate upside-down overnight at 37 °C.

6. The next day, store plates at 4 °C, wrapped in parafilm to seal. At the end of the day, pick single colonies and inoculate 5 ml overnight cultures in LB with ampicillin.

7. The next day, recover plasmid using Plasmid Miniprep kit and make glycerol stocks as described in Subheading 3.1.

8. Run a diagnostic digest to screen for correct insertion. If your oligos have been correctly inserted, the BbsI sites you used to do so will be eliminated, so BbsI should no longer cut your plasmid. Therefore cutting with NotI and BbsI should give a single ~9.2 kb band if your insert is right, and 3 kb and 6.2 kb bands if your plasmid does not have the insert.

   5 μl CutSmart Buffer.
   1 μl NotI.
   1 μl BbsI HF.
   X μl Plasmid (2 μg).
   X μl ddH_2O (to 50 μl total).
   Incubate at 37 °C, 1 h.

9. Run digest product on an agarose gel (1.2% w/v agarose in TAE buffer), and analyze bands. Send any plasmids showing a single 9.2 kb band for sequencing to verify they are correct. Sequencing primers are those listed in **item 8** Subheading 2.2 (Forward: 5′-CGGCCTTTTTACGGTTCCTGGC -3′; Reverse: 5′-GTTGGGCGGTCAGCCAGG-3′).

   At this point, you will have two plasmids with different selection markers. The next step is to create a single vector containing both guide RNAs so only one selection strategy need be used. For this step, decide which marker to use. pX461 carries EGFP, pX462 carries puromycin resistance (*see* **Note 9**). The plasmid bearing whichever marker you want to *keep* will now be referred to as Plasmid/sgRNA **#**1. The other will be Plasmid/sgRNA #2.

10. Make more Plasmid #1. Inoculate a small chunk of glycerol stock into 6 ml LB with 100 μg/ml ampicillin, grow overnight at 37 °C, 250 RPM, and the next day perform four minipreps in parallel as described in **step 7** above. Use the same 50 μl water for all four elutions to get concentrated plasmid.

11. Run PCR reaction to amplify sgRNA #2 cassette, using Plasmid #2 as template. Using the primers listed in **item 9** Subheading 2.2 (Forward: 5′-CACCGCTAGCGAGGGCCTATTTCCCATGATTCCTTC -3′;

    Reverse: 5′-GTACCTCTAGAGCCATTTGTCTGCAG-3′) will add the needed restriction sites to allow cloning sgRNA #2 into Plasmid #1:

    X μl Plasmid #2 (100 ng).
    5 μl Pfu Buffer.
    2 μl dNTPs.
    1 μl Forward primer:
    1 μl Reverse primer.
    1 μl Pfu Ultra II polymerase.
    X μl nuclease-free to 50 μl total volume.

    Amplify using the following cycling conditions: 95 °C 2 min; 30 cycles of 95 °C for 20 s, 56 °C for 20 s, 72 °C for 1 min; 72 °C for 3 min. *See* **Note 10**.

12. Run the PCR product on a 1.2% agarose gel to separate the PCR product from the plasmid template and excise only the product using a clean razor blade. Perform gel extraction using a Gel Extraction Kit according to the manufacturer protocol (*see* **Note 7**).

13. Run digests on Plasmid #1 and sgRNA #2 PCR product:

X μl Plasmid #1 (5 μg)	*X* μl PCR product (2 μg)
5 μl Restriction Enzyme Buffer	5 μl Restriction Enzyme Buffer
2.5 μl XbaI	1 μl XbaI

(continued)

X µl nuclease-free water (to 50 µl total)	1 µl NheI
	X µl nuclease-free water (to 50 µl total)

Incubate 37 °C, 1 h

14. Add 1 µl CIP/rSAP phosphatase to Plasmid #1 digest to dephosphorylate ends, and incubate another hour at 37 °C (*see* **Note 11**).
15. Run reaction cleanup on both digest products, as described in **step 3**.
16. Do ligation of sgRNA #2 into Plasmid #1:

    X µl plasmid #1 digest.
    Y µl sgRNA #2 digest (use equal masses of these two; *see* **Note 12**).
    1 µl 10× T4 Ligase Buffer.
    1 µl T4 Ligase.
    Incubate at room temp at least 1 h.
17. Transform competent *E. coli* as in **step 5**, using 5 µl ligation mix. Plate cells onto LB agar plates with 100 µg/ml ampicillin and incubate overnight at 37 °C.
18. The next day, pick single colonies and grow overnight in 5 mL LB broth with ampicillin.
19. The next day, do minipreps and make glycerol stocks for each culture, as described in **step 7**. Determine plasmid concentrations by absorbance at 260 nm.
20. Run a diagnostic digest to look for insertion of a second sgRNA cassette. Cutting your plasmid with KpnI and NotI will produce a 6 kb band and either a 3.1 kb band (one sgRNA) or a 3.6 kb band (both sgRNAs—successful insertion). Run a digest of Plasmid #1 from before ligation as a negative control:

    5 µl CutSmart Buffer.
    1 µl KpnI HF.
    1 µl NotI HF.
    X µl plasmid (1 µg).
    X µl nuclease-free water (to 50 µl total).
    Incubate at 37 °C, 1 h.
21. Run digest products on a 1.2% agarose gel, and look for correct banding pattern. Send those that show 6 kB and 3.6 kB bands for sequencing to confirm, using the same primers as in **step 9**. The forward primer will read the first sgRNA cassette going forwards, and the reverse primer will read the second sgRNA going backwards (*see* **Note 13**).

22. If sequencing is correct, plasmid is ready to use for transient transfection.

    At this point, you can transfect your plasmid into the target cells. The following steps assume transfection of adherent cells. Your target cells may require optimization of transfection that would alter the timing of these steps (*see* **Note 3**).

23. Plate cells in two T25 flasks, such that cells will reach ~70% confluence the following day.
24. The next day, transfect 5 μg plasmid into one flask of cells in OptiMEM medium. To the other flask, add transfection reagent only, without plasmid, as a control for selection. After 4–6 h, replace medium with normal growth medium.
25. The following day, begin selection. For puromycin, add drug to both flasks and monitor flasks and discontinue puromycin selection when all control cells are dead. For GFP, perform flow-assisted cell sorting for green cells at optimum time post transfection, using control cells to set gates for negative GFP expression. *See* **Notes 14** and **15** for additional details.

You may find that the short (~5 days) window for selection is not sufficient to give robust knockout. If this is the case, you can try clonal expansion, discussed in the next section, to obtain a pure knockout population. The resulting cell line will also be genetically identical.

3.5 Derivation of Clonal Knockout Cell Lines

It is often desirable to have a homogeneous cell population that is genetically identical. The exact genetic changes in the target cells, both on- and off-target, can then be determined by sequencing. The following procedure will allow you to find single-cell-derived clonal lines.

1. After selection, trypsinize and count cells. Pellet cells and resuspend in growth medium to 100,000 cells/ml to break up pellet (Suspension 1). Perform a 100-fold dilution to make Suspension 2 (1000 cells/ml), and a second 100-fold dilution for a final concentration of 10 cells/ml in 10 ml total volume (Suspension 3).
2. Aliquot 100 μl of Suspension 3 to each well of a 96-well plate, with the exception of well A1.
3. To A1, add 90 μl medium and 10 μl of Suspension 1, for ~1000 cells in this well. This will allow for easy focusing of a microscope.
4. Monitor wells under the microscope to find wells with one cluster of cells growing, indicating a single cell of origin.
5. As cells reach confluence, passage all cells from a well to one well of a 24-well plate, then to a 6-well plate.

6. As you expand cells from the 6-well plate, harvest cells and verify knockout by western blot and sequencing analyses.

4 Notes

1. Original work in our laboratory was performed with the original pX462 (i.e., Addgene #48141). We, however, recommend pX462 V2 (i.e., Addgene #62987). This plasmid is an improved version that, according to the depositors, fixes a mutation in the puromycin resistance gene, yielding superior selection.
2. Enzymes from other manufacturers may also work. The original protocol from Feng Zhang et al. on which these procedures are based utilizes enzymes from Fermentas. However, all listed enzymes except for BsmBI are available from NEB in "HF" forms that minimize unwanted activity and all cut in a single buffer, facilitating double digests required in this protocol.
3. Transfection should be optimized for your cell line of interest. Existing protocols for transfection within your laboratory should be tried first, but in the event of low efficiency, or no prior protocol, suggestions are given here: We have had success with polyethyleneimine or XtremeGene9 in the past. It may also be worth trying to transfect cells either in suspension prior to plating or 24 h post-seeding in attachment conditions. Transfection efficiency of cells can be assessed by looking for the expression of a plasmid-borne fluorescent reporter by microscopy.
4. As a general starting point, it is advisable to use the sequence from the ATG start codon to the end of the exon in which it is found as the region to search for cut sites. However, for genes with alternate transcripts or splicing variants that have a secondary start codon, the cut site should be after this second ATG if full knockout is the goal. Sequence should be confined to a single exon.
5. If your thermal cycler is unable to ramp down in this manner, then most gradual ramp down in temperature may suffice. Alternatively, following 37 °C incubation, the reaction tube can be placed in a 95 °C heat block for five minutes. Once the 5 min has elapsed, remove the entire metal block from the heating unit, and place it on the benchtop. It will slowly cool to ambient temperature. If the block cannot be removed, turning the unit off will also slowly cool the reaction, though it will take longer. Note that as per the original protocol from the Zhang laboratory, the buffer for T4 Ligase should be used as it includes the ATP required by PNK.

6. For best results, use freshly prepared DTT. Also, BsmBI cuts optimally at 55 °C, but we have found that 1 h at 37 °C yields sufficient cutting. If your yield appears low, NEB offers the enzyme Esp3I, which has the same cut pattern as BsmBI but will cut at 37 °C in CutSmart buffer. Note also that NEB will be discontinuing BsmBI in favor of a re-engineered BsmBI-v2 in 2020, but this enzyme will still require Buffer 3.1.
7. A key to successful gel extraction is minimizing the amount of excess (empty) gel input into the reaction. If you do not possess a comb with wells large enough to accommodate the entire PCR reaction volume, plus loading dye, do not run multiple lanes side by side, as the gaps in between become wasted space, or else have to be removed. To save time and effort, use laboratory tape to join neighboring teeth of the comb together to form one larger tooth, yielding a single well on the gel.
8. The original protocol from the Zhang laboratory suggests 1:200, but we have found that 1:100 gives greater yield.
9. Where possible, our laboratory has used puromycin resistance as our marker of choice. This selection strategy eliminates the need for FACS sorting of green cells, meaning the only additional expense is purchasing puromycin. If the target cell line already expresses one of these markers, the opposite should be used for CRISPR.
10. You can substitute the PCR reagents of your choice; however, we recommend a polymerase, such as Pfu Ultra II Fusion, that has proofreading ability to prevent unwanted mutations in the finished plasmid product.
11. We recommend restriction enzymes and either calf intestinal phosphatase (CIP) or recombinant shrimp alkaline phosphatase (rSAP) from New England Biolabs. Either enzyme will work in the CutSmart buffer used in the preceding digestion reaction.
12. A useful rule of thumb for ligation is to have at least a tenfold molar excess of insert over vector backbone. The insert is approximately 24 times smaller than the backbone (~450 bp vs ~9 kb), so using equal masses will give a 24 molar excess of insert, which we have found works well. To determine volumes for the reaction, use the following two equations:

$$X + Y = 8$$

X * plasmid concentration = Y * insert concentration

13. This digest will determine if the second guide has been inserted, but not in which orientation it has been inserted. If you wish to confirm orientation by diagnostic digest, a digest can be run with NotI and XbaI. If the two sgRNA cassettes are

in the same orientation, the same 6 kB + 3.6 kB banding pattern will appear. If a 6 kB + 3.1 kB pattern appears, the second guide is in the reverse orientation. Sequencing will also confirm orientation. We have exclusively obtained and used plasmids in which both guides are in the same orientation and recommend doing the same.

14. Selection conditions should be optimized ahead of time. For puromycin, cells should be treated with various concentrations of puromycin to determine a dose that will kill sensitive cells within 5 days. 0.5–5 μg/ml is a helpful range to begin.
15. It is helpful to do a time course experiment in the target cells ahead of time, transfecting with empty parental pX461 vector and observing transfected cells for strength of GFP expression over time. The time of maximal expression should be noted. Following transfection of the target cells with the finished CRISPR vector, cells should be incubated for the same length of time prior to cell sorting. Non-transfected cells in the control flask will not express GFP, and so can be useful as a way to gate GFP positivity. In the event that transfection efficiency is poor and too few cells are positive for a successful sort, transfection can be scaled up using proportionally larger numbers of cells, higher volume of transfection mix, and appropriate plasticware (e.g. 100 mm dishes or T75 flasks).

Acknowledgments

Support for the research of which the design and optimization of these protocols was a part was provided by American Cancer Society Postdoctoral Fellowship 131420-PF-17-236-01-DMC.

References

1. Chylinski K, Makarova KS, Charpentier E, Koonin EV (2014) Classification and evolution of type II CRISPR-Cas systems. Nucleic Acids Res 42(10):6091–6105. https://doi.org/10.1093/nar/gku241
2. Barrangou R (2015) The roles of CRISPR-Cas systems in adaptive immunity and beyond. Curr Opin Immunol 32:36–41. https://doi.org/10.1016/j.coi.2014.12.008
3. Deltcheva E, Chylinski K, Sharma CM, Gonzales K, Chao Y, Pirzada ZA, Eckert MR, Vogel J, Charpentier E (2011) CRISPR RNA maturation by trans-encoded small RNA and host factor RNase III. Nature 471 (7340):602–607. https://doi.org/10.1038/nature09886
4. Jinek M, Chylinski K, Fonfara I, Hauer M, Doudna JA, Charpentier E (2012) A programmable dual-RNA-guided DNA endonuclease in adaptive bacterial immunity. Science 337 (6096):816–821. https://doi.org/10.1126/science.1225829
5. Cong L, Ran FA, Cox D, Lin S, Barretto R, Habib N, Hsu PD, Wu X, Jiang W, Marraffini LA, Zhang F (2013) Multiplex genome engineering using CRISPR/Cas systems. Science 339(6121):819–823. https://doi.org/10.1126/science.1231143
6. Mali P, Yang L, Esvelt KM, Aach J, Guell M, DiCarlo JE, Norville JE, Church GM (2013) RNA-guided human genome engineering via Cas9. Science 339(6121):823–826. https://doi.org/10.1126/science.1232033

7. Guirouilh-Barbat J, Huck S, Bertrand P, Pirzio L, Desmaze C, Sabatier L, Lopez BS (2004) Impact of the KU80 pathway on NHEJ-induced genome rearrangements in mammalian cells. Mol Cell 14(5):611–623. https://doi.org/10.1016/j.molcel.2004.05.008
8. Durai S, Mani M, Kandavelou K, Wu J, Porteus MH, Chandrasegaran S (2005) Zinc finger nucleases: custom-designed molecular scissors for genome engineering of plant and mammalian cells. Nucleic Acids Res 33 (18):5978–5990. https://doi.org/10.1093/nar/gki912
9. Maeder ML, Thibodeau-Beganny S, Osiak A, Wright DA, Anthony RM, Eichtinger M, Jiang T, Foley JE, Winfrey RJ, Townsend JA, Unger-Wallace E, Sander JD, Muller-Lerch F, Fu F, Pearlberg J, Gobel C, Dassie JP, Pruett-Miller SM, Porteus MH, Sgroi DC, Iafrate AJ, Dobbs D, McCray PB Jr, Cathomen T, Voytas DF, Joung JK (2008) Rapid "open-source" engineering of customized zinc-finger nucleases for highly efficient gene modification. Mol Cell 31(2):294–301. https://doi.org/10.1016/j.molcel.2008.06.016
10. Miller JC, Tan S, Qiao G, Barlow KA, Wang J, Xia DF, Meng X, Paschon DE, Leung E, Hinkley SJ, Dulay GP, Hua KL, Ankoudinova I, Cost GJ, Urnov FD, Zhang HS, Holmes MC, Zhang L, Gregory PD, Rebar EJ (2011) A TALE nuclease architecture for efficient genome editing. Nat Biotechnol 29 (2):143–148. https://doi.org/10.1038/nbt.1755
11. Zhang F, Cong L, Lodato S, Kosuri S, Church GM, Arlotta P (2011) Efficient construction of sequence-specific TAL effectors for modulating mammalian transcription. Nat Biotechnol 29(2):149–153. https://doi.org/10.1038/nbt.1775
12. Ran FA, Hsu PD, Lin CY, Gootenberg JS, Konermann S, Trevino AE, Scott DA, Inoue A, Matoba S, Zhang Y, Zhang F (2013) Double nicking by RNA-guided CRISPR Cas9 for enhanced genome editing specificity. Cell 154(6):1380–1389. https://doi.org/10.1016/j.cell.2013.08.021
13. Haeussler M, Schonig K, Eckert H, Eschstruth A, Mianne J, Renaud JB, Schneider-Maunoury S, Shkumatava A, Teboul L, Kent J, Joly JS, Concordet JP (2016) Evaluation of off-target and on-target scoring algorithms and integration into the guide RNA selection tool CRISPOR. Genome Biol 17(1):148. https://doi.org/10.1186/s13059-016-1012-2
14. Sanjana NE, Shalem O, Zhang F (2014) Improved vectors and genome-wide libraries for CRISPR screening. Nat Methods 11 (8):783–784. https://doi.org/10.1038/nmeth.3047
15. Shalem O, Sanjana NE, Hartenian E, Shi X, Scott DA, Mikkelson T, Heckl D, Ebert BL, Root DE, Doench JG, Zhang F (2014) Genome-scale CRISPR-Cas9 knockout screening in human cells. Science 343(6166):84–87. https://doi.org/10.1126/science.1247005

Chapter 19

Determining Cell Death Pathway and Regulation by Enrichment Analysis

Katherine Gurdziel

Abstract

Bioinformatics tools and resources are valuable for the analysis of data sets focusing on programmed cell death. This chapter discusses methods for the generation of gene sets as well as enrichment analysis using publicly available databases.

Key words Programmed cell death, Gene ontology, Enrichment analysis

1 Introduction

Resistance to programmed cell death (PCD) is acquired by many cancer types, which make determination of induced or altered PCD signaling pathways critically important [1]. Classification of cell death pathways in global expression datasets is well suited to functional enrichment analysis. Enrichment analysis involves detection of over-representation of members from gene sets that have an association to particular biological functions. Enrichment analysis to determine PCD mechanisms can be applied using both publicly available tools and by applying appropriate statistical tests after data-mining repositories to generate relevant associations to novel biological questions.

1.1 Enrichment Analysis

Understanding the functional significance of genes linked to a phenotype is critical to determining biological significance. Functional enrichment analysis performs a statistical test for overrepresentation by querying a gene list against sets of genes with established biological associations to determine if more genes from the list occur in a gene sets than expected by chance. This is analogous to measuring the probability of the frequency of successes in a finite number of draws, without replacement, from a finite population size that contain a percentage of objects of

Ayesha B. Alvero and Gil G. Mor (eds.), *Detection of Cell Death Mechanisms: Methods and Protocols*, Methods in Molecular Biology, vol. 2255, https://doi.org/10.1007/978-1-0716-1162-3_19,

interest. By applying a one-tailed variant of Fisher's exact test (hypergeometric test), it is possible to verify if genes of interest are more often associated to certain biological functions than what would be expected in a random set of genes by comparing the count the frequency (k) of genes in the list (n) that are associated to the biological gene set, and the frequency (K) of genes in the population set (N) that are associated to the same set. By comparing the likelihood of obtaining at least k genes associated to the biological gene set if n genes were randomly sampled from the population, given the frequency K and size N of the population establishes the probability of observing the sample frequency, given the population frequency.

Each gene set comparison results in a p-value indicating the probability that there is no difference between the observed frequency of the occurrence of genes from the gene set in the list and the frequency expected by chance. Since multiple comparisons are conducted between the list and different gene sets, the probability of encountering a false positive is increased and a correction needs to be made for to account for the multiple testing. False-Discovery Rate correction (FDR) adjusts p-values to lower the proportion of false positives [2].

1.2 Gene Sets

1.2.1 Predefined Gene Sets GO

The complexity of data generated by high-throughput sequencing created a need to interpret biological relevance from global datasets. The Gene Ontology consortium was founded to classify the function of genes into Gene Ontology terms (GO) by creating a structured, controlled vocabulary for the classification of gene function at the molecular and cellular level [3]. GO terms comprise gene sets based on the experimentally derived shared function of each gene member of the set. Terms relating to PCD (GO:0012501) are annotated under the biological process category and include the major cell death pathways (Table 1).

Although creation of new annotations and inclusion of additional genes to existing terms occurs continuously to keep up with published work, the information contained in the GO database should be considered incomplete with some unevenness resulting from underrepresented regions of scientific focus. Apoptotic processes have been extensively studied with ferroptosis is a relatively recently discovered mechanism of PCD [4]. For this reason, it is important to note for GO analysis that absence of evidence of function does not imply absence of function.

1.2.2 Defining Gene Sets Using Data Mining

GO is focused on gene function and does not incorporate noncoding RNAs (ncRNAs), which have been shown to influence the occurrence and development of several diseases [5]. ncRNAs mediate gene expression by transcriptional and post-transcriptional regulation [6] and have an established role in regulation of cell death [7, 8]. Data repositories for ncRNAs involved in cell death

Table 1
Gene Ontology terms affiliated with major cell death pathways. Gene members indicates the total number of genes in each GO term

PCD category	GO term	Gene members
Apoptotic process	GO:0006915	1879
Autophagic cell death	GO:0048102	12
Cornification	GO:0070268	4
Ferroptosis	GO:0097707	2
Mitochondria outer membrane premeabilization	GO:1902686	34
Necrotic cell death	GO:0097300	41
Pyroptosis	GO:0070269	20

processes can be used to establish gene sets for evaluating regulatory mechanisms of PCD [9].

2 Methods

The following methods provide stepwise instructions for using enrichment analysis either with the publicly available DAVID GO webtool, which allows a user to test for enrichment in their gene list using the database of GO terms or for generating gene sets derived from available databases (ncRDeathDB) and analyzing enrichment using the R statistical environment. User gene lists can be generated from differential expression analysis (i.e., between control and treatment) that have been filtered for significance. Increasing or decreasing fold change cutoff criteria can be used to modify the size of the gene list. The output for both enrichment analyses will include enrichment scores with statistical assessments.

2.1 DAVID Bioinformatics Database

DAVID Bioinformatics Database is a GO webtool available at https://david.ncifcrf.gov/tools.jsp [10, 11]. Selecting the "Start Analysis" tab redirects the page to the GO tool. In this section, the user will determine enriched GO categories for a gene list. After filtering by multiple test corrected p-values, the GO categories can be searched for terms related to PCD.

1. Gene List—Gene lists can be generated from a differential expression analysis and must be less than 3000 genes. To achieve the target range for list size of a few hundred to a few thousand genes, it may be necessary to adjust the filtering criteria such as the magnitude of fold change or statistical cut-off criteria.

(a) Select "Upload" on the in the left pane to create a list of genes for submission.

(b) Select the proper identifier type.

(c) Select "Gene List".

(d) After submitting, you may be prompted to select the correct species if the identifier type is not species specific.

2. Background—For a differential expression analysis, filter out genes that have no counts in any of the conditions in order restrict the background to only genes that have the potential to be positive.

   (a) Select "Upload" again on the left pane to submit a list of genes for the background.

3. Select "Functional Annotation Chart".

   (a) Uncheck Check Defaults.

   (b) Open the Gene Ontology menu select GOTERM_B-P_ALL (Cell death GO:0008219 is classified as a biological process).

4. Data output.

   (a) Clicking "Functional Annotation Chart" button will open a new window with the results.

   (b) Right click on "Download File" to save the output.

   (c) The output contains the following information.

   - Category—records the original annotation source of the term.
   - Term—a descriptor of the gene set evaluated for enrichment.
   - Count—total number of genes from the gene list that were found in the gene set.
   - %—percentage of genes from the submitted gene list that appear in the gene set. Redundant identifiers are removed from the total count. For example, if three gene transcripts for the same gene were included in the gene list.
   - PValue—Modified Fisher Exact *p*-value.
   - Genes—names of the members of the gene list that were found in the gene set.
   - List Total—number of genes in the gene list contained within the annotation source.
   - Pop Hits—number of genes from the background list that belong to the gene set.
   - Pop Total—total number of genes in the background list that are contained within the annotation source.

- Fold Enrichment—(Count/List Total)/(Pop Hits/Pop Total)
- Multiple correction tests (Bonferroni, Benjamini, FDR on a 0–100 scale).

5. Evaluation/Interpretation of the results.

2.2 Enrichment of Genes Regulated by Known PCD Elements

ncRDeathDB is a publicly available database containing annotations for ncRNAs that have been shown to influence PCD [9]. In this section, the user will create two genes sets from ncRDeathDB data that can be used to test for enrichment of PCD ncRNA regulation in a gene list.

1. If not already installed, download R the free environment for statistical computing (https://cran.r-project.org/). Select the correct download based on the operating system. In brief, the R graphical user interface (RGui) contains a console for execution of codes and an editor window for recording commands.
2. The R package "bc3net" will be used to determine enrichment.
   (a) In the editor window enter the following lines.
   - install.packages ("bc3net") #this command installs the package into R and only needs to be executed once
   - library (bc3net) #the library command loads the specified package into the environment which enables use of the package components

3. Inputting the gene lists.
   (a) GeneList <− read.txt ("UserDEGenes.txt", header = TRUE) #inputs a text document containing one gene name per line
   (b) Background <− read.txt ("UserBackground.txt", header = TRUE) #inputs a text document containing one gene name per line
4. Collecting the gene sets.
   (a) Download ncRNAs that associated with PCD http://www.rna-society.org/ncrdeathdb/
   - Select Download & API followed by the Download tab.
   - Download the text file.

   (b) Import data table into R.
   - ncData <− read.csv ("allNcRNACelldeathData.txt", sep = "\t", header = TRUE)

   (c) Subset the data into gene sets.

- HSncData <− ncData[ncData$Organism == "Homo sapiens",] #subset the database to include only human annotations
- lncHS <− HSncData[HSncData$RNA.Category == "lncRNA",]
- lncGene <− unique(lncHS[!lncHS$Gene_Symbol==“",6]) #returns unique gene symbols contained in colum 6 without including the blank entries,
- miHS <− HSncData[HSncData$RNA.Category == "miRNA",]
- miGene <−unique(miHS[!miHS $Gene_Symbol==“",6])

5. Performing the analysis.
   (a) Generate a list containing each of the gene sets.
   - ncSets <− list (lnc = lncGene, mi = miGene) #the left side of the equal sign contains the collection name,

   (b) Hypgnc <− enrichment(GeneList, Background, ncSets, adj = "fdr", verbose = TRUE).
   - Hypgnc #contains results from the enrichment function performing the comparison for the gene list against each collection.
     – TermID—collection name.
     – Genes—number of genes from the gene list.
     – All.
     – pval—*p*-value,
     – padj—*p*-value adjusted for multiple comparisons using the false discovery rate method.

References

1. Speirs CK, Hwang M, Kim S, Li W, Chang S, Varki V et al (2011) Harnessing the cell death pathway for targeted cancer treatment. Am J Cancer Res 1(1):43–61
2. Jafari M, Ansari-Pour N (2019) Why, when and how to adjust your P values? Cell J 20 (4):604–607
3. The Gene Ontology Resource (2019) 20 years and still GOing strong. Nucleic Acids Res 47 (D1):D330–D338
4. Li J, Cao F, Yin HL, Huang ZJ, Lin ZT, Mao N et al (2020) Ferroptosis: past, present and future. Cell Death Dis 11(2):88
5. Lekka E, Hall J (2018) Noncoding RNAs in disease. FEBS Lett 592(17):2884–2900
6. Wang Z (2018) Diverse roles of regulatory non-coding RNAs. J Mol Cell Biol 10 (2):91–92
7. Su Y, Wu H, Pavlosky A, Zou LL, Deng X, Zhang ZX et al (2016) Regulatory non-coding RNA: new instruments in the orchestration of cell death. Cell Death Dis 7 (8):e2333
8. Zhao M, Zhu N, Hao F, Song Y, Wang Z, Ni Y et al (2019) The regulatory role of non-coding RNAs on programmed cell death four in inflammation and cancer. Front Oncol 9:919

9. Wu D, Huang Y, Kang J, Li K, Bi X, Zhang T et al (2015) ncRDeathDB: a comprehensive bioinformatics resource for deciphering network organization of the ncRNA-mediated cell death system. Autophagy 11 (10):1917–1926
10. Huang W, Sherman BT, Lempicki RA (2009) Systematic and integrative analysis of large gene lists using DAVID bioinformatics resources. Nat Protoc 4(1):44–57
11. Huang d W, Sherman BT, Lempicki RA (2009) Bioinformatics enrichment tools: paths toward the comprehensive functional analysis of large gene lists. Nucleic Acids Res 37(1):1–13

Chapter 20

Transcription Factor–Binding Site Identification and Enrichment Analysis

Joe L. Guy and Gil G. Mor

Abstract

Transcription factors orchestrate complex regulatory networks of gene expression. A better understanding of the common transcription factors, and their shared interactions, among a set of coregulated or differentially expressed genes can provide powerful insights into the key pathways governing such expression patterns. Critically, such information must also be considered in the context of the frequency in which a transcription factor is present in a properly selected background, and in the context of existing evidence of gene and transcription factor interaction. Given the vast amount of publicly available gene expression data that can be further scrutinized by the user-friendly analysis tools described here, many useful insights are assuredly to be revealed. The proceeding methods for application of the analysis tool CiiiDER for transcription factor–binding site identification, enrichment analysis, and coregulatory factor identification should be applicable to any dataset comparing differential gene expression in response to various stimuli and gene coexpression datasets. These methods should assist the researcher in identifying the most relevant regulators within a gene set, and refining the list of targets for future study to those which may share biologically important regulatory networks.

Key words Transcription factor, DNA-binding motifs, Enrichment analysis, Gene expression

1 Introduction

The ~1600 transcription factors recognize and bind sequence-specific sites of the genome and play the central role in gene expression by interacting with regulatory regions of the genome [1]. These regulatory regions include promoters and enhancers, and transcription factors frequently co-ordinate within these regions to activate or repress transcription [2]. Given the massive impact these proteins have on cellular fate, it is of critical importance to bring to light the key figures that are responsible for alterations in transcriptional programs in the context of human disease.

Various experimental techniques are employed to improve our understanding of the specificity of transcription factors for their

Ayesha B. Alvero and Gil G. Mor (eds.), *Detection of Cell Death Mechanisms: Methods and Protocols*, Methods in Molecular Biology, vol. 2255, https://doi.org/10.1007/978-1-0716-1162-3_20,

preferred DNA-binding motifs. A common method in cell-based experiments for determining transcription factor–binding specificity involves fixation of cells with DNA-crosslinking agents, followed by chromatin immunoprecipitation and sequencing (ChIP-Seq) [3, 4]. This method has enabled a tremendous expansion of experimentally validated transcription factor–binding site (TFBS) Position Frequency Matrices (PFMs or "motifs") for hundreds of human transcription factors. Systematic evolution of ligands through exponential enrichment (SELEX) is an in vitro technique that minimizes some of the technical issues involved with ChIP-Seq data (such as indirect binding and dependence on highly specific ChIP antibodies for the transcription factor of interest) to improve the accuracy and specificity of PFM data through a process of alternate rounds of enrichment of oligonucleotides with high affinity for the transcription factor under investigation among a random pool of oligonucleotides, and amplification of bound ligands [5].

The data derived from transcription factor–binding motif experiments are commonly visualized as sequence logos that represent the underlying data stored in a PFM. Those underlying data represent a transcription factor's preference for each base position in a TFBS [2, 6]. Other models have been developed to predict TFBSs, such as those based on the shape of DNA [7], but PFMs are the most widely used. The major open-source databases rely on various experimental techniques to establish PFMs, which may be an important consideration for some researchers when determining which PFM library to use for transcription factor enrichment analysis. JASPAR database PFMs are derived from ChIP-Seq, DAP--Seq, SMILE-Seq, PBM, and HT-SELEX experiments [6]. The Jolma 2013 PFM library [8] is derived from HT-SELEX and ChIP-Seq experiments. The HOCOMOCO v11 [9] PFM library is derived from ChIP-Seq experiments.

CiiiDER [10] is a very user-friendly program that has proven to be a valuable tool for uncovering the hidden drivers of complex transcriptional programs. It performs three types of analyses. The "Scan" analysis will search the regulatory regions of genes of interest, or sequences supplied by the user, and will predict TFBS using the well-established MATCH algorithm [10, 11]. The "Enrichment" analysis reveals the key transcription factors (frequently among hundreds of others) that are over- or underrepresented in terms of their binding sites in regulatory regions of genes of interest compared to an appropriate background set. The third type of analysis, "Proximal Enrichment," highlights patterns in colocalization of transcription factors, which are calculated to occur to a greater extent in the analyzed gene set compared to background. A summary of the major analyses (Scan and Enrichment), which are explained in [10], is displayed in Fig. 1. It is worth noting that there are several high-quality web-based programs that can perform transcription factor enrichment analysis [1, 12–15], but one

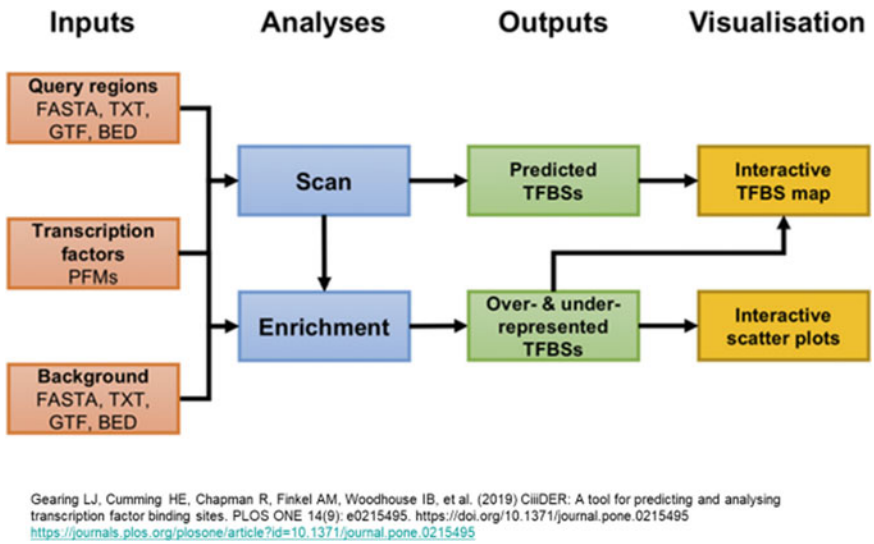

Fig. 1 Overview of CiiiDER: the workflow depicts required inputs, options for analyses (Proximal Enrichment not shown), potential outputs, and options for visualization of results. Reproduced from [10]

major distinguishing quality of CiiiDER is that it is a downloadable program, which is operating system agnostic that enables the researcher to conduct and save all analyses offline.

This chapter describes a step-by-step procedure for application of the analysis tool CiiiDER for transcription factor–binding site analysis. Three types of methods are described, including transcription factor–binding site identification, enrichment analysis, and coregulatory factor identification (proximal enrichment analysis), which are applicable to any dataset comparing differential gene expression in response to various stimuli and gene coexpression datasets.

2 Requirements

CiiiDER program acquisition and installation

- CiiiDER runs on Java and is platform agnostic.
- Download CiiiDER from ciiider.org, and select the file "CiiiDER with Human genome," which includes the human GRCh38 genome and gene look-up manager (GLM) files. The download also includes a very useful document (CiiiDER Documentation Draft) that explains in greater detail the various features and underlying statistical calculations of this tool.
- Download Java Runtime Environment (https://www.java.com/en/download/) if your operating system does not already have it installed. Note that 64-bit Java will dramatically speed up

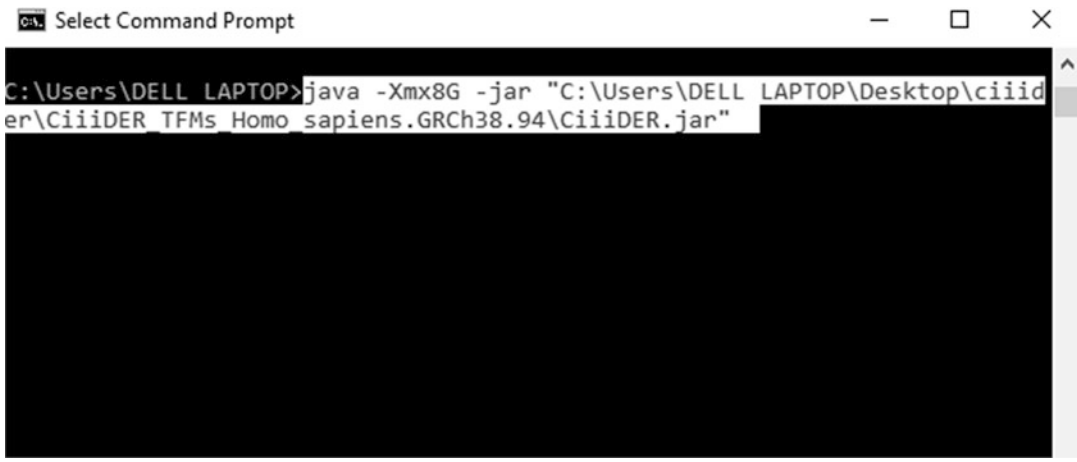

Fig. 2 Some analyses performed in CiiiDER require a large amount of memory to be performed efficiently. Using Terminal or Command Prompt, the user can run the CiiiDER jar file with additional memory using the indicated command. This command specifies the maximum size of the memory allocation pool (8G, for instance, translates to 8 GB of memory) for the application. Note that, based on the author's experience, the 64-bit version of JRE enables the user to specify a larger memory allocation pool. Otherwise, an error message such as "could not create the Java Virtual Machine" may be encountered with the 32-bit installation of JRE

analyses, but the program must be initiated in the Command Prompt (per the below instructions):

- In Windows, this is achieved by pressing the "Window" + "R" buttons simultaneously on the keyboard to open the "Run" box, and then typing "cmd" and clicking "OK."
- In the command line, enter the following: java -Xmx8G -jar "C:\ ~ \ciiider\CiiiDER_TFMs_Homo_sapiens.GRCh38.94 \CiiiDER.jar"; note that the contents of the quotations will be specific to the file path of the CiiiDER.jar file on the end user's machine, and note that the quotations must be typed into the command line. Figure 2 provides an example of the entry in Command Prompt.

3 Methods

3.1 Transcription Factor–Binding Site Identification

This analysis is useful for determining whether promoters or other regulatory regions (as defined by the user) contain TFBSs for transcription factors of interest to the user.

1. The user opens the CiiiDER.jar file in the "CiiiDER_TFMs_Homo_sapiens.GRCh38.94" subfolder.
2. Click on the "Start" button at the center of the window.
3. On the next window (Fig. 3), the user can choose to upload a list of ENSEMBL IDs or gene names that have been pasted

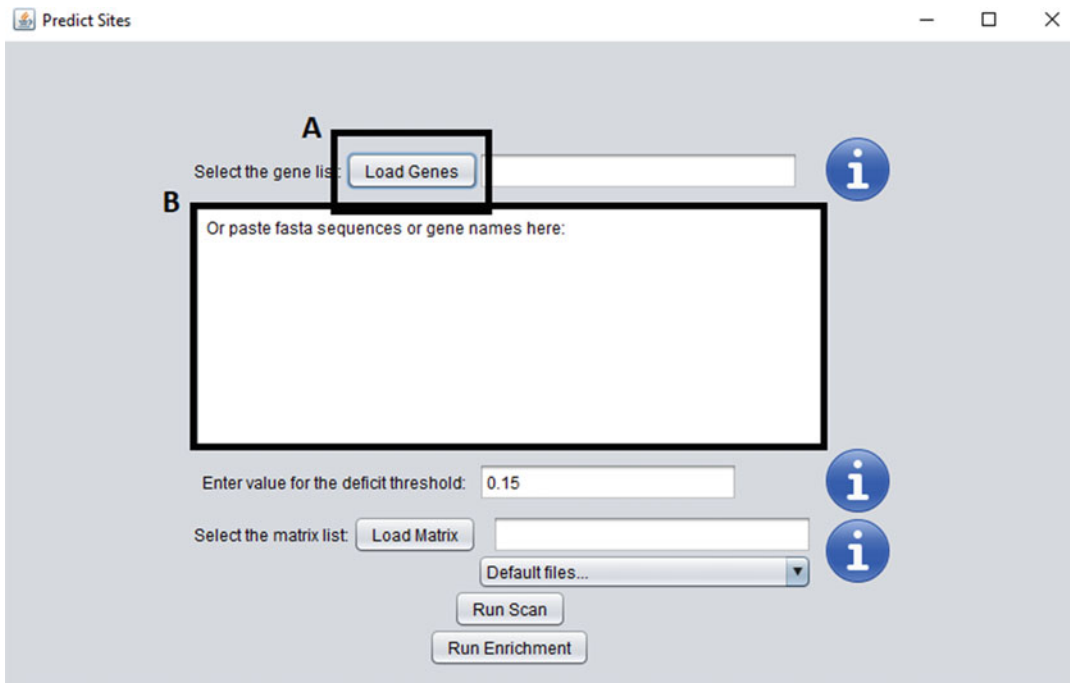

Fig. 3 The user can upload a list of ENSEMBL IDs or gene names that have been pasted into a .txt file to identify putative TFBSs, or the user can analyze specific sequences by uploading a list of sequences in FASTA format in a .txt file, using the "LOAD GENES" button (selection A). Alternatively, the user can simply type or paste a list of gene names or FASTA sequences in the text box (selection B)

into a .txt file, or a list of sequences in FASTA format in a .txt file, using the "LOAD GENES" button (selection A). Alternatively, the user can simply type or paste a list of gene names or FASTA sequences in the text box (selection B).

4. CiiiDER will recognize the input information, and the GUI will either be updated or remain the same based on whether a GLM (gene lookup manager) is required in order to perform the TFBS identification. If the input is a list of FASTA sequences, CiiiDER will read the sequences directly to identify TFBSs, and the GUI will appear the same as above. If the input is a list of genes or Ensembl IDs, then a GLM is required in order to identify the promoter region of a gene of interest. The GLM contains information regarding transcription start sites (TSSs) for all of the genes and transcripts for the human GRCh38 genome. The view will appear as in Fig. 4.
   (a) If the input is a list of genes as in the image above, then the user will be prompted to identify the region of interest to be analyzed for TFBSs. The default setting is 1500 bp upstream and 500 bp downstream of the TSS, which generally corresponds to a gene's promoter region. Additionally, the user may select the genome to be scanned for

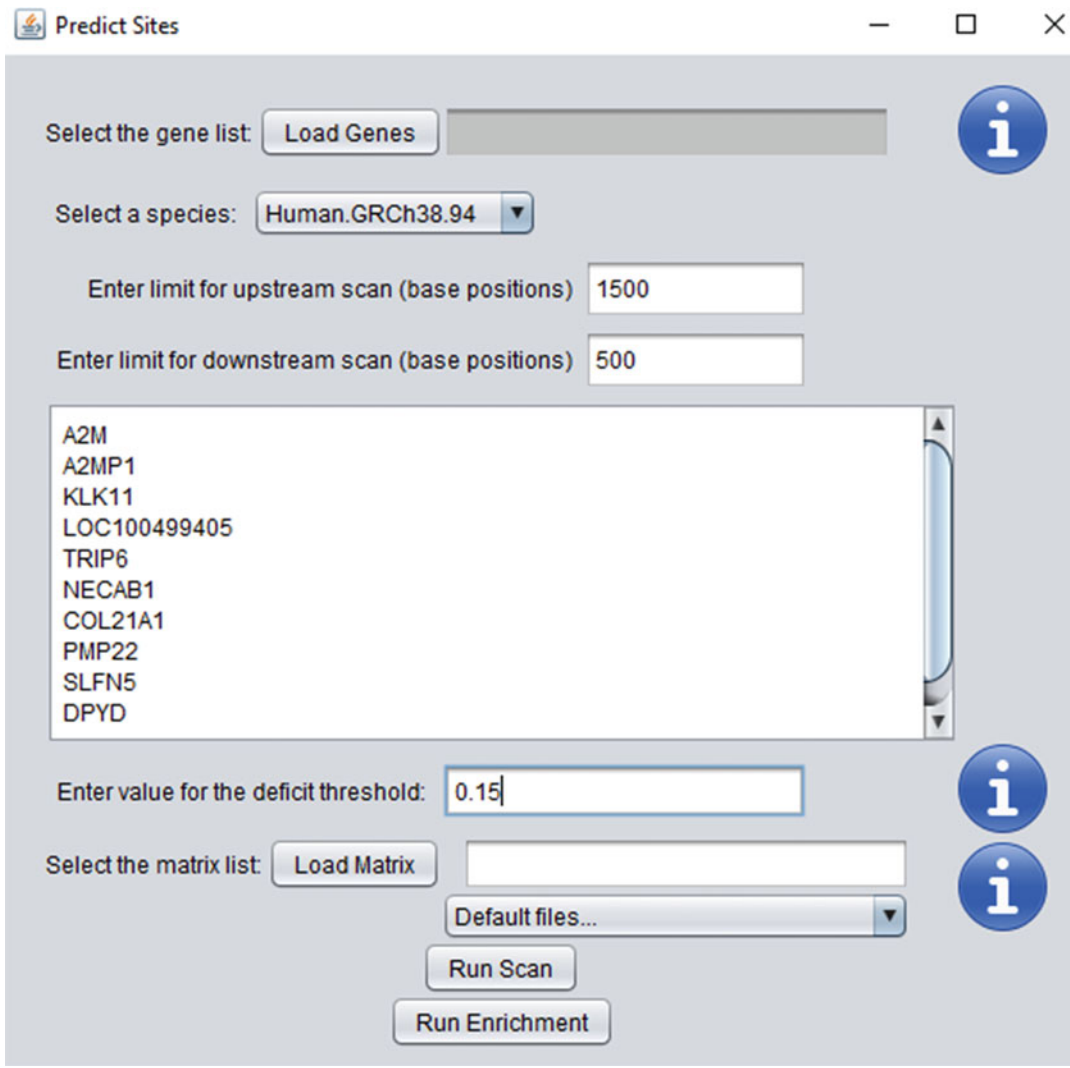

Fig. 4 If the input is a list of genes, then the user will be prompted to identify the region of interest to be analyzed for TFBSs. The default setting is 1500 bp upstream and 500 bp downstream of the TSS, which generally corresponds to a gene's promoter region. Additionally, the user may select the genome to be scanned for the TFBS identification. The default is the human genome that is included in the CiiiDER installation. The user will also be prompted to select a value for the deficit threshold (the quality of a match between a sequence and the PFM of a given transcription factor). The default setting is 0.15. A position frequency matrix (PFM) library must also be selected from either the dropdown list or by clicking on the "Load Matrix" button

the TFBS identification. The default is the human genome that is included in the CiiiDER installation.

5. The user will be prompted to select a value for the deficit threshold (the quality of a match between a sequence and the PFM of a given transcription factor). The default setting is 0.15, which correlates to the scan accepting any TFBS with a

MATCH score of 0.85 or above. A perfect MATCH score is 1. The user can choose to apply more stringent parameters (a deficit threshold of 0.05, for instance), or more lenient parameters (a deficit threshold of 0.25, for instance). As can be expected, the number of identified TFBSs decreases as the deficit threshold moves closer to 0. Values closer to 0 return fewer TFBSs but more perfect matches between PFM and sequence; values closer to 1 return more TFBSs but less perfect matches between PFM and sequence.

6. A position frequency matrix (PFM) library must then be selected. The CiiiDER package includes two PFM libraries: JASPAR 2018 CORE nonredundant vertebrate matrices and matrices from [16], which is a large experimental dataset. The user can easily add additional PFM libraries provided that they are in a format recognizable by CiiiDER (TRANSFAC or JASPAR format).
   (a) As an example, the author downloaded the HOCOMOCO v11 PFM library from https://hocomoco11.autosome.ru/downloads_v11 (H11_HUMAN_mono_transfac_format.txt), and saved the .txt file in the "Matrices" subfolder under the "CiiiDER_TFMs_Homo_sapiens.GRCh38.94" subfolder in the CiiDER program files. The HOCOMOCO v11 PFM library can then be found as an option in the list of default matrix files (Fig. 5).
7. The user then clicks on the "Run Scan" button to initiate identification of the TFBSs for the FASTA sequences or selected regulatory regions for the list of genes or Ensembl IDs.
8. The output screen (Fig. 6) displays putative TFBSs per regulatory region of each gene, on an interactive map. At this screen, the user can do the following:
   (a) Right-click on the name of the transcription factor on the right side of the screen, which gives options for the following:
      - Choose color.
      - Hide.
      - Hide all other transcription factors.
      - Save genes with this transcription factor.
      - Show only promoters with this transcription factor.
   (b) Adjust the order of gene promoter or regulatory regions by clicking on each track and dragging up or down.
   (c) Show additional transcription factors on the gene maps. By default, 10 transcription factors will be shown. Additional transcription factors can be added to the interactive

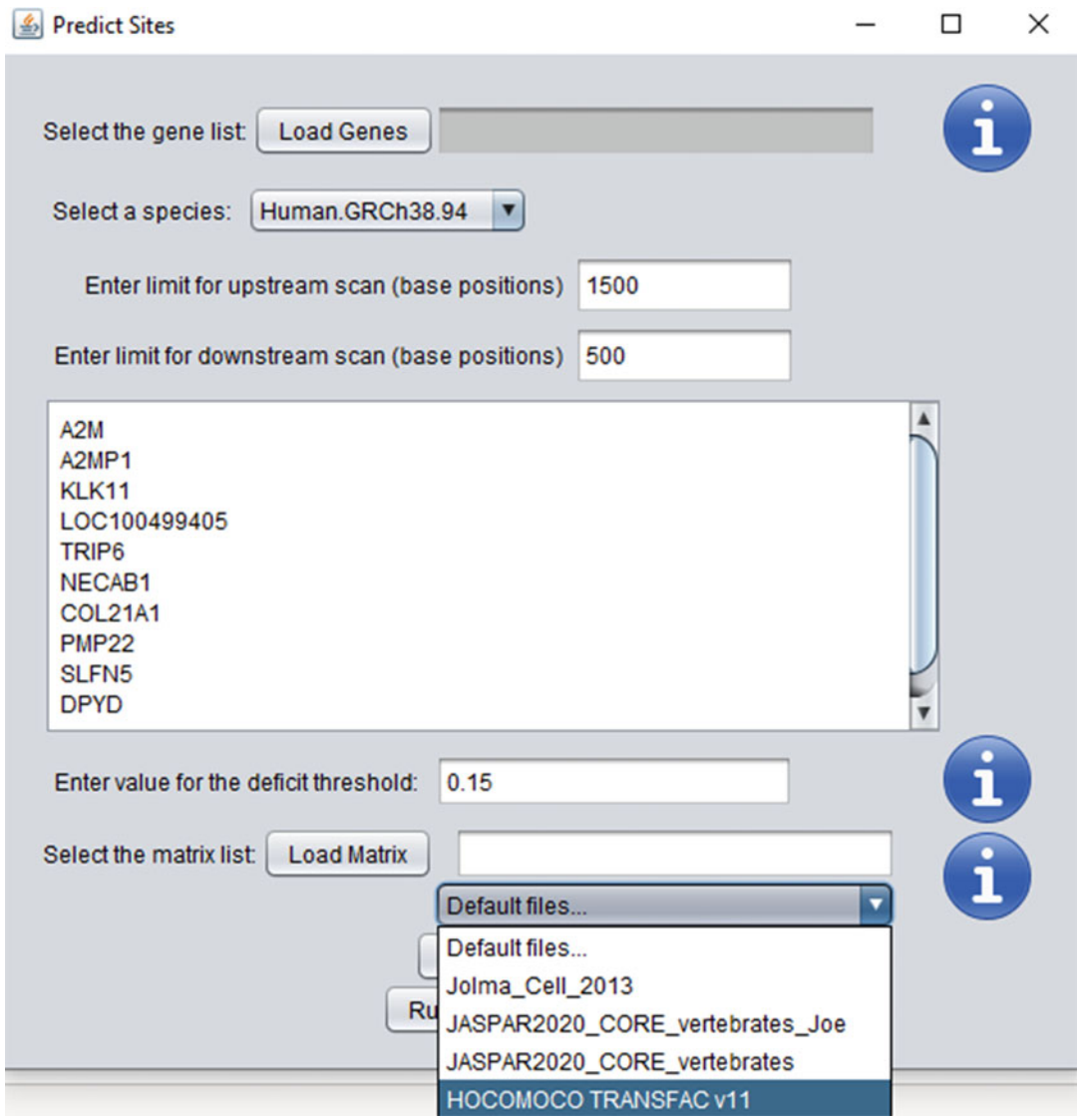

Fig. 5 Additional PFM libraries can easily be added to CiiiDER to repeat analyses across various publicly available matrix libraries. Libraries stored in the "Matrices" subfolder in the CiiiDER software folder will be displayed in the dropdown list of default files. PFM libraries must be in JASPAR or TRANSFAC format

map by double-clicking on transcription factors of interest in the list in the lower right box.

(d) Adjust the zoom level of the gene map, and adjust the deficit cutoff to increase scan stringency.

9. The results of the TFBS identification analysis can be saved as a project (file name ending in .cdr), and publication-quality images of the TFBSs can be saved in *PNG*, *TIFF*, or *GIF* format.

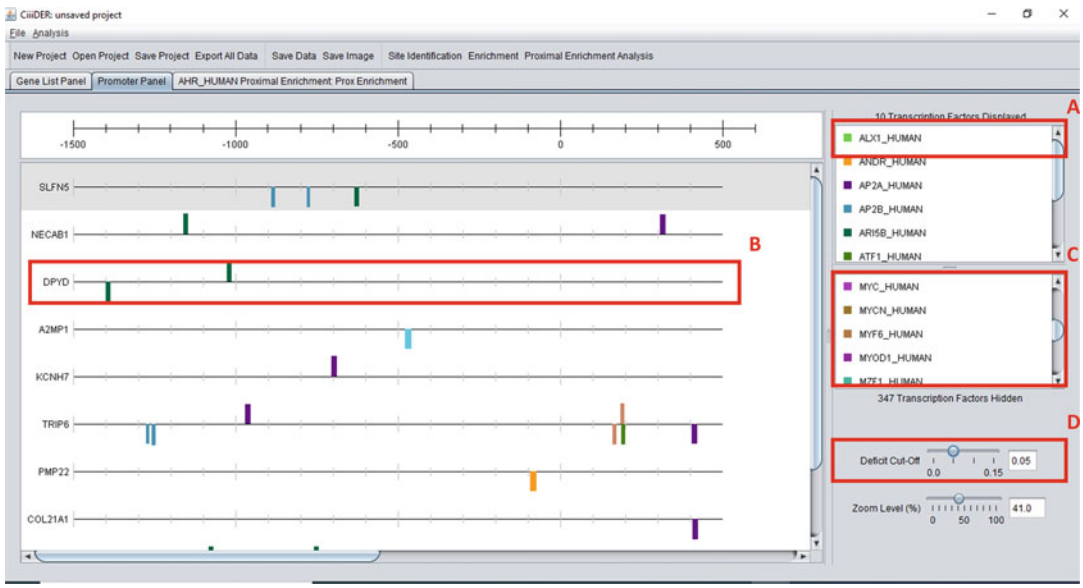

Fig. 6 TFBS identification results screen. (**a**) Right-clicking on the name of the transcription factor on the right side of the screen gives options for the changing transcription factor display parameters. (**b**) The order of gene maps can be adjusted by clicking on each track and dragging up or down. (**c**) Additional transcription factors can be displayed on the gene maps. By default, ten transcription factors will be shown. Additional transcription factors can be added to the interactive map by double-clicking on transcription factors of interest in the list in the lower right box. (**d**) The zoom level of the gene map can be adjusted to show specific regions or the entire region of interest (for example, the zoom can be decreased to show the entire range of 1500 bp upstream to 500 bp downstream of the TSS); the deficit cutoff can be adjusted to increase scan stringency

3.2 Transcription Factor Enrichment Analysis

This analysis enables the user to sort out which transcription factors are overrepresented (or underrepresented) in the regulatory regions of a differentially expressed set of genes, compared to a background list of genes. The selection of an appropriate background list of genes is critical for ensuring that meaningful results are returned. Rather than randomly picking a list of genes, it is best to select genes that are expressed in the organism being studied. An example of a relevant background list could be genes with a very small or no fold change in expression between comparison groups, or genes that do not correlate with expression of a gene of interest.

1. For an example of this analysis, the author retrieved data from the TCGA Ovarian Serous Cystadenocarcinoma Firehose Legacy using the cBioPortal platform [17, 18]. There are numerous publicly available datasets for a variety of disease states and cancer types that have yet to be mined for the type of information that the following analysis uncovers.
   (a) In this example, the author is interested in examining a list of genes that are strongly correlated (Spearman's correlation ≥ 0.6) with expression of XAF1, which has been

shown to be a strong inducer of apoptosis in various disease states, including ovarian cancer [19–25].

(b) The background list for this analysis are genes that are very weakly correlated (Spearman's correlation ≤ 0.2 and ≥ -0.2) with expression of XAF1.

2. To begin the analysis, the user opens the CiiiDER.jar file in the "CiiiDER_TFMs_Homo_sapiens.GRCh38.94" subfolder.
3. The user then clicks on the "Start" button at the center of the window.
4. On the next window that opens, the user can choose to upload a list of ENSEMBL IDs or gene names that have been pasted into a .txt file, or a list of sequences in FASTA format in a .txt file, using the "LOAD GENES" button. Alternatively, the user can simply type or paste a list of gene names or FASTA sequences in the text box.
   (a) For example, the list of genes strongly correlated with XAF1 expression are pasted into the text box, and XAF1 is added to the bottom of the list to include this gene in the analysis.
5. The user then specifies the region of interest to be analyzed based on the TSS of each gene. The default setting is 1500 bp upstream and 500 bp downstream of the TSS, which generally corresponds to a gene's promoter region.
6. The user may select the genome to be scanned for the TFBS identification. The default is the human genome that is included in the CiiiDER installation.
7. The value for the deficit threshold (the quality of a match between a sequence and the PFM of a given transcription factor) is 0.15 by default, but the user can enter any value from 0 to 1 to alter the match stringency (values closer to 0 return fewer TFBSs but more perfect matches between PFM and sequence; values closer to 1 return more TFBSs but less perfect matches between PFM and sequence).
   (a) For example, the author selected a deficit threshold of 0.15 for this analysis.
8. A position frequency matrix (PFM) library must then be selected. The CiiiDER package includes two PFM libraries: JASPAR 2018 CORE nonredundant vertebrate matrices and matrices from [6], which is a large experimental dataset.
   (a) For example, the author selected the Jolma et al. PFM library for this analysis.
9. The user then clicks on the "Run Enrichment" button to proceed in the analysis.

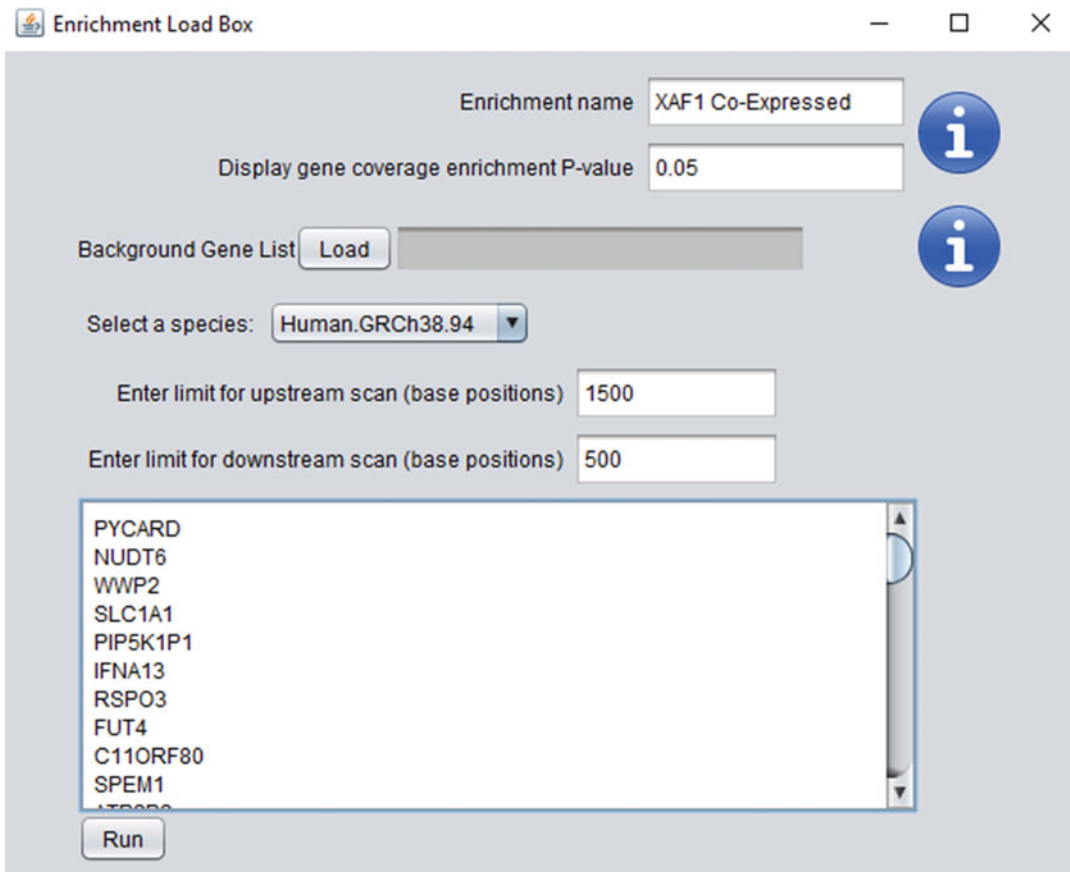

Fig. 7 The Enrichment Load Box directs the user to name the enrichment analysis (Enrichment name), to choose a *P*-value for gene coverage enrichment, and to upload or paste a background gene list. The authors of the CiiiDER program recommend a background list of at least 100 genes (per the CiiiDER Documentation Draft included in the download). Additionally, if a list of genes is pasted into the text box, then the user will be prompted to define the promoter region to be scanned for TFBSs for each gene. The default is 1500 BP upstream and 500 BP downstream of the TSS

10. The proceeding screen (Enrichment Load Box) (Fig. 7) directs the user to name the enrichment analysis (Enrichment name), to choose a *P*-value for gene coverage enrichment, and to upload or paste a background gene list. The authors of the CiiiDER program recommend a background list of at least 100 genes (per the CiiiDER Documentation Draft included in the download). Additionally, if a list of genes is pasted into the text box, then the user will be prompted to define the promoter region to be scanned for TFBSs for each gene. The default is 1500 BP upstream and 500 BP downstream of the TSS. The user then clicks "Run".
    (a) For example, the author named the enrichment analysis "XAF1 Co-Expressed," left the gene coverage enrichment and region scan limits at the default settings, and pasted a

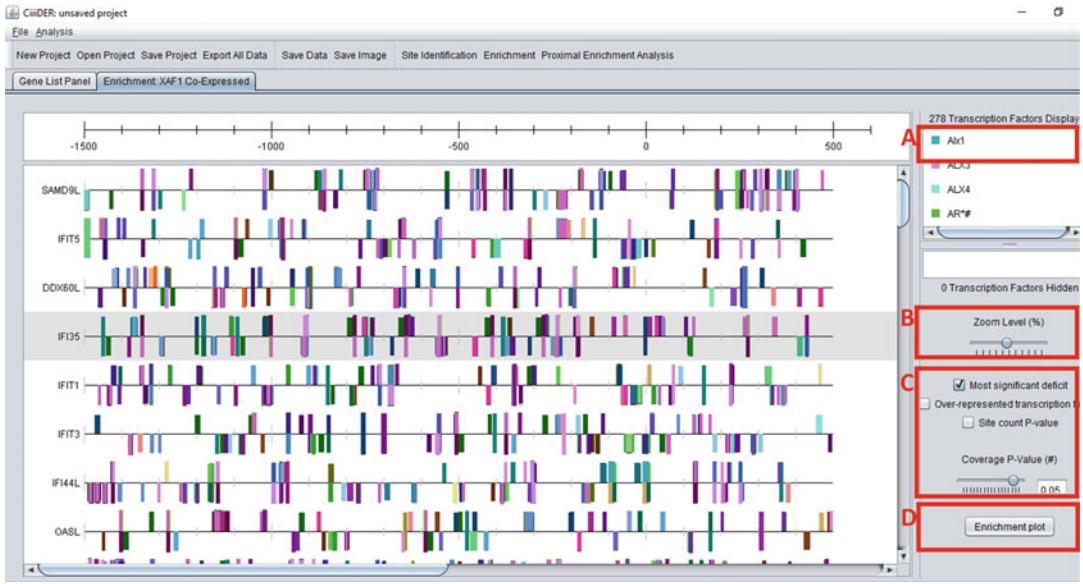

Fig. 8 Transcription factor enrichment analysis output screen. (**a**) Right-clicking on the name of a transcription factor on the right side of the screen presents several options for modulating the displayed results. (**b**) The user can adjust the zoom level to expand or shrink the range of regulatory region that is viewable in the interactive map window. (**c**) Options to modulate analysis parameters (detailed descriptions is found in the text). (**d**) The enrichment analysis can be displayed in an intuitive graphical format by clicking on the "Enrichment plot" button

list of 5000 genes that were very weakly correlated with XAF1 expression.

11. The output screen displays putative TFBSs per regulatory region of each gene on an interactive map. At this screen, the user can do the following (Fig. 8, boxes a–d relate to **steps a–d** that follow):

    (a) Right-click on the name of the transcription factor on the right side of the screen, which gives options for the following:

    - Choose color.
    - Hide.
    - Hide all other transcription factors.
    - Save genes with this transcription factor.
    - Show only promoters with this transcription factor.

    (b) Adjust the zoom level to expand or shrink the range of regulatory region that is viewable in the interactive map window.

    (c) Select/modulate the following options:

    - Whether to display all transcription factors at the deficit in which they are most significantly enriched

(default) (checkbox for "Most significant deficit"). This will increase the number of significant results.

- Whether to display only over-represented transcription factors (default), as opposed to displaying both over- and underrepresented transcription factors.
- Whether to incorporate an additional *P*-value threshold for site count statistical significance (default is that the checkbox "Site count *P* value" is unchecked).
  - Site Count *P*-Value: This statistic is based on the Mann-Whitney *U* test, and determines significance based on whether the number of TFBS per regulatory region is different between the list of genes of interest and the list of background genes. Note that this significance test depends on differences in the number of TFBS per individual genes, and does not necessarily inform as to whether a transcription factor is present or absent (one or the other, yes or no, regardless of the number of TFBS per regulatory region) from regulatory regions in the target list significantly more or less compared to background. A few genes with many TFBS could skew the results of this calculation.
- Select the Gene Coverage *P*-value (default is 0.05).
  - Gene Coverage *P*-Value: This statistic is based on Fisher's exact test, and calculates the proportion of regulatory regions bound or unbound by a transcription factor, and compares the proportions bound or unbound between the target genes and the background list. This calculation does not consider differences in the number of TFBS per regulatory region between comparison groups; it answers whether a given transcription is present or absent anywhere in the specified regulatory region of the gene.

(d) Generate an enrichment plot (additional information follows in **step 12**).

(e) Save the project ("Save Project"), save enrichment analysis data ("Save Data") in .csv format, and save images ("Save Images") of the TF-TFBS maps.

(f) The .csv file includes the following data:

- Transcription Factor Name.
- Deficit.
- No. of Search Sites.
- Mean Sites Per Search Gene.

- No. of Background Sites.
- Mean Sites Per Background Gene.
- Site Representation.
- Mann-Whitney *U*.
- Site *P*-Value.
- Total No. of Search Genes.
- No. of Transcription Factor Search Genes.
- Total No. of Background Genes.
- No. of Transcription Factor Background Genes.
- Gene Representation.
- Gene *P*-Value.
- Average Log2 Proportion Bound.
- Log2 Enrichment.
- Significance Score.

12. Enrichment Plot—data from the enrichment analysis can be viewed in an intuitive graphical format (Fig. 9).

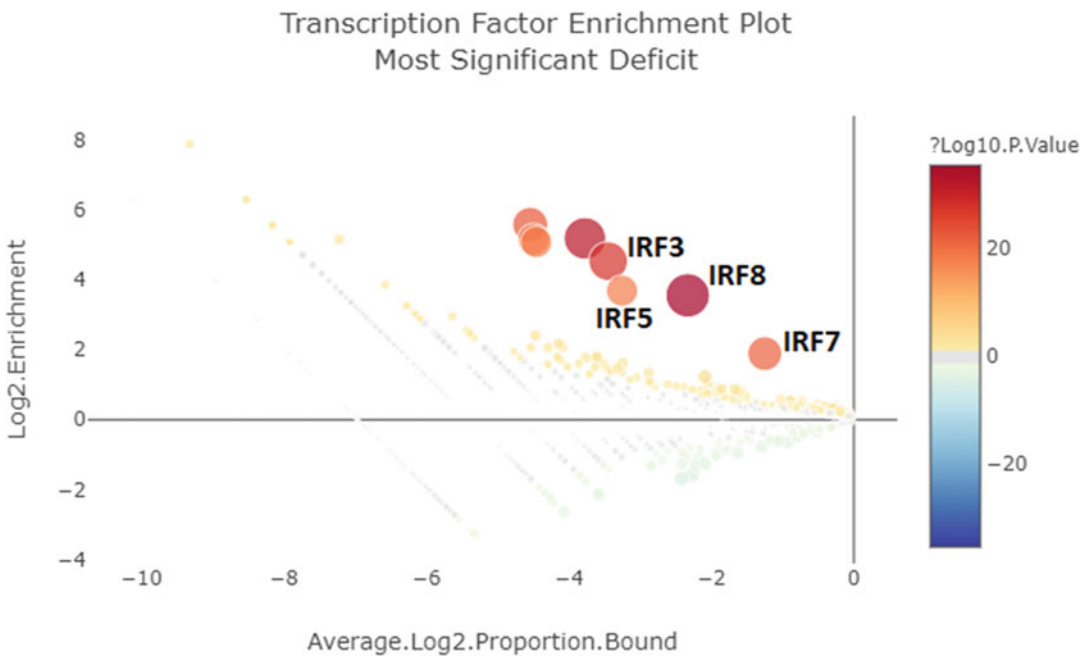

Fig. 9 Enrichment plot example. The results of the enrichment analysis are plotted according to their degree of over- or underrepresentation (*y*-axis), the degree to which TFBSs exist in the regulatory regions of the gene set of interest and background (*x*-axis), and the statistical significance of the enrichment (the size of the circle for each transcription factor). A detailed description of the calculations and interpretation of the plot is found in the text

(a) The enrichment calculation (y-axis) indicates to what extent a transcription factor is over- or underrepresented. The value is greater than zero if the transcription factor occurs in a greater proportion of search genes than of background genes, and less than zero if the transcription factor is underrepresented. If a given transcription factor has binding sites in n_S out of N_S genes and in n_B out of N_B background genes, then:

$$\log_2(\text{Enrichment}) = \log_2\left(\frac{n_S + 1/2}{N_S + 1/2} \div \frac{n_B + 1/2}{N_B + 1/2}\right)$$

(b) The proportion bound calculation (x-axis) indicates to what extent a transcription factor is present in the analyzed regulatory regions for both the genes of interest and the background genes. The closer the value is to 0, the more ubiquitous the transcription factor is in the regulatory regions analyzed. As the value decreases below zero, the TFBSs are less frequently present in the analyzed regions of the target and background gene lists (e.g., -1 if sites are present in $1/2$ of the genes, -2 if $1/4$ genes, -3 if $1/8$ of the genes, etc.).

$$\text{Average } \log_2(\text{Proportion Bound}) = \frac{1}{2}\log_2\left(\frac{n_S + 1/2}{N_S + 1/2}\right) + \frac{1}{2}\log_2\left(\frac{n_B + 1/2}{N_B + 1/2}\right)$$

(c) The size of the dot on the graph which corresponds with a transcription factor increases as the P value decreases, and the P value is $\log_{10}$ transformed to generate a "Significance Score." The size of the dot therefore increases as the "Significance Score" increases.

(d) As an example, when the author performed the enrichment analysis as outlined in previous steps, the enrichment plot reveals a number of IRF TFBSs as overrepresented in the list of genes that strongly correlate with XAF1 expression in ovarian cancer.

3.3 Proximal Enrichment Analysis

This analysis builds off the results of the transcription factor enrichment analysis, and can help the user to identify the transcription factor sites that are enriched near a particular transcription factor. This analysis can also identify proximal transcription factor sites that are underrepresented in a gene set of interest compared to background. This analysis uses the identified TFBSs from the enrichment analysis, in both the gene list of interest and the background gene list, to analyze over- or underrepresentation. An example is included in the proceeding steps describing this analysis.

Fig. 10 Proximal enrichment analysis can be performed following transcription factor enrichment analysis by clicking on the button in the ribbon indicated by the red box in the figure

1. Proximal enrichment analysis can be performed starting at the screen where the transcription factor enrichment analysis procedure ended in the steps above. To begin proximal enrichment analysis, the user clicks on the "Proximal Enrichment Analysis" button on the top ribbon of the screen (identified in the red box in Fig. 10).
2. The user is then brought to a new screen with prompts for selecting the transcription factor to explore further for proximal enrichment analysis (Fig. 11). The user is also able to change the transcription factor deficit for the transcription factor of interest (the default value is the deficit value used for transcription factor enrichment analysis for that specific transcription factor), proximal enrichment window size, and deficit threshold values for transcription factors to be identified. A matrix list is selected, and the default selection is the matrix list previously used for the transcription factor enrichment analysis. The user then clicks on the "Run Enrichment" button.
   (a) For example, in the analysis the author performed above, IRF8 was found to be the most overrepresented transcription factor in the list of genes strongly correlated with XAF1 expression, compared to background. In the previous analysis, 62 TFBSs for IRF8 were identified in the list of 62 genes, which strongly correlate with XAF1 expression (1 binding site per search gene). In the background list, only 295 TFBSs for IRF8 were identified in the list of

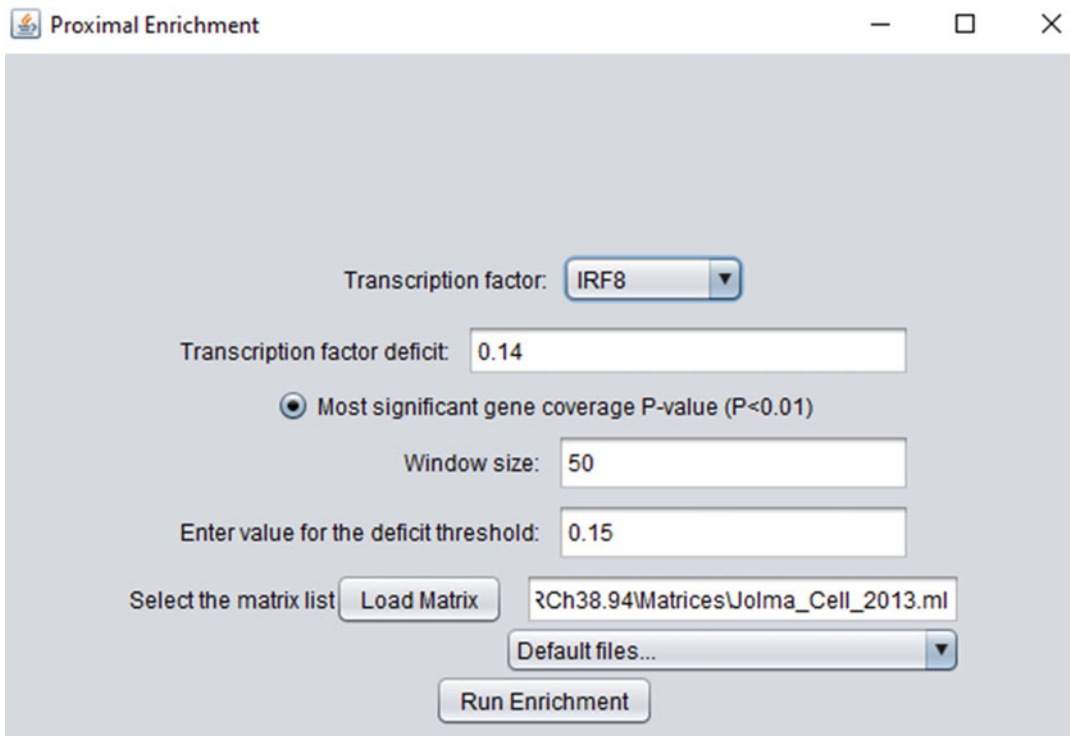

Fig. 11 Prompts for selecting the transcription factor to explore further for proximal enrichment analysis. The user can change the transcription factor deficit for the transcription factor of interest (the default value is the deficit value used for transcription factor enrichment analysis for that specific transcription factor), proximal enrichment window size, and deficit threshold values for transcription factors to be identified. A matrix list is selected, and the default selection is the matrix list previously used for the transcription factor enrichment analysis

4909 background genes (0.06 binding sites per background gene). The proximal enrichment analysis identifies what transcription factor–binding sites near the binding sites for IRF8 occur more frequently in the IRF8-binding sites for the genes of interest compared to their presence near IRF8-binding sites in the 295 genes in the background list.

3. The enrichment results (Fig. 12) present an interactive map as in the TFBS scan and Transcription Factor Enrichment Analysis, showing the binding sites for the transcription factor of interest in the regulatory region of the genes of interest, and the over- or underrepresented transcription factors with proximal binding sites to the gene of interest. From here, the user can save the proximal enrichment analysis data in .csv format, save images, and generate an enrichment plot.
   (a) For this example, IRF3, IRF4, and IRF5 had the highest significance scores, meaning that their TFBSs are

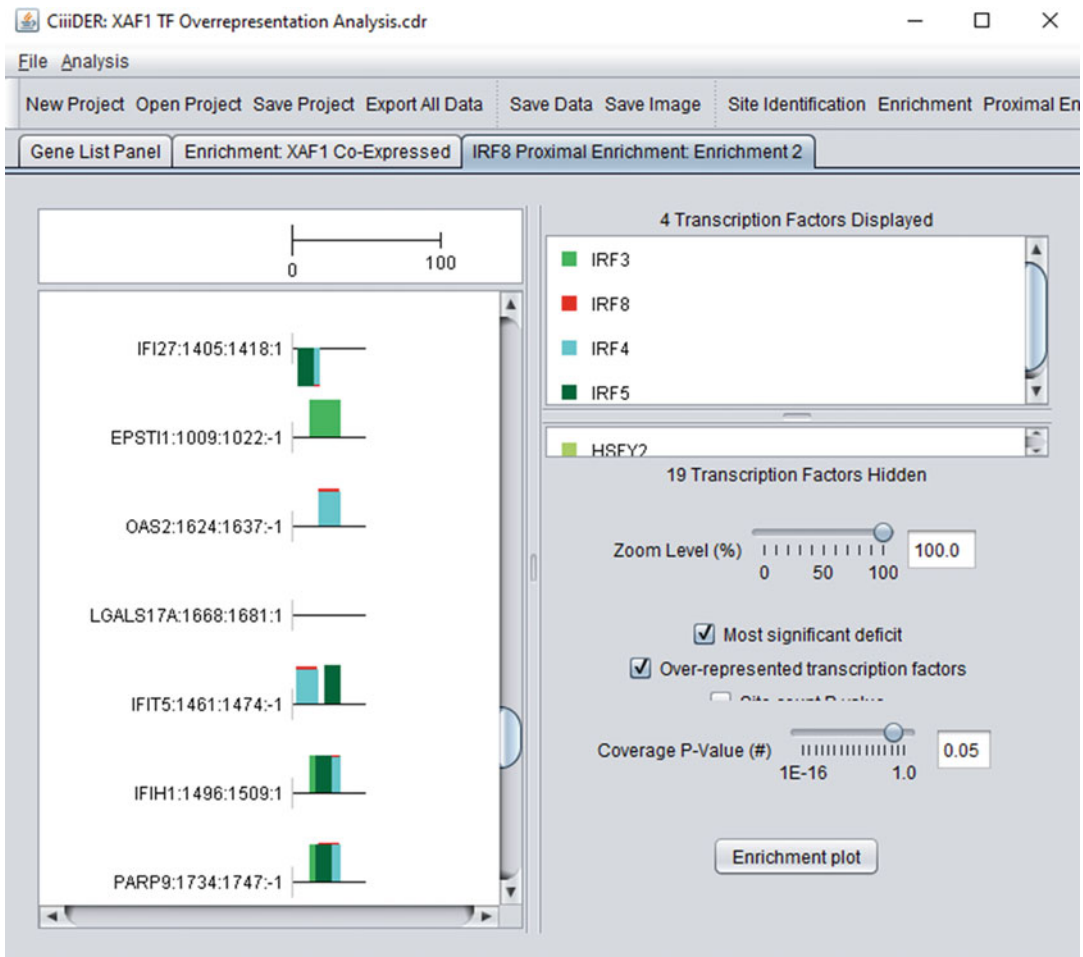

Fig. 12 Proximal enrichment analysis output screen. Over- or underrepresented transcription factors with TFBSs proximal to the transcription factor of interest are displayed

colocated with IRF8 TFBSs to a much higher degree in the gene set of interest compared to background. The interactive map displayed in Fig. 12 demonstrates the coordination of these sites with IRF8.

(b) The enrichment plot in Fig. 13 shows the overrepresentation of colocalization of transcription factor–binding sites in an intuitive graphical format. As one can see, IRF9-binding sites are also significantly overrepresented as being proximal to IRF8-binding sites in the target gene set compared to background.

(c) For the example shown here, the table in Fig. 14 displays the data represented in the enrichment plot. The number of colocalized TFBS per gene for each significantly overrepresented transcription factor vs. the total number of

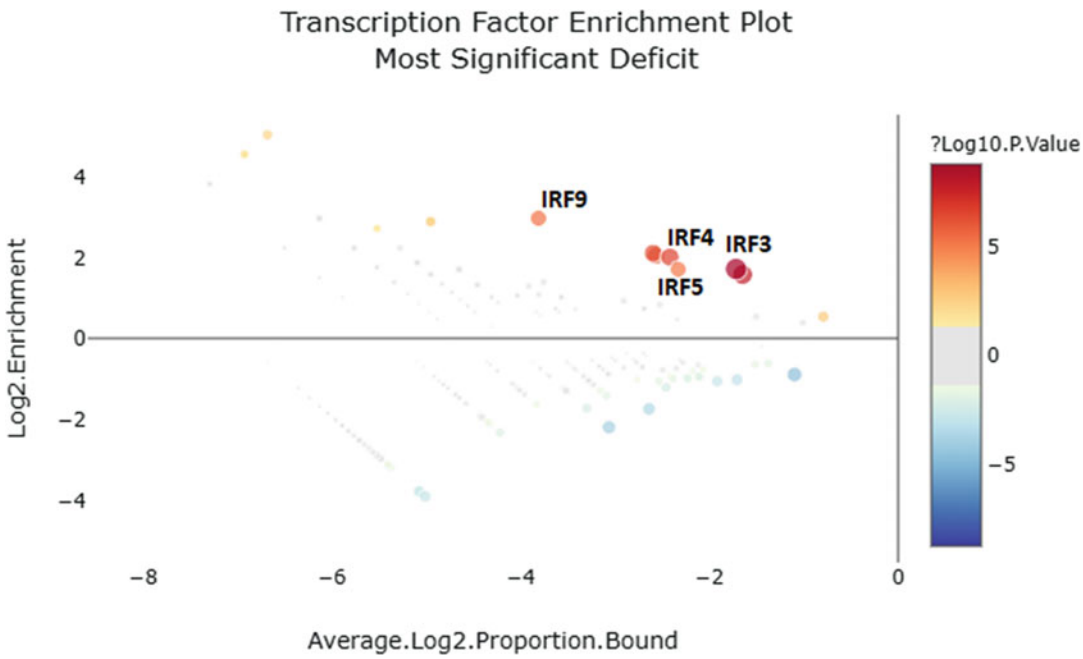

Fig. 13 Enrichment plot example for proximal enrichment analysis results

Transcription Factor ID	Transcription Factor Name	Deficit	Total No. Search Genes	No. Genes with TFBS Colocalized with IRF8	Total No. Background Genes	No. Genes with TFBS Colocalized with IRF8	Gene Representation	Gene P-Value	Average Log2 Proportion Bound	Log2 Enrichment	Significance Score
IRF3_H01	IRF3	0.13	62	34	295	49	Up	1.76E-09	-1.717458764	1.720397872	8.754050077
IRF4_H01	IRF4	0.13	62	23	295	27	Up	2.40E-07	-2.41842502	2.014459174	6.619199168
IRF5_H02	IRF5	0.07	62	21	295	24	Up	7.45E-07	-2.565912003	2.052784946	6.12760968
IRF9_H01	IRF9	0.11	62	12	295	7	Up	5.34E-06	-3.81102591	2.97819563	5.272718244

Fig. 14 Tabulated results of the data presented in the example enrichment plot. The number of colocalized TFBS per gene for each significantly overrepresented transcription factor vs. the total number of relevant genes (in both the genes of interest and the background genes) is calculated as per the enrichment equation described in the text, to determine the Significance Score (log10-transformed *P*-value)

relevant genes (in both the genes of interest and the background genes) is calculated as per the equation in **step 12a** to determine the Significance Score.

(d) For the example shown here, the Proximal Enrichment results may indicate that IRF3, IRF4, IRF5, and IRF9 are critical cofactors with IRF8 for orchestrating the expression of genes strongly correlated with the expression of an important mediator of apoptosis (XAF1) in ovarian cancer.

References

1. Keenan AB, Torre D, Lachmann A, Leong AK, Wojciechowicz ML, Utti V, Jagodnik KM, Kropiwnicki E, Wang Z, Ma'ayan A (2019) ChEA3: transcription factor enrichment analysis by orthogonal omics integration. Nucleic Acids Res 47(W1):W212–W224. https://doi.org/10.1093/nar/gkz446
2. Lambert SA, Jolma A, Campitelli LF, Das PK, Yin Y, Albu M, Chen X, Taipale J, Hughes TR, Weirauch MT (2018) The human transcription factors. Cell 172(4):650–665. https://doi.org/10.1016/j.cell.2018.01.029
3. Johnson DS, Mortazavi A, Myers RM, Wold B (2007) Genome-wide mapping of in vivo protein-DNA interactions. Science 316 (5830):1497–1502. https://doi.org/10.1126/science.1141319
4. Robertson G, Hirst M, Bainbridge M, Bilenky M, Zhao Y, Zeng T, Euskirchen G, Bernier B, Varhol R, Delaney A, Thiessen N, Griffith OL, He A, Marra M, Snyder M, Jones S (2007) Genome-wide profiles of STAT1 DNA association using chromatin immunoprecipitation and massively parallel sequencing. Nat Methods 4(8):651–657. https://doi.org/10.1038/nmeth1068
5. Tuerk C, Gold L (1990) Systematic evolution of ligands by exponential enrichment: RNA ligands to bacteriophage T4 DNA polymerase. Science 249(4968):505–510. https://doi.org/10.1126/science.2200121
6. Khan A, Fornes O, Stigliani A, Gheorghe M, Castro-Mondragon JA, van der Lee R, Bessy A, Chèneby J, Kulkarni SR, Tan G, Baranasic D, Arenillas DJ, Sandelin A, Vandepoele K, Lenhard B, Ballester B, Wasserman WW, Parcy F, Mathelier A (2018) JASPAR 2018: update of the open-access database of transcription factor binding profiles and its web framework. Nucleic Acids Res 46(D1): D260–D266. https://doi.org/10.1093/nar/gkx1126
7. Pal S, Hoinka J, Przytycka TM (2019) Co-SELECT reveals sequence non-specific contribution of DNA shape to transcription factor binding in vitro. Nucleic Acids Res 47 (13):6632–6641. https://doi.org/10.1093/nar/gkz540
8. Jolma A, Yan J, Whitington T, Toivonen J, Nitta KR, Rastas P, Morgunova E, Enge M, Taipale M, Wei G, Palin K, Vaquerizas JM, Vincentelli R, Luscombe NM, Hughes TR, Lemaire P, Ukkonen E, Kivioja T, Taipale J (2013) DNA-binding specificities of human transcription factors. Cell 152(1):327–339. https://doi.org/10.1016/j.cell.2012.12.009
9. Kulakovskiy IV, Vorontsov IE, Yevshin IS, Sharipov RN, Fedorova AD, Rumynskiy EI, Medvedeva YA, Magana-Mora A, Bajic VB, Papatsenko DA, Kolpakov FA, Makeev VJ (2018) HOCOMOCO: towards a complete collection of transcription factor binding models for human and mouse via large-scale ChIP-Seq analysis. Nucleic Acids Res 46(D1): D252–D259. https://doi.org/10.1093/nar/gkx1106
10. Gearing LJ, Cumming HE, Chapman R, Finkel AM, Woodhouse IB, Luu K, Gould JA, Forster SC, Hertzog PJ (2019) CiiiDER: a tool for predicting and analysing transcription factor binding sites. PLoS One 14(9):e0215495. https://doi.org/10.1371/journal.pone.0215495
11. Kel AE, Gößling E, Reuter I, Cheremushkin E, Kel-Margoulis OV, Wingender E (2003) MATCHTM: a tool for searching transcription factor binding sites in DNA sequences. Nucleic Acids Res 31(13):3576–3579
12. Chen EY, Tan CM, Kou Y, Duan Q, Wang Z, Meirelles GV, Clark NR, Ma'ayan A (2013) Enrichr: interactive and collaborative HTML5 gene list enrichment analysis tool. BMC Bioinformatics 14:128. https://doi.org/10.1186/1471-2105-14-128
13. Kuleshov MV, Jones MR, Rouillard AD, Fernandez NF, Duan Q, Wang Z, Koplev S, Jenkins SL, Jagodnik KM, Lachmann A, McDermott MG, Monteiro CD, Gundersen GW, Ma'ayan A (2016) Enrichr: a comprehensive gene set enrichment analysis web server 2016 update. Nucleic Acids Res 44(W1): W90–W97. https://doi.org/10.1093/nar/gkw377
14. Fu Y, Frith MC, Haverty PM, Weng Z (2004) MotifViz: an analysis and visualization tool for motif discovery. Nucleic Acids Res 32(Web Server Issue):W420–W423. https://doi.org/10.1093/nar/gkh426
15. Frith MC, Fu Y, Yu L, Chen J-F, Hansen U, Weng Z (2004) Detection of functional DNA motifs via statistical over-representation. Nucleic Acids Res 32(4):1372–1381. https://doi.org/10.1093/nar/gkh299
16. Jolma A, Kivioja T, Toivonen J, Cheng L, Wei G, Enge M, Taipale M, Vaquerizas JM, Yan J, Sillanpää MJ, Bonke M, Palin K, Talukder S, Hughes TR, Luscombe NM, Ukkonen E, Taipale J (2010) Multiplexed massively parallel SELEX for characterization of human transcription factor binding specificities. Genome Res 20(6):861–873. https://doi.org/10.1101/gr.100552.109

17. Cerami E, Gao J, Dogrusoz U, Gross BE, Sumer SO, Aksoy BA, Jacobsen A, Byrne CJ, Heuer ML, Larsson E, Antipin Y, Reva B, Goldberg AP, Sander C, Schultz N (2012) The cBio cancer genomics portal: an open platform for exploring multidimensional cancer genomics data. Cancer Discov 2(5):401–404. https://doi.org/10.1158/2159-8290.CD-12-0095
18. Gao J, Aksoy BA, Dogrusoz U, Dresdner G, Gross B, Sumer SO, Sun Y, Jacobsen A, Sinha R, Larsson E, Cerami E, Sander C, Schultz N (2013) Integrative analysis of complex cancer genomics and clinical profiles using the cBioPortal. Sci Signal 6(269):pl1. https://doi.org/10.1126/scisignal.2004088
19. Choo Ze KRYL, Wallis K, Koh TJW, Kuick CH, Sobrado V, Kenchappa RS, Loh AHP, Soh SY, Schlisio S, Chang KTE, Chen ZX (2016) XAF1 promotes neuroblastoma tumor suppression and is required for KIF1B-β-mediated apoptosis. Oncotarget 7 (23):34229–34239. https://doi.org/10.18632/oncotarget.8748
20. Jeong S-I, Kim J-W, Ko K-P, Ryu B-K, Lee M-G, Kim H-J, Chi S-G (2018) XAF1 forms a positive feedback loop with IRF-1 to drive apoptotic stress response and suppress tumorigenesis. Cell Death Dis 9(8):806. https://doi.org/10.1038/s41419-018-0867-4
21. Long X, Li Y, Qi Y, Xu J, Wang Z, Zhang X, Zhang D, Zhang L, Huang J (2013) XAF1 contributes to dengue virus-induced apoptosis in vascular endothelial cells. FASEB J 27 (3):1062–1073. https://doi.org/10.1096/fj.12-213967
22. Xia Y, Novak R, Lewis J, Duckett CS, Phillips AC (2006) Xaf1 can cooperate with TNFalpha in the induction of apoptosis, independently of interaction with XIAP. Mol Cell Biochem 286 (1–2):67–76. https://doi.org/10.1007/s11010-005-9094-2
23. Yu LF, Wang J, Zou B, Lin MCM, Wu YL, Xia HHX, Sun YW, Gu Q, He H, Lam SK, Kung HF, Wong BCY (2007) XAF1 mediates apoptosis through an extracellular signal-regulated kinase pathway in colon cancer. Cancer 109 (10):1996–2003. https://doi.org/10.1002/cncr.22624
24. Zhao W-J, Deng B-Y, Wang X-M, Miao Y, Wang J-N (2015) XIAP associated factor 1 (XAF1) represses expression of X-linked inhibitor of apoptosis protein (XIAP) and regulates invasion, cell cycle, apoptosis, and cisplatin sensitivity of ovarian carcinoma cells. Asian Pac J Cancer Prev 16(6):2453–2458. https://doi.org/10.7314/apjcp.2015.16.6.2453
25. Zhu C, Li B, Frontzek K, Liu Y, Aguzzi A (2019) SARM1 deficiency up-regulates XAF1, promotes neuronal apoptosis, and accelerates prion disease. J Exp Med 216(4):743–756. https://doi.org/10.1084/jem.20171885

INDEX

Ayesha Alvero and Gil G. Mor (eds.), *Detection of Cell Death Mechanisms: Methods and Protocols*, Methods in Molecular Biology, vol. 2255, https://doi.org/10.1007/978-1-0716-1162-3, © Springer Science+Business Media, LLC, part of Springer Nature 2021

F

G

H

I

K

L

M

N

O

P

R

S

T

U